Developing microbial biotherapeutics for the immunotherapy of cancer

Christopher A. Price

A thesis submitted for the degree of Doctor of Philosophy (PhD) in biomolecular science

University of East Anglia
School of Biological Sciences

Quadram Institute Biosciences
Food, Microbes, and Health

October 2023

Abstract

Over recent decades, the microbial communities of the gut have been validated as powerful regulators of human immunity and cancer. Both animal and human studies have shown that the supplementation with specific beneficial gut bacteria can significantly improve outcomes, yet no bacteria-based drugs have yet been successfully translated to the clinic. One of the major challenges facing the field, is a lack of understanding of the detailed molecular mechanisms of action which govern efficacy, both in the context of bacterial active compound production and the host anti-tumour response. This lack of understanding prevents the rational use of response-predicting biomarkers, which in turn prevents proper patient stratification and leads to inconsistent clinical responses. Additionally, poor characterisation of the key active compounds produced by therapeutic bacteria prevents the isolated administration of functional ingredients and thus requires the utilisation of live bacteria, whose activity are inherently dictated by individual host conditions (e.g., diet, abundance of competing bacteria, antibiotic use). The research presented here shows a mechanism-focused approach to bacterial drug discovery, focusing on the commensal *Bifidobacterium* and *Bacteroides*, which have received significant attention for cancer-protective properties. Specifically, we show that *Bifidobacterium*, as a genus, are broadly protective against pre-clinical breast cancer models through a range of unique, strain-specific mechanisms. We show for the first time, that a strain of *Bifidobacterium pseudocatenulatum* (LH663) activates host $CD8^+$ T cell anti-tumour immunity against the major subtypes of breast cancer. We validate that this effect is specifically mediated by cell surface exopolysaccharide (EPS), which functions mechanistically to enhance the activity of $CD8^+$-specific dendritic cells. Finally, we also demonstrate the novel utility of *Bacteroides thetaiotaomicron* outer membrane vesicles (OMVs) as anti-cancer therapeutic agents against pre-clinical melanoma.

Contents

List of Figures

List of Tables

Acknowledgements

I have so many wonderful people to thank for getting me to a completed PhD thesis. Firstly, to my parents, I could not have reached this position without your unwavering belief and support. In more ways than one, I wouldn't be here without you. Also, to my sister Jess, for always being there for me. To my partner, Meg, thank you for being my daily champion, comfort, and inspiration. You're my best friend and I'm so lucky to be able to walk through life with you. I love you.

I'd like to thank the BigC cancer charity for funding my research, and the Quadram Institute for funding my continued study following the COVID-19 pandemic. Members of the Robinson lab past and present have been a huge part of my growth and journey to get here, both scientifically and personally. JT, Chris B, Ali, Wes, Rob, Sally, Luke, Alicia, Aleks, Nancy, and Nilda, all of you have contributed so much to the kind, supportive, and collaborative culture that makes Robinson lab special. I'd particularly like to thank Wes, Nilda, Ali, Alicia, and Luke as people who dedicated a significant amount of their time directly helping me produce the work in this thesis.

Externally, I'd like to say a huge thank you to Dr Magda Kujawska for her expert bioinformatic support analysing *Bifidobacterium* genomes and isolation of EPS, Dr Emily Jones for her essential help producing bacterial OMVs and conducting key OMV tracking experiments, and to Dr Trey Koev for his (very much needed!) chemistry expertise analysing polysaccharide structure. I have also been blessed to have excellent students to mentor through my PhD, and I'd like to recognise both Avani and Mitch for delivering some brilliant research from their projects and helping contribute key data to the project.

Finally, I want to express my deep gratitude to both my PhD supervisors Lindsay Hall and Stephen Robinson. Lindsay continues to inspire me and everyone else around her with her ingenuity and endless fountain of ideas, and I feel so fortunate to have been mentored by a scientific mind whose greatness is only matched by her kindness. To my primary supervisor, Stephen, words cannot do justice to how much I owe you. You were one of the first people to really believe in me and gave me the opportunity to start my career in science. You are a truly remarkable mentor, both scientifically and personally, and bouncing ideas off you has given me some of the most enjoyable

moments of my professional life. On a personal note, I am so unbelievably grateful to leave this PhD not just with a mentor, but a lifelong friend.

1. Introduction

1.1. Cancer biology and the current therapeutic landscape

In the age of modern medicine, cancer remains one of the single biggest threats to human health. Alongside cardiovascular disease, cancer accounts for a majority of premature deaths worldwide(*1*), with variable response to existing therapies and a lack of new therapies continuing to hamper progress. The problem of cancer is only expected to grow bigger, as global cancer burden is expected at around 28 million cases by 2040 (a 47% increase from 2020)(*2*) and the total cost to society is expected to reach $25.2 trillion by 2050(*3*). To summarise, cancer poses of one the single greatest challenges to biomedical research this century, with higher numbers of more effective, better tolerated, and more accessible therapies desperately needed to make a dramatic improvement to patient outcomes.

1.1.1. Cancer aetiology and progression

Cancer is an umbrella term describing a range of diseases across the body which arise from the aberrant uncontrolled proliferation of mammalian cells. Cancerous cells can develop from anywhere in the body, usually emerging due to the accumulation of genetic mutations (either from passive or actively mutagenic processes) which fundamentally damage cell cycle regulation. Cancer is appreciated as a stepwise disease, whereby the sequential acquisition of mutations in oncogenes, tumour suppressor genes (TSGs), and DNA repair genes incur gradual defects to normal cellular processes until uncontrolled proliferation is achieved. Cancer progresses through further stages from here in the formation of small legions, which eventually develop into larger tumours. Occurring concurrently to this tumour formation is the process of cancer metastasis, whereby a metastatic cascade of events leads to the escape of cancerous cells from the primary tumour and eventual seeding at other organs in the body, which precedes the development of secondary tumours. During the progression of the metastatic process, cancer becomes a truly systemic disease which involves the host ‘fighting’ tumours across multiple sites. The growth of these primary and secondary tumours drains energy and nutrients from the host, causes high levels of tissue damaging inflammation, and ultimately disrupts and shuts down the normal essential functions of the organ which houses the cancer, causing host mortality. The

seminal review published by Hanahan and Weinberg in 2000(*4*) describes several fundamental 'hallmarks of cancer', these seemingly ubiquitous traits of tumours (regardless of tissue origin) include self-sufficient proliferation, insensitivity to growth inhibiting signals, resistance to apoptosis, ability to recruit vasculature (angiogenesis), and acquired capabilities for invasion and metastasis. This review series has since been updated over the past two decades(*5, 6*) to reflect our advancing understanding behind the complexity of cancer, now including cancer immune escape, metabolic reprogramming, phenotypic plasticity, nonmutational epigenetic reprogramming, senescence, and polymorphic microbiomes.

1.1.2. Breast cancer

Breast cancer (BrCa), tumourigenesis of the mammary epithelium, is the most diagnosed cancer in the world and leading cause of cancer-related death in women(*2*). Although breast cancer survival is broadly improving in developed countries such as the UK, likely due to better early screening and healthcare availability(*7*), BrCa is an increasing problem in developing countries with enhanced incidence and comparatively worse survival statistics(*8*). Despite improvement to overall BrCa survival in developed countries, with 85% five-year survival in UK women(*9*), survival for patients diagnosed with metastatic disease (i.e., Stage IV) is far lower at only 25% five year survival(*10*). An unfortunate reality for most patients is the requirement of aggressive treatments, such as chemotherapy and radiotherapy, which have undesirable side effects and variable efficacy. The combination of huge clinical incidence, poor late-stage survival, and inconsistent therapeutic efficacy makes BrCa research and therapy development a huge unmet clinical need.

Like all cancers, BrCa progresses through the stepwise acquisition of mutations which ultimately result in a tumorigenic phenotype. The most common mutation in BrCa is that of the BRCA (BReast CAncer susceptibility) genes(*11*). Both BRCA1 and BRCA2 are TSGs which activate processes of DNA repair(*11*). Consequently, individuals with BRCA mutations have reduced capacity to repair DNA breaks, potentially causing improper transcription of mutated proteins, a reduction in apoptosis and a shift towards oncogenesis(*12*). There is a high level of genetic variability between individual cases of BrCa, and other mutations common in BrCa include TP53, PTEN, KRAS, APC, and an array of other TSGs and oncogenes (OGs)(*13*). Indeed, the acquisition of tumorigenic

mutations will also influence the clinical staging of the tumour, with a high frequency of mutations correlated with a more aggressive phenotype. Staging is performed according to the TNM model, with stage I BrCa describing a small, localised tumour with limited/no lymph node involvement, and stage IV BrCa describing metastatic cancer which has spread from the primary tumour to distant organs(*14*).

1.1.2.1. Breast cancer classification

BrCa classification can be defined by physiological or molecular characteristics. Clinically, BrCa is described based on the site of the primary tumour, lymph node involvement and metastatic spread; known as the 'Tumour, Node, Metastasis' model(*15*). BrCa can also be described physiologically, lobular carcinoma in situ (LCIS) and ductal carcinoma in situ (DCIS), for example, describe non-invasive tumours emanating from the breast lobules and ducts respectively(*16, 17*). Infiltrating lobular carcinoma (ILC) and infiltrating ductal carcinoma (IDC) on the other hand, describe tumours derived from these same tissues but with an invasive phenotype(*18, 19*). A more common and clinically useful (predictive) method of BrCa classification describes the disease on molecular grounds. This type of classification defines the 'molecular subtypes' of BrCa based on the expression of key hormone receptors (HRs); oestrogen receptor (ER), progesterone receptor (PR) and human epidermal growth factor receptor (HER2)(*20*). The utility of this system lies in a classification of BrCa which describes tumour proliferative capability(*21*), response to therapy(*22*) and likely prognosis(*23*). Outside of hormone receptor status, some proliferative markers (e.g. Ki67) and basal markers (e.g. claudin) can be used to further distinguish BrCa type(*24*).

<u>Luminal and Normal-like BrCa</u>

Luminal BrCa can be split into two major subtypes; Luminal A and Luminal B(*25*). The main relation of these subtypes lies in their ability to express both ER and PR. Contrastingly though, only Luminal B can overexpress HER2 and is typically associated with a reduced PR expression compared to Luminal A(*25*). HER2 overexpressing Luminal B tumours will also display higher levels of Ki67 and have a resulting proliferative phenotype which is more resistant to existing therapies(*26*). Both Luminal A and B tumours are however susceptible to adjuvant hormone therapy (e.g. tamoxifen) due to the expression of cell surface hormone receptors (i.e. ER and/or PR)(*27*). There are further similarities between Luminal BrCa (particularly Luminal A)

and ‘Normal-like’ BrCa – with the latter also capable of expressing ER and PR. Normal-like BrCa is categorised independently however, due to a distinct genomic background from luminal cancer which mimics that of healthy breast tissue(*28*). Prognosis is generally positive for these types of tumours.

HER2-Enriched BrCa

The HER2-enriched subtype of BrCa is defined by a HER2 amplification which results in an over-expression of cell surface growth factor receptors, causing increased sensitivity to human epidermal growth factor(*29*). The result of this is a highly proliferative phenotype which displays high levels of Ki67(*24*). The prognosis for these tumours is generally poor(*30*), although the overexpression of growth factor receptors confers susceptibility to adjuvant hormone therapy(*31*).

Triple negative (Basal-like) BrCa

The triple negative (also described as ‘basal-like’) subtype of BrCa is named due to the common absence of ER and PR expression, as well as HER2 overexpression(*32*). This type of BrCa emanates from the basal epithelium of the breast and is highly proliferative (demarcated by high Ki67 expression)(*33*). In the absence of the major hormone receptors, triple negative BrCa can be identified through the expression of basal markers such as laminin, claudin and cytokeratin 5, 14 and 17(*34*). The clinical outlook for triple negative BrCa patients is particularly poor, as a proliferative and invasive tumour phenotype is exacerbated by resistance to hormone therapy; caused by reduced expression of hormone receptors at the cell surface(*35*). A small positive in the treatment of these cancers is that high tumour proliferation sensitises triple negative BrCa to chemotherapy and higher than usual T cell infiltration sensitises these tumours to some checkpoint immunotherapy(*36*), although treatment-resistance and tumour relapse is common and patient survival remains low(*37*).

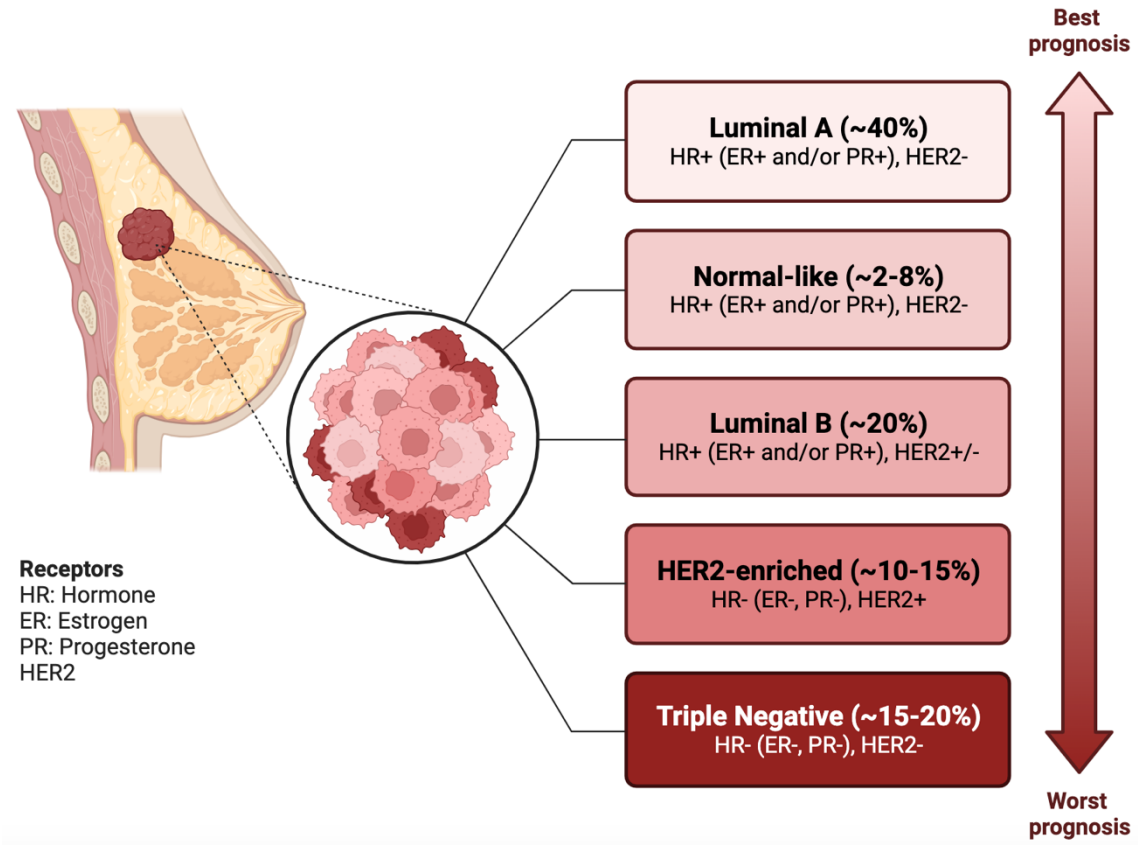

Figure 1.1. The molecular subtypes of breast cancer. Breast cancers can be broadly distinguished based on the expression of various hormone receptors and HER2 growth factor receptor. The intrinsic molecular subtype of breast cancer correlates strongly with prognosis. Adapted from "Intrinsic and Molecular Subtypes of Breast Cancer", by Biorender.com (2023). Retrieved from https://app.biorender.com/biorender-templates.

1.1.2.2. The therapeutic outlook for breast cancer

The therapeutic outlook for BrCa differs significantly depending on the subtype and clinical stage of disease (Figure 1.1). A given treatment regime which is effective in one type of BrCa can be ineffective in another, meaning many patients have tailored treatment regimens depending on prior clinical evaluation(*38*). The amount of clinical evaluation of patients prior to therapy has become increasingly extensive, and thus treatment regimens are now beginning to be tailored between individuals with the same BrCa subtype, but different biomarker or mutational profile(*39*). Despite the complexity in treatment combination approaches which can exist within BrCa, the idealistic aim of care is relatively simple: getting patients to a stage where surgical resection of the

cancer is possible. Metastatic BrCa diagnosed at stage IV is usually considered inoperable and incurable, thus patients these patients are normally administered systemic therapy with the goal of managing symptoms to end of life(*38*).

Surgery and neoadjuvant therapy

Surgical removal of BrCa is the common goal of clinical practice. The majority of BrCa patients (more than 80%)(*40*) receive this treatment immediately prior to the commencement of any adjuvant approaches, particularly those with early stage BrCa (stage I-II) with minimal lymph node involvement or metastases. Surgical approaches can broadly be categorised into breast conserving surgery (BCS) and mastectomy, whereby a localised region of breast (BSC) containing the tumour, or the whole breast (mastectomy) is removed, depending on the primary tumour size and potential regional spread(*41*). Five-year survival following surgery is excellent, at around 90%(*42*), but is not always possible due to a larger tumour size (>2cm^2) or a complex morphology. In such situations, neoadjuvant chemotherapy is usually prescribed to reduce the primary tumour burden prior to surgery. This is particularly recommended for triple negative and HER2$^+$ patients due to a positive correlation with pathological complete response(*43*).

Adjuvant approaches

The adjuvant stage of the BrCa treatment pathway is where most systemic therapy begins. The standard for most, particularly for high risk patients with later stage disease, is a regime of chemotherapy (either post-operatively or immediately for inoperable patients)(*44*). Precise regimes of chemotherapy can differ depending on subtype, but a combination or sequence of anthracycline and taxane agents is generally most effective in preventing recurrence(*45*). Common therapy combinations (across the major subtypes of disease) include AC (doxorubicin and cyclophosphamide) in combination with paclitaxel (AC-T) or docetaxel (DAC), as well as the anthracycline-free combination of docetaxel and cyclosphosphamide (TC) (which can have survival benefits when compared with AC treatment)(*46*). Specifically for patients with triple negative disease, trial data indicates that standard anthracycline and taxane approaches (e.g., AC-T) can be combined with platinum to increase pathological complete response(*47-49*), with the caveat that adverse side effects are generally also enhanced in these patients(*50*). It is generally considered that use of adjuvant chemotherapy is more effective in preventing recurrence in HR negative than

HR positive disease(*51*), despite these patients generally having worse outcomes overall.

For patients with HR^+ disease, endocrine therapy is generally prescribed as standard in addition to other treatments. Tamoxifen treatment offers significant clinical benefit in preventing recurrence and mortality over a prolonged (15 year) time horizon(*52*), functioning to antagonise ER and thus prevent the tumour proliferative effects of oestrogen(*53*). Despite the long-term protective effects of tamoxifen, increasing resistance occurs over time. Thus, supplementation with other types of endocrine therapy, such as aromatase inhibitors, is also common(*27*). Aromatase inhibitors are usually prescribed to post-menopausal women only and function to block the action of the aromatase enzyme, which demethylates androgen carbon 19 to phenolic 18-carbon oestrogens(*54*), supressing systemic oestrogen levels and providing a 40% reduction to BrCa recurrence when used sequentially after tamoxifen(*55*).

For $HER2^+$ patients, an additional option of targeted therapy is available. HER2 targeting antibodies, such as trastuzumab, can be used to specifically target BrCa cells alongside standard chemotherapy (mainly taxane-based) regimens, incurring antibody-dependent cell-mediated cytotoxicity and providing a 50% reduction to disease recurrence(*56*). More recent work has seen the clinical translation of other antibodies targeting HER2 or its downstream pathways, such as Pertuzumab(*57*) and Lapatinib(*58*). Although outcomes are generally worse for patients with germline BRCA1/BRCA2 mutated BrCa, the recent translation of novel PARP inhibitor therapy is providing hope. The PARP1 and PARP2 proteins are vital components of the DNA damage response (DDR) pathway which prevent the formation of double strand DNA (dsDNA) breaks(*59*). Inhibition of the PARPs causes an increase in these dsDNA breaks and genome instability, which normally can be repaired by the homologous recombination repair (HRR) pathway mediated by the BRCA1 and BRCA2 proteins(*60*). However, in BRCA mutated BrCa, these proteins are non-functional and thus BrCa cells cannot repair dsDNA breaks caused by PARP inhibitors, with the resulting genome instability causing BrCa cell death(*61*). PARP inhibitors such as olaparib and talazoparib are effective in prolonging progression free survival in this particularly vulnerable subset of patients(*62, 63*).

Although there are also other approved breast cancer therapies that have entered the clinic over recent decades, such as cyclin dependent kinase (CDK) inhibitors against metastatic HR^+ BrCa(*64*), an advance sparking broader interest is the introduction of

checkpoint immunotherapy to triple negative BrCa patients. Due to the immense promise of immunotherapy (outlined in section 1.2.5.), the number of trials focusing on this therapeutic modality in BrCa are continually increasing(*65*). Administration of the PD-1 targeting monoclonal antibody (mAb) pembrolizumab alongside chemotherapy for advanced metastatic ($PD\text{-}L1^{+}$) triple negative BrCa was approved in 2021, achieving a significantly increased pathological complete response and estimated event free survival compared with chemotherapy alone(*66*). Early results using checkpoint inhibitors in HR^{+} BrCa have thus far been disappointing(*67*), likely owing to a reduced infiltration of inflammatory T cells in these tumours(*68*), although exploration of immunotherapy in BrCa remains a huge therapeutic goal for researchers and clinicians.

1.1.3. Melanoma

Melanoma is the deadliest form of skin cancer. The disease arises due to the carcinogenic mutation and uncontrolled proliferation of melanin producing melanocytes in the basal skin epidermis. Melanoma is relatively rare disease which only represents 1% of diagnosed skin cancer, yet accounts for 80% of skin cancer deaths(*69*). Survival for melanoma is highly stratified depending on clinical stage, with cutaneous resectable early stage (I-II) melanoma patients having a 99.6% five-year survival, compared with 73.9% for stage III and 35.1% for stage IV(*69*). Melanoma is more common in Caucasian individuals(*70*) and has broadly increased in incidence in recent decades in fair-skinned, developed countries(*2*). In the US, melanoma represents the 5^{th} most common cancer diagnosis, though fortunately the transformational advent of checkpoint immunotherapy has decreased melanoma mortality in recent years(*71*).

1.1.3.1. Melanoma development and classification

Melanoma onset is driven by a combination of hereditary and environmental factors. Hereditary mutations in drivers such as CDKN2A, PTEN, and TP53 significantly increase the risk of disease onset(*72*) and can be compounded by exposure to UVA and UVB sunlight, which can further enhance melanocyte mutational burden, acquisition of key driver mutations, and development from benign nevi to malignant tumours(*73, 74*) (Figure 1.2). Most driver mutations for melanoma are thought to occur through the UV exposure, with BRAF (e.g., V600E) and MAPK mutations particularly prevalent in clinical cases(*75*). The progression of melanoma through to stage IV

metastasis is the key determinant of poor clinical outcomes, as the disease is generally very aggressive once it progresses subcutaneously to surrounding regional lymph nodes(*76*). Common sites of melanoma metastasis include the lungs, liver, and bone(*76*).

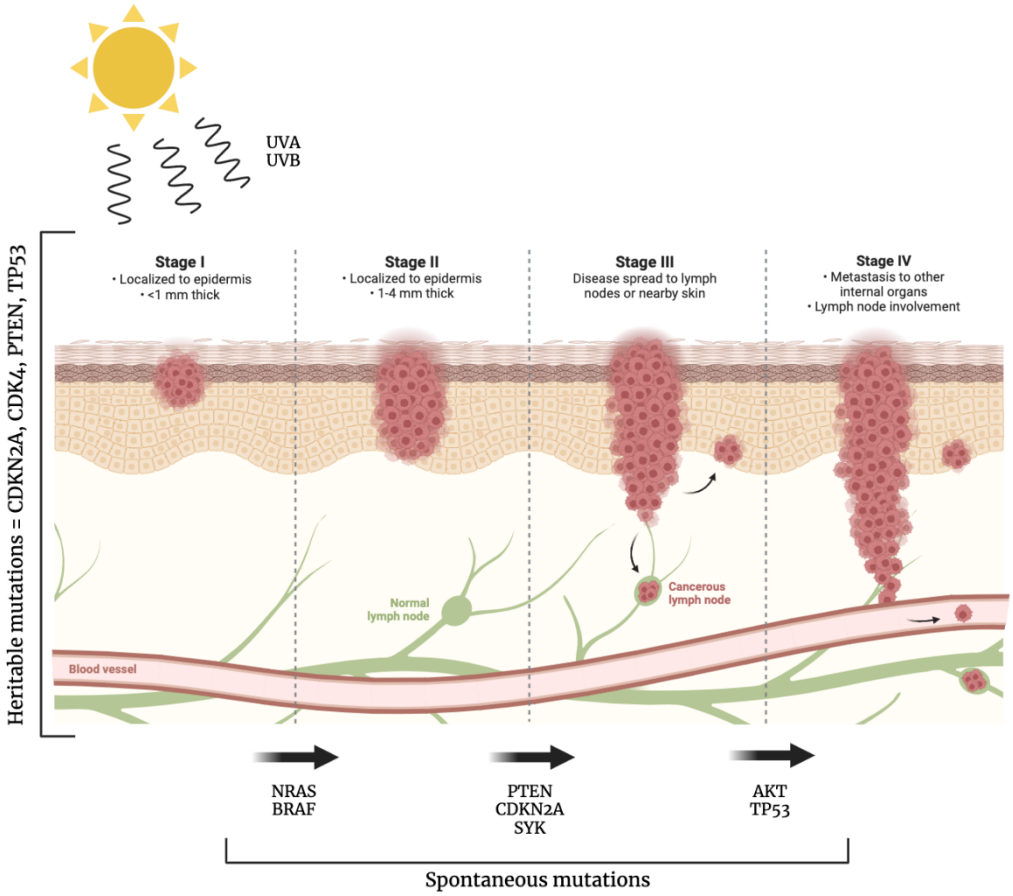

Figure 1.2. The genetic and molecular events of malignant melanoma. Heritable mutations in genes such as PTEN and TP53 are known to increase risk of metastatic disease. Exposure of melanocytes in skin the ionising UV-radiation can incur mutations in canonical drivers such as NRAS and BRAF, promoting the growth of a stage I benign nevus. Sequential acquisition of further oncogenic mutations in proto-oncogenes and tumour suppressor genes (e.g., APC, CDKN2A) allow transition to the stage II radial growth phase (RGP) and stage II vertical growth phase (VGP). The RGP is associated with the migration of tumour cells within the epidermis, whilst the VGP triggers melanoma invasion into the underlying dermal tissue. Dermal invasion provides the platform for stage IV tumour metastasis to distal sites, the dominant cause of mortality. Adapted from “Melanoma staging”, by Biorender.com (2023). Retrieved from https://app.biorender.com/biorender-templates.

1.1.3.2. The therapeutic outlook for melanoma

Like BrCa, the front-line preferred treatment for melanoma is surgical removal of the tumour. Surgery is currently the only near-curative therapy for melanoma, although these excellent outcomes are primarily confined to stage I-II disease, highlighting the importance for early diagnosis in melanoma(*77*). In cases of stage III disease, surgical resections of metastatic sentinel lymph nodes are also possible to contain the potential of further metastasis or recurrence, however surgical intervention for metastatic stage IV disease is not designed to be curative and further systemic treatment is required(*78*). Until advancements in targeted and immunotherapies in recent decades, the only available front-line treatment from melanoma was chemotherapy. Unfortunately, chemotherapy has never been a particularly effective course of treatment for the disease, with the only clinical approval having been dacarbazine and a median 1-year survival of 27%(*79*). No other tested chemotherapy was more effective with fewer side effects, demonstrating a major unmet need. Many targeted therapies, primarily against the driver mutations within melanoma, have been trialled in recent decades in the attempt to boost outcomes. The most successful of these have been the selective BRAF inhibitors vemurafenib(*80*) and dabrafenib(*81*) approved for metastatic unresectable BRAF-mutated melanoma. Although a relatively strong response of around 50% of patients is observed with these therapies, an unfortunate longer-term reality is the development of secondary resistance in many patients, which has led researchers to explore possible combination approaches targeting multiple pathways(*82, 83*).

The translation of immunotherapy has been transformative for melanoma outcomes. Approved therapies are based on immune checkpoint inhibition (see section 1.2.5.) and include the anti-CTLA-4 antibody ipilimumab(*84*) and two anti-PD-1 antibodies nivolumab(*85*) and pembrolizumab(*86*). Each of these therapies represented a significant advance on dacarbazine alone, with the example of nivolumab showing a 12-month overall survival rate of 73% compared to 43% of patients treated with dacarbazine(*85*). A more recent addition to the drug paradigm is the approval of dual Nivolumab with the LAG-3 inhibitor relatlimab, with this combination increasing median progression free survival to 10.1 months from 4.6 months (from Nivolumab alone), as well as increasing overall survival(*87*). Although these immunotherapies have made great advancements in the treatment of metastatic melanoma, they do suffer from adverse effects for patients based on enhanced inflammation of mucosal tissues (e.g.,

the skin and gastrointestinal tract), which does cause a significant minority of patients to withdraw from treatment(*88*). Additionally, over half of patients still do not respond to melanoma immunotherapy(*85, 87*), showing much research is still required to overcome problematic resistance mechanisms.

1.2. The immune system and cancer

The mammalian immune system is a spawling network of cells which serve as potentially our single greatest protection against systemic infection and disease. During a normal 'healthy' state, the immune system conducts active surveillance and guards against the action of potentially dangerous pathogenic bacteria, viruses, and fungi. Where these initial defences are overcome, the immune system attacks infection-causing pathogens, preventing their long-term colonisation and protecting against host damage and mortality. Under diseased states, such as cancer, the immune system functions to identify and destroy aberrant cells, representing a key determinant of long-term clinical outcomes(*89, 90*). Despite the immense benefit to human health which is provided by the immune system, the regulation of the complex processes governing proper function can also become imbalanced and cause serious disease. This is usually caused by the magnitude and regularity of the immune response becoming dysregulated, such as during cases of overactive (auto-) immunity in inflammatory bowel disease (IBD), where the immune response is triggered prematurely and is improperly targeted towards healthy host gastrointestinal cells, causing the host cell death, dysfunction of normal digestion, and potential mortality(*91*). Alternatively, the immune system can also be underactive and supressed, such as during cases of late-stage cancer, where tumours function to evade and inhibit the immune destruction of cancer cells(*92*) (outlined in section 1.2.3.4.). There is also evidence to suggest that immune dysfunction contributes to the natural decline in health during aging. This process is termed 'inflammaging' and describes an increasing propensity for the immune system to autoreact against the host and damage normal cell, tissue, and organ function with increasing age, increasing the risk of disease and frailty(*93*). Given the central role of the immune system to human health, the ability to control immunity represents a fundamental obstruction to improving and prolonging health.

1.2.1. An overview of the mammalian immune system

The action of the immune system can broadly be split into two arms, the innate and adaptive immune system. Innate immunity describes a set of biological responses which are genetically pre-programmed against defined molecular patterns, such as pathogen-associated molecular patterns (PAMPs) from microbes and damage-associated molecular patterns (DAMPs) from aberrant host cells(*94*). The receptors typically used by the cells of the innate immune system, such as toll-like receptors (TLRs) and C-type lectin receptors (CLRs), are widely expressed by many cell types to permit a rapid protection against pathogenic or inflammatory challenge, limiting damage to the host(*94*). Examples of key innate immune cells include monocytes, macrophages, and granulocytes (e.g., eosinophils, basophils, and mast cells), although innate immunity can also be non-cellular through the action of circulating plasma defensins, complement proteins, and ficolins(*95*).

Contrastingly, adaptive immunity describes the arm of cellular responses mediated by 'adaptable' receptors targeted with extreme specificity to a foreign structure (antigen), resulting from a process of somatic rearrangement of hundreds germ-line genetic elements to form unique functional receptors(*96*). The key cells of the adaptive immune system are T cells and B cells, which rely on the activity of the T cell receptor (TCR) and B cell immunoglobulin (Ig) receptors respectively(*97*). The adaptive process generates a small number of cells with specific activity against an antigen (e.g., a pathogen cell wall component or toxin), meaning antigenic challenge stimulates a broad adaptive cell proliferation process prior to significant inflammatory response(*97*). The acquisition of antigen-specificity by adaptive cells causes adaptive immunity to generally occur after an initial innate immune response, but offers the key advantage of remnant adaptive cells circulating for extended periods (years, or potentially decades) to protect against rechallenge from the same antigen, providing an immunological 'memory'(*98*).

Although innate and adaptive immunity are described separately with distinct functions, they functionally interact and operate synergistically to ensure health of the host. The innate immune response occurs more rapidly than the adaptive response, but also functions to inform adaptive immunity through 'presenting' antigens on cell surfaces to immature (antigen naïve) T and B cells(*99*). Likewise, the downstream activation of adaptive immune cells is associated with further recruitment of innate cells to facilitate

complete removal of the infectious challenge(*100*). Communication between immune cells is facilitated through an array of secretory proteins, such as chemokines (which generally recruit immune cells to an inflammatory site) and cytokines (which generally alter the activity and function of nearby immune cells)(*101*). The action of synergistic immune cells and immunomodulatory signals allows one type of immune cell to behave in a multitude of ways, permitting fine tuning of the immune response to each unique challenge.

1.2.2. Haematopoiesis and basic immune cell function

The array of cell types constituting the immune response is responsible for the adaptability and potency of the system. Generally, all immune cells begin from the same haematopoietic stem cells (HSCs) in the bone marrow, which also give rise to non-immune blood cells (erythrocytes, megakarocytes etc.)(*102*) (Figure 1.3). Here, HSCs differentiate either into common myeloid progenitors (CMPs) or common lymphoid progenitors (CLP), which spawn the myeloid and lymphoid lineages of immune cells respectively(*102*). CLPs can rapidly differentiate into functional populations of B lymphocytes, T lymphocytes, and natural killer (NK) cells(*103*). Discrimination of these cell types is possible based on the presence of surface markers and functional outputs. B cells are characterised by the presence of membrane-bound Ig and the production of antibodies (soluble secretory Igs) with cytotoxic action(*104*). T cells are demarcated by the presence of the TCR, whilst NK cells are larger granular lymphocytes which lack either B-cell Ig or the TCR (functioning as innate rather than adaptive immune responders)(*105*).

The output of CMPs is more widespread than that of CLPs, as they can differentiate into lineages of erythrocytes, megakaryocytes, and the myeloid immune lineage. Once differentiated to the granulocyte monocyte progenitor, differentiation through subtype dependent intermediaries precedes the formation of monocytes, neutrophils, basophils, eosinophils, and mast cells(*103*). As these myeloid cells are innate immune populations, they all broadly serve as first-line defences against host infection or tissue damage. In this context, neutrophils are usually the first responders, rapidly phagocytosing bacterial pathogens and targeting them for killing through release of cytotoxic granules loaded with reactive oxygen species (ROS)(*106*). Neutrophils also play an active role in tissue repair following infectious or inflammatory damage, secreting key enzymes such as elastase and cathepsin G.(*107*) Monocytes are highly

phagocytic and are also responsible for primary defence against pathogens(*108*). They can be recruited through the activity of neutrophils whilst persisting far longer in inflammatory tissues, killing internalised pathogens through nitric oxide products and processing antigens on their cell surface(*108*). Macrophages function similarly to monocytes in this context, although macrophages are derived primarily from the embryonic yolk sac(*109*), remaining as tissue-resident cells throughout life rather than being renewed through the action of HSCs. The antigen processing and production of immunomodulatory cytokines (e.g., TNFα, IL-10, IL-6) makes monocytes and macrophages key mediators of downstream adaptive immune responses(*110, 111*). The remaining granulocytes of the myeloid immune cells are lower in abundance than monocytes and neutrophils and have discrete functions(*112*). Eosinophils for example, function similarly to neutrophils but with cytoplasmic granules targeted to parasites (e.g., helminths) and a broad propensity for the release of chemoattracting chemokines(*113*). The activity of mast cells and basophils is relatively comparable during an allergenic challenge (e.g., from pollen), releasing histamine and other proteases to create a local inflammatory environment(*114*).

A final important cellular subset generated (primarily) from CMP are dendritic cells (DCs). Following a pathway from CMP to a common dendritic progenitor (CDP) population, then to subsets of conventional DCs (cDCs) and plasmacytoid DCs (pDCs)(*115*), these key cells function as 'professional' antigen presenting cells (APCs). Here, DCs within inflammatory tissues take up antigens from pathogens and damaged host cells and present them to the adaptive T cells through major histocompatibility complex (MHC) type I and II(*116*). Due to the expression of several powerful co-stimulatory molecules, such as CD80/CD86, DCs are the most potent APCs across the immune system(*117*). These interactions between DCs and T cells usually occur in the lymphoid organs (spleen and lymph nodes) and represent a key bridge between the innate and adaptive immune systems(*115*). Plasmacytoid DCs are distinct from cDCs in their prominence in plasma, where they appear to be particularly responsive to viral infection through secretion of type I interferon (IFN)(*118*).

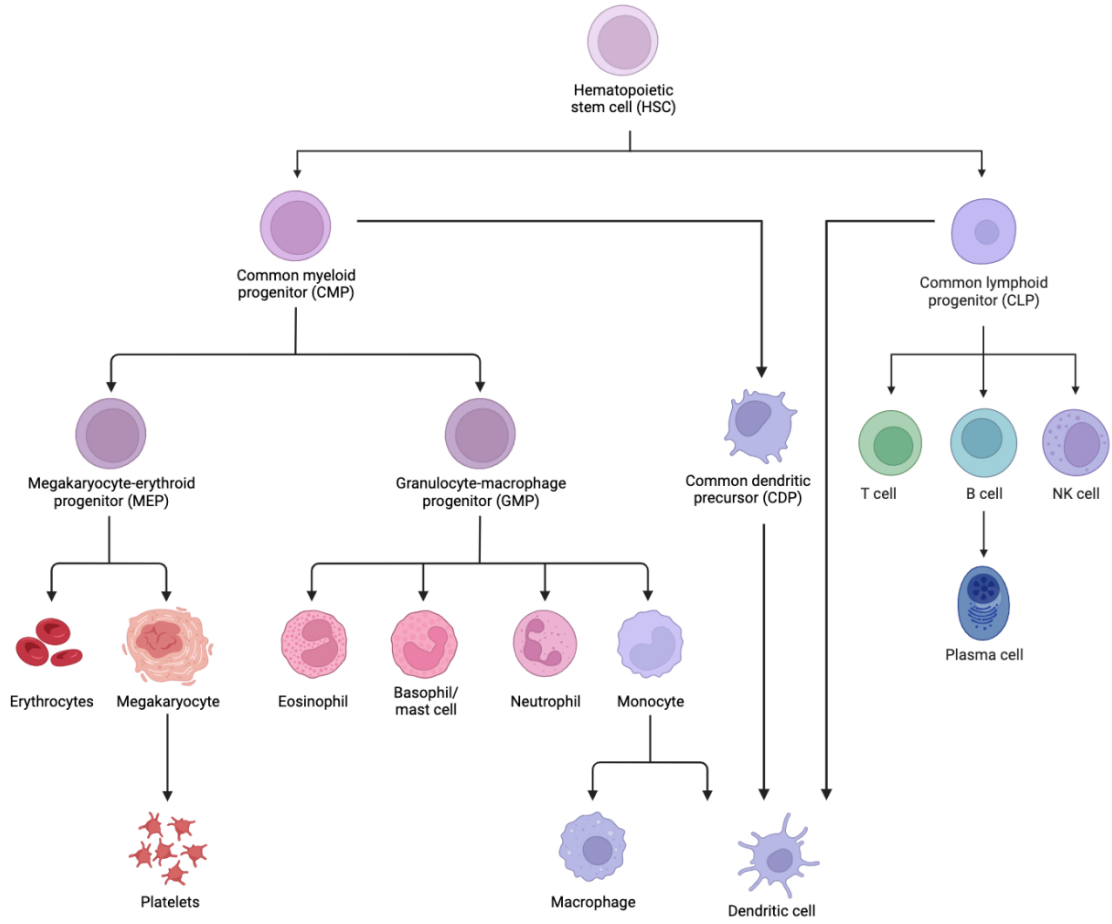

Figure 1.3. Schematic of haematopoietic lineage development. Flow chart showing progression of HSCs to immune progenitors (CMP and CLP) through to mature immune populations. Adapted from "Differentiation of Hematopoietic Stem Cells: Myeloid Lineage", by Biorender.com (2023). Retrieved from https://app.biorender.com/biorender-templates.

1.2.3. Anti-tumourigenic immune responses

Immune-mediated suppression of cancer is a highly coordinated process encompassing the innate and adaptive immune system. Control of these processes and ensuring their proper function is a major aim within cancer research. Enhanced pro-inflammatory immune activation associated with response to therapy and beneficial long-term outcomes(*119, 120*), however control over the myriad of cell types contributing to tumour immunity has proven difficult(*121, 122*). For future success in the immunomodulation of cancer, understanding of the fundamental mechanisms of the tumour immune response is vital to enable effective therapy development.

1.2.3.1. The innate response: Dendritic cells and macrophages

As cancerous cells develop into tumours, they initially meet the responders of the innate immune system. Whilst many innate responses are not beneficial (see section 1.2.4.1. and 1.2.4.2.), the role of inflammatory macrophages and dendritic cells is key in supressing tumour development.

Tumour associated macrophages (TAMs) are broadly characterised into two subtypes, pro-inflammatory 'M1' macrophages and anti-inflammatory 'M2' macrophages. Although this classical description of macrophages is now appreciated to be overly simplistic and unreflective of the nuanced roles of macrophage subsets(*123-125*), it is a useful paradigm through which to explore the opposing function of macrophages during tumourigenesis (immunosuppressive macrophages in cancer are described in section 1.2.4.2.). M1-like macrophages are typically defined through the higher expression of distinct markers, such as MHCII and iNOS, and are associated with an enhanced phagocytic capability alongside presentation of tumour-associated antigens (TAA) to adaptive immune cells(*126*). Although the phagocytosis of tumour cells by TAMs is a relatively slow process(*126*), pre-clinical research has shown that targeting of inhibitory signal complexes (e.g., CD47/SIRPα) on TAMs can result in meaningful increases to tumour phagocytosis and overall outcomes(*127*). The repolarisation of suppressive M2-like macrophages to inflammatory M1-like macrophages is a major theme of TAM research, and has also shown promise preclinically(*128*), highlighting the important role of inflammatory TAMs in directly killing tumour cells and presenting TAA to adaptive cells.

The cross-presentation of TAA is particularly vital to the induction of cancer immunity, primarily because it is the backbone of the adaptive T cell response and long-lived cancer immunity. Although this process can be enhanced by inflammatory macrophages, it is the action of DCs that is considered most central to T cell priming(*129*). The role of cancer cell antigen uptake is highly specialised even among DCs, with type I cDCs (cDC1) having the major role(*130*). These cDC1 cells are demarcated by the expression of CD103 and are described as 'migratory', reflecting their ability to travel from inflammatory tissues to secondary lymphoid organs(*131*). In the context of cancer cDC1 cells typically accumulate within tumours and sample TAA from dead tumour cells. Upon the loading of TAA to the DC cell surface, a programme of DC 'maturation' occurs involving the expression of T cell co-stimulatory factors (e.g.,

CD80/CD86), secretion of inflammatory cytokines (IL-12), and upregulation of the migratory chemokine receptor CCR7 (enabling CCR7-dependent migration)(*132*). The cDC1 cells then migrate to the resident tumour draining lymph node, where they cross-present TAA to antigen naïve T cells, sparking T cell polarisation, migration, and anti-tumour activation(*116*) (Figure 1.4). Binding of co-stimulatory CD80/CD86 to T cell CD28/CTLA-4 is vital for enhanced T cell activation(*133, 134*), as well as the cDC1 secretion of IL-12 inducing the cytotoxic differentiation of $CD8^+$ T cells and T helper cells to inflammatory subtypes(*135-137*) (Figure 1.5). Seminal research has further indicated that $CD103^+$ cDC1 cells could be responsible for an amount of constitutive priming from within the tumour microenvironment (TME) of more mature T cells, being the only DC subset seemingly capable of this action(*138*). From the same study, analysis from The Cancer Genome Atlas database highlighted that the $CD103^+/CD103^-$ gene ratio correlates strongly with increased patient survival across 12 tumour types, reinforcing the relevance of cDC1 cells to robust tumour immunity(*138*).

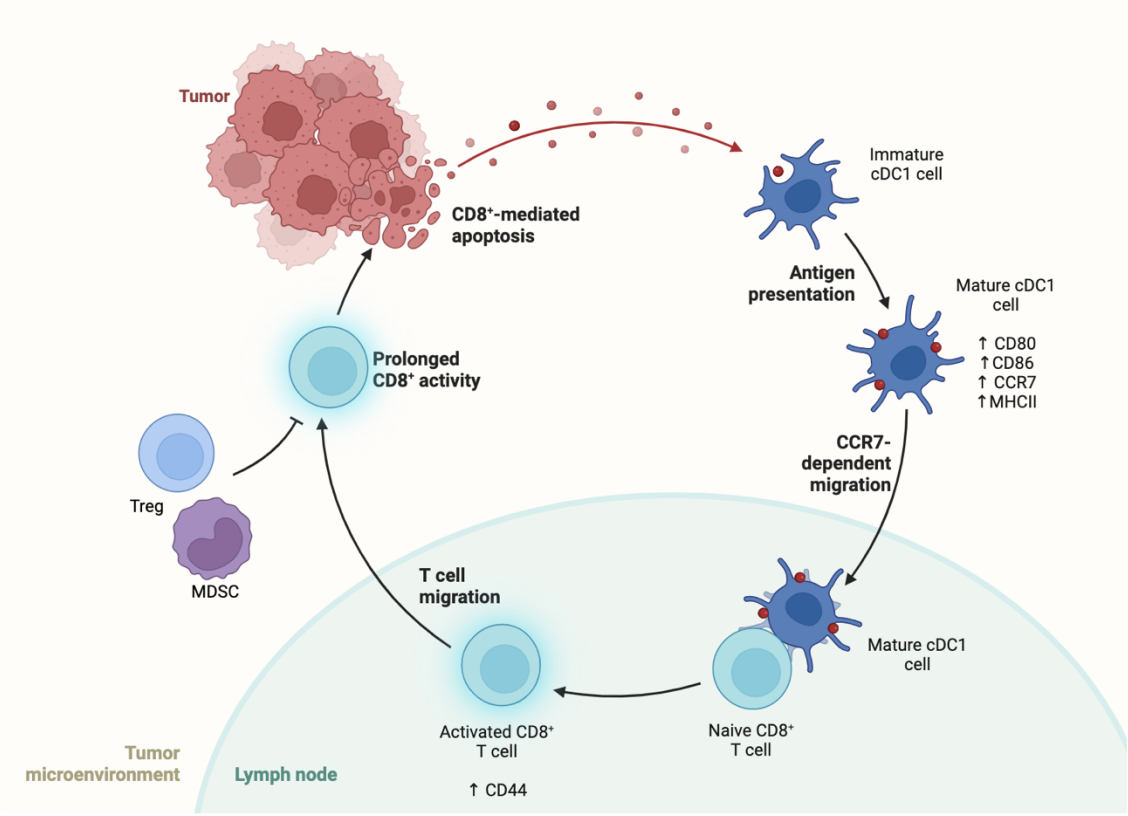

Figure 1.4. Dendritic cell priming of CD8⁺ T cell anti-tumour immunity. Immature cDC1 cells sample tumour-associated antigen from dead cells and undergo a programme of maturation, with enhanced expression of several activation factors. Mature cDC1 cells then undertake CCR7-dependent migration to the local tumour draining lymph node, where they cross present antigen and activation signals (CD80/CD86) to naïve $CD8^+$ T cells. Activated $CD8^+$ T cells migrate to the primary tumour and release cytotoxic effectors to induce tumour cell apoptosis. Adapted from "Tumor-Specific T Cell Induction and Function", by Biorender.com (2023). Retrieved from https://app.biorender.com/biorender-templates.

In addition to the central role of cDC1 cells, cDC2 cells are now also understood to be capable of uptake and presentation of TAA, mediating a T helper cell-dependent anti-tumourigenic effect(*139*). This effect was however dependent on the depletion of regulatory T cells (summarised in section 1.2.4.3) and suggests a more nuanced or limited role of cDC2 cells in tumour immunity. Although it is broadly accepted that cDC2 cells are the main primers of $CD4^+$ T helper cells, research has shown that cDC1 cells have a higher expression of T helper specific MHCII-restricted antigens than cDC2 cells(*140*), suggesting that cDC1 cells may still dominate in this context.

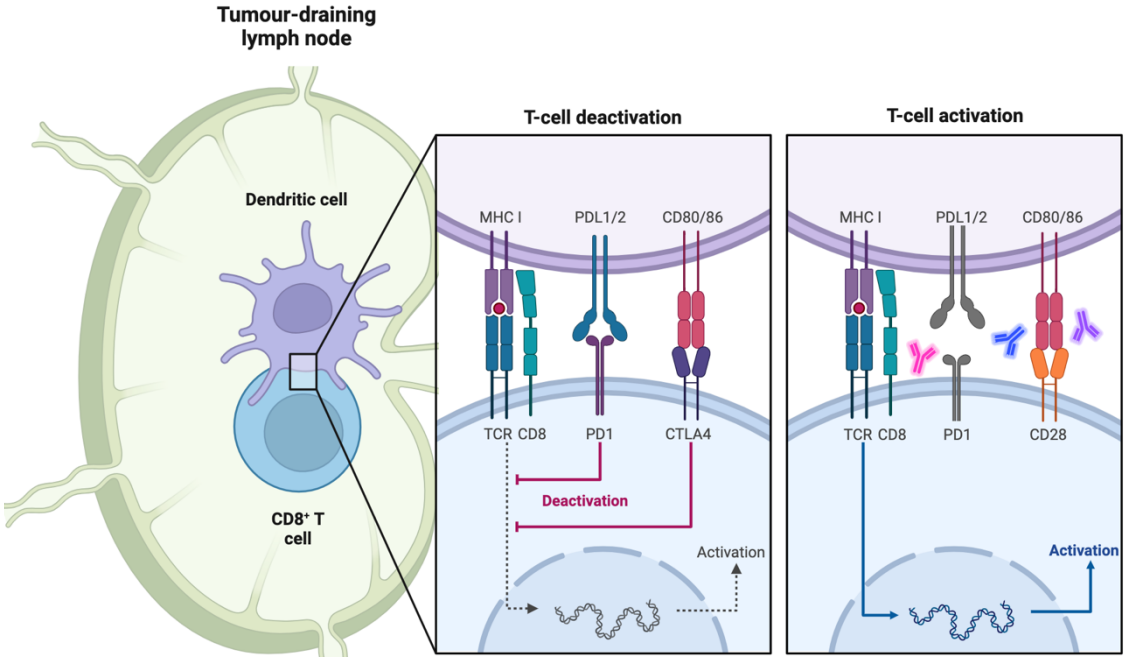

Figure 1.5. The presence of dendritic cell co-stimulatory receptors dictates effective T cell activation. $CD8^+$ T cell activation is mediated by the expression of dendritic cell co-stimulatory receptors CD80/86, which bind to CD28 of T cells. Activation of the T cell receptor can be prevented by binding of inhibitory dendritic cell CD80/CD86 by T cell CTLA-4, which competitively inhibits CD28-dependent co-stimulation. Binding of inhibitory PD-L1 to T cell PD-1 receptor also causes a downregulation of T cell stimulation by dendritic cells. Adapted from "T-cell Deactivation vs. Activation", by Biorender.com (2023). Retrieved from https://app.biorender.com/biorender-templates.

1.2.3.2. The cytotoxic $CD8^+$ T cell response

$CD8^+$ T cells are perhaps the most powerful and ubiquitously potent anti-cancer immune effector populations. They form a key part of the adaptive immune response and are the foundation of most current approaches to cancer immunotherapy. Like most T cells, $CD8^+$ T cells are antigen restricted and are initially bystander cells lacking an inflammatory target(*141, 142*). Circulating and lymphoid-resident $CD8^+$ cells in this phase express L-selectin (CD62L), which allows their adhesion, rolling and extravasation from vasculature to inflammatory sites(*143*). In the context of the anti-cancer response, naïve $CD8^+$ T cells are generally primed in the tumour draining lymph nodes by migratory $CD103^+$ cDC1 cells through MHC class I (MHCI)(*99, 132*). Antigen loaded MHCI binds to the $CD8^+$ TCR, which uptakes the antigen and is co-stimulated by $CD8^+$-derived CD28 and DC-derived CD80/CD86 interactions. This stimulation of the TCR initiates an intracellular signalling cascade which induces $CD8^+$ proliferation and differentiation to an activated state. Activation of the TCR is correlated with the expression of CD44 and signals a shift to either a central memory ($CD8^+$ Tcm) or an effector memory ($CD8^+$ Tem) subset(*144*). $CD8^+$ Tcm cells are responsible for long-lived immunological memory and can remain in the circulatory system and lymphoid organs to proliferate producing more activated $CD8^+$ cells, whilst $CD8^+$ Tem cells are short-lived tissue resident populations which actively respond to inflammatory stimuli (demarcated by the loss of L-selectin)(*144*). Following antigen priming, $CD8^+$ Tem cells migrate from the lymph nodes to the TME where they initiate cytotoxic programmes against the tumour cells. The major mechanism for this is the cellular degranulation of proteolytic enzymes, such as perforin, to puncture the outer membrane of the cancer cells, and granzymes (e.g., granzyme B), to cytolytically cleave the intracellular contents and ultimately kill the target cells(*145*). An additional mechanism for $CD8^+$ Tem-mediated tumour apoptosis is the activation of tumour cell FasL, which results in

cytochrome *c*-dependent caspase production and apoptosis(*146*). The direct cytotoxic activity is not the only mechanism of $CD8^+$ Tem cells, as they also release pro-inflammatory cytokines such as IFNγ and TNFα to stimulate M1-like macrophages to phagocytose tumour cells and cross-present more TAA(*147*).

Although this system has been demonstrated to be immensely powerful in the destruction of tumours, in-built homeostatic mechanisms (termed 'immune checkpoints') exist to limit the inflammatory response of $CD8^+$ cells and prevent the onset of autoimmunity(*148*). Whilst prevention of excess inflammation is important upon the clearance of the cancer, tumour cells can adopt theses pathways to prevent a complete immunological response (Figure 1.6). The first of these checkpoints, CTLA-4, was discovered in seminal work by Krummel and Allison(1995)(*149*), and functions to competitively inhibit the binding of CD28 and thus prevent $CD8^+$ T cell co-stimulation and antigen-dependent activation. Another major checkpoint is the programmed death pathway, with the expression of the key receptor (PD-1) being upregulated on activated $CD8^+$ T cells in response to sustained production of IFNγ(*150*). PD-1 is bound by the programmed-death ligand (PD-L1) which is produced by tumour and immune cells within the TME, causing the $CD8^+$ cells to undergo a process of 'exhaustion' (a decline in cytotoxic effector production until eventual cell apoptosis)(*151*). Other negative regulators of $CD8^+$ function have been discovered more recently, including LAG-3, TIGIT, and TIM-4, sparking a major step change in immuno-oncology to focus on the prevention of T cell exhaustion(*152*) (see section 1.2.5.1. for immune checkpoint inhibition therapy).

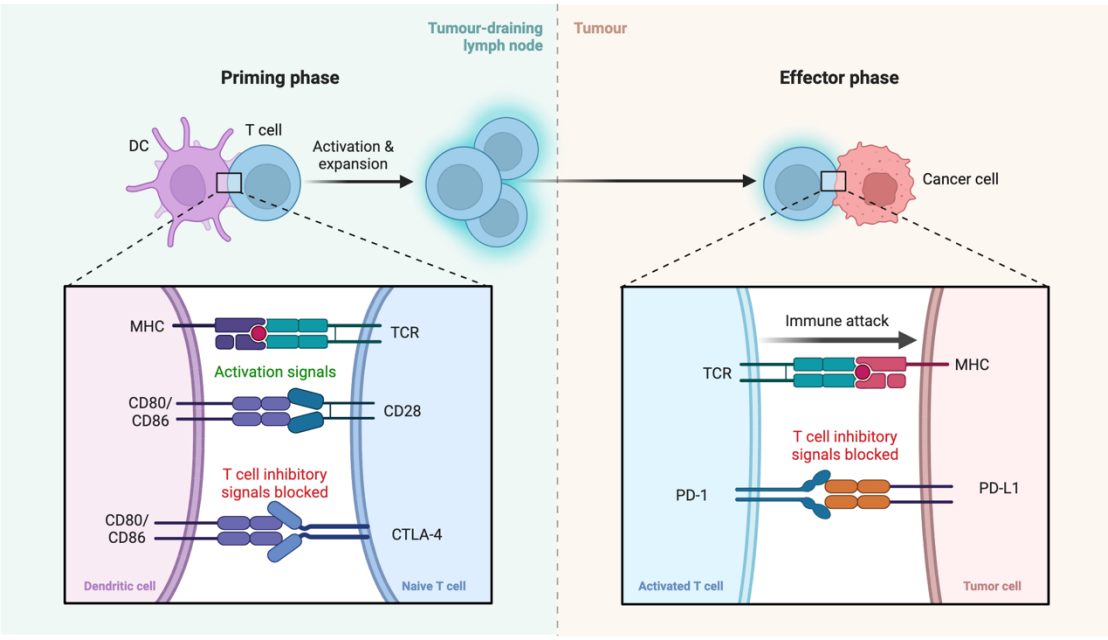

Figure 1.6. Immune checkpoints operate at several stages of the anti-tumour immune response to enable cancer immune evasion. In the antigen priming phase of the tumour immune response, T cell CTLA-4 is the dominant immune checkpoint which binds to dendritic cell CD80/CD86 to prevent CD28-dependent T cell co-stimulation. Within peripheral tissues, the PD-1 immune checkpoint becomes more dominant, as tumour cell and tumour microenvironment secreted PD-L1 binds to T cell PD-1 receptor to downregulate cytotoxic effector release, promoting a state a T cell exhaustion and initiate apoptosis. Adapted from "Blockade of CTLA-4 or PD-1 Signalling in Tumor Immunotherapy", by Biorender.com (2023). Retrieved from https://app.biorender.com/biorender-templates

1.2.3.3. T helper cells

The activity of T helper cells has historically been considered complementary to that of $CD8^+$ T cells but is now appreciated to encompass a broader range of tumour targeting functions. T helper cells can be categorised into various subsets depending on their effector function release, dictated during thymic development(*153*) (Figure 1.7). T helper cells are primed with TAA in a very similar fashion to $CD8^+$ T cells, with the exception that the cDC2 cell subset appears to play a more prominent role in lymph node antigen priming. The T helper 1 (Th1) subset are particularly important for cancer, as they produce high levels of pro-inflammatory cytokines such as IFNγ and TNFα and enhance the downstream effector function of $CD8^+$ T cells through numerous mechanisms(*154*). Within primary tumours, activated T helper cells can enhance and prolong the activation of $CD8^+$ T cells through the release of IL-2, which binds IL-2 receptor (CD25) and enhances $CD8^+$ proliferation(*155*). In the lymph nodes, T helper cells can function to increase $CD8^+$ T cell priming by DCs by co-operatively binding and co-stimulating the antigen presenting cell(*156*). This typically occurs through presentation of CD40 ligand to DC CD40, which upregulates the expression of $CD8^+$-promoting co-stimulatory components and the secretion of IL-12, enhancing CD8 memory and effector differentiation(*155*). CD40 expression has dual anti-tumour functionality here, as it also stimulates the differentiation of B cells into the active plasma subtype, whose abundance correlates with the magnitude of serum antibodies against tumour antigens(*157, 158*). Completely differentiated Th1 cells within the TME further exert anti-tumourigenic function, as their secretion of these key cytokines can function to directly stress and apoptose tumour cells, as well as indirectly enhancing the activity of anti-tumour M1-like macrophages and cDCs(*154, 159*).

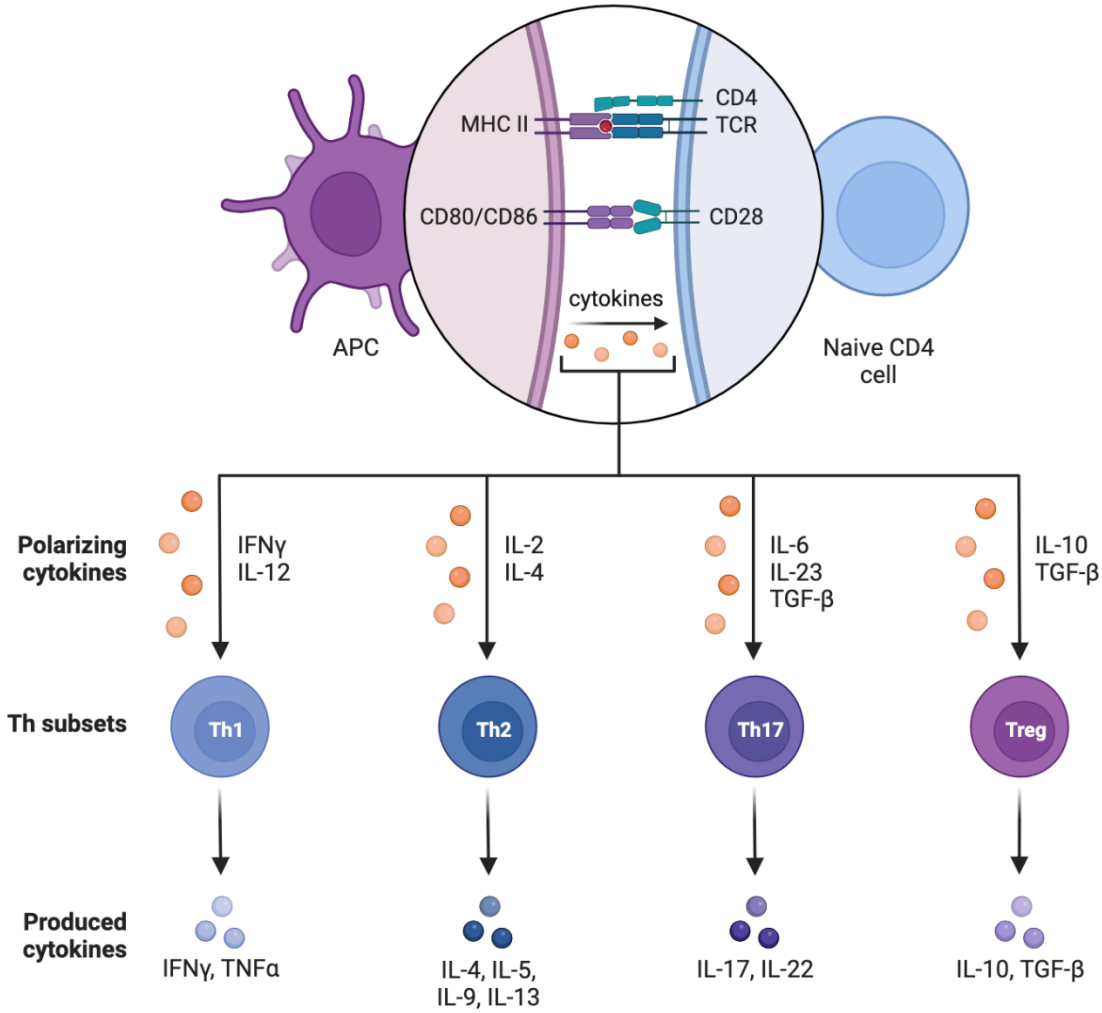

Figure 1.7. CD4⁺ T helper cell differentiation. Flow chart showing antigen presenting cell (APC) priming of naïve CD4⁺ T helper cells with subset-dependent cytokine gradients, causing differential T helper differentiation to the Th1, Th2, Th17 and Treg subtypes. Adapted from "T cell activation and differentiation", by Biorender.com (2023). Retrieved from https://app.biorender.com/biorender-templates

The role of other T helper subsets is not as well studied or clearly defined as that of Th1 cells, although Th2 cells have also been associated with influence over cancer progression(*160*). Th2 cells are known to secrete IL-4, IL-5, and IL-10, associated with the immunosuppression of inflammatory effectors cells and tissue remodelling (e.g., induction of tumour angiogenesis)(*160, 161*). Some research has indicated that elevated levels of these Th2 cytokines results in the accumulation of immunosuppressive M2-like macrophages, mast cells, and eosinophils via an upregulation of TGF-β signalling(*162*). Clinical associations have shown that a higher

Th1/Th2 ratio is correlated with better outcomes in luminal breast cancer patients but worse outcomes for triple negative patients, suggesting a context dependent role for the subsets(*163*). Recent approaches have even attempted to weaponise Th2 cells specifically, with Liu et al.(*164*), demonstrating that inhibition of TGF-β signalling in Th2 cells induced a protective restoration of leaky vasculature, inhibition of tumour angiogenesis, and resultant induction of tumour cell hypoxia and death. With such clear mechanistic differences between T helper subsets, proper characterisation of the T helper immune compartment is essential for concrete conclusions on T helper function to be drawn.

1.2.3.4. Natural killer cells

NK cells are innate immune cells descended from the lymphoid cell lineage, termed innate lymphoid cells. NK cells are the dominant effector population of this lineage and predominantly inhabit the circulatory system and immune organs (spleen and bone marrow) prior to an inflammatory challenge, where they infiltrate into inflammatory tissues in response to chemokine signals (e.g., CXCL16)(*165*). Effector NK cells have the unusual properties of sharing the cytolytic properties of $CD8^+$ and Th1 cells, whilst being non-antigen-specific innate responders. Through a set of NK-specific receptors, such as the NK cell activating receptor (NKG2D) and natural cytotoxicity receptors (NCRs), NK cells can recognise and kill cells with downregulated MHCI (preventing immune evasion) and opsonised antibodies on their surface(*166-168*). In the context of tumours NK cells induce tumour cell death through $CD8^+$ T cell-like mechanisms, releasing proteolytic enzymes (e.g., granzyme B) from cytolytic lysosomes and expressing membrane-bound FasL to induce TRAIL-dependent apoptosis(*169*). Like anti-tumour T cells, NK cells also produce high levels of inflammatory IFNγ and TNFα to boost CD8 T cell responses(*170*), as well as producing high levels of cytokines (CCL3, CCL4, and CCL5) to boost complementary adaptive and innate immune infiltration(*171*). High levels of NK infiltration in primary tumours have correlated with better outcomes and survival across several cancers, such as breast(*172*), renal(*173*), and head and neck(*174*), reinforcing the strong pre-clinical evidence of protective effects of NK cells. Although most cancer immunotherapy research has focused on the $CD8^+$ paradigm, innovate therapeutic approaches are now exploring the use of NK cells has an alternative and complementary target (outlined more in section 1.2.5.).

1.2.4. Pro-tumourigenic immune responses

Where the immune system functions properly, cancer should not develop. The requirement of cancer cells to mutate to acquire ability for perpetual self-renewal results in the production of new antigens (neo-antigens), which should be recognised by the host innate immune system (particularly macrophages and dendritic cells). These initial innate responders should not only begin the process of tumour cell phagocytosis, but also present the tumour-specific neo-antigens to inflammatory T cell effectors to induce immune mediated destruction and long-lived immunity against recurrence. However, a range of factors within the TME secreted from a range of cell types (e.g., other immune cells, tumour cells, and stromal cells) coordinate to supress the pro-inflammatory anti-cancer responses (outlined in section 1.2.3.).

1.2.4.1. Myeloid-derived suppressor cells

Myeloid-derived suppressor cells (MDSCs) are perhaps the most quintessential immunosuppressive immune cells operating within the TME. These myeloid infiltrating cells encompass a mixture of innate cells, such as monocytes, neutrophils, and poorly differentiated granulocytes, and collectively function to secrete inhibitory signals to anti-tumourigenic responders(*175*). MDSCs are broadly split across two major groups of monocytic (M-MDSCs) and granulocytic (G-MDSCs) cells, which describe monocyte-like and neutrophil-like cells respectively(*176*). The differing morphology and originating cell type does confer slightly different functions and effector release from these subpopulations, but both broadly act to supress inflammatory responses. The term MDSC can be used to define the action of pathological monocytes and neutrophils(*177*). In contrast to their usual acute stimulation by PAMPs and DAMPs outlined in section 1.2.1., MDSCs are typically stimulated by a more sustained signalling from growth factors and cytokines from chronically inflamed milieu (e.g., tumours)(*178*). Examples of these signalling factors include granulocyte-macrophage colony stimulating factor (GM-CSF), vascular endothelial growth factor (VEGF), IL-6, IL-1β, adenosine, and HIF1α(*178*).

As previously mentioned, the defining feature of MDSCs is the suppression of adaptive T cells. The mechanisms for this are varied, occurring both directly and indirectly. MDSCs are known to produce high levels of reactive nitric oxide (NO) species through inducible nitric oxide synthase (iNOS), with the resulting NO responsible for direct

inhibition of proliferation and induction of apoptosis in T cells and DCs(*179, 180*). Production of another NO intermediate called peroxynitrite (PNT) also acts directly on T cells, nitrating the TCR complex and impairing antigen response and cell proliferation(*181*). Indirectly, MDSCs decrease metabolites involved in potentiating T cell function, such as L-arginine and tryptophan, through the secretion of degrading enzymes arginase 1 (ARG1) and indoleamine 2, 3-dioxygenase (IDO)(*182*). MDSC enzyme production can also impede proper trafficking of naïve T cells to antigen priming sites, as the production of ADAM17 enzyme cleaves CD62L and thus prevent cell adhesion and extravasation(*183*). By expressing high levels of PD-L1(*184, 185*) and in some cases CTLA-4(*186*), MDSCs co-opt immune checkpoint circuits to induce inflammatory T cell apoptosis, which is compounded by the production of potent immunosuppressive cytokines IL-10 and TGF-β(*187*). The inflammatory T cell suppression induced by IL-10 for instance is also associated with an induction of T regulatory (Treg) cells (described in section 1.2.4.3.), which are additionally recruited by MDSC IL-10, CCR5 binding ligands, and cell surface CD40 (which binds the Treg cells to increase their function)(*188-190*). In addition to suppressive effects on $CD8^+$ and Th1 cells, MDSCs have also been shown to inhibit innate anti-tumour responders. NK cell and DC inhibition is obtained through similar NO-dependent apoptosis mechanisms(*180, 191*), as well as the production of TGF-β1 which downregulates NKG2D expression and NK cell effector functionality(*192*). Correlating with this extensive mechanistic work, is the inverse relationship between MDSCs and inflammatory T cell(*193*), NK cell(*194*) and DC(*195, 196*) activity and downstream clinical outcomes. Overall, the mechanisms of MDSC-induced suppression of anti-tumour responses are varied and potent, presenting a major challenge to the induction of durable immunological responses and response to cancer immunotherapy in highly MDSC-infiltrated tumours (such as pancreatic ductal adenocarcinoma).

1.2.4.2. Immunosuppressive macrophages

Although some inflammatory TAMs (M1-like subsets) can be protective in anti-tumour immunity (outlined in section 1.2.3.1), most TAMs are considered immunosuppressive and negative prognostic indicators of clinical outcomes. Although under normal conditions, tissue-resident macrophages are derived from the embryonic yolk sac rather than from a systemic pool of precursors, under the pathological conditions of tumour formation, TAM accumulation appears to be dependent on differentiation from bone marrow-derived monocytes and M-MDSCs in response to the tumour chemokine

milieu. Unlike their inflammatory counterparts M2-like macrophages are defined by the production of a host of immunosuppressive cytokines, such as IL-10 and IL-1β, as well as enzymes and growth factors like matrix metalloproteinase (MMP) and VEGF(*197*). Acting concordantly, these factors function to reduce local inflammatory responses and increase tissue remodelling through angiogenesis and extracellular matrix (ECM) metabolism(*197*). These processes are particularly beneficial in a wound healing context, however cancer is famously described as a 'wound that never heals'(*198*) and thus such mechanisms only contribute to further pathology.

In a very direct pro-tumourigenic TAM mechanism, M2-like macrophages are known to secrete growth factors used by tumour cells to increase proliferative responses, such as epidermal growth factor (EGF), platelet-derived growth factor (PDGF), and epithelial growth ligands of the factor receptor (EGFR)(*199*). Migratory metastatic responses are also directly influenced by immunosuppressive TAMs, as the release of matrix degrading enzymes (MMPs, serine proteases, cathepsins) damages basement membrane boundary of tumour endothelial cells, encouraging the migration, vascular intravasation, and metastasis of tumour cells(*126*). Many of the cytokines, growth factors, and enzymes described here are also important in the promotion of angiogenesis, meaning TAM accumulation often precludes enhanced tumour vascularisation and growth(*200*). In purely immunological terms, M2-like TAMs inhibit adaptive T cell responses through very similar mechanisms to MDSCs and are associated with a decreased infiltrate of T cells in patients(*201, 202*). The release of high IL-10 for example, functions to directly reduce inflammatory T cell proliferation whilst simultaneously inducing the differentiation and activation of Treg cells(*202, 203*). By producing the similar reactive NO species to MDSCs through iNOS, M2-like macrophages also metabolise key $CD8^+$-promoting metabolites like L-arginine(*204*). Taken together, immunosuppressive M2-like TAMs exert a range of pro-tumourigenic functions through direct and indirect mechanisms, targeting tumour cells, stromal cells, and immune cells to enhance cancer progression. Targeting M2-like TAMs and inducing their repolarisation to inflammatory M1-like TAMs is seen as a compelling potential therapeutic axis.

1.2.4.3. T regulatory cells

Treg cells represent the dominant immunosuppressive T cell subset. They are defined by expression of CD4, CD25 and the master transcriptional regulator forkhead box protein P3 (FOXP3), being vital for the prevention of autoimmunity onset(*205*). During

an inflammatory challenge, such as cancer, Treg cells migrate into tissues and supress the activity of the dominant inflammatory cell types ($CD8^+$ T cells, Th1 cells, NK cells etc.). Treg cells can be both antigen and non-antigen specific(*206*), with each subset functioning slightly differently (antigen restricted Treg cells are thought to have superior immunosuppressive characteristics). In contrast to inflammatory $CD8^+$ and T helper cells, Treg cells recognise 'self' antigens and function in a variety of ways to supress downstream adaptive responses. This poses a major problem in cancer, as cancer cells are derived from healthy host cells, which despite the acquired presence of tumour-associated neoantigens, contain high levels of 'self' antigens recognised by the Treg cells(*207*). Treg cells are also recruited into tumours with relatively high efficiency through a multitude of chemokine gradients, such as Treg CCR4 recognition of CCL17 and CCL22(*208*). The high infiltrate of Treg cells in the TME is associated with a reduced infiltration of $CD8^+$ T cells and poor prognoses(*209*).

Upon stimulation of the TCR of Tregs with tumour-associated 'self' antigens, in addition to other TCR stimulating immunosuppressive signals (e.g., TGF-β), Tregs undergo a programme of proliferation and immunosuppressive activation(*210*). Within the TME, high expression of CD25 (IL-2 receptor) and negligible *de novo* production of IL-2 by Tregs enables them to sequester locally available IL-2, which is required for inflammatory $CD8^+$ T cell proliferation and longevity(*211*). Concurrently, Treg cells produce high levels of anti-inflammatory IL-10 and TGF-β to downregulate cytotoxic effector release from inflammatory cells(*211, 212*). Treg cells themselves produce cytotoxic granzymes and perforins, but these effectors are targeted at host $CD8^+$ and T helper cells to induce apoptosis and further halt inflammatory responses(*213*). In addition to directly inhibitory effects on other T cells, Tregs are also potent inhibitors of the function of upstream APCs. One mechanism for this is Treg expression of the immune checkpoint CTLA-4, which competitively binds DC CD80/CD86 and thus inhibits T cell co-stimulation during antigen priming(*214*). This effect is further bolstered by a process of trogocytosis, where CTLA-4 bound CD80/CD86 is physically cleaved from the surface of the DCs(*215*). A reduction in DC co-stimulatory signalling decreases the number of total tumour-antigen specific T cells trafficked to primary tumours, as well as decreasing the activity of the remaining inflammatory T cells which do successfully reach the tumour(*216*). These key interactions between CTLA-4 and DC CD80/CD86 have further downstream consequences, as they trigger the production of IDO enzyme by DCs, which causes degradation of local tryptophan needed by T cells to maintain functionality(*217*). When Treg activity is combined with

the array of immunosuppressive functions of MDSCs and M2-like macrophages, the local TME can rapidly become a hostile environment to the key anti-tumour effector populations, representing a key reason for the failure of immunosurveillance to curtail the progression of cancer in patients.

1.2.4.4. The immunosuppressive tumour microenvironment

Although much of the focus of cancer immunosuppression has thus far focused on the roles of individual subpopulations of immune cells, the action of the non-immune compartment of the TME plays a vital role in potentiating the previously outlined immunosuppressive responses, as well as contributing entirely unique anti-inflammatory mechanisms. A major contributor to this phenomenon is the action of tumour cells themselves. Crosstalk between cancerous and non-cancerous host cells form a cornerstone of tumourigenesis, whereby aberrant tumour cells (through physical interactions and secreted intermediaries) remodel the local TME to enable further growth, increasing ECM deposition, promotion of angiogenesis and suppression of anti-tumour immunity (Figure 1.8)(*218*). Many mechanisms for tumour cell induced immunosuppression have been identified, with some being specific to individual cancer indications. Perhaps the most well characterised of these mechanisms is tumour cell induction of the PD-1 exhaustion pathway, whereby tumour cells express PD-L1 to downregulate inflammatory $CD8^+$ and Th1 responses(*219*). Additionally, the process of tumour cell surface glycan sialylation (the addition of sialic acid residues to surface glycans) enables physical crosstalk with many immune cells through sialic acid-binding immunoglobulin-type lectins (Siglecs), enabling immune evasion responses(*220*). For example, the binding of TAMs expressing singlec-9 to tumour-bound ligand (e.g., sialylated mucin-1), polarises the TAM to an M2-like phenotype(*221*). On the inflammatory side of the immune system, binding of tumour sialic acid residues to NK cell singlec-7 and singlec-9 inhibits their cytotoxic effector release(*222*). Tumour cell-TAM interactions are particularly well studied, with tumour cells known to promote pro-tumourigenic TAM function through the secretion of sonic hedgehog(*223*), kynurenine(*224*), and osteopontin(*225*). Tumour cell secreted products are also known to directly supress $CD8^+$ T cell responses, with tumour-derived TGF-β binding to $CD8^+$ cells causing the activation of Smad/ATF1 and the suppression of cytotoxic effectors (IFNγ, granzyme B, FasL etc.)(*226*). Another direct example of this is the secretion of cathepsins by melanoma cells for the degradation of cytotoxic perforin from $CD8^+$ T cells, preventing granzyme B-induced cell death(*227*). An emerging mechanism of

tumour-immune cross talk are tumour cell extracellular vesicles (EVs), with pre-clinical evidence showing that EVs can facilitate oncogenic signals locally and systemically(*228*). For example, melanoma EVs can traffic from the primary tumour to the bone marrow to induce the immunosuppressive differentiation of bone marrow myeloid progenitor cells, causing enhanced downstream metastasis(*229*). Though there are far too many mechanisms of tumour cell-induced immunosuppression to describe here, it is clear that tumour cells play a major role in contributing to the anti-inflammatory TME.

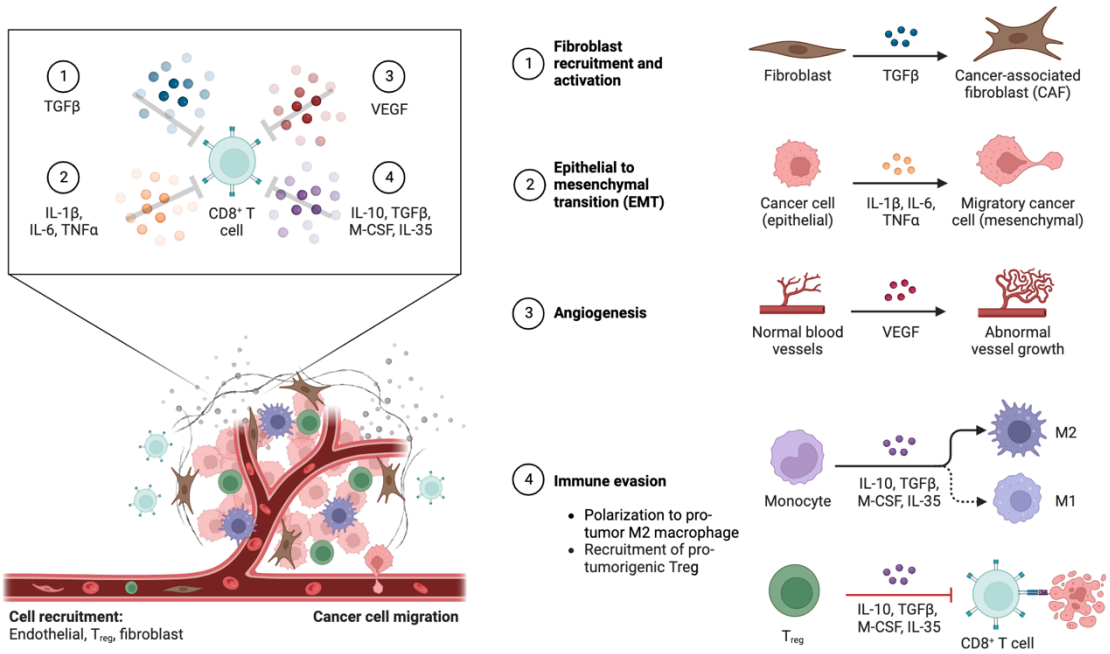

Figure 1.8. Cells of the tumour microenvironment contribute to anti-tumour immune evasion. Various immune and non-immune cells secrete immunosuppressive cytokines, chemokines, and growth factors to suppress the adaptive response. TGFβ from cancer associated fibroblasts (CAFs) increases the activity of myeloid derived suppressor cells (MDSCs) and tumour-associated macrophages (TAMs) whilst decreasing the proliferation and activation of T helper and $CD8^+$ T cells. Cancer cells respond to various fibrotic cytokines (e.g., IL-1b) to increase their mesenchymal metastatic phenotypes, whilst secreting VEGF to enhance angiogenesis. Treg, MDSCs, and TAMs also function to secrete directly and indirectly $CD8^+$-suppressive cytokines (e.g., IL-10). Adapted from "The Tumor Microenvironment: Overview of Cancer-Associated Changes", by Biorender.com (2023). Retrieved from https://app.biorender.com/biorender-templates.

Outside of tumour cells, another major cell type of the TME which has received significant attention over recent years are cancer-associated fibroblasts (CAFs). CAFs are an umbrella term for fibrotic cells of various origins, including tissue-resident fibroblasts, adipocytes, stellate cells, and bone marrow-derived mesenchymal stem cells(*230*). The heterogeneity within CAFs makes specific mechanistic characterisation challenging, although they are broadly considered pro-tumourigenic through their fibrotic ECM deposition and various immunosuppressive functions(*230*). CAFs can become activated within the TME through a variety of tumour cell-dependent signals, such as growth factor secretion (TGF-β, PDGF, fibroblast-derived growth factor etc.), tumour cell EVs, and tumour cell-derived DAMPs(*231*). CAFs secrete a number of directly anti-inflammatory cytokines and chemokines to bolster anti-inflammatory myeloid cells, such as the release of CXCL12 for the recruitment of MDSCs(*232*) and IL-6 for the suppressive activation of regulatory DCs(*233*). The high infiltration of CAFs in primary tumour correlates with low $CD8^+$ T cells and a poor prognosis in cancer patients(*234*), with the links to adaptive immune system being direct in addition to the innate immune modulation. One mechanism for this is CAF expression of MHCI complexes to allow direct binding to intra-tumoural $CD8^+$ T cells, whereby CAF co-expression of FasL can directly induce $CD8^+$ cell apoptosis(*235*). CAFs can also express conventional immune checkpoint ligands (PD-L1 and PD-L2) to further induce inflammatory exhaustion(*236, 237*), whilst the increase ECM deposition by CAFs contributes a physical barrier to $CD8^+$ cell permeation to the core of tumours (termed 'immune exclusion')(*238*).

1.2.5. Cancer immunotherapy

The rise of immunotherapy, the concept of weaponising the host immune system against disease, has completely revolutionised the treatment of cancer. In recent decades, the clinical translation of immune checkpoint inhibitors (ICIs) and adoptive cell transfer immunotherapy has rejuvenated interest in therapeutically targeting anti-cancer immune cells. Remarkably, these therapies can successfully regress tumours in subsets of patients and obtain durable recurrence-free survival, however response rates remain low and restricted to specific tumour types(*239*). A major confounding factor for this is the complexity of the TME and the various subsets of immune cells introduced in section 1.2.3 and 1.2.4., which vary between individuals and collectively dictate immunotherapy clinical outcomes(*122*). The relative success of clinically approved approaches has highlighted the great potential and current challenges of

immunotherapy, demonstrating a need for new immunotherapy approaches which can complement and overcome resistance to current therapies. Although there are breakthrough immunotherapy approaches, namely DC-based cell therapies (cancer vaccines against personalised TAAs)(*240, 241*) and oncolytic virus therapies (which increase tumour secretion of TAA)(*242*), as well as traditionally used (but largely ineffective) recombinant cytokine therapies(*243*), the review herein will focus on the major clinically approved immunotherapies which have the most relevance for patients in the short-medium term.

1.2.5.1. Immune checkpoint inhibitors

The concept and mechanisms of immune checkpoints were described in section 1.2.3.2. and are a consistent theme of the core cancer immunology introduced in later sections. Briefly, immune checkpoints describe inhibitory mechanisms hardwired into the immune system which prevent the onset of excess inflammatory responses and autoimmunity(*244*). However, cancer cells, non-cancer cells of the TME, and anti-inflammatory immune cells converge during cancer progression to co-opt these inhibitory mechanisms and permit tumour immune evasion and cancerous growth(*244*). ICIs are typically monoclonal antibodies (mAbs) which deplete these inhibitory checkpoints to allow the enhancement of acute inflammation, 'releasing the brakes' on anti-tumour immunity(*151*). The common targets of ICIs are CTLA-4 (ipilimumab), PD-1 (pembrolizumab and nivolumab), and PD-L1 (Durvalumab), although depletion of novel therapeutic targets is also becoming more common (such as LAG-3, TIM-4, TIGIT). The first wave of ICIs entered the clinic in the 2010's, as ipilimumab, nivolumab, and pembrolizumab each demonstrated significantly enhanced patient survival compared to the previous standard of care chemotherapy regimens(*84-86*). More recent approaches and active trials are exploring combination approaches targeting multiple immune checkpoint simultaneously, such as the dual use of nivolumab with the LAG-3 inhibitor relatlimab, which increases overall survival and median progression free survival to 10.1 months from 4.6 months (from Nivolumab alone)(*87*). The combination of ipilimumab and nivolumab was the first ICI combination to be approved and also showed enhanced progression free survival than either monotherapy, although at the expense of more immune-related adverse events(*245*). Although ICIs are relatively well tolerated, common adverse events are typically excess inflammation of the gastrointestinal tract leading to diarrhoea or colitis, which can cause some patients to cease treatment(*245*).

The success of ICIs has now seen the therapy approved across various indications, such as non-small cell lung cancer (NSCLC), renal cell carcinoma, head and neck cancer, triple negative breast cancer and others(*246*), the efficacy is typically no better (often worse) when compared with melanoma, where 40-60% of patients do not respond (depending on the precise regime)(*247, 248*). Even where responses to ICIs do occur, most patients still die from their disease due to primary or acquired resistance(*248*). The dominant resistance to ICI is caused by the immunosuppressive responses of MDSCs, TAMs, Tregs and the non-immune cells of the TME(*122*) (reviewed extensively in section 1.2.4), but can also be caused by tumour intrinsic mechanisms. An example of this is the relative mutational burden of a given tumour type, whereby less mutated tumour types typically have lower expression of neoantigens for recognition by APCs, causing lower adaptive activation and inferior response to ICIs(*249*). Tumour cells can also downregulate neoantigen expression to achieve similar effects(*250*), as well as altering key signalling pathways(*251*) and metabolism(*252*) to acquire resistance to ICIs. Broader host factors also appear to play a role and predict ICI efficacy, with factors such as age, diet, gender hormone levels, and importantly, gut microbiome composition (reviewed in section 1.3.2.) all correlating with ICI response(*253, 254*).

1.2.5.2. Adoptive transfer immunotherapy

In addition to ICIs, the other major immunotherapy option which is approved and used clinically are adoptive transfer immunotherapies. These therapies involve the utilisation of autologous immune cells (usually T cells), which are isolated, expanded (with potential genetic manipulation) and reintroduced into patients for an enhancing immune targeting of tumour cells(*255*). The use of these techniques can be traced back to the 1980's(*256*), with modern approaches generating genetically modified tumour reactive T cells against an overexpressed tumour antigen(*257*). The two dominant types of genetic manipulations are chimeric antigen receptor (CAR)-T cells and TCR-engineered T cells. The basis of CAR T cell therapy is the CAR, whereby the normal TCR is engineered to include an extracellular domain of an antigen specific antibody alongside co-stimulatory factors (CD28)(*258*). This engineering enables specific T cell targeting of the tumour-specific antigen independently of MHCI-related co-stimulation from host cells, whilst retaining the core activity of the TCR and resulting anti-tumour cytotoxicity(*258*). Although the efficacy of CAR-T therapy has been inconstant in solid

tumour types, it has shown excellent efficacy in haematological tumours, with most approved CAR-T cell therapies targeting lymphoma with a CD19-targeting CAR(*259*). TCR-engineered T cell therapy follows a similar principal of CAR-T, but genetically transfers a TCR with its normal binding domain specific tumour-overexpressed antigen, rather than the attachment of a tumour-specific extracellular antibody domain(*260*). The result of this are tumour reactive T cells which are dependent on MHCI coactivation, so are considered lower risk of major off-target effects(*260*). Recent years have seen the development of adjacent approaches using CAR-NK cell therapy, involving the attachment of a tumour-specific antibody domain to the NK activating NKG2D receptor(*261*). Early results from phase I/II trials are showing promise in haematological malignancies, with a seemingly lower risk of overproduction of cytokines (cytokine storms)(*262*). Although adoptive transfer therapies generally work well and achieve complete responses in haematological malignancies, they do not work nearly as well in solid tumour types, are expensive, and require specialist manufacturing, making their broader translation difficult.

1.3. The role of gut bacteria in cancer progression and therapy

1.3.1. The gut microbiota: development and composition

The gut microbiota is a complex ecosystem home to some 100 trillion microorganisms, including bacteria, viruses, fungi, and protozoa(*263*). Numbers of these gut microbes rival the cells of the human body by 1.3x(*264*), and it follows that this vast community has a huge influence over human health. Bacteria are the most well-characterised modulators of human physiology within the gut microbiome, so will be the focus of the discussed literature. The complexity and scale of the human microbiota have historically made studying the system difficult. However, advancements of metagenomic and transcriptomic technologies (such as shotgun metagenomics) have made phylogenetic characterisation of individual microbiomes possible(*265*), allowing an unprecedented view into the species and even strain-level effects of the microbiota on human health. Use of metabolomic techniques (e.g. liquid-chromatography mass spectroscopy) has also allowed characterisation of some mechanisms behind these physiological changes to health, and the last 10-15 years of research has revealed systemic roles for the microbiota relating to metabolism, the immune system and cancer(*266*).

The microbiota contains a diverse community of bacteria. The dominant phyla are the *Firmicutes* and *Bacteroidetes*, whilst *Proteobacteria*, *Actinobacteria*, *Fusobacteria* and *Verrucomicrobia* also represent significant populations(*267*). Within these phyla, genera containing hundreds more species inhabit the various regions of the GI tract, extending from the duodenum to the base of the colon(*268*). Bacterial diversity is highly variable between individuals, and microbial composition of the microbiota is fundamentally determined by the environmental conditions (e.g. O_2 levels, pH, bile, pathogenesis etc)(*269*). Such environmental factors are in-turn influenced by age, diet, stress, and antimicrobial use, alongside an increasing list of other factors we are discovering to be crucial for the health of the microbiota(*269*). Variability within the microbiota is particularly apparent during development, where the dominant phyla of the microbiota shift in a predictable, age-dependent manner(*270*). The colonisation of the microbiota mostly occurs after birth, as the infant microbiota display low bacterial load and low microbial diversity. The first week post-birth is demarcated by the dominance of aerobic enterobacteria, enterococci and staphylococci, whilst other anaerobic species (e.g. *Bifidobacterium*) are not highly represented(*271*). A shift in conditions from aerobic to anaerobic, as well as the intake of breast milk, accompanies a change in bacterial diversity (at ~1 month of age) as *Bifidobacterium* and L*actobacillus* become dominant genera(*272, 273*). Relative abundance of bacteria shifts yet again upon the cessation of breastfeeding (weaning), as the intake of carbohydrates and fibre accompanies increased representation of *Firmicutes* and *Bacteroidetes*, and decreased levels of *Bifidobacterium(274, 275)*. Whilst these developmental changes in microbiota composition are considered natural and healthy, further bacterial variation can be driven by external factors and cause negative consequences to health(*276*). Examples here include the use of antibiotics, replacement of breast milk with formula-milk, or birth via caesarean (rather than vaginal delivery)(*276*).

1.3.2. The gut microbiota regulates human health

The gut microbiota, both collectively and on the single strain level, is vital for optimal host health. These effects can be local to the gastrointestinal tract (GIT) or systemic in nature, ranging from the programming of the immune system to core digestion and metabolism of nutrients.

Immune education and modulation

Human immune development and education occurs primarily during the neonatal period, with recent studies suggesting that bacterial colonisation and immune education during this critical window shape health and disease susceptibility into adulthood. The issue of initial microbial contact in humans is somewhat controversial, with some major studies indicating that these microbial interactions begin *in utero*, such as Rackaityte et al.(*277*), isolating *Micrococcaceae* and *Lactobacillaceae* from the foetal intestine which were able to supress *ex vivo* IFNγ production by T cells. Circumstantial evidence also exists from studies showing antigen primed DCs and memory T cells in the foetal intestine(*278*), whilst detection of microbial gene signatures in the placenta and amniotic fluid further supported the idea(*279, 280*). However, the presence of a placental microbiome has been largely dismissed due to apparent contamination and improper interrogation in low biomass microbiome studies(*281, 282*), and many doubt that microbial colonisation of infants does occur *in utero* in healthy individuals(*283*). Far more agreed upon however, is that initial microbial colonisation post birth initiated a vital chain of immunological events. This process begins in a birth-route dependent manner, whereby newborns are initially colonised by bacteria more dominated by *Bifidobacterium* (and fewer pathogenic *Enterococcus*, *Enterobacter*, and *Klebsiella* species) when delivered vaginally compared to Caesarian section (C-section), which is in turn associated with colonisation with skin and environmental species(*284*). C-section neonates broadly experience delayed microbial colonisation and lower microbiome diversity over the first years of life, resulting in an increased risk of inflammatory diseases in later life (such as allergies and asthma)(*284*). Feeding from breast milk is also vital during early life immune education and health, as maternal breast milk is known to contain crucial antibodies (IgA and IgG), cytokines, and nutrients. Maternal IgG and IgA have been shown to dampen inflammatory $CD4^+$ T helper cells for example(*285*), and can cross react with pathogens (e.g., *E. coli*) to prevent the premature onset of infection(*286*). Concurrently, the availability of the breast milk nutrient source encourages the proliferation of human milk oligosaccharide (HMO) metabolisers, such as *Bifidobacterium(287)*, which can in turn contribute to immune development by inducing the differentiation of Treg cells through HMO-metabolite release and direct bacteria-immune cell interactions(*288, 289*). The cells of the innate immune system are largely immature in neonates and require stimulation and maturation from beneficial bacterial species, such as the induction of DC antigen priming and maturation by

Lactobacillus(290, 291), with these processes vital for the prevention of infection (the major cause of infant mortality).

Aside from the initial development of the infant immune system, the microbiota has vital roles both locally and systemically in immune responses throughout life. These effects are commonly initiated by microbial activity within the microbiota, such as pathogenesis, metabolite production, and the expression of commensal surface antigens(*292*), which can cause profound immunological changes. The gut associated lymphoid tissue (GALT) is the major site of mucosal immune response (Figure 1.9)(*293*). Changes at the GALT dictate both the local immune response and the delivery of immune populations into the blood stream – representing one of the major effector mechanisms of host systemic changes. The major site of immune priming in the gut is the small intestine, where the GALT is comprised of the surface luminal epithelium and lamina propria, as well as antigen sampling lymphoid structures called payers patches (PPs). PPs can also be referred to as lymphoid follicles; this denotes the follicle-associated epithelium (FAE) which encases the outer layer of the structure(*294*). Within the FAE are specialised microfold cells (M cells), which function to transport antigens to the major APCs of the GIT, DCs and macrophages(*295*). DCs are primarily localised to the underlying sub-epithelial dome (SED), and migrate deeper-still during pathology and antigen sampling into the inter-follicular region (IFR)(*295*). The activity of the IFR can be thought of as a precursor of wider mucosal immune changes, harbouring naïve T and B cells which undergo clonal expansion upon DC-mediated antigen cross presentation(*296*). Antigen-presenting DCs, as well as expanded T- and B-cell populations, can then migrate out of the PPs through afferent lymph vessels into adipose-associated mesenteric lymph nodes (MLNs)(*297*). From here, mature (Ag-educated) lymphocytes are distributed back to the lamina propria (to modulate mucosal/local immune responses) and to the wider circulatory system (to modulate systemic immune responses) via the thoracic duct(*297*).

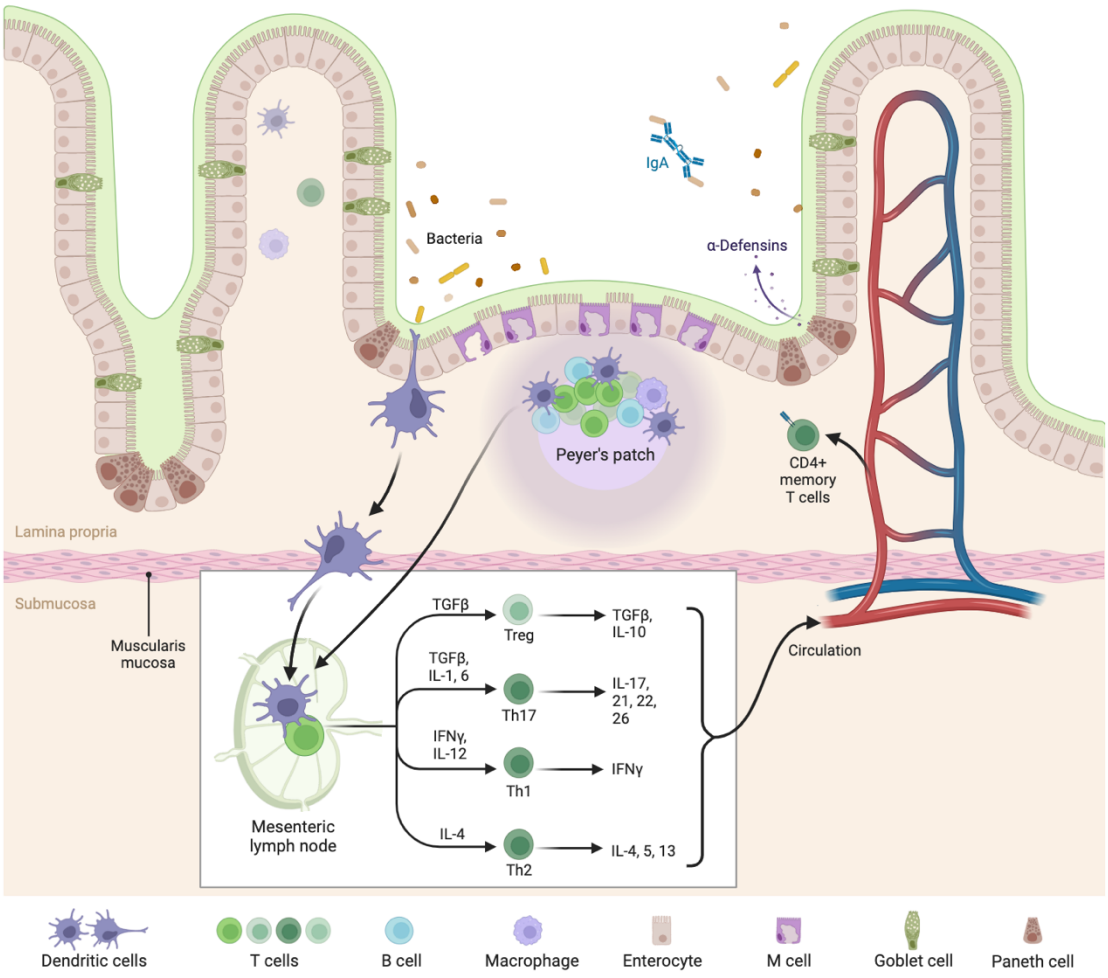

Figure 1.9. The structure function of the gut associated lymphoid tissue. Antigen (Ag) sampling occurs predominantly at microfold cells within the follicle associated epithelium of the Peyer's patches. Ags pass through the sub-epithelial dome (SED), where they are expressed up by dendritic cells, and promote expansion of immature T- and B-cell populations within draining mesenteric lymph nodes (MLNs) to enable an Ag-specific response. Mature lymphocytes travel through efferent lymphatics (the thoracic duct) into the blood stream, where they can return to the lamina propria (locally) or circulate systemically. Ag sampling can also occur through an alternative route directly across the epithelium via DCs, which instigate lymphocyte expansion at peripheral lymph nodes. Adapted from "Intestinal Immune System (Small Intestine)", by Biorender.com (2023). Retrieved from https://app.biorender.com/biorender-templates.

Metabolism

Perhaps the most apparent function of the gut microbiota is its role in nutrient metabolism. The digestion of carbohydrates, for example, is mostly enacted by resident *Bacteroidetes* (as well as some *Roseburia* and *Bifidobacterium*), and results in

the production SCFAs(*298*). The importance of SCFAs, such as acetate, propionate, and butyrate, to health and disease is well documented in the literature(*299-301*). These SCFAs can be viewed as 'active' metabolites of carbohydrate digestion, and can be used both as an energy source and in prevention of disease(*302*). A key example of this is butyrate, which is the primary energy source for luminal colonocytes whilst also having direct anti-inflammatory properties in the GIT(*303*). High levels of butyrate are associated with less severe IDB symptoms(*304*), and with the decreased accumulation of toxic metabolites such as D-lactate(*305*). Elsewhere, it is also known that acetate production by *Bifidobacterium* prevents enteric infections through inhibition of epithelial translocation of toxins (e.g. by enterohaemorrhagic *Escherichia coli*)(*306*). Outside of carbohydrate metabolism and SCFA production, the microbiota has defined roles in the metabolism of proteins, lipids, and dietary polyphenols, which themselves have important health consequences. In the context of protein metabolism, colonic bacteria convert amino acids into antimicrobial bacteriocins through the action of resident proteinases. Probiotic *Lactobacillus plantarum* convert host glutamate into γ-amino butyric acid (GABA) through the action of bacterial glutamate decarboxylase(*307*). Here, GABA acts as an indirect bacteriocin through its induction of host β-defensin-2 and filaggrin(*307*).

GI Barrier Maintenance

Maintenance of the luminal epithelial layer (and its overlying mucosa) is vital for local GI homeostasis. Specifically, a structurally compromised GI epithelium increases the exposure of sensitive underlying tissue to resident pathobionts, increasing the frequency of intestinal infection(*308*). A simultaneous consequence of a perturbed epithelium is disruption of surface mucosa, causing increased colonisation of pathogens and an exaggerated inflammatory response(*308*). Epithelial permeability is associated with a range of diseases, such as IBD, irritable bowel syndrome (IBS) and colon cancer(*309*). Specific members of the microbial community have emerged as being important in epithelium-protective processes, such as the development and preservation of epithelial goblet cells by *Bacteroides thetaiotaomicron*(*310*), or the prevention of epithelial apoptosis by *Lactobacillus rhamnosus*(*311*). A more general mechanism for the maintenance of the GI barrier function is the propagation of TLR2 signalling at mucosal tight junctions(*312*). This process is mediated by interactions between TLR2 and microbial cell wall peptidoglycan and promotes a healthy inflammatory response during pathogenic challenge(*312*).

Antimicrobial protection

As mentioned previously, the gut microbiota plays important roles in protecting from enteric infection. The mechanisms utilised here are varied and represent both direct and indirect protection from pathogens. For direct antimicrobial protection, physiological aspects of the GIT (namely, the mucosal layer) intersect with the action of resident bacteria to produce anti-microbial proteins (AMPs)(*313*). More precisely, pattern recognition receptors (PRR) such as TLRs and CLRs are stimulated by specific microbe associated molecular patterns (MAMPs)(*314*). Examples of MAMPs may include microbe-specific lipopolysaccharide (LPS), flagella or DNA, and stimulation of PRRs triggers pro-inflammatory signalling cascades and production of AMPs (e.g., defensins)(*313*). As previously mentioned, AMPs can also be produced through the action of bacterially metabolised SCFAs. AMPs of this lineage have been shown to protect against infection by pathogenic *Escherichia coli*(*315*) and *Clostridium difficile*(*316*).

As well as direct anti-microbial action of the microbiota, competition for scarce resources within the ecosystem can also promote an indirect inhibition of pathogens; a process termed 'colonisation resistance'(*317*). Here, symbionts and pathobionts alike compete for resources such as GI niches, O_2 or dietary nutrients, and so can outcompete one another(*317*). The significance of colonisation resistance is best exemplified in cases of microbiota dysbiosis. Deadly infections such as *C. difficile* are typically initiated through the depletion of normal microbial diversity (e.g. after antibiotic use), whilst the most effective treatment relies on microbiota restoration through faecal microbial transfer (FMT)(*318*).

1.3.2.1. Links between the gut microbiota and disease

Alongside the gut microbiota's role in development and maintenance of physiological health, the function of these residential bacteria also has strong links to disease initiation and progression. Much of these associations stem from the adaptability of the gut microbiota in response to common stressors, such as the use of antibiotics, changes in diet, hormonal imbalances, alcohol consumption, emotional stress, alongside many more microbiota-modulating factors(*319*). The dysfunctional modulation of the microbiota, which is commonly assigned to a decrease in community diversity, is referred to as a state of dysbiosis and associated with a host of serious diseases(*319*). Inflammatory bowel diseases, such as Crohn's disease and ulcerative colitis, are perhaps the disease indications most associated with gut dysbiosis(*320*). Many studies over the last decades have demonstrated a decrease in microbial

diversity and an enhancement of inflammatory bacteria abundance (e.g., *Enterobacteriaceae*)(*321-323*), which correlates with the main symptoms of enhanced autoimmunity against healthy gut epithelium cells. In experimental pre-clinical models, restoration of anti-inflammatory commensal bacteria such as *Faecalibacterium prausnitzii(324)* or *Lactobacillus murinus(325)* has successfully reversed the gut inflammation, demonstrating an intrinsic link between gut microbes and disease progression. Mechanistically, resident gut bacteria have been shown to be vital for the balance of suppressive and inflammatory cell types in IBD, with an absence of symbiotic commensals intrinsically associated with a decrease in inflammatory Treg cell activation(*320*). IBD patients have a higher proportion of inflammatory and pathogenic bacteria (e.g., *E. coli*) invading the mucosal barrier, which may contribute to the loss of epithelial barrier integrity and enhanced inflammation observed in patients(*326, 327*).

Given the proximity between gut microbes and the intestinal epithelium, it makes intuitive sense that microbial changes could have direct impacts over GIT diseases like IBD. However, it is also now clear that gut microbes have significant influence over many extra-intestinal systemic diseases, including cardiovascular disease (CVD), neurological disease, liver disease, diabetes, and cancer(*328*). CVD is the most lethal disease in the world(*329*) and heavily associated with the gut, which is in turn considered the largest endocrine organ in the body. Most of the links between the gut (microbiota) and CVD emanate from the microbiota's role in metabolism. The best characterised of these mechanisms is the microbiota metabolism of choline, phosphatidylcholine, and carnitine, which collectively generate the by-product trimethylamine-N-oxide (TMAO)(*330*). Systemic levels of TMAO are associated with the balance of bile acids and cholesterol and risk of early onset atherosclerosis(*331*), with TMAO also directly responsible for the activation of the mitogen-activated protein kinase (MAPK) and NF-κB signalling pathways in endothelial cells and smooth muscle cells(*330*), which likely make further contributions to vascular damage. The truly systemic effects of the gut microbiota are further exemplified by the close associations with neurological and neurodegenerative diseases, such as anxiety, depression, Parkinson's disease (PD), and Alzheimer's disease, among many others which have broad microbiota changes associated with their incidence and prognosis(*332*). The broad phenomenon which describes this is the 'gut-brain axis', and mechanistically describes the production of neurotransmitters (e.g., GABA, serotonin) and inflammatory mediators (e.g., cytokines) in the gut which travel systemically to the brain(*332*). PD is a particularly associated indication with the gut microbiota, as the

disease aitiology is even postulated to originate in the gut through the accumulation of immunoreactive α-synuclein misfolded proteins in neurons(*333*). Analysis of patients in the early stages of PD were found to have unbroken chains of these neurons from within the gut enteric nervous system which were spreading systemically towards the CNS, suggesting gut microbial pathogens may initiate PD-causing neuronal damage(*333*). These types of findings coincide with nearly 80% of PD patients suffering from GIT issues (e.g., constipation) in earlier life years prior to PD onset(*334*), and the identification of highly sensitive predictive biomarkers such as reduced *Prevotellaceae* and increased *Enterobacteriaceae(335)*. Although there are too many systemic diseases associated with the gut microbiota to fully review, gut microbial communities clearly impact disease initiation, progression, prognosis both locally and systemically, reaching tissues across most major organs through an array of diverse mechanisms. Better understanding of these links is vital to utilising the fundamental biology to improve human health

1.3.3. The gut microbiota and cancer

One of the major breakthroughs of cancer over recent decades has been the discovery of close links to the gut microbiota. We are increasingly understanding that gut bacteria are key regulators of cancer progression and responses to therapy, which has made gut microbial manipulation a major avenue for novel therapeutics.

Although rare across the broad spectrum of known microbes, some members of the microbiota are known to directly modulate cells to enable tumourigenesis. Perhaps the best characterised of these is *Helicobacter pylori*, which predisposes individuals to gastric cancer through epigenetic modification(*336*). Specifically, *H. pylori* promote oxidative stress and the accumulation of reactive oxygen species (ROS) via the recruitment of macrophages and neutrophils, which increases the frequency of local DNA mutation and cancer formation(*337*). *H. pylori* also use specific virulence factors (e.g. ‘cytotoxin-associated gene A’) to exacerbate this carcinogenic inflammation and mutation(*338*). Elsewhere, it has also been shown that *Salmonella typhi* can cause the development of gallbladder cancer and that *Salmonella enteridus* has a similar effect in colorectal cancer (CRC)(*339*). CRC is unsurprisingly susceptible to microbial dysbiosis due to its proximity to the gut microbiota; disease progression is known to be furthered by *Fusobacterium nucleatum* through enterotoxin secretion and oncogenic *c*-MYC activation(*340*). It is not solely through the action of bacteria that cancer can be

modulated either, as human papillomavirus (HPV) is well known in its ability to insert oncogenic proteins (e.g. E6 and E7) into the host genome to promote cervical cancer(*341*).

Certainly, microbes can, directly or indirectly, promote the progression of a variety of cancers – particularly those which have direct contact with the GI tract. Excitingly, research in the field is increasingly implicating the anti-tumour protective effects of gut microbes on cancers anatomically separated from the GI tract. Some examples of these malignancies include liver cancer(*342, 343*), pancreatic cancer(*344*) and melanomas(*345*) – highlighting a huge promise for further research into different cancer types. Many of these findings were borne from observational studies demonstrating different microbiome profile between cancer patients and healthy controls(*346*). These associations are notable in the context of the host of epidemiological studies implicating differing cancer susceptibility and mortality depending on diet, ethnicity, obesity, alcohol consumption, and antibiotic exposure, with each of these factors known to impact the gut microbiota(*347-349*). As cohort studies have become more sophisticated, these microbiome discrepancies have been further demonstrated between responders and non-responders to standard of care therapies(*350-352*), further implicating a functional role for the gut microbiota. Pre-clinical studies have been vital to validate the protective effects of the gut microbiota mechanistically, with most focus on the response to standard of care therapies. Breakout studies within the field have demonstrated that efficacy of chemotherapy and immunotherapy is lost pre-clinically in response to antibiotic exposure. Iida et al.(*353*), for example, demonstrated that use of antibiotics to disrupt the microbiota impaired response to CpG-oligonucleotide immunotherapy and platinum chemotherapy through dampening of the inflammatory myeloid TNFα. This effect was dependent on TLR4 signalling and correlated with the abundance of *A. shahii*, with administration of this bacteria sufficient to rescue to effects of antibiotic treatment. In a similar study, Viaud et al.(*354*), also demonstrated the negative effects of gut microbiota-depletion with antibiotics, with antibiotic administration impairing pre-clinical response to cyclophosphamide chemotherapy. This effect was mediated in a reduced Th1 and Th17 response, which was rescued following an FMT from a healthy donor. More recent studies are further demonstrating the protective nature of the gut microbiota in cancer outside of response to therapy, as antibiotic induced dysbiosis has been demonstrated to increase breast cancer primary tumour burden(*355*) and metastasis(*356, 357*) in separate pre-clinical studies through the activation of tumourigenic mast cells. The significance of these findings has only been further

bolstered by human studies demonstrating that antibiotic use correlates with worse survival outcomes in breast cancer patients(*358, 359*), where cyclophosphamide is a cornerstone of standard of care therapy and prophylactic antibiotic administration is common. More broadly, clinical use of antibiotic correlates with worse outcomes across a range of tumour types and treatment regimens (chemotherapy, immunotherapy, combination approaches)(*360, 361*), further suggesting a ubiquitous role for the gut microbiota in cancer.

The various studies which have used microbiota depletions to demonstrate the protective role of gut bacteria in cancer responses have been vital for our understanding but left the open question as to whether the microbiota can be used therapeutically to improve cancer response. This question was first answered in a seminal study by Sivan et al.(*362*), who demonstrated that the therapeutic administration of *Bifidobacterium* (four strains from four species) was able to enhance response to αPD-L1 immunotherapy. This effect was shown to be dependent on the *Bifidobacterium*-stimulated DC maturation and activity, which in turn enhanced priming of TAAs by $CD8^+$ T cells and resulted in enhanced $CD8^+$ effector release and tumour cell death. The therapeutic use of bacteria against cancer has grown to a major field of study over intervening years, as many groups have separately demonstrated pre-clinical efficacy of many types of therapeutic bacteria against many types of cancers(*363-366*). In a more recent Nature study, Tanoue et al.(*367*), developed an eleven-strain consortium of bacteria isolated from a human donor microbiota which induced a strong CD8 IFNγ response (compared to other human donors) in the colon of germ-free mouse models. These eleven strains (which were uniquely elevated in the human donor) were able to reduce primary tumour burden in subcutaneous colon and melanoma tumour models through the activation of gut resident $CD103^+$ cDC1 cells. With the attention received from the microbiome in the context of cancer, the field has been seen as a tool to convert immunotherapy non-responders to responders in the clinic. This drive has spurred an influx of human studies validating the therapeutic potential of gut microbiota, with major works demonstrating that enhanced microbiota diversity broadly associates with a favourable response to ICIs(*368, 369*), whilst specific genus (such as *Lactobacillus*, *Streptococcaceae*, *Enterobacter*) are associated with non-response(*370, 371*) across multiple geographical cohorts. (*372*). FMTs from immunotherapy responders in human melanoma and epithelial tumour cohorts has been shown to improve ICI response in mouse models (relative to non-responder controls), demonstrating a distinct functional difference between the gut bacterial communities(*373, 374*). Excitingly, these findings are now being replicated in clinical

trial cohorts, as responder to non-responder FMT therapy is meeting initial efficacy thresholds in combination with ICIs in refractory patients(*375, 376*). In another recent study, the first positive clinical trial data using a single strain (*Clostridium butyricum*) showed positive phase I results in renal cell carcinoma patients alongside nivolumab plus ipilimumab, showing for the first time (in humans) that entire bacterial communities are not necessarily required to achieve a beneficial response(*377*).

1.3.3.1. *Bifidobacterium*

Bifidobacterium are a genus of gram-positive anaerobic bacteria within the phylum of Actinobacteria, which are characterised as non-motile, non-spore forming, with a 'Y'-shaped morphology, generally found in the mammalian GIT(*378*). Members of the *Bifidobacterium* genus are among the first to initially colonise the gut during early life, performing an array of vital functions for host immune education and development. *Bifidobacterium* are generally considered to be 'beneficial' bacteria and are commonly used in commercial probiotic products, with many commonly used species classified as 'generally recognised as safe' (GRAS)(*379*). During early life, *Bifidobacterium* are essential for the development of the adaptive immune system. As introduced in section 1.3.2., much of this action is associated with the degradation of sugars, such as nutrient derived cellulose, fructans and pectins, as well as host derived HMOs from breast milk, which provide selection and growth advantages for resident *Bifidobacterium* and stimulate the production of bioactive downstream metabolites (e.g., the SCFA acetate)(*378*). This activity is mediated by the particularly wide arsenal of Carbohydrate-Active Enzymes (CAZymes) found in *Bifidobacterium* (such as the glycosyl hydrolyses), which facilitate SCFA and indole-3-lactic acid (ILA) production, inducing immune tolerance through Treg differentiation, prevention of Th2 polarisation, and increased expression of tolerogenic T helper receptors (e.g., galactin-1)(*289, 379*). Infants delivered pre-term, through C section, and those fed on formula rather than breast milk have all been demonstrated to have lower abundances of gut *Bifidobacterium(380)*. These children in turn display higher risk of immunological disease, such as asthma and allergy, as well as a higher risk of serious infections like necrotising enterocolitis (NEC)(*284*). The functional link here has been demonstrated in clinical intervention studies, where administration of a *Bifidobacterium*/*Lactobacillus*-based probiotic to pre-term infants reduces the onset of NEC and all-cause mortality by 50%(*381*). These types of protective results have been replicated elsewhere(*382-384*),

with a probiotic (*Bifidobacterium*) intervention to deficient infants (e.g., those which are pre-term) is now included in WHO guidelines as recommended clinical practice(*385*).

Within the context of the gut microbiome and cancer, *Bifidobacterium* have some of the most consistent and potent associations with positive outcomes, both in clinical cohort studies and mechanistic pre-clinical studies. Many of these associations with cancer were spurred from the previously referenced Sivan study (2015)(*362*) showing *Bifidobacterium* enhancing response to αPD-L1 immunotherapy in melanoma. Preclinical studies emerging in the following years have further expanded these findings, and separate studies have demonstrated that both strains of *Bifidobacterium breve(386)* and *Bifidobacterium bifidum(387)* could reduce subcutaneous colon tumour burden as a monotherapy and synergically enhancing response to oxaliplatin chemotherapy and αPD-1 immunotherapy. A notable finding from each of these studies was that the protective effects were strain specific. The finding that different strains within the same species had different functional effects on cancer response highlights the mechanistic variety and specificity within the *Bifidobacterium* genus, and the great potential the bacteria have therapeutically. The study by Lee et al.(*387*), highlighted a particularly interesting mechanism whereby the strain-specific composition of peptidoglycan mediated a TLR2-dependent response, which in turn stimulated enhanced downstream immunity against the tumour. Elsewhere, the production of metabolites by *Bifidobacterium* has also been shown to mediate anti-cancer immune responses, as Mager et al.(*363*), demonstrated a mechanism of *Bifidobacterium pseudolongum* production of inosine mediating enhancement of αCTLA-4 and αPD-1 ICI response in CRC and melanoma. This mechanism took advantage of the 'leaky gut' induced by ICI administration (a common clinical adverse effect) which allowed the systemic translocation of inosine, which bound to adenosine 2A receptor ($A_{2A}R$) on $CD8^+$ and T helper cells to induce enhanced anti-tumour effector release (IFNγ, granzymes etc.) and increased of ICI response. In addition to the mechanism-focused pre-clinical studies on *Bifidobacterium* and cancer, a number of high profile human observational studies have identified *Bifidobacterium* as being associated with favourable cancer responses. For example, Lee et al.(*351*), conducted a shotgun metagenomic sequencing across five sperate cohorts of ICI-treated melanoma patients, which despite not completely replicating findings across all cohorts, showed both that the microbiome profile was broadly associated with response and that abundance of *Bifidobacterium pseudocatenulatum* (alongside *Roseburia spp*. and *A. muciniphila*) correlated with enhanced overall response rates and progression-free survival. This study reinforced previous findings from Matson et al.(*388*), who identified

Bifidobacterium longum and *Bifidobacterium adolescentis* as being associated with favourable response to ICI in melanoma patients, with a B. longum containing community able to functionally enhance ICI response in a melanoma mouse model. Another major cohort study, this time in NSCLC, revealed that an enhanced abundance of *A. muciniphila*, *Bifidobacterium adolescentis* and *E. hallii* were associated with improved clinical outcomes and pro-inflammatory responses following ICI treatment(*352*), demonstrating the protective associations of *Bifidobacterium* in humans is not restricted by tumour type.

1.3.3.2. *Bacteroides*

As one of the dominating phyla of the gut microbiota, *Bacteroides* have huge influence over the functional outputs of the gut. *Bacteroides* are particularly known for their role in metabolism, representing key degraders of diet- and host-derived glycans, which enables the downstream production of functional metabolites and vitamins to influence the host and allow cross-feeding for other commensal organisms(*389*). Particularly abundant species include *B. fagilis*, *B. thetaiotaomicron* (Bt), *B. vulgatus*, and *B. ovatus*. As obligate anaerobes, *Bacteroides* can be found in both the small intestine and colon, whereby they provide crucial nutrients for other microbes and provide protection from pathogens(*389*). As an example, Bt is known to metabolise starch via a catalogue of polysaccharide utilisation loci (PUL), which generates maltose and glucose for use by *Eubacterium ramulus* (which does not have the capability to metabolise dietary fibre)(*390*). *E. ramulus* can then ferment glucose to the SCFA butyrate, as well as enhance the degradation of polyphenolic compounds such as quercetin, generating bioactive metabolites with defined roles in activating the host immune system(*390*). One of the key mechanisms of *Bacteroides* functional communication with other organisms and the host is through the secretion of outer membrane vesicles (OMVs) (outlined in detail in section 1.3.5.4.), which contain proteases, glycosyl hydrolases, bacterial antigens, and AMPs(*391*). Bacteroides fragilis OMVs, for example, have been shown to contain *Bacteroidales* secreted antimicrobial protein (BSAP-1) within the internal structure, which is endocytosed upon contact with a cellular target to form membrane pores and kill the pathogenic cell(*392*). Alongside this, Bt OMVs have separately been demonstrated to be potent stimulators of the host immune system, inducing a strong TLR2-dependent IL-10 response in monocytes(*393*) and a corresponding regulatory IL-10 response in colonic DCs(*394*), indicating a homeostatic role for Bt during gut immune tolerance. Interestingly, Bt OMVs have also

been shown to cross the gut epithelium and travel systemically(*395*), implicating a potentially broader role in systemic immunity. Although generally considered a beneficial commensal, a subset of Bacteroides strains do behave as opportunistic pathogens when translocated past the initial mucosal barrier (e.g., because of a leaky gut). Enterotoxic *Bacteroides fragilis* strains are those which produce the *Bacteroides fragilis* toxins (Bfr toxin), which are associated with enhanced intestinal inflammation and tissue damage, causing increased risk of ulcerative colitis, diarrhoea, and CRC(*396*).

Despite the negative association with some strains of Bacteroides fragilis with CRC development, *Bacteroides* species are generally associated with favourable outcomes in cancer, likely due to their role in gut homeostasis and immune regulation. One of the major studies in this area by Vétizou et al.(*397*), showed that both *Bacteroides fragilis* and Bt mediated response to αCTLA-4 ICIs, with this effect lost in antibiotic-treated or germ-free mice. Further experiments found that the polysaccharide on the surface of each species induced a specific IL-12 response in (colonic) DCs, inducing a stronger Th1 polarisation and enhanced induction of anti-tumour immunity, with the administration of isolated *Bacteroides* polysaccharide sufficient to replicate this effect. Since this study, further beneficial effects of *Bacteroides* polysaccharide have been identified, with the administration of non-enterotoxic *Bacteroides fragilis* able to inhibit CRC tumourigenesis in a chemically induced animal model through cell surface polysaccharide A (PSA) interaction with TLR2, which in turn reduced local expression of CCR5 and was strongly associated with tumour protection(*398*). In another mouse study, a *Bacteroides fragilis* and Bt stimulating FMT was sufficient to confer an enhanced response to αPD-1 immunotherapy in a subcutaneous model of colon cancer, again highlighting a synergy between non-eneterotoxic *Bacteroides* strains and ICI response(*399*).

1.3.4. The tumour microbiome

The tumour microbiome is a relatively recent concept which has gathered huge attention in major research papers, referring to the colonisation of tumours with a distinct population of microorganisms. Although this concept is broadly accepted in the case of intestinal tumours, e.g., *Fusbacterium nucleautum* promoting the formation of CRC(*400*), extraintestinal tissues and tumours have long been considered sterile (outside of incidences of major infection). Although the identification of bacteria within

tumours can be traced to more than 100 years ago, the poor control over potential microbial contaminants limited scientific interest(*401*). Modern experimental methodologies have attempted to overcome this issue through employment of rigorous controls, with one of the first major studies analysing human tumours by Nejman et al.(*402*), showing a remarkable level of positive FISH staining against bacterial 16S rRNA, immunohistochemical staining of LPS, and species level genomic signatures within a wide range human primary tumour types. Particularly striking, was the extent of bacteria discovered in breast and bone tumours (considered unlikely sites for bacterial colonisation), alongside a unique community of bacteria within distinct associations with outcomes depending on tumour type. In another significant study from the same year, Poore et al.(*403*), published astonishing analysis of 17,625 samples from the Cancer Genome Atlas (TCGA) showing a microbial genomic signature in 32/33 cancer types. They developed a machine learning algorithm which could not only discriminate tumour types based on microbial signatures but could also infer prognosis for many cancer types with >95% accuracy. Many studies have corroborated apparent microbial infiltration into tumours alongside distinct mechanisms of action, with Parida et al.(*404*), detecting enhanced levels of *Bacteroides fragilis* in human breast tumours compared with normal breast tissue. Mechanistically, the group showed that specifically enterotoxic *Bacteroides fragilis* contributed to enhanced tumour growth and metastasis in transplanted mouse models through activation of the Notch/β-catenin pathways.

The incidence and mechanistic function of an extra-intestinal tumour microbiome has been supported by both clinical and pre-clinical mouse studies in pancreatic tumours(*405, 406*), breast tumours(*407, 408*), melanoma(*409, 410*) and many more(*401, 411, 412*), which proport both positive and negative associations between intratumoural bacteria and prognosis. Of particular relevance, are a number of studies showing protective roles for intra-tumoural bacteria and bacterial gut-tumour translocation as a mechanism of action. A recent example of this by Bender et al.(*413*), showed that oral administration of *Lactobacillus reuteri* resulted in a direct translocation to subcutaneous melanoma tumours (validated through selective culture). Mechanistically, *L. reuteri* released indole-3-aldehyde, a dietary tryptophan metabolite, which bound aryl hydrocarbon receptor on $CD8^+$ T cells to increase cytotoxic effector release, reduce primary tumour burden, and enhance response to ICIs. In addition to bacterial studies, breakthrough works are also implicating a fungal tumour mycobiome as have mechanistic and prognostic relevance across a number of tumour types(*414, 415*), although this field is more poorly understood.

Although the weight of literature (including major studies in high impact journals) provides convincing evidence for the presence and relevance of a tumour microbiome(*401, 416*), several recent studies have called methodologies and specific major works into question. A point of contention is the reliance on metagenomic sequencing of tumours from patients to validate human findings, which is problematic due to the difficulty in maintaining truly sterile environmental conditions clinically and during sample transit, as well as major concerns around the accuracy of bacterial databases. Studies have indicated that human reads are major contaminants of thousands of assembled genomes of bacterial species(*417*), with another study confirmation this human contamination is prevalent across 2 million entries in the GenBank database(*418*), which is used to assign microbial signatures to tumour-derived DNA reads. Some spurious results have also raised eyebrows, as bacterial and viral genera that were not known to exist in humans have been identified in tumours(*419*). In 2023, major preprints have brought into question some of the foundational studies within the tumour microbiome field, as Gihawi et al.(*420*), have validated major data handling errors in the Poore (2020) Nature paper which completely invalidate the findings, showing false positive identification of bacterial signatures due to database contamination with human reads alongside the data transformation methodology creating an artificial discriminatory signature which was picked up by the machine learning algorithm. The correction of these errors dramatically demonstrated a loss of the microbial signatures identified in the tumours and a corresponding loss in the discriminatory prediction of the algorithm. Another preprint published recently has further casted doubt over the Nejman (2020) science paper, as de Miranda et al.(*421*), analysis of 129 human breast tumours did not reveal the presence of any bacterial LPS as previously reported.

Overall, the broader field and previous findings have recently been bought into question by many, and as such the role of the tumour microbiome is less clear. However, the weight of corresponding substantiating studies does suggest there is likely to be an extra-intestinal tumour microbiome in at least some tumours, perhaps in an individual specific manner. It is plausible, for example, that a cancer patient with a chemotherapy- or immunotherapy-induced leaky gut may be suspectable to gut-tumour bacterial translocation, which could in-turn influence tumour progression. Although, with the difficulty in handling such low biomass bacteria, it may be increasingly difficult to distinguish which microbial signatures are genuine, environmental contaminants, or artificial through human contamination of bacterial databases

1.3.5. Mechanisms of host-microbe interactions in immunity and cancer

The promise of using bacteria for enhancing outcomes in cancer is clear. A huge volume of studies have outlined countless associations between gut bacteria and cancer outcomes, outlining uniquely important bacteria in specific indications and therapeutic utilisation of these bacteria in pre-clinical models. However, a common issue for the field is a lack of mechanistic specificity. A poor understanding of what active compounds a bacterium is producing, which receptors they are specifically binding, and how this mounts a (usually complex) multi-system anti-cancer response, fundamentally holds the field back from proper clinical translation. Without this mechanistic understanding, the identification and prediction of mechanisms of resistance becomes increasingly difficult and prevents informed patient stratification. Lack of mechanistic insight simultaneously prevents prescription or control of host-derived factors (e.g., diet, antibiotic use) which may fundamentally shape a therapeutic response. The promise of a more detailed mechanism of action further allows innovative 'post-biotic' therapeutic approaches, which utilise the active compound of a bacterium rather than the host live cells, simplifying manufacture and removing the confounder of bacterial viability/activity being different in different host patients.

Broadly speaking, the active compounds produced by therapeutic bacteria fall into two categories, actively produced/secreted compounds (referred to as 'metabolites'), and inactively produced and stable bacterial cell membrane components. The active compounds mechanistically mediating host-microbe interactions will be discussed in detail below, with a particular focus on *Bifidobacterium*-relevant pathways.

1.3.5.1. Microbial metabolites

Microbial metabolites are actively synthesised and secreted compounds which result from bacterial cell metabolism of a nutrient energy source. Metabolites are a vital functional output from the gut microbiota, as they facilitate crosstalk and cross-feeding between gut bacteria members, can behave as AMPs against pathogens, and facilitate communication with the host(*422*). The interactions between microbial metabolites and the immune system are particularly important for health of the host, providing one of the most cited links between bacteria and cancer progression(*423*).

A key group of metabolites commonly associated with protective immunological and anti-cancer responses are the SCFAs, including acetate, propionate, and butyrate(*424*). Here the protective action of SCFAs is two-fold, supressing the chronic inflammation which often precedes cancer development, whilst later enhancing anti-tumour immunity once a tumour has established(*424*). SCFAs operate through a variety of mechanisms of action, but often bind to the host through G protein-coupled receptors (GPCRs). In a spontaneous $APC^{min/+}$ colon cancer model, butyrate binds to GPR109a on dendritic cells and macrophages to induce a downstream polarisation of $CD4^+$ lymphocytes to differentiated IL-10^+ Treg cells, which in turn mediates a downregulation of Th17 polarised cells(*425*). The suppression of Th17 cells by butyrate/GPR109a programmed Tregs reduced the chronic inflammation observed in the model and slowed the onset of colon tumourigenesis(*425*). In the context of established colon tumours, butyrate can also bind free fatty acid receptor 2 (FFAR2) on DCs to inhibit the production of $CD8^+$ T cell suppressive IL-27(*426*). A SCFA known to be highly produced by *Bifidobacterium*, acetate, has been shown to directly increase the effector activity of anti-tumour $CD8^+$ T cells under glucose-restricted conditions through an epigenetic mechanism(*427*). Here, acetate enters $CD8^+$ T cells through monocarboxylate transporters (MCTs) or aquaporins and is converted to acetyl-coenzyme A (CoA), which functions to enhance histone acetylation and chromatin accessibility, enabling the downstream enhancement of transcription of IFNγ, granzymes, and TNFα(*427*). Very similar mechanisms of direct $CD8^+$ T cell modulation and enhancement of anti-tumour effector function (through histone acetylation and enhanced transcription) have also been validated for the SCFAs butyrate and pentanoate in a separate study(*428*).

Although SCFAs often get most attention in mechanistic research outlining host-microbe interactions, an array of other key metabolites have been shown to be important in mediating cancer responses. One group of these metabolites are the indoles (dietary tryptophan metabolites), as outlined in the previously referenced study by Bender (2023) showing *L. reuteri* released indole-3-aldehyde enhancing melanoma tumour $CD8^+$ activity(*413*). Another recent study by Zhang et al.(*429*), showed a similar finding, as *Lactobacillus plantarum*-derived indole-3-lactic acid was shown to cross the intestinal barrier and elicit epigenetically anti-cancer effector release in DCs and $CD8^+$ T cells, which resulted in reduced subcutaneous colon tumour progression and enhancement of ICIs. Another type of microbial metabolite introduced previously in the context of CVD, TMAO, has also been shown to have links with cancer progression. TMAO is produced dominantly by members of the *Clostridiales* genera, and can

mechanistically induce pyroptosis in triple negative breast cancer cells through endoplasmic reticulum stress kinase (PERK), which functionally enhances anti-tumour $CD8^+$ T cell immunity and the response to ICIs(*430*). Many other microbial metabolites have been implicated in cancer responses, such as the previously discussed study by Mager (2020) showing *Bifidobacterium pseudolongum* and *Lactobacillus johnsonii* produced inosine enhancing $CD8^+$ effector activity(*363*), as well as types of secondary bile acids(*431*), sulfonic acids (taurine)(*432*), and even antibiotics (*Streptomyces spp*. produced Manumycin A)(*433*).

1.3.5.2. Bacterial surface-associated exopolysaccharides

Bacterial surface-associated exopolysaccharides (EPS) are extracellular sugar macromolecules which are either tightly bound to the capsule (CPS) or weakly bound to the bacterial slime layer(*434*). Due to the difficulty in separating the EPS from either origin, they will be discussed as one group for the purposes of this review. Though not the focus of the literature discussed, one of the most famous microbial polysaccharides is pathogenic lipopolysaccharide (LPS), which induces damaging inflammation to the host through TLR4 activation. Outside of this context, EPS has gained a significant amount of attention over recent years as key modulators of host-microbe interactions, mediating beneficial mechanisms for many types of probiotic bacteria. Some of the dominant producers of EPS are the lactic acid bacteria *Bifidobacterium* and *Lactobacillus*, where the EPS structures produced have been implicated in altering microbiota composition, enhancing gut barrier integrity, and mediating host GIT immune responses(*435*).

Structurally, EPS can be described as homopolysaccharide or heteropolysaccharide, which respectively describe EPS structures comprised of one type of sugar monomer or several(*435*). Examples of common sugar monomers include glucose, galactose, mannose, rhamnose, and fructose. The monomer composition and structural (i.e., linkage position and branching) configuration of microbial EPS is highly variable (Figure 1.10.), not just between different genus and species, but even different strains of the same species (particularly for *Bifidobacterium*)(*436*). This inconsistency produces a huge variety of unique EPS structures, which can in turn be metabolically influenced by the local availability of sugar monomers(*437*), providing a wide range of potential functions for microbial EPS depending on strain and context.

One of the first major roles identified for microbial EPS is utilisation as a prebiotic for other commensals within the microbiota. Although the extent of this phenomenon is very much dependent on the specific EPS structure, a study by Korakli et al.(*438*), demonstrated that several specific strains of *Bifidobacterium* were able to ferment EPS from *Lactobacillus sanfranciscensis* into SCFAs, such as acetate, lactate and formate. Given the protective roles of SCFA in a variety and health as disease contexts, EPS could indirectly promote GIT health and immune tolerance. Additionally, another study by Salazar et al.(*439*), showed that EPS isolated from strains of *Bifidobacterium* (mostly comprised of glucose and galactose monomers) was also readily digestible by the human gut microbiota, resulting in an increased abundance of gut *Bifidobacterium* and levels of SCFAs. Aside from fermentation by other commensals, EPS has also been implicated in having more direct roles in mediating microbial interactions with the host, having been consistently implicated in increasing gut epithelial barrier integrity(*435*). Mechanistically, pre-treatment of intestinal epithelium cells with *Bifidobacterium* EPS was shown to inhibit the cytotoxic effects *Bacillus cereus* toxins on barrier integrity, potentially through provision of a protective polysaccharide boundary(*440*). Elsewhere, *Bifidobacterium* EPS has been shown to increase the expression of tight junction proteins (claudins) in gut epithelial cells as another mechanism of enhanced barrier integrity(*441*).

The interaction between microbial EPS and the host immune system is a key mechanism supporting host-microbe interactions. The unique structure and composition EPS ultimately dictates binding affinity to immunological receptors and the resulting downstream activity. TLR2 is the TLR most associated with EPS binding, having been implicated in interacting with EPS from *Thermus aquaticus*, *B. breve*, and *Streptococcus suis(442-444)*. The result of this TLR2 activation is typically an inflammatory response in monocytes and macrophages, however EPS from a number of strains has also been demonstrated to inhibit pathological TLR4 inflammatory pathways during pathogen exposure (e.g., to enterotoxic *E. coli*)(*445*). Another group of receptors linked with recognition of microbial EPS are the C-type lectin receptors (CLRs), commonly found on innate macrophage and DC lineages. Although research on EPS binding to immunological receptors is lacking generally, particularly in the case of CLRs, CLRs have been historically implicated in the recognition of sugar constituents of fungal cell during pathogenesis(*446*). Major CLRs include Dectin-1 (high affinity for glucan residues)(*447, 448*), Dectin-2 (high affinity for mannose)(*449*), and DC-sign (high affinity for mannose and fucose-terminated glycans)(*450*), with

many in the field postulating CLRs to have a role for immune recognition of microbial EPS sugars.

The role of EPS from commensal bacteria has been shown to be relevant for immunity and disease progression through several pre-clinical studies. One of the most well studied bacterial polysaccharides is *B. fragilis* PSA, which has been shown to bind TLR2 on plasmacytoid DCs and stimulate the production of IL-12, TNFα and IFNγ(*451*). PSA-loaded DCs can subsequently cross-present deaminated PSA antigen to $CD4^+$ T cells via MHCII(*452*), whilst also showing the ability to induce IL-10^+ Treg cells to promote GIT immune tolerance(*453*). The roles of *Bifidobacterium* EPS in modulating the immune system are highly varied, as Hidalgo-Cantabrana et al.(*454*), demonstrated differential inflammatory effects of different strains of the same species of *Bifidobacterium animalis subsp. lactis*, with only one strain producing EPS which stimulated a pro-inflammatory response (higher TNFα/IL-10 ratio) in human peripheral blood mononuclear cells (PBMCs). Contrastingly, a key study by Fanning et al.(*455*), validated a key anti-inflammatory effect of *B. breve* EPS *in vivo* and *in vitro* to enable increased persistence and induce protection against pathogenic *Citrobacter rodentium* colonisation. The same strain of *B. breve* has also been implicated in regulatory DC responses for immune tolerance, preventing DC maturation and cross-presentation of antigen to $CD4^+$ T helper cells(*456*). Alongside these studies, an array of other literature has further described pro- and anti-inflammatory roles for EPS (particularly from *Bifidobacterium*)(*457-459*), with the wide variety of immunological effects matching the wide variety of EPS structures. Although the link between microbial EPS and an anti-cancer host immune response has not yet been validated, some studies have implicated various types of EPS to have directly apoptotic effects on cancer cell lines *in vitro(460-462)*, however the biological relevance of these studies is not yet clear from *in vivo* work. Overall, microbial EPS represents a crucial interface between bacteria and the host response, but the highly variable EPS composition and configuration is crucial for the initiation of a very specific host immune response. More research is required to better understand the *in vivo* relevance of microbial EPS structures to the mechanisms of action of therapeutic bacteria.

1.3.5.3. Other bioactive structural components

In addition to surface-associated polysaccharides, there are many other immunomodulatory components present on microbial membranes which can be

involved in host-microbe interactions (Figure 1.10). A key example of this is bacterial peptidoglycan (PG), which functions to provide strength against pH and osmotic pressure(*463*). PG is comprised of N-acetylglucosamine (GlcNAc) and N-acetylmuramic acid (MurNAc) monomers connected by β-1,4-O-glycosidic bonds, which is cross-linked via peptide chain to form the solid three-dimensional structure(*463*). PG can be subclassified based on amino acid composition and the type of binding at the amino acid bridge. Innate immune cells have a range of receptors capable and recognising PG, such as nucleotide-binding oligomerization domain-containing protein 1 (NOD1), NOD2, peptidoglycan recognition proteins (PGRP) and TLR2(*464*). Whilst PGRPs are thought to be involved in the recognition of pathogenic PG (owing to their bactericidal activity), probiotic PG is more commonly associated with recognition by NOD-like receptors and TLR2(*465*). Associations between PG and cancer in fact trace to the 1980s, where Sekine et al.(*466*), observed strong inhibition of Meth-A fibrosarcoma tumour formation (resulting in some regressions) when tumour cells were inoculated with *B. longum ssp. infantis* cell wall preparation. Historical issues with impure peptidoglycan preparations have made specific conclusions difficult however, due to contaminating polysaccharide and surface proteins. More recent studies have, however, shown a directly apoptotic effect of bacterial cell wall peptidoglycan on various tumour cell lines(*467*), as well as induction of inflammatory cytokines in macrophages *in vitro(468)*. A significant study by Lee et al.(*387*), showed that differences in cell wall peptidoglycan between therapeutic and non-therapeutic strains of *B. bifidum* mediated therapeutic response in subcutaneous colon cancer through a TLR2-dependent effect. Though mechanistic knowledge of the role of peptidoglycan in mediating anti-cancer responses is thin, preliminary literature suggests a potentially significant role, owing to PG being a key mediator of host-microbe interactions.

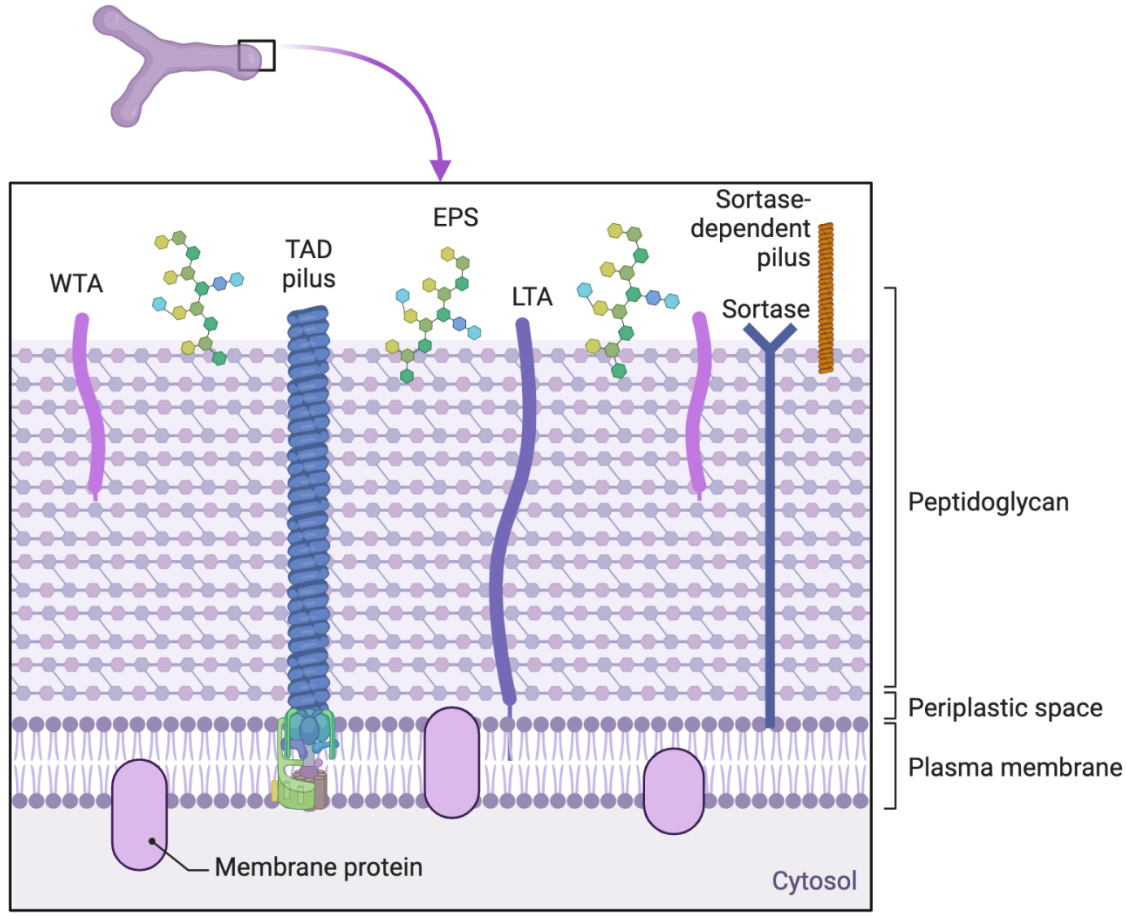

Figure 1.10. Schematic showing macromolecular structures exposed on the bifidobacterial surface. Membrane protein (MP), exopolysaccharide (EPS), wall and lipoteichoic acids (WTA and LTA), with sortase-dependent and Tad pili. Adapted from "Gram-Positive Bacteria Cell Wall Structure", by Biorender.com (2023). Retrieved from https://app.biorender.com/biorender-templates.

A common contaminant of bacterial cell wall preparations are teichoic acids, which are cell wall-bound negatively charged polymers, typically made up of 30–40 subunits(*469*). Common subunits include glycerol phosphate and ribitol phosphate, alongside sugar monomers (e.g., glucose, rhamnose). Teichoic acids can be subdivided into lipoteichoic acid (LTA) and wall teichoic acid (WTA), which are respectively bound to either the cell membrane or PG(*469*). Though the functional roles of these membrane components are poorly defined, it is thought that they may have discrete roles in stimulating the immune system, as Mizuno et al.(*470*), showed that LTA from *Lactobacillus plantarum* stimulated a TLR3-specific response at the intestinal epithelium. Another bioactive structural component thought to be relevant for host-microbe interaction of pili, which are thin proteinaceous projections which facilitate bacterial cell adhesion to mucosal surfaces(*471*). Two major types of pili are found in

Bifidobacterium, sortase-dependent pili and tight-adherence (TAD) pili. Like teichoic acids, little is known of the functional mechanistic roles of pili in immune activation, although they have been shown to activate both TLR2 on monocytes(*472*) and DC-sign on DCs(*473*). *In vivo*, *B. bifidum* pili have been shown to increase pro-inflammatory TNF and decrease IL-12 responses at the gut epithelium(*474*), demonstrating a role in mediating the host immune response.

1.3.5.4. Bacterial extracellular vesicles (BEVs)

Bacterial extracellular vesicles BEVs are nano-sized (~20-400nm) structures exocytosed from the membranes of bacteria. These structures fundamentally differ depending on the bacteria of origin, as Gram-negative bacteria (e.g., *Bacteroides*) produce BEVs with an outer membrane, termed outer membrane vesicles (OMVs), and Gram-positive bacteria (such as *Bifidobacterium*) produce standard membrane extracellular vesicles (EVs) which lack an outer membrane layer(*475*). Due to the focus work of chapter 6 focusing on Bt OMVs for the treatment of cancer, this review section will focus specifically on the function of Gram-negative OMVs in health and disease.

OMVs have a diverse array of functions, particularly in the environment of the gut microbiota, such as cell communication, pathogenesis and secretion of superfluous proteins(*476*). Bacterial OMV secretion is an active and selective process which can occur in response to several extracellular cues, such as nutrient availability, pH, quorum sensing and temperature(*477*). Bioactive proteins can be differentially expressed on and within the OMV bilayer surface, which ultimately determines the nature of OMV-cell (bacterial or host) interactions (Figure 1.11)(*478*). The outer layer of OMV membranes is known to contain LPS, outer membrane proteins, polysaccharides, and periplasmic proteins, whilst the intra-vesicle cargo of OMVs can include RNA, DNA, proteins, and virulence factors(*479, 480*). The effects of interactions facilitated by OMVs can be wide-ranging, with OMVs having been implicated in biofilm formation and bacterial pathogenesis(*476*). During pathogenesis, OMVs can modulate host immune responses through the expression of virulence factors such as LPS(*481*). OMVs are known to be secreted by a range of pathogenic bacteria in this context, such as *H. pylori* (which secrete VirD4-containing OMVs)(*482*) and enteropathogenic *E. coli* (which secrete HtrA containing OMVs)(*483*). Importantly for the perspective of microbiota-host interactions, OMVs secreted in the gut are also known to cross the GI epithelium and translocate systemically(*395*). The nano-particle structure of OMVs,

which allows efficient diffusion across capillary and extra-cellular membranes, coupled with potent immunomodulatory effects(*393, 394*), has led to excitement over OMVs as novel therapeutic agents, particularly in immunogenic diseases such as cancer. The acellular (non-replicative) nature of OMVs also permits a low risk of major systemic infection, although toxicity is a concern when delivering non-attenuated vesicles.

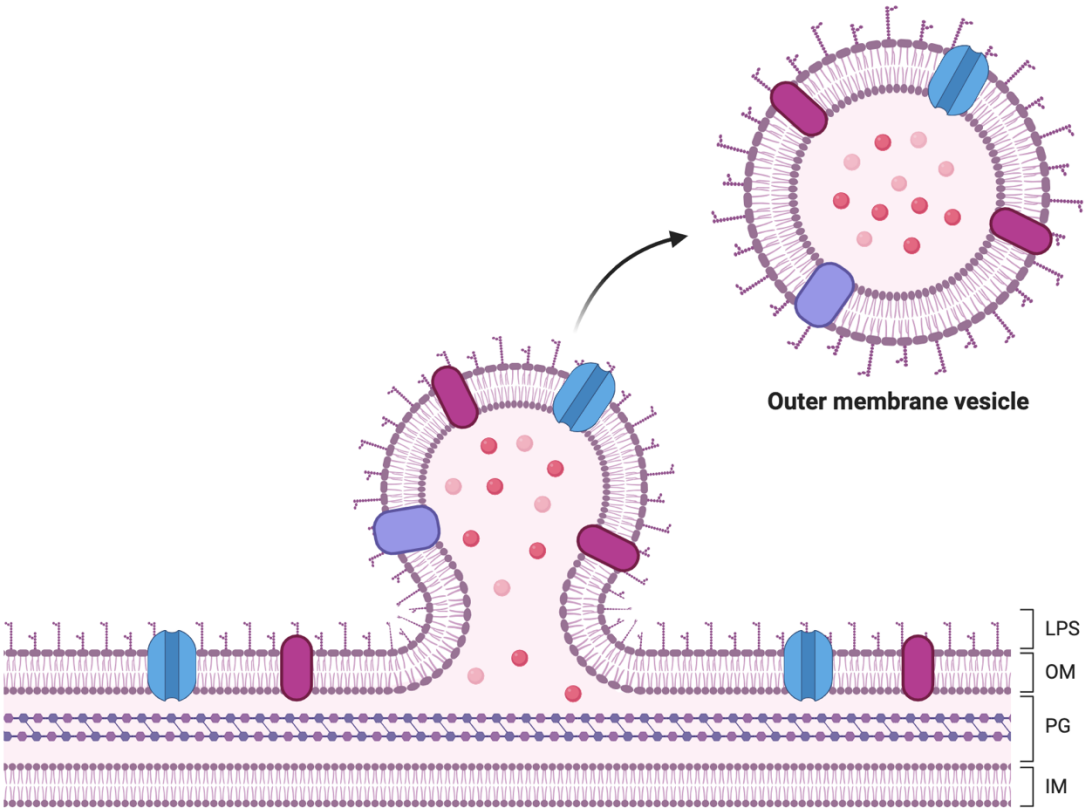

Figure 1.11. The formation of bacterial outer membrane vesicles (OMVs). Gram-negative bacteria cell initially have homogenous distribution of vesiculation-inducing proteins. The linking between outer membrane and peptidoglycan is lost through the movement of periplasmic linking proteins. OMVs may be produced without enrichment of periplasmic proteins, with intra-vesicular enrichment of periplasmic proteins or with enrichment with specific periplasmic proteins on the outer membrane. LPS = Lipopolysaccharide, OM = Outer membrane, PG = Peptidoglycan, IM = Inner membrane. Adapted from “Gram Negative Bacteria Outer Membrane Vesicle Formation”, by Biorender.com (2023). Retrieved from https://app.biorender.com/biorender-templates.

Although there has not been extensive study of microbial OMVs as anti-cancer therapeutics, the research which has been conducted has yielded promising results. A key example here by *Kim et al.*(*484*) showed that OMVs generated from *E. coli*, *S. enterica*, *Staphylococcus aureus* and *Lactobacillus acidophilus* were all able to induce anti-tumour responses against subcutaneously implanted CT26 colon tumours in mice. *E. coli* OMVs were further able to reduce subcutaneous melanoma and breast tumour size through an IFNγ-dependent mechanism, with $IFN\gamma^{-/-}$ mice displaying resistance to OMV-mediated tumour effects. Excitingly, this immune defence against tumours was long-lived, as CT26 colon tumours were completely rejected after 2^{nd} and 3^{rd} implantation attempts. The ability of OMVs to uptake extra-vesicular material has also promoted interest in OMVs as a platform for delivery of conventional therapeutics. Uptake of by the chemotherapeutic drug 'tegafur' by attenuated *Salmonella typhimurium* OMVs was shown to be effective in reducing melanoma tumour size and metastasis. Importantly, these OMVs had greater anti-tumourigenic effects than 'WT' *S. typhimurium* OMVs, and tumour targeting efficiency was also improved through co-expression of the Arg-Gly-Asp (RGD) peptide at the OMV surface, which enabled increased OMV tracking to αvβ3-overexpressing tumour cells. Taken together, the prospects for utilising OMVs in cancer therapy is exciting, and advancements in OMV optimisation for increased therapeutic efficacy represents a vital avenue for future research. There are still knowledge gaps, however, and there remains a lack of mechanistic study of OMVs in sophisticated cancer models (e.g., orthotopic BrCa studies), as well as consistent issues with OMV toxicity due to OMV derivation from pathogens(*485*). Use of attenuated OMVs is now becoming prominent, but further research using commensal derived OMVs would represent an ideal methodology to combat undesirable side effects.

1.4. Research aims and objectives

The gut microbiota has emerged as a frontier of cancer research over research decades. Microbial modulation of the host immune response has been validated repeatedly as a viable effector mechanism for cancer therapy, yet bacterial therapies have not yet made it to the clinic. One of the key reasons for this, is a poor understanding of the molecular mechanisms of action of protective bacteria against cancer, as most research is currently limited to associations and observational changes. To progress the field forward, detailed knowledge of the host immunological mechanism driving anti-cancer responses, alongside the microbial active compounds responsible for initiating those responses, is vital for more effective clinical translation. More mechanistic knowledge allows better patient stratification (through more informative biomarkers) and more flexibility in therapeutic delivery (live bacteria, or isolated active compounds). From prior literature, *Bifidobacterium* and *Bacteroides* strains have received particular attention for having close associations with positive cancer outcomes. Broadly, the aims of this thesis are to assess therapeutic potential and decipher clear mechanisms of action for therapeutic bacteria. Specifically, we aim to:

1) Characterise the breadth of therapeutic utility of various species of *Bifidobacterium* against BrCa when delivered orally to the gut microbiota

2) Identify and experimentally validate specific host-driven mechanisms of action of a promising therapeutic strain of *Bifidobacterium*

3) Validate the bacteria-produced active compounds driving the host anti-cancer response

4) Determine the potential of *Bacteroides thetaiotaomicron* OMVs as anti-cancer therapeutics when administered systemically (bypassing the commensal gut microbiota)

2. Materials and methods

2.1. Mouse models

C57 BL/6 mice were purchased and maintained in-house at the Disease Modelling Unit at the University of East Anglia. BALB/C mice were purchased from Charles River and maintained in-house. Animals used throughout were age 8-12 weeks and were randomly mixed between cages prior to experiment onset. All animal experiments were performed in accordance with UK Home Office regulations and the European Legal Framework for the Protection of Animals used for Scientific Purposes (European Directive 86/609/EEC).

2.1.1. Orthotopic breast tumour models

Synergic breast cancer cells were injected in 50μl of a 1:1 mixture of phosphate buffered saline (PBS) and Matrigel (Corning Life Sciences, Corning, USA) into the left inguinal mammary fat pad of age-matched female mice. PyMT-BO1, E0771 and 4T1 cells were each injected $1x10^5$ and BRPKp110 cells were injected at $5x10^5$. The experimental duration for each breast model used is outlined in the associated figures. *In situ* tumour volumes were measured thrice weekly with digital calipers from the onset of a palpable tumour, using the formula: length x $width^2$ x 0.52(*486*).

2.1.2. Subcutaneous melanoma and lung carcinoma tumour models

$4x10^5$ B16F10 melanoma or $1x10^6$ CMT19T lung carcinoma cells were administered subcutaneously into the flank of age-matched male mice in 100μl of PBS. Tumours were allowed to develop until day 15 (B16F10) or day 18 (CMT19T).

2.1.3. B16F10 experimental metastasis model

$1x10^6$ B16F10 cells were injected intravenously (IV) into the tail vein of age matched male and female mice. Tumour cells were allowed to seed at metastatic sites until day 14 before harvest of metastatic tissues.

2.2. *In vivo* experiments

2.2.1. Bacteria and bacterial product administration

Animals were orally administered thrice weekly with live *Bifidobacterium* strains ($1x10^{10}$ CFU/200μl) or isolated EPS (80μg/200μl) from the onset of a palpable tumour to endpoint. For OMV experiments, OMVs were administered via intraperitoneal injection thrice weekly or intravenously every three days from the onset of a palpable tumour. Treatments were administered on tumour model-specific outlines as detailed in the experimental workflow figures.

2.2.2. Cyclophosphamide chemotherapy experiments

Following the formation of palpable tumours, cyclophosphamide (Sigma) was administered by intraperitoneal injection at 100mg/kg on days 10 and 17 (for BRPKp110 experiment) or days 7 and 14 (PyMT-BO1 experiment).

2.2.3. aPD-1 immune checkpoint experiments

Tumour-bearing animals were intraperitoneally administered 20mg/kg anti-PD-1 mAb (Clone J43, BioXCell) or matched isotype control on day 7, 10, 13 (4T1 experiment) or day 10, 13, 16, 19 (BRPKp110 experiment).

2.2.4. aCD-8 depletion experiment

Cellular depletion was induced through intraperitoneal injection of 400μg anti-CD8-α (clone 2.43, BioXCell) or matched isotype control mAb one day prior to *Bifidobacterium* administration (day 9), followed by 200μg injections thereafter on days 13, 16, and 19. Depletion was verified by flow cytometry of primary tumour immune cells.

2.2.5. FITC dextran analysis of gut permeability

Mice were orally administered FITC-Dextran solution (44mg/100g) (Sigma) 2 hours prior to sacrifice. FITC was detected in serum samples by fluorescence spectrophotometry (excitation:490nm, emission:530nm).

2.2.6. Antibiotic administration

BRPKp110 tumour-bearing animals were treated with antibiotics by oral gavage (200μl in water vehicle) on day 3, 6 and 8 prior to therapeutic intervention. The antibiotic cocktail contained 1mg/ml Amphoteracin B, 25mg/ml Vancomycin, 50mg/ml Neomycin

and 50mg/ml Metronidazole (all purchased from Sigma). Animal drinking water was also supplemented with 1mg/ml Ampicillin (Sigma).

2.2.7. Mammary tumour microbiome experiment

BRPKp110 tumours were allowed to develop until day 13, when *Bifidobacterium* or vehicle control (PBS) was administered at $1x10^{10}$ CFU/200μl. On day 14, animals were sacrificed, and tumours harvested following the dissection outline from Fu et al(*408*). Tumour dissection was carried out in a sterile tissue culture hood using autoclaved tools, with care taken to avoid contamination of tumour tissue with human or mouse skin. For bacterial isolation, tumour pieces (around 200mg) were homogenised with in an Eppendorf in 1ml of chilled PBS. A PBS-only control was exposed to autoclaved tools taken through the experimental process, serving as the environmental control. For bacterial culture, 100μl of tissue homogenate was plated on the following growth mediums and conditions. Aerobic culture: Columbia blood agar (Oxoid) + 5% horse blood, Man Rogosa Sharpe (MRS) agar (Oxoid), and brain heart infusion (BHI) (Oxoid) at 37°C (+ 5% CO_2) aerobically for 5 days. Anaerobic culture: MRS agar (+ 50mg/L L-cysteine) and BHI agar (+ 50mg/L L-cysteine) at 37°C (+ 5% CO_2) anaerobically for 3 days. Upon completion of incubation, culture plates were sealed and stored at 4°C until used for DNA extraction.

DNA extraction was performed according to Serghiou et al.(*487*). All colonies on agar plates corresponding to an individual tumour were picked using a sterile loop and inoculated in 400μl of sterile PBS. The inoculate was transferred to a 2ml Lysing Matrix E tube (MPBio) with 3 μl of Thermo Fischer lysozyme (diluted to 250 U/μl in Tris-EDTA Buffer) and incubated under agitation at 300 RPM at 37°C for 18 hours. Samples were then incubated for 3 minutes in the Qiagen Tissue Lyser instrument at 20 Hz. Samples underwent off-board lysis at 68°C for 15 minutes with the addition on 40μl proteinase K, 165μl Buffer ATL, 120μl of 1μg/μl Carrier RNA, and 315μl Buffer ACL (all purchased from Qiagen). The samples were centrifuged at 14000 g for 15 minutes and bacterial cell supernatants were loaded onto the Maxwell® RSC 48 Instrument for DNA extraction using the Maxwell® RSC Blood DNA Kit, following the manufacturer's instructions. The recovered DNA was measured using a Qubit® 2.0 fluorometer (Invitrogen), with sequencing and bioinformatic processes conducted as outlined in sections 2.9.2. and 2.9.3. respectively.

2.2.8. Nano-luciferase OMV (OMV^{NLuc}) in vivo tracking

Nano-luciferase OMV (OMV^{NLuc}) experiments were conducted in collaboration with the Carding laboratory (Quadram Institute, Norwich, UK). Nano-luciferase was genetically inserted into parental *Bacteroides thetaiotaomicron* (Bt) VPI-5482(*488*), then $OMVs^{NLuc}$ were isolated according to the section 2.3.4. For *in vivo* tracking, $1x10^{10}$ OMV^{NLuc} (or respective vehicle controls, as outlined in the figures) were IV injected into the tail vein of B16F10 tumour-bearing (D10) mice. Animals were sacrificed at 3-hours post-dose and organs were excised, immersed in sterile PBS, blotted dry, and an arranged in large petri dishes. Organs were then immersed in 10ml of nano-luciferase substrate furimazine (Nano-Glo luciferase assay system kit, Promega, UK) at a 1:20 dilution in PBS. Immersed organs were left for 5 minutes and then imaged using the Bruker In-Vivo Xtreme (Bruker, Coventry, UK) machine. A pre-set of 1 minute exposure bioluminescence image was used, with ROIs drawn around each organ and bioluminescent quantification conducted using ImageJ software.

2.3. Bacterial culture and preparation

2.3.1. Bifidobacterium

All *Bifidobacterium* strains used for this study were isolated previously by the laboratory of Prof. Lindsay Hall. The strains were cultured at 37°C in MRS broth with L-cysteine (50mg/L) (Sigma) in an anaerobic chamber (Don Whitley Scientific, Bingley, UK). Strains were cultured for one week and then preserved by lyophilisation in the exponential phase of growth. Lyophilised bacteria were equally distributed across individual dosage vials which were stored at -80°C. To ensure accurate dosing, at least 3x vials from each lyophilisation batch were enumerated by counting CFUs on MRS agar plates across serial PBS dilutions. The mean CFU was calculated for each batch and vials were resuspended in PBS (to $1x10^{10}$ CFU/200μl/animal) immediately prior to experimental administrations. Strains LH13 and LH14 were cultured in Wilkins-Chalgren anaerobe broth under the same conditions as above and lyophilised by Cultech Ltd, Port Talbot, UK.

2.3.2. Peracetic acid preparation of killed bacteria

For acid-killed experiments, peracetic acid pre-treatment of bacteria was performed as previously described(*489*). Briefly, lyophilised bacteria were reconstituted in 10ml of sterile PBS at a concentration of ~$1x10^{10}$ CFU/ml. Peracetic acid (Sigma) was added to

a final concentration of 0.4% and bacteria were incubated at RT for 1 hour. The bacteria were washed three times in sterile PBS and then resuspended to the appropriate final concentration for animal administrations. Bacterial killing was confirmed by culturing 100μl of acid-killed bacteria on MRS agar under aerobic conditions (outlined in section 2.3.1.) and validating the absence of bacterial growth.

2.3.3. Exopolysaccharide isolation and purification

The Hall laboratory (Technical University of Munich, Munich, Germany) conducted EPS isolation and purification based on the protocol by Ruas-Madiedo (2021)(*490*). A 20ml bacterial suspension in MRS broth was cultured overnight at 37°C under anaerobic conditions. 200µl of the liquid culture were plated on MRS + L-cysteine (50mg/L), MRS + L-cysteine (50mg/L) + fructose, or MRS + L-cysteine (50mg/L) + arabinose agar plates and incubated for 96 hours anaerobically at 37°C. The bacterial lawn was harvested by adding 1ml of MilliQ water to the plate and scraping with a spreader. This step was repeated as required. One volume of 2M NaOH was added to the harvested bacterial biomass and the resulting solution was stirred gently for 16 h at 150rpm. Next, the bacterial biomass solution was centrifuged for 25 minutes at 9200 rpm at 4°C and the resulting supernatant was collected. EPS was precipitated by adding two volumes of ice-cold absolute ethanol to the supernatant and storing at 4°C for at least 48 hours. The precipitated mixture was centrifuged for 25 minutes at 9200 rpm at 4°C. The supernatant was discarded, the precipitate was dissolved in 10ml MilliQ water and transferred to a pre-soaked Spectra/Por® Dialysis Membrane (Spectrum Laboratories, Inc., USA) with a molecular weight cut off of 8,000 or 10,000 Da. The dissolved precipitate was dialysed against MilliQ water with a daily water change for at least 48 hours. The dialysis product was transferred to sterile empty petri dishes (5ml/petri dish), covered with parafilm which was then poked, and lyophilized overnight using Alpha 1-4; CHRIST LOC-1m (Christ, Germany) lyophilizer. The lyophilized crude EPS (cEPS) was harvested using a 10µl sterile plastic loop, transferred to a sterile cryotube and stored at 4°C.

20mg of crude EPS were dissolved in 4ml of Buffer I (50 mM Tris-HCl pH 7.5, 10 mM MgSO4*7H2O), after which 1000x stock of DNase I (dissolved in Buffer I) was added to a final concentration of 5.5µg/ml. The solution was gently stirred on a shaker at 37°C for 6 hours. Then, stock of 100x Pronase E dissolved in Buffer II (50 mM Tris-HCl pH 7.5, 2% EDTA pH 7-8) was added to a final concentration of 50µg/ml. The solution was gently stirred on a shaker for 18 hours at 37°C. As a next step, 60% TCA

were added to a final concentration of 12%. The solution was transferred to 2ml Eppendorf tubes and incubated on a shaker at 21.5°C for 30 minutes at 350rpm, after which it was centrifuged at 13000 g for 25 minutes at 4°C. The supernatant was collected and adjusted to a pH of 5 with 10M NaOH. The solution was transferred to a pre-soaked Spectra/Por® Dialysis Membrane (Spectrum Laboratories, Inc., USA) with a molecular weight cut off of 10,000 Da and dialysed against MilliQ H2O at 4°C for 48 hours with a daily water exchange. The dialysed sample was then lyophilised and transferred to a sterile cryotube and stored at 4°C.

2.3.4. *Bacteroides thetaiotaomicron* OMV generation and quantification

OMV isolations were conducted by the Carding laboratory (Quadram Institute, Norwich, UK). Bt VPI-5482 was grown anaerobically at 37°C in BHI medium (Oxoid) or *Bacteroides* defined media (BDM)(*393*) supplemented with 15 μM hemin. Bt OMVs were purified as previously described(*491*). Briefly, Bt cultures were centrifuged at 5500 *g* for 45 min at 4°C and the supernatants filtered through 0.22-μm polyethersulfone membranes (Sartorius). The supernatants were concentrated by ultrafiltration (100 kDa MWCO, Vivaflow 50R, Sartorius) and rinsed with 500 mL of PBS. OMV solutions were concentrated to 1 ml in sterile PBS and filtered through 0.22 μm pore-size syringe-filters (Sartorius). OMVs were stored at 4°C and sterility was confirmed by plating onto BHI–hemin agar. OMVs were characterised (sizes and concentrations) using the ZetaView nanoparticle tracking analyser (Particle Metrix).

2.4. Cancer cell culture

All tumour cell lines were cultured in high glucose DMEM (Thermofisher) supplemented with 10% foetal bovine serum (FBS) (Hyclone, Thermofisher) and 100 units/ml penicillin/streptomycin (Thermofisher). Cells were seeded onto flasks coated with 0.1% porcine gelatin (Sigma) and incubated at 37°C and 5% $C0_2$.

2.5. *In vitro* experiments

2.5.1. THP1-Blue reporter cell culture and assays

THP1-Blue cells were purchased from Invivogen and cultured in RPMI1640 (Sigma) supplemented with 10% FBS (Hyclone, Thermofisher); 1% Penicillin-Streptomycin (Thermofisher), 100 μg/mL Normocin (Invivogen) and 10 μg/mL blasticidin (Invivogen).

For NF-κB activity assays, $1x10^5$ cells were seeded in 96-well plates and cultured for 24 hours with excipients and LPS positive control. NF-κB activity was measured using QUANTI-Blue detection medium (Invivogen) according to the manufacturer's instructions. Absorbance was read at 650nm in a microplate reader (Biotec, USA).

2.5.2. HEK-Blue hTLR reporter cell culture and assays

HEK-Blue hTLR2, HEK-Blue hTLR4, and HEK-Blue hTLR5 cells were all purchased from Invivogen. Cells were cultured in RPMI1640 supplemented with 10% FBS (Hyclone, Thermofisher); 1% Penicillin-Streptomycin (Thermofisher), 100 µg/mL Normocin (Invivogen). TLR2 and TLR4 reporter cells were additionally supplemented with 1x HEK-Blue™ Selection cocktail, and TLR5 reporter cells were supplemented with 30 µg/ml of blasticidin (Invivogen) and 100 µg/ml of Zeocin (Invivogen). For TLR activity assays, reporter cells were seeded at $5x10^4$ cells in 96-well plates in HEK-Blue detection media with experimental interventions and respective positive controls; LTA-BS (TLR2), LPS (TLR4), and recFLA-ST (TLR5), all purchased from Invivogen. Cells were incubated overnight, and absorbance measured at 650nm in a microplate reader (Biotec, USA).

2.5.3. $CD8^+$ T cell co-cultures

$CD8^+$ T cells were isolated from spleens (see section 2.7.1. for spleen cell preparation) using the $CD8a^+$ T Cell Isolation Kit, mouse (Miltenyi Biotec) according to the manufacturer's instructions. Purified $CD8^+$ T cells were cultured in RPMI1640 medium supplemented with 10% FBS, 1% penicillin/streptomycin (Gibco). Cells were seeded at $2x10^5$ cells per well of a 96-well plate in combination with the indicated treatment. After 24 hours, supernatants were analysed for cytokine levels by MSD multiplex assay.

2.5.4. Bone marrow dendritic cell (BMDC) co-cultures

BMDCs were generated from flushed bone marrow from tibias and femurs of C57 BL/6 mice. Isolated bone marrow was treated with red blood cell lysis buffer for 5 minutes, washed twice in PBS, and cultured overnight in RPMI1640 medium supplemented with 10% FBS, 1% penicillin/streptomycin (Gibco), 20ng/ml IL-4 (R&D) and 10ng/ml GM-CSF (R&D). On the second day, supernatant with non-adherent cells was removed and culture media replaced. Cell culture medium was replaced again on the fifth day, and semi-adherent BMDCs were collected on the seventh day for experimental use. Purified BMDCs were seeded at $2.5x10^5$ cells per well in 24 well plates, incubated for

48 hours with indicated treatments and LPS positive control, then analysed by flow cytometry for markers of cell maturation.

2.5.5. Alamar Blue tumour cell viability assay

PyMT-BO1 or B16F10 cells were seeded onto 96-well plates at 2000 cells/well for 24 hours, then exposed to the indicated treatments for a further 24 hours. The cells were then incubated AlamarBlue™ Cell Viability Reagent (A50100, Invitrogen) for 4 hours. Fluorescence intensity was measured at 590nm.

2.5.6. Tumour cell cycle and apoptosis analysis by flow cytometry

Cell cycle analysis with propidium iodide (PI) and intracellular Ki67 quantification was performed simultaneously as previously described(*492*). Briefly, $1x10^6$ cells/sample were washed in 10ml of PBS and then resuspended in 0.5ml PBS. Then, 4.5ml of pre-chilled (at -20°C) 70% ethanol was added dropwise under agitation and fixed cells were incubated at -20°C for 2 hours. Samples were washed twice with FACS buffer (2% FBS in PBS) and stained with Ki67-BUV395 antibody (BioLegend, 1/50) for 30 minutes. Cells were washed again with FACS buffer, resuspended in 500µl of PI staining solution (50µg/ml propidium iodide (Sigma), 100µg/ml RNaseA, 2µM $MgCl_2$), then analysed by flow cytometry.
For apoptosis analysis, $1x10^6$ cells/ml were washed twice with FACS buffer and then resuspended in Annexin V Binding Buffer (BioLegend, Cat. No. 422201). Cell surface was stained with Annexin V-APC antibody (BioLegend, 1/100) and 5mg/ml PI solution for 15 minutes in the dark (RT) before cytometric analysis.

2.6. Organ histology and immunostaining

2.6.1. Cryo-sectioning snap frozen tumours for immunofluorescence

Harvested tumours were immediately snap-frozen in liquid nitrogen and stored at 80°C. Tumours were then sectioned at 5µm thickness using a Microm HM-560 Cryostat (Thermofisher, Waltham, USA) and stored on slides at -80°C.

2.6.2. Formaldehyde fixed paraffin embedded tissue for histology

Harvested organs were incubated overnight in 4% paraformaldehyde (PFA) at 4°C and processed with the Leica Tissue Processor ASP-300-S (Leica Biosystems, Milton Kenes, UK). The tissues were incubated in formalin, dehydrated through increasing

concentrations of ethanol (from 70% to 100%), washed in three changes of xylene (Sigma-Aldrich) and then embedded in paraffin (Sigma-Aldrich). Paraffin blocks were sectioned at 6µm using a rotary microtome (Leica Biosystems, RM2235), mounted onto positively charged glass slides (Thermofisher), and incubated overnight at 37°C.

2.6.3. Haematoxylin & eosin (H&E) staining

Prior to histological staining, FFPE tissue sections were deparaffinised in xylene (Sigma) and rehydrated through sequentially decreasing concentrations of ethanol (100%-70%), then into water. H&E staining was performed using a Leica ST5020 tissue multi-stainer (Leica Biosystems, Nussloch, Germany) and sections were then mounted with coverslips with Neo-Mount™ (Sigma). Images were captured using the Olympus BX60 microscope (Olympus, Southend-on-Sea, UK) with a microscope camera Jenoptik C10 and ProgRes CapturePro software v.2.10.

2.6.4. Picrosirius red staining and quantification

Snap-frozen tumour sections were air dried at room temperature and then fixed in 4% PFA for 10 minutes. Sections were immersed in Picro-Sirius Red solution (Abcam) for 60 minutes and then washed twice in a 0.5% solution of acetic acid. Sections were dehydrated in three washes in 100% ethanol and cleared in xylene prior to mounting with Neo-Mount™ (Sigma). Brightfield images were captured using an Olympus BX60 microscope and fibrosis was measured using ImageJ software to calculate the intensity of the red staining across individual tumours.

2.6.5. Immunofluorescent staining

Frozen tumour sections were air dried and fixed in ice cold methanol (each for 10 minutes) before washing in PBS/0.1% Tween-20. Sections were blocked using Dako serum-free protein block (Agilent Dako, X0909) and incubated over-night (4^{o}C) with antibodies against Ki67 (ab16667, 1/500, Abcam) and Endomucin (sc-65495, 1/500, Santa-Cruz) diluted in PBS/1% donkey serum. Sections were incubated in Alexa Fluor 594- Donkey anti-Rat IgG secondary antibody (A-21209, 1/1000, Thermo) or Alexa Fluor 488-Donkey anti-Rat IgG secondary antibody (A-21206, 1/1000, Thermo) blocked in Sudan Black B (Sigma) and mounted with Fluoromount-G with DAPI (eBiosciences). Images were captured using the Zeiss Axioplan 2ie widefield microscope (Carl Zeiss Microscopy, Jena, Germany) and processed using imageJ.

2.6.6. TUNEL staining

Apoptotic cells within frozen tumour sections were visualised using a Click-iT™ TUNEL Alexa Fluor™ 594 Imaging Assay (Thermofisher) following the manufacturer's instructions. Images were captured using the Zeiss Axioplan 2ie widefield microscope and processed using imageJ.

2.7. Flow cytometry

2.7.1. *In vivo* tissue single cell isolation

Tumours and lungs were excised and mechanically homogenised using scalpels. Tumours were digested in 0.2% collagenase IV (Thermofisher) and lungs in 0.2% collagenase I (Thermofisher), with 0.01% hyaluronidase (Sigma) and 0.01% DNase I (in HBBS) at 37°C under agitation for 60 minutes (tumours) or 30 minutes (lungs). Tissues were then passed through a 70µm filter (Thermofisher) and washed in PBS before further staining. Spleens and lymph nodes were mechanically dissociated through 70µm strainers. Lymph nodes were immediately processed for staining and tumours, lungs and spleens were resuspended red blood cell lysis buffer (Thermofisher) for 5 minutes. Cells were washed in PBS and counted, with 1 million cells being stained per sample in FACS buffer (2% FBS in PBS).

2.7.2. Cell staining protocol

For intracellular cytokine analysis, cells were resuspended in 200µl RPMI supplemented with 10% FBS, 50µM 2-Mercaptoethanol, 50ng/ml Phorbol 12-Myristate 13-Acetate (PMA), 750ng/ml Ionomycin and 10µg/ml Brefeldin-A (all purchased from Sigma) and incubated in a 96-well U-bottom plate (Sigma) at 37°C, 5% CO_2 for 4 hours. Cells were blocked with Fc-receptor blocking reagent (Thermofisher) and incubated in relevant antibody (Table 2.1) and fixable Live/Dead Red (Invitrogen) solutions for 30 minutes (at 4°C in the dark). Cells were washed twice in FACS buffer, fixed with 4% PFA for 30 minutes, and then resuspended in FACS buffer prior to analysis. Where intracellular staining was required, cells were treated using the eBioscience™ Foxp3 / Transcription Factor Staining Buffer Set, as per the manufacturer's instructions, then stained with intracellular antibodies.

2.7.3. Data collection and analysis

Data collection was conducted on the BD LSR Fortessa cell analyser and analysed using FlowJo software (BD). All samples were initially gated using FSC-A vs. FSC-H to identify single cells (Singlets), which were then gated for Live/Dead Red negative. Major immune populations were identified using the marker profiles outlined in Table 2.2.

Table 2.1. List of conjugated flow cytometry antibodies

Target	Conjugate	Clone	Source	Category number	Dilution
CD45	PerCP-Cy5.5	30-F11	Invitrogen	45-0451-02	1:200
CD3	APC	17A2	BioLegend	100236	1:200
CD8a	APC-Cy7	53-6.7	Invitrogen	A15386	1:200
CD44	eFluor450	1M7	Invitrogen	48-0441-82	1:200
CD62L	BV605	MEL-14	BioLegend	104438	1:200
NK1.1	PE-Cy7	PK136	BioLegend	108714	1:200
IFNy	BV711	XMG1.2	BioLegend	505836	1:100
IL-2	PerCP-Cy5.5	JES6-5H4	Invitrogen	45-7021-80	1:100
FOXP3	eFluor450	FJK-16s	Invitrogen	48-5773-82	1:100
CD45	BUV395	30-F11	BD	564279	1:200
CD4	PE	GK1.5.	Invitrogen	12-0041-82	1:200
FOXP3	AF700	FJK-16s	Invitrogen	56-5773-82	1:100
Granzyme B	PE-Cy7	NGZB	Invitrogen	25-8898-82	1:200
CD11b	BV605	M1/70	BD	563015	1:200

Ly6C	eFluor450	HK1.4	Invitrogen	48-5932-82	1:200
Ly6G	APC-Cy7	1A8	BD	560600	1:200
F4/80	APC	BM8	Invitrogen	17-4801-82	1:200
MHCII (I-A/I-E)	PE-Cy7	M5/114.15.2	Invitrogen	25-5321-82	1:200
CD206	FITC	CO68C2	BioLegend	141704	1:200
CD11c	BUV395	HL3	BD	564080	1:200
CD103	BV711	2E7	BioLegend	121435	1:200
Ki67	BUV395	B56	BD	564071	1:100
PD-1	PE-Cy7	29F.1A12	BioLegend	135216	1:200
CD80	Super Bright 600	GL1	Invitrogen	63-0862-82	1:200
CD86	BV421	16-10A1	BD	562611	1:200
CD19	BV650	6D5	BioLegend	115541	1:200
CD107a	eFluor450	104B	Invitrogen	48-1071-82	1:100
GFP	PE-Cy7	FM264G	BioLegend	338014	1:100
Luciferase	AF647	EPR17789	Abcam	ab237252	1:100
IL-4	PerCP-Cy5.5	11B11	BioLegend	504123	1:100
TNFα	PE	MP6-XT22	BioLegend	506306	1:100
Annexin V	APC	N/A	BioLegend	640920	1:50

Ki67	APC	16A8	BioLegend	652402	1:50

Table 2.2. List of flow cytometry gating strategies for the identification of immune cell populations

Population	Gating strategy
Lymphoid cells	Singlet, Live, CD45+, CD3+
T helper cells	Singlet, Live, CD45+, CD3+, CD4+, CD8-
CD8+ T cells	Singlet, Live, CD45+, CD3+, CD4-, CD8+
CD8+ effector memory	Singlet, Live, CD45+, CD3+, CD4-, CD8+, CD62L-, CD44+
CD8+ central memory	Singlet, Live, CD45+, CD3+, CD4-, CD8+, CD62L+, CD44+
Naïve CD8	Singlet, Live, CD45+, CD3+, CD4-, CD8+, CD62L+, CD44-
Treg cells	Singlet, Live, CD45+, CD3+, CD4+, CD8-, FOXP3+
NK cells	Singlet, Live, CD45+, CD3-, NK1.1+
B cells	Singlet, Live, CD45+, CD3-, CD19+
Myeloid cells	Singlet, Live, CD45+, CD11b+
M-MDSCs	Singlet, Live, CD45+, CD11b+, Ly6C+, Ly6G-
G-MDSCs	Singlet, Live, CD45+, CD11b+, Ly6C-, Ly6G+
Macrophages	Singlet, Live, CD45+, CD11b+, Ly6C-, F4/80+
Dendritic cells (DCs)	Singlet, Live, CD45+, CD11c+
cDC1 cells	Singlet, Live, CD45+, CD11c+, MHCII+, $CD103^{hi}$, $CD11b^{lo}$
cDC2 cells	Singlet, Live, CD45+, CD11c+, MHCII+, $CD103^{lo}$, $CD11b^{hi}$
Lung alveolar macrophages	Singlet, Live, CD45+, CD11b+, Ly6C-, F4/80+, $CD11c^{hi}$
Lung interstitial macrophages	Singlet, Live, CD45+, CD11b+, Ly6C-, F4/80+, $CD11c^{lo}$

2.8. Untargeted serum metabolomics

2.8.1. Serum preparation

Blood was collected by cardiac puncture immediately following animal sacrifice by rising level of CO_2. Blood was allowed to coagulate for 30 minutes and then centrifuged at 12000 g for 15 minutes at 4°C. Serum was removed from the separated pellet of coagulated blood and stored at -80°C.

2.8.2. MxP® Quant 500 assay

The untargeted metabolomics assay was performed by Biocrates (Innsbruck, Austria). The commercially available MxP® Quant 500 kit from Biocrates was used for the quantification of endogenous metabolites of various biochemical classes. Lipids and hexoses were measured by flow injection analysis-tandem mass spectrometry (FIA-MS/ MS) using a SCIEX API 5500 QTRAP® (AB SCIEX, Darmstadt, Germany) instrument with an electrospray ionization (ESI) source, and small molecules were measured by liquid chromatography-tandem mass spectrometry (LC MS/MS), also using a SCIEX API 5500 QTRAP@ (AB SCIEX, Darmstadt, Germany) instrument. The experimental metabolomics measurement technique is described in detail by patents EP1897014B1 and EP1875401B1. Briefly, a 96-well based sample preparation device was used to quantitatively analyse the metabolite profile in the samples. This device consists of inserts that have been impregnated with internal standards, and a predefined sample amount was added to the inserts. Next, a phenyl isothiocyanate (PITC) solution was added to derivatise some of the analytes (e.g., amino acids), and after the derivatization was completed, the target analytes were extracted with an organic solvent, followed by a dilution step. The obtained extracts were then analysed by FIA-MS/ MS and CC-MS/ MS methods using multiple reaction monitoring (MRM) to detect the analytes. Concentrations were calculated using appropriate mass spectrometry software (Sciex Analyst®) and data were imported into biocrates' MetIDQ™ software for further analysis

2.8.3. MetaboAnalyst bioinformatic analysis

Metabolomics analysis to generate PCoA plots, heatmaps and differential metabolite comparisons were conducted using the MetaboAnalyst (V5.0) platform. The data was first normalised by sum, $\log_{10}$ transformed, and auto scaled prior to univariate analyses, as described previously(*493*). Differential metabolite levels were compared by two-sample *t* test with statistical FDR threshold value < 0.05. Metabolite abundances were

then input into the MetaboAnalayst platform to allow comparisons of perturbed metabolic pathways, as previously described(*494*).

2.9. Caecal shotgun metagenomics

2.9.1. Caecal DNA extraction

Caecal DNA was extracted using the MPBio FastDNA™ SPIN Kit for Soil (MPBio) following the manufacturers protocol, with an extension of the bead beating time to three minutes. The recovered DNA was validated using a Qubit® 2.0 fluorometer (Invitrogen) prior to library preparation.

2.9.2. Library preparation and sequencing

Sequencing was performed as previously described by McKee (2021)(*355*) and Alikhan (2022)(*495*). A modified Illumina Nextera low input tagmentation approach was used. A master mixture containing 9µL of TD Tagment DNA Buffer, 0.09µL TDE1, Tagment DNA Enzyme and 4.01 µL PCR grade water was loaded at 3µL/reaction to a chilled 96 well plate. Genomic DNA was normalised to 0.5ng/µL with 10mM Tris-HCl. 2µL of normalised DNA (1ng total) was pipette mixed with the 5µL of the tagmentation mix and heated to 55 °C for 10 minutes in a PCR block.

A PCR master mix (4ul kapa2G buffer, 0.4 µL dNTP's, 0.08 µL Polymerase and 4.52 µL PCR grade water) from the Kap2G Robust PCR kit (Merck Life Science) was added at 9µL per samples. 2µL of each P7 and P5 of Nextera XT Index Kit v2 index primers (Illumina) were added to each well. Then, the 7µL of Tagmentation mix was added and mixed. The PCR was run with 72°C for 3 min, 95°C for 1 min, 14 cycles of 95°C for 10s, 55°C for 20s and 72°C for 3 minutes.

Following the PCR reaction, the libraries were quantified using the Quant-iT dsDNA Assay Kit, high sensitivity kit and run on a FLUOstar Optima plate reader. Libraries were pooled in equal quantities. The final pool was double-SPRI size selected between 0.5 and 0.7X bead volumes using KAPA Pure Beads (Roche, Burgess Hill, UK). The final pool was quantified on a Qubit 3.0 instrument and run on a D5000 ScreenTape (Agilent) using the Agilent Tapestation 4200 to calculate the final library pool molarity.

The pool was run at a final concentration of 1.5pM on an Illumina Nextseq500 instrument using a Mid Output Flowcell (NSQ® 500 Mid Output KT v2(300 CYS) following the Illumina recommended denaturation and loading recommendations which

included a 1% PhiX spike in (PhiX Control v3 Illumina Catalog FC-110-3001). Data was uploaded to Basespace (www.basespace.illumina.com) where the raw data was converted to FASTQ files for each sample.

2.9.3. MicrobiomeAnalyst bioinformatic analysis

Primary analysis was conducted using the MicrobiomeAnalyst (V2.0) platform(*496*). Default filtering settings were used to remove low count and low variance and ensure robust results. Total sum scaling was applied and downstream analysis at the phyla and species level was conducted using the platform in-built tools. Analysis included microbiome α diversity (Shannon measure with t-test), β diversity plotted as PCoA (Bray–Curtis distance method), and univariate species abundance comparisons using *t* test (adjusted cut-off < 0.05).

2.10. *Bifidobacterium* comparative genomics analyses

2.10.1. *Bifidobacterium* DNA extraction and WGS

Bacterial pellets were resuspended into MPBio Lysing Matrix E bead beating tubes (MPBio) in sodium phosphate buffer and DNA was extracted using the MPBio FastDNA™ SPIN Kit for Soil (MPBio) following the manufacturers protocol. The recovered DNA was validated using a Qubit® 2.0 fluorometer (Invitrogen).

2.10.2. Comparative genomics sequencing and bioinformatic analysis

Comparative genomics was conducted by Magdalena Kujawska from the Hall laboratory. Genomes of *B. pseudocatenulatum* strains were sequenced as previously described(*497*). The sequencing reads for strains *B. bifidum* LH_80 and *B. animalis* LH_506 were pre-processed with fastp v0.22(*498*) with default settings and assembled using Unicycler v0.4.9(*499*) in “conservative” mode, with the minimum contig length set to 1000bp. The sequencing reads for strain *B. longum subsp. longum* NCIMB 8809 generated on the Illumina instrument were processed with fastp v0.22 as above, while the nanopore reads were processed using a modified Porechop v0.2.4 (https://github.com/rrwick/Porechop) script with “--discard_middle” option to remove custom sequencing adapters. After pre-processing, Unicycler v0.4.9 was used to generate a hybrid assembly using both short and long reads, with the minimum contig length of 1000bp. Completeness and contamination of new assemblies were estimated

at >99.5% and <0.5% at the family level, respectively, using CheckM v1.2.0(*500*). All genomes were annotated with Prokka v1.14.6(*501*).

For EPS genomics comparison, BLAST+ v2.13.0 (blastp e-value of 1e-50)(*502*) was used to screen genomes of the strains used in this study against an in-house *Bifidobacterium* EPS cluster database, built based on previously reported data(*436, 503*). Clinker v0.0.27 was used to visualise homologous comparisons indicative of the presence of potential complete or partial clusters (blastp identity score >50% and/or >5 consecutive genes present in the putative cluster)(*504*).

2.11. *Bifidobacterium* qPCR

Bacterial load was of *B. pseudocatenulatum* LH663 was estimated by qPCR using a species-specific primer (GroEL gene) designed previously by Junick and Blaut (2012)(*505*). The reactions were performed in duplicate in 12.5μl of LightCycler® 480 SYBR Green I Master (Roche Diagnostics, cat. 0470751600), 2.5μl of forward and reverse 10μM primers, 7.3μl of RNase-free water (Qiagen), and 0.2μl of template DNA. Standard curves were generated by serial dilutions of 100 ng/μL of monoculture-extracted DNA to reach the lowest concentration of 0.001 ng/μL. Samples were run on the LightCycler® 480 system (Roche) with the programme as follows: 5 minutes incubation at 95 °C, followed by 45 cycles with 15 seconds at 94°C, 15 seconds at 64°C and 15 seconds at 72°C. The melting curve analysis followed with 5 seconds at 95°C, 5 minutes at 65°C and continuous temperature increase to 97°C. Samples were finally cooled to 40°C for 30 seconds before completion. Data was analysed with the LightCycler® 480 Software (v.1.5) (Roche).

2.12. Mesoscale discovery (MSD) multiplex cytokine arrays

Tissue samples were weighed into a MPBio Lysing Matrix E bead beating tube (MPBio) with 1ml of homogenisation buffer (150 mmol/L NaCl, 20 mmol/L Tris, 1 mmol/L EDTA, 1 mmol/L EGTA, 1% Triton X-100, pH 7.5+ cOmplete™ protease inhibitor (Roche)). An MPBio Fast Prep bead beater (MPBio) was used to homogenise the tissues at a speed 4.0 for 40 seconds, followed by speed 6.0 for 40 seconds. Samples were centrifuged at 12,000 x g for 12 minutes (4°C) and then stored at −80°C until analysed. Samples were run on a custom Mesoscale Discovery U-PLEX Mouse

Kit (MSD) according to the manufacturer's instructions. Plate was read using an MSD QuickPlex SQ 120 imager (MSD, Rockville, MD, USA).

2.13. *Bifidobacterium* exopolysaccharide structural analyses

2.13.1. Monosaccharide composition analysis by alditol acetate derivatisation

Glycosyl composition analysis was performed by combined gas chromatography-mass spectrometry (GC-MS) of the alditol acetates (AAs) as described by Peña et al. (2012)(*506*). The exopolysaccharide sample was hydrolysed in 2M trifluoroacetic acid (TFA) for 2 hours in a sealed tube at 120 °C, reduced with $NaBD_4$, and acetylated using acetic anhydride/TFA. The resulting alditol acetates were analysed on an Agilent 7890A GC interfaced to a 5975C MSD, electron impact ionisation mode. Separation was performed on a 30-m Supelco SP-2331 bonded phase fused silica capillary column.

2.13.2. Glycosyl linkage analysis

Glycosyl linkage analysis was performed by combined gas chromatography-mass spectrometry (GC-MS) of the partially methylated alditol acetate (PMAA) derivatives produced from the sample. The procedure is described by Anumula and Taylor (1992)(*507*). Briefly, permethylation of the sample was achieved by two rounds of treatment with sodium hydroxide (15 minutes) and methyl iodide (30 minutes). The sample was then hydrolysed using 2M TFA (2 hours in sealed tube at 120 °C), reduced with $NaBD_4$, and acetylated using acetic anhydride/TFA. The resulting PMAAs were analyzed on an Agilent 7890A GC interfaced to a 5975C MSD (mass selective detector, electron impact ionisation mode); separation was performed on a 30 m Supelco SP-2331 bonded phase fused silica capillary column for the neutral residues and an EC-1 column for the amino containing residue.

2.14. Statistical analysis

Statistical analyses were performed using GraphPad Prism 9 software. Unless otherwise stated, Kolgorov-Smirnov tests were performed to confirm normality of data and Student's *t*-test (unpaired, two-tailed, at 95% confidence interval) were using to generate *P*-values. Where multiple *t*-tests were performed, a false discovery rate (FDR) of $q<0.05$ was used. Significant observations are represented according to the

following annotation: ****$P < 0.001$, ***$P < 0.001$, **$P < 0.01$, *$P < 0.05$. In some figures, raw *P*-values which did not meet statistical significance are presented next to the corresponding data. Where no *P*-value is presented, statistical analyses did not identify a significant observation. Full details of specific statistical tests performed corresponding to each dataset can be found the respective figure legends.

3. *Bifidobacterium* have broad anti-cancer properties in murine cancer models and can enhance response to standard of care treatments

Inconsistent patient responses to standard of care therapy are one of the great challenges within cancer research. Over recent decades, particularly with the clinical translation of checkpoint immunotherapy, it has become clear that a host-intrinsic factors could underlie key roadblocks to a consistent clinical benefit(*122*). The mechanisms defining host-intrinsic factors which influence cancer progression, beyond genetics, are poorly understood and thus difficult to meaningfully target(*508-510*). Major advances in metagenomic sequencing technologies have spurred influx of research into the microbiome and have revealed concrete links to cancer(*511*). These studies began as largely correlative(*512, 513*), but have now progressed to deeper mechanism-based understandings of how the microbiome can be manipulated to improve cancer outcomes(*365, 376, 514*).

A common thread through many studies showing beneficial manipulation of the microbiome is the presence and activity of lactic acid bacteria, particularly *Bifidobacterium(515)*. The mechanisms of action of *Bifidobacterium spp.* in protection against cancer have predominantly centred around the activation of the adaptive immune system (i.e., activation of inflammatory $CD8^+$ and/or T helper cells by dendritic cells), but the key bacterial drivers to obtain this have been encouragingly varied. Some examples include the production of immune modulatory metabolites(*363*), cell wall structural components(*387*) and even evidence for direct translocation of *Bifidobacterium* from the gut to the tumour(*409*). Importantly, human cohort studies are also revealing that reduced abundances of *Bifidobacterium* in cancer patients negatively correlate with clinical outcomes across multiple indications(*351, 352*), supporting the rationale for using *Bifidobacterium* therapeutically in humans.

The continued association of this genus with beneficial cancer outcomes, alongside highly varied mechanisms of action, suggests that *Bifidobacterium* could have huge untapped potential in the treatment of cancer, and may represent a well-tolerated adjuvant approach to improving cancer therapy responses. A better understanding of how widely beneficial *Bifidobacterium* are for cancer outcomes, alongside more detail on key mechanistic determinants, could allow for future *Bifidobacterium*-based

therapies which utilise multiple microbial pathways synergistically to induce even more profound reductions in cancer progression. To assess the first of these key points, the work in this chapter sought to understand the broader utility of the *Bifidobacterium* genus in cancer protection and therapy. Using a suite of different strains from different species, both in isolation and combination, *Bifidobacterium spp*. displayed a remarkable ability to inhibit tumour progression across multiple models of breast cancer and melanoma, as well as enhancing therapeutic response to standard of care therapies. Of note was the therapeutic potential of a strain of *Bifidobacterium pseudocatenulatum*, with this species yet to be characterised in the context of a cancer therapeutic.

3.1. A four-strain *Bifidobacterium* cocktail effectively reduces luminal A breast cancer primary tumour burden and early metastatic dissemination

In order the study the effects of the *Bifidobacterium* genus, we employed several unique pre-clinical cancer models. Our predominant focus was breast cancer, and in the first instance we utilised the BRPKp110 HR^+ luminal A-like tumour model previously characterised by Allegrezza (2016)(*516*) and Rosean (2019)(*356*). These tumour cells were orthotopically engrafted into the inguinal mammary fat pad, and following formation a solid palpable mass, we began therapeutic intervention with *Bifidobacterium* thrice weekly to endpoint (Figure 3.1A). To provide a broad assessment for the potential of *Bifidobacterium* in inhibiting breast cancer, we combined four different strains from four different species (*B. bifidum*, *B. pseudocatenulatum*, *B. animalis* and *B. longum subsp. longum*) into a bacterial cocktail (*Bif* cocktail*)* which was orally administered. Assessment of endpoint BRPKp110 tumour volumes showed that intervention with the *Bif* cocktail was successful in inhibiting primary tumour growth (Figure 3.1B). Despite primary tumour reduction being a key metric for the action of a cancer therapeutic, metastatic spread of the primary tumour cells to distal organs remains the major cause of mortality in breast cancer(*517*). Due to the poorly metastatic nature of the BRPKp110 model, we were unable to use histological techniques to assess this metastatic outgrowth due to the absence of overt legions. To overcome this, resolution at the single cell level was necessary to identify changes in these early metastatic stages. Using flow cytometry, we assessed the lungs of BRPKp110 tumour-bearing animals at experimental endpoint for the presence of GFP, which had been tagged on the BRPKp110 cells. Use of non-

tumour bearing controls and relevant FMOs validated the approach, and comparison between groups revealed that administration of the *Bif* cocktail inhibited the metastatic dissemination of GFP+ BRPKp110 to the lungs to near statistically significant levels, despite a low number of replicates (Figure 3.1C-D).

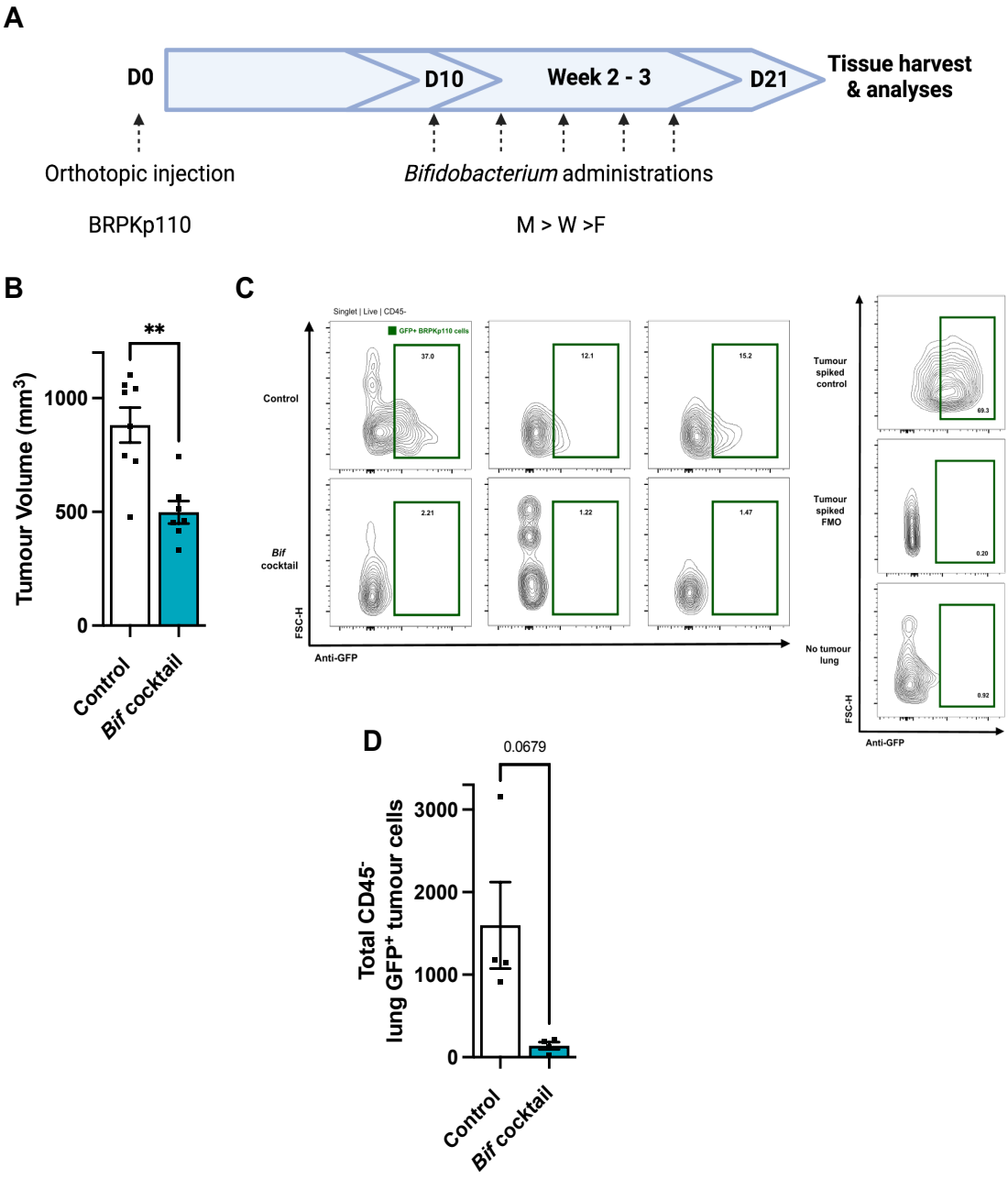

Figure 3.1. A four-strain *Bifidobacterium* (*Bif*) cocktail reduces luminal A breast tumour growth and early metastasis. (A) Experimental design BRPKp110 tumour growth experiments. C57 BL/6 mice were orally dosed with ~1x10^{10} CFU/ml *Bifidobacterium* thrice weekly upon the onset of a palpable tumour (day 10). (B) Primary tumour size (± SEM) of *Bif* cocktail-treated animals compared with PBS vehicle control. n=7-8 mice per group. (C) Representative flow cytometry plots of treatment and control groups for the assessment of GFP^+ BRPKp110 cell infiltration into the lungs of primary tumour-bearing animals. (D) Quantification of GFP^+ BRPKp110 cell infiltration to the lungs following treatment with the *Bif* cocktail, n=4. (B and D) Quantifications represent mean (± SEM), with statistical significance calculated by two-tailed unpaired t test. $^{**}P < 0.01$, $^{*}P < 0.05$.

Existing research across the field has shown that the immune system is the most common effector pathway initiated by *Bifidobacterium* spp. upon successful inhibition of cancer progression in pre-clinical models(*362, 386, 515*). To gain an initial understanding of how the administration of the *Bif* cocktail may have been specifically inhibiting BRPKp110 tumour progression, we undertook multi-parameter flow cytometry of primary tumours to measure the infiltration of several key immune populations spanning the innate and adaptive arms of the immune system (Figure 3.2A). This analysis revealed no significant alterations in infiltration of these populations, or any alterations in the polarisation of T cells across their major subsets ($CD8^+$, T helper and Treg), which have typically been implicated in pre-clinical studies showing beneficial effects of the microbiome against cancer (Figure 3.2B). Although gross infiltration of immune cells only provides a limited information on the relevance of immune cells within tumours (i.e., only showing cell presence rather than activity), these data did suggest that the mechanism of the *Bif* cocktail against BRPKp110 tumours may differ from previously published research.

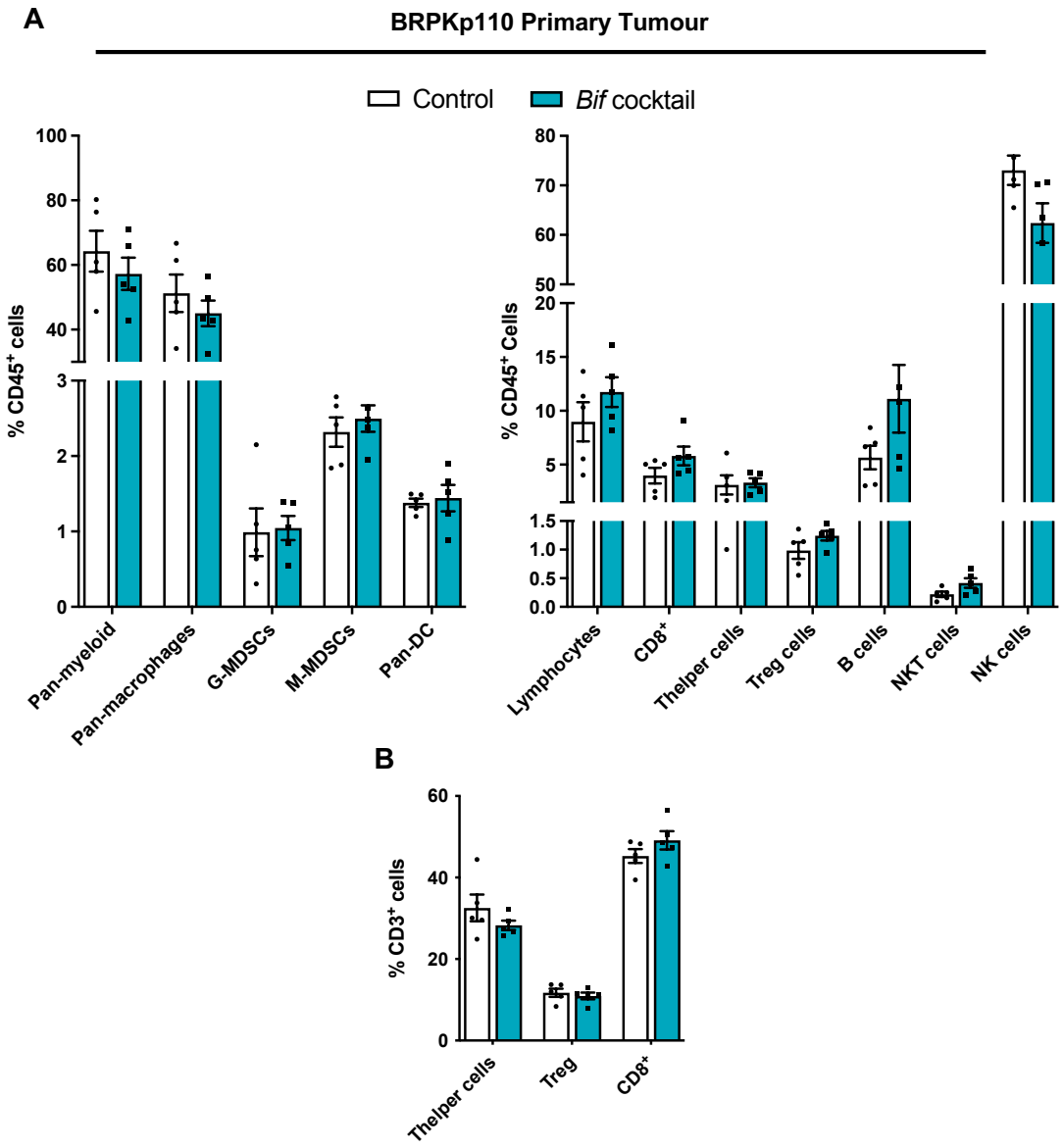

Figure 3.2. Administration of a four-strain *Bif* cocktail does not induce changes to immune cell infiltrate in BRPKp110 primary tumours. (A) Quantification infiltration of primary tumour myeloid (left) and lymphoid (right) populations by flow cytometry as a percentage of total CD45⁺ immune cells. (B) Quantification of major tumour infiltrating T cells as a percentage of total CD3⁺ lymphocytes. Data shows the mean values (± SEM), n=5.

3.2. Comparative testing of *Bifidobacterium spp.* reveals several strains capable of reducing luminal B breast tumour growth

Whilst the results of the BRPKp110 tumour experiment showed valuable evidence for the potential of *Bifidobacterium* as a novel therapeutic against breast cancer, the important question of mechanism remained open. We reasoned that whilst the use of a *Bif* cocktail provided proof of concept, it would become difficult to unpick the downstream mechanism of action of the *Bifidobacterium* due to the presence of four different strains from different species. Beyond the challenge of four different experimental variables, these strains have the potential to have unique mechanisms of action, interact with or inhibit each other, or differentially interact with other members of the commensal microbiota. The effect of just one of these factors would make gaining a clear mechanism of action highly challenging. To allow a more realistic downstream route to discovering mechanism, we next conducted parallel testing of the *Bif* cocktail against each of the cocktail's constituent strains individually. Alongside this experimental setup, we also used a second model of breast cancer, the PyMT-BO1 luminal B-like model, which is more aggressive than the previously tested BRPKp110 model. Using a similar outline to prior experiments, we allowed orthotopically engrafted PyMT-BO1 tumours to grow to a palpable mass before thrice weekly oral administration of the relevant interventions of *Bifidobacterium* (Figure 3.3A). Analysis of the endpoint PyMT-BO1 tumour volumes showed, in contrast to the BRPKp110 tumour experiments, administration of the *Bif* cocktail did not significantly inhibit primary tumour growth. Despite this, three out of the four individually administered strains (*bifidum*, *pseudocatenulatum* and *animalis*) were successful in inhibiting PyMT-BO1 tumour growth, whilst only the species of *B. longum* was ineffective. These results suggest both that the combination of several individually effective strains does not always cause an additive effect on efficacy, and that the presence of an ineffective strain within a therapeutic consortium (i.e., *B. longum 8809*) can nullify the protective properties of other beneficial members.

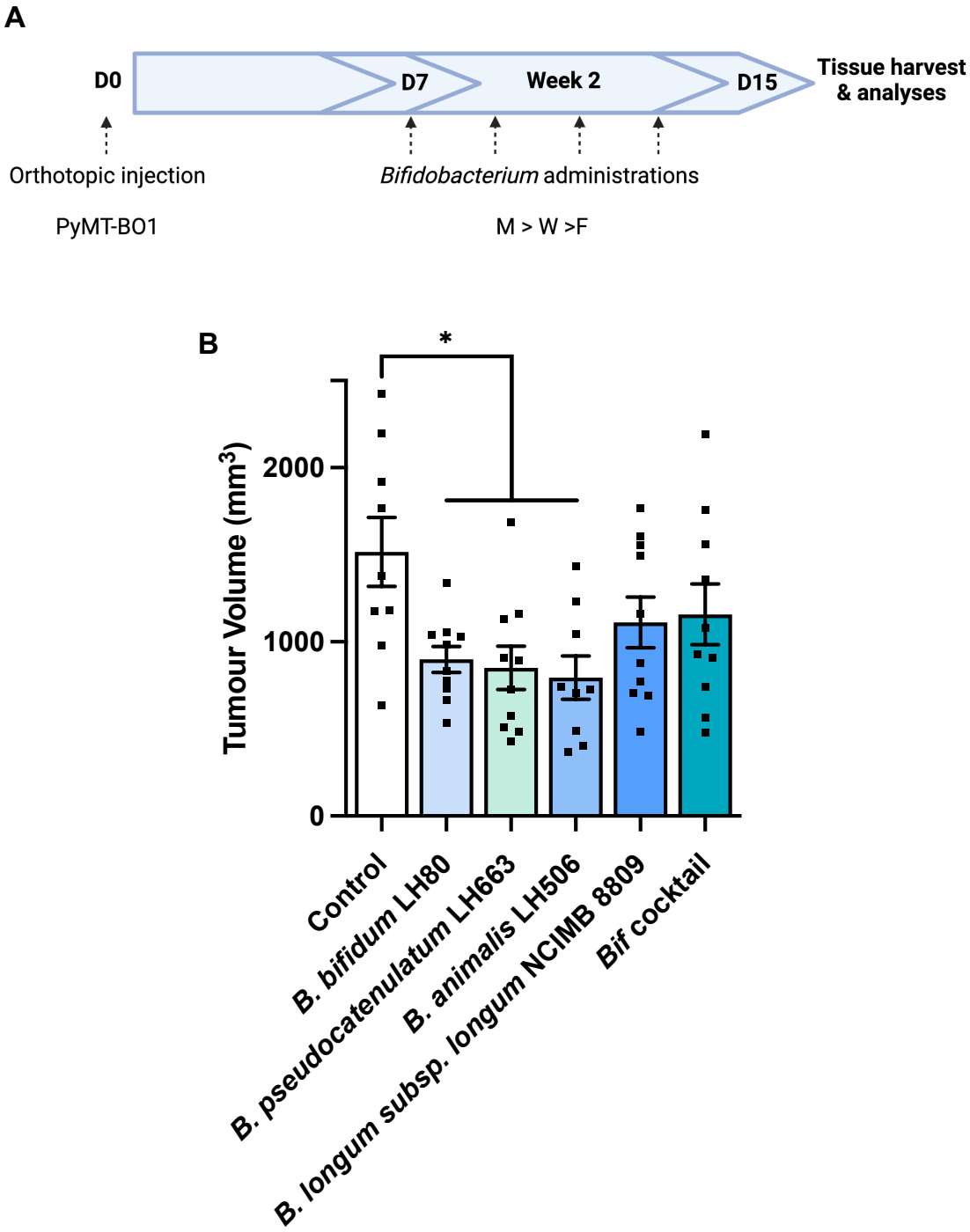

Figure 3.3. Several strains of *Bifidobacterium* can reduce PyMT-BO1 luminal B breast tumour burden. (A) Experimental outline for PyMT-BO1 tumour experiments. *Bifidobacterium* strains are orally administered, at an approximate dose of $1x10^{10}$ CFU, thrice weekly upon the onset of a palpable tumour (day 7). (B) Endpoint PyMT-BO1 tumour volumes following administration of various unique strains of *Bifidobacterium* or four-strain consortia (*Bif* cocktail) comprised of each the individual strains. Data shows mean tumour volumes ±SEM. n=9-10 animals per group. Statistical significance was calculated by one-way ANOVA with Tukey's multiple comparisons test. *$P < 0.05$.

The experimental setup of testing several strains simultaneously provided an opportunity to look for conserved anti-tumour mechanisms from strains which did inhibit tumour growth, compared to treatments which did not. To assess this, we again employed flow cytometry to assess the immune landscape in the PyMT-BO1 tumours, with the additional focus on the polarisation of intra-tumoural $CD8^+$ T cells, which had been implicated in prior research as being modulated by *Bifidobacterium* in other cancer indications(*362*). Analysis revealed that administration of the strain *B. pseudocatenulatum* 'LH663' (LH663) caused the largest polarisation of $CD8^+$ T cells from naïve to effector memory (Figure 3.4A), a significant increase compared with the *Bif* cocktail alongside a corresponding decrease in the percentage of naïve $CD8^+$ T cells (Figure 3.4B).

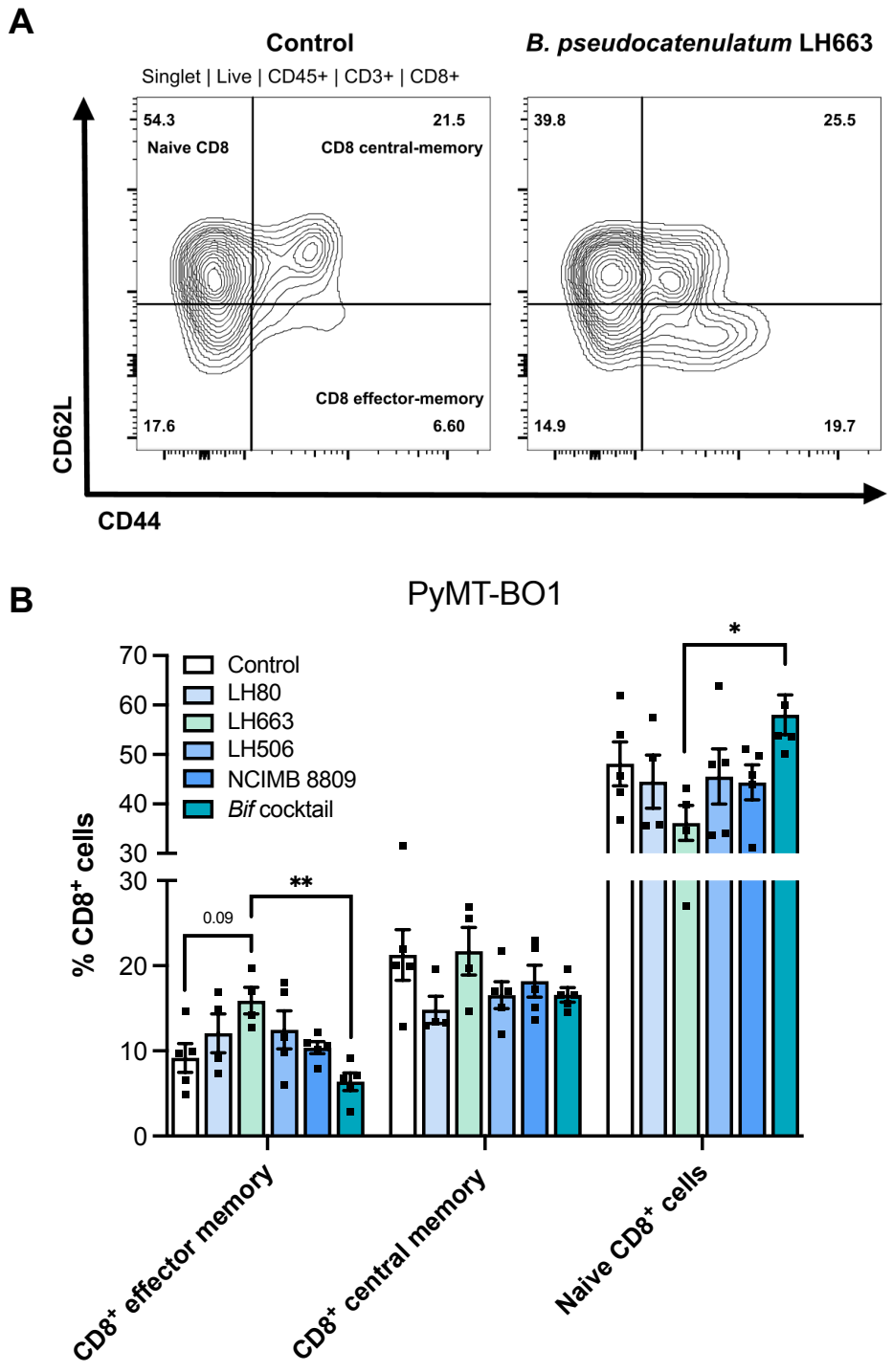

Figure 3.4. *B. pseudocatenulatum* LH663 induces the polarisation of naïve CD8⁺ T cells to CD8⁺ effector memory cells within PyMT-BO1 primary tumours. (A) representative flow cytometry plot showing a pro-inflammatory polarisation of CD8⁺ effector memory cells following administration of *B. pseudocatenulatum* LH663 compared to PBS vehicle control. (B) Quantification of CD8⁺ effector memory polarisation following administration of *Bifidobacterium* treatments. Data show mean values (± SEM), statistical significance was calculated by one-way ANOVA with Tukey's multiple comparisons test. n=4-5. $^{**}P < 0.01$, $^{*}P < 0.05$.

3.3. *Bifidobacterium pseudocatenulatum* 'LH663' inhibits *in vivo* breast cancer progression in luminal and triple negative mouse models

Due to the unique $CD8^+$ activation we observed following strain LH663 administration, we decided to focus on this bacterium as our most promising and mechanistically characterised therapeutic. To further test the potential of LH663 for inhibition of breast cancer, we administered the strain as a monotherapy in both the BRPKp110 and PyMT-BO1 models, showing a significant reduction in primary tumour growth (Figure 3.5A-B).

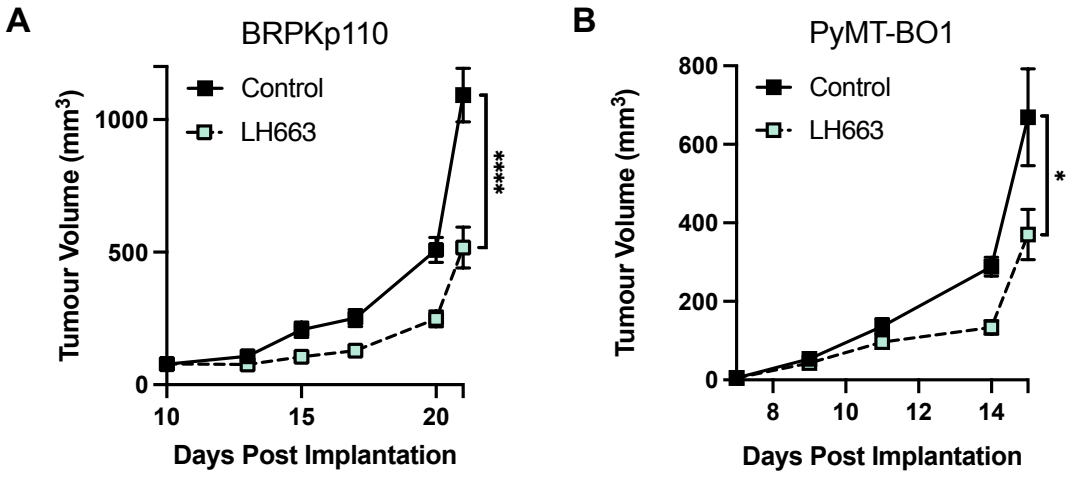

Figure 3.5. *B. pseudocatenulatum* LH663 administration reduces luminal breast tumour burden. Tumour growth over time in (A) BRPKp110 (n=16-18, N=2) and (B) PyMT-BO1 (n=8-9, N=1) luminal breast tumours following administration of *B. pseudocatenulatum* LH663. Data shows mean values (± SEM) with statistical significance calculated by two-tailed unpaired t test. ****$P < 0.0001$, *$P < 0.05$.

Although luminal breast cancer accounts for around 70% of patients, the triple negative subtype (around 15% of patients) has the poorest prognosis and the greatest clinical need for new therapies(*518*). Additionally, therapies which are effective in one subtype of breast cancer can also be ineffective in others, so testing prospective therapeutics across the major breast cancer subtypes is essential for this indication. Alongside our

existing approach with luminal tumour models, we also tested LH663 administration in the 4T1 triple negative breast cancer model in BALB/C mice. Following the same principals as with the luminal models, 4T1 tumours were allowed to form a palpable mass before thrice weekly administration of LH663 (Figure 3.6A). LH663 administration was again effective in significantly reducing primary tumour volume (Figure 3.6B), and likewise reduced the number of metastatic legions in the lung (Figure 3.6C-D). The mean size of lung nodules in the lungs were also smaller (non-significant trend), with this experimental readout potentially becoming more meaningful at later stages of metastatic outgrowth.

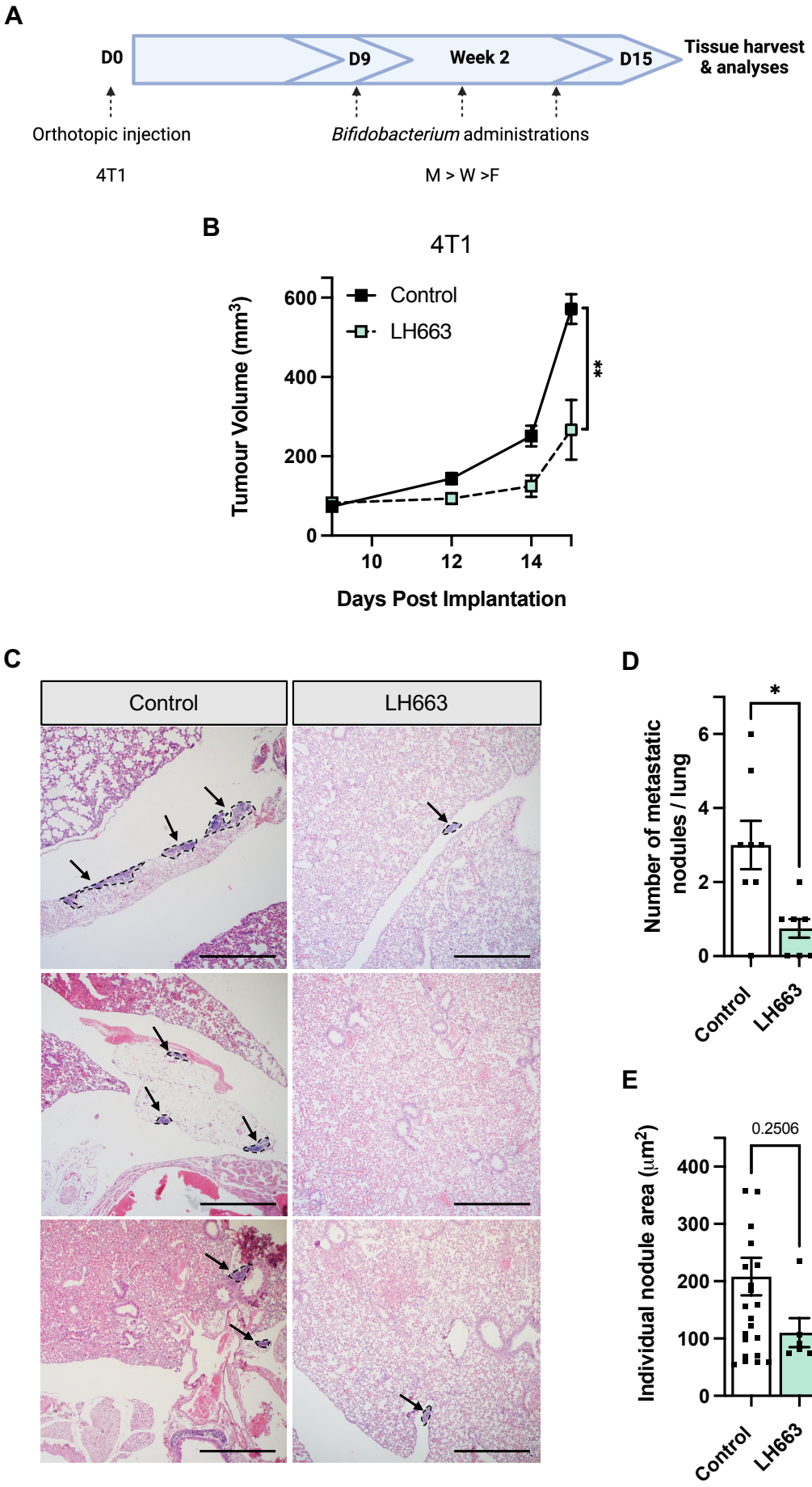
A
D0
D9
Week 2
D15
Tissue harvest & analyses
Orthotopic injection
4T1
Bifidobacterium administrations
M > W >F
B
4T1
Control
LH663
Tumour Volume (mm3)
600
400
200
0
10
12
14
Days Post Implantation
**
C
Control
LH663
D
Number of metastatic nodules / lung
6
4
2
0
*
Control
LH663
E
Individual nodule area (μm2)
400
300
200
100
0
0.2506
Control
LH663

Figure 3.6. *B. pseudocatenulatum* LH663 administration reduces triple negative 4T1 primary tumour volume and metastasis. (A) experimental outline of 4T1 orthotopic tumour growth experiments. (B) 4T1 mean (± SEM) tumour growth over time following administration of *B. pseudocatenulatum* LH663, n=9. (C) Representative images showing the presence of metastatic nodules in H&E-stained endpoint lungs of 4T1-bearing animals. Scale bar = 200μm. (D) Quantification showing the average number, and (E) size of individual metastatic nodules in the lungs of 4T1-bearing animals. Statistical significance calculated by, (B) two-tailed unpaired t test, (D) two-tailed unpaired *t* test with Welch's correction, (E) Mann-Whitney U test. $^{**}P < 0.01$, $^{*}P < 0.05$.

3.4. *B. pseudocatenulatum* LH663 administration can enhance the effectiveness of chemotherapy and immunotherapy in mouse breast cancer models

Though our data showed that LH663 administration could be effective as a monotherapy, successful translation to patients in the clinic will almost certainly involve a combination approach with existing standard of care. This is particularly relevant for microbiome-based inventions with *Bifidobacterium*, as this genus has an excellent safety record in humans and is already used in infants to prevent onset of necrotising enterocolitis (NEC)(*519*). Even more broadly, *Bifidobacterium* strains are already purchasable over the counter within most commercial probiotic products, and many species are classified as Generally Recognised as Safe (GRAS). The safety of this genus suggests that the issue of additive side effects is unlikely to be a factor when combining with other cancer therapeutics. Given these factors, we first decided to test strain LH663 in our luminal models in combination with the chemotherapeutic cyclophosphamide. Cyclophosphamide is commonly prescribed frontline chemotherapeutic for luminal breast cancer in the UK and USA, typically in combination with an anthracycline (deoxyrubicin) and a taxane (pactitaxel)(*38*).

The regime for BRPKp110 cyclophosphamide experiments follows the outline shown in Figure 3.7A, with co-administration of LH663 significantly enhancing the therapeutic response to cyclophosphamide treatment compared with chemotherapy alone (Figure 3.7B). To assess whether this finding was sustained across our PyMT-BO1 luminal B breast cancer model, which followed a similar experimental outline (Figure 3.7C) but

did not observe the same magnitude of therapeutic benefit, with only a small non-significant enhancement of therapeutic response following LH663 co-administration (Figure 3.7D). Whilst chemotherapy represents one of the few broadly effective treatments against breast cancer, a major problem for its use is the prevalence of major side effects(*520*). A particular issue for patients is gastrointestinal cell death and subsequent inflammation. These phenomena leads to the onset of a 'leaky gut', whereby the lining of the gastrointestinal epithelium becomes damaged and allows unwanted bacteria and bacterial products to cause inflammation locally and systemically(*521*). The severity of these types of side effects can be so severe that patients are forced to cease treatment. Many beneficial bacterial species, including *Bifidobacterium*(*522, 523*), have been implicated in gut barrier repair and this trait would offer great additional patient benefit for any live biotherapeutic. Oral administration of fluorescein isothiocyanate (FITC) to PyMT-BO1 tumour bearing animals did not, however, highlight any differences in barrier integrity following the indicated treatments, as measured by detection of FITC in the serum (Figure 3.7E).

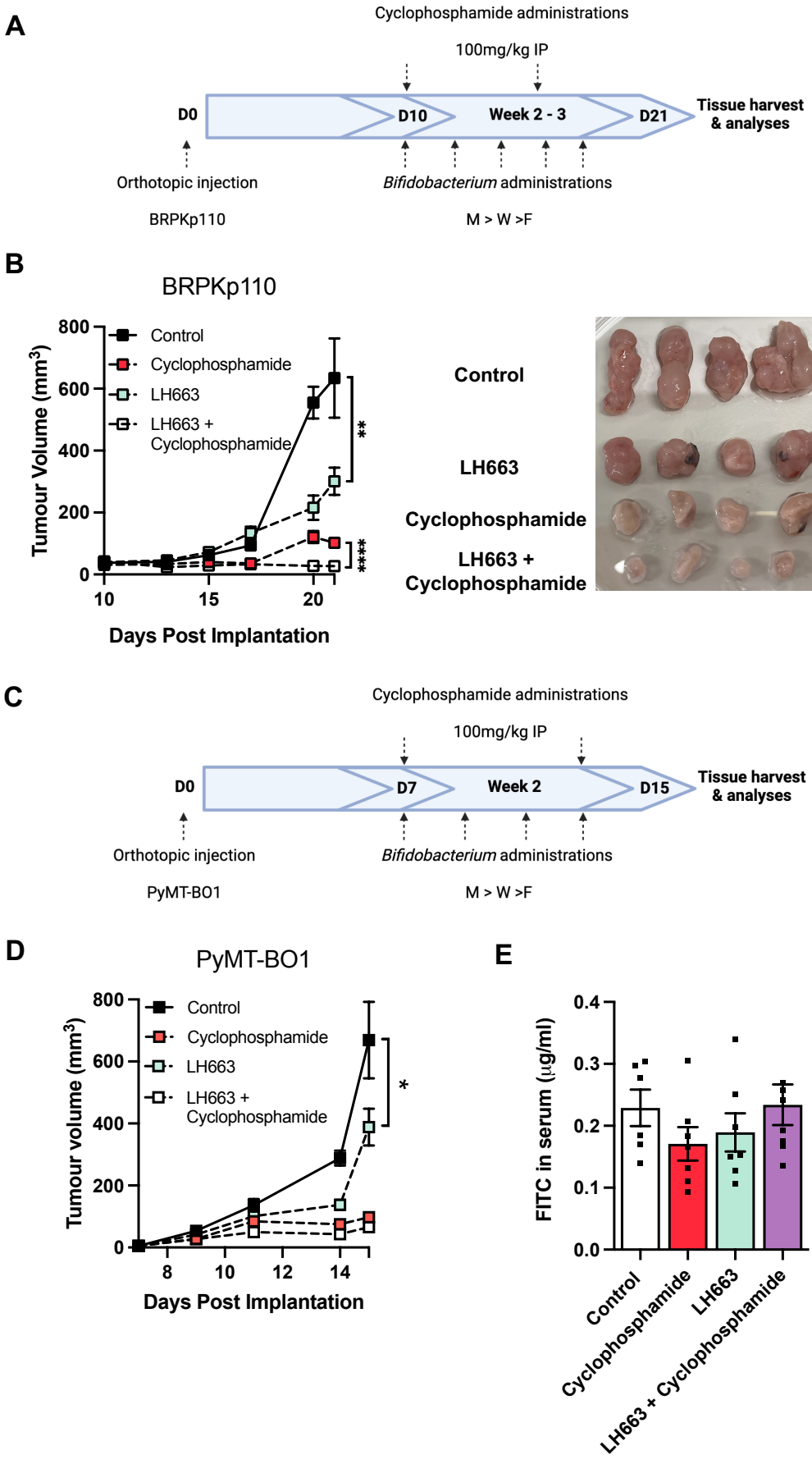
A
Cyclophosphamide administrations
100mg/kg IP
D0
D10
Week 2 - 3
D21
Tissue harvest & analyses
Orthotopic injection
Bifidobacterium administrations
BRPKp110
M > W >F
B
BRPKp110
Tumour Volume (mm3)
Control
Cyclophosphamide
LH663
LH663 + Cyclophosphamide
**
****
Days Post Implantation
Control
LH663
Cyclophosphamide
LH663 + Cyclophosphamide
C
Cyclophosphamide administrations
100mg/kg IP
D0
D7
Week 2
D15
Tissue harvest & analyses
Orthotopic injection
Bifidobacterium administrations
PyMT-BO1
M > W >F
D
PyMT-BO1
Tumour volume (mm3)
Control
Cyclophosphamide
LH663
LH663 + Cyclophosphamide
*
Days Post Implantation
E
FITC in serum (µg/ml)
Control
Cyclophosphamide
LH663
LH663 + Cyclophosphamide

Figure 3.7. Combination treatment of *B. pseudocatenulatum* LH663 with cyclophosphamide chemotherapy enhances therapeutic response in a model specific manner. (A) *B. pseudocatenulatum* LH663 + cyclophosphamide tumour experiment outline for the BRPKp110 tumour model. (B) Tumour growth over time (mean values ± SEM) of BRPKp110 tumour-bearing animals (n=7-10) treated with the indicated treatment combinations with a representative photograph of excised tumours. (C) *B. pseudocatenulatum* LH663 + cyclophosphamide tumour experiment outline for the PyMT-BO1 tumour model. (D) Tumour growth over time (mean values ± SEM) of PyMT-BO1 tumour-bearing animals treated with the indicated treatment combinations, n=8-10. (E) Quantification of circulating FITC in the serum (mean values ± SEM) following oral administration to animals in the indicated groups, n=6-8. Statistical significance calculated by two-tailed unpaired t test. ****$P < 0.0001$, **$P < 0.01$, *$P < 0.05$.

Whilst chemotherapy represents a core component of standard of care at present, there is significant interest in translating current immune checkpoint inhibitors (ICIs) immunotherapy approaches into breast cancer. Currently, ICI (pembrolizumab) is only approved for use in a limited patient subset of metastatic TNBC expressing PD-L1 in combination with chemotherapy(*524*). As such, it was most clinically relevant to test for potential synergy between LH663 and αPD-1 immunotherapy in the 4T1 triple negative model (Figure 3.8A), with results showing that LH663 significantly enhanced the therapeutic response (Figure 3.8B). With results indicating that LH663 could be effective co-therapy in a model where ICIs are already approved, we next asked whether LH663 could have a similar effect in luminal breast cancer and offer a potential route to future immunotherapy approval in a new indication. Results showed however that the additional beneficial effect of LH663 with αPD-1 in the BRPKp110 luminal A model was only marginal (non-significant) compared with LH663 or αPD-1 alone (Figure 3.8C).

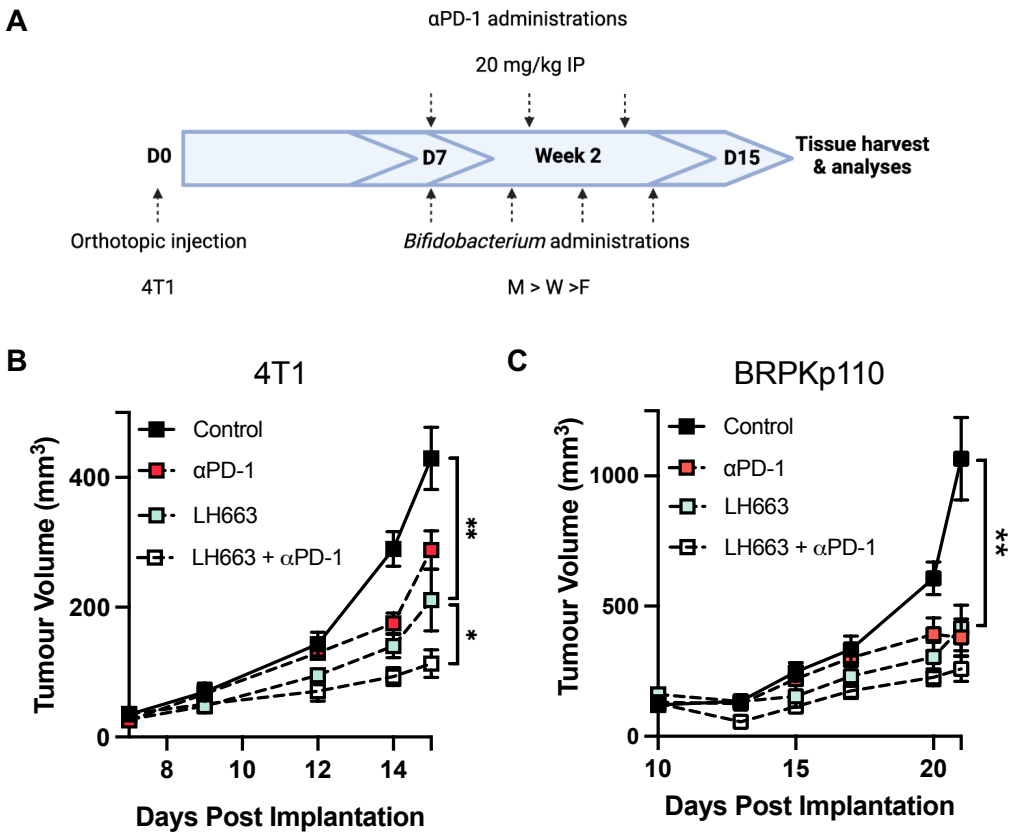

Figure 3.8. Combination treatment of *B. pseudocatenulatum* LH663 with αPD-1 immune checkpoint blockade can enhance therapeutic response. (A) Experimental outline of αPD-1 combination experiments in the 4T1 breast cancer model. αPD-1 or isotype control was administered intraperitoneally every 3 days from the onset of a palpable tumour alongside the standard regimen of oral *Bifidobacterium* administration. (B) Mean (± SEM) 4T1 tumour growth over time following administration of various combinations of LH663, αPD-1 or isotype control, n=6-9. (C) Mean (± SEM) BRPKp110 tumour growth over time following administration of the same treatment combinations as in panel B, n=7-8. Statistical significance calculated by two-tailed unpaired t test. $^{**}P < 0.01$, $^{*}P < 0.05$.

3.5. *B. pseudocatenulatum* LH663 can also protect against B16F10 melanoma tumour growth

Although most of our investigation focused on breast cancer, due to the relatively limited success and attention this indication has received in the context of microbiome

and immunotherapy, we also felt it important to test whether the potential of LH663 could extend to other tumour types. To this aim, we used the B16F10 model of melanoma (Figure 3.9A), which represents a well characterised, immunotherapy resistant model with poor infiltration of $CD8^+$ T cells. Administration of LH663 was indeed effective in reducing B16F10 primary tumour burden despite the immune excluded nature of the tumours, providing strong evidence for the translational potential of LH663 across multiple solid tumour types.

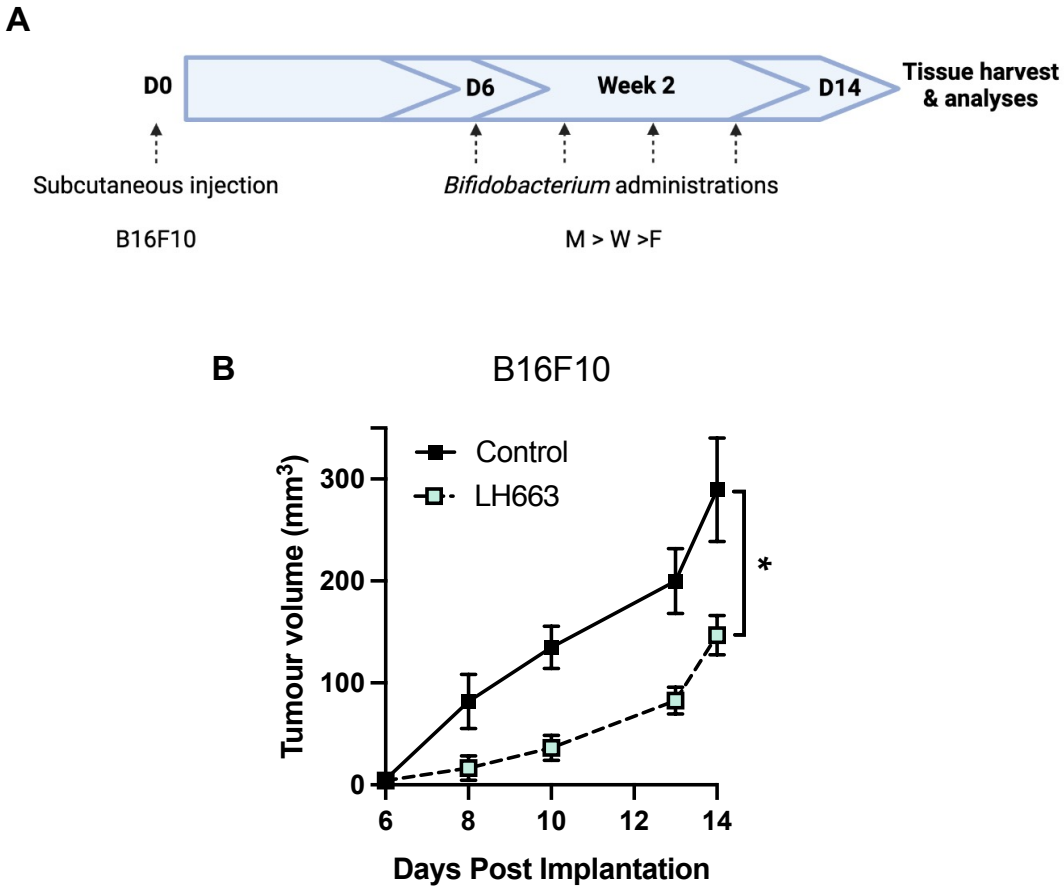

Figure 3.9. *B. pseudocatenulatum* LH663 administration reduces B16F10 primary tumour burden. (A) Experimental outline of B16F10 syngenic growth experiments. (B) Mean (± SEM) B16F10 tumour growth over time following *B. pseudocatenulatum* LH663 administration, n=8. Statistical significance calculated by two-tailed unpaired t test. *P < 0.05.

3.6. Discussion

With the consistently positive associations drawn between the abundance of *Bifidobacterium* and cancer outcomes in humans(*351, 352, 388*) and animal models(*362, 363, 386, 387*), a more thorough assessment of the breadth and depth of the therapeutic potential of this genus is required. In the context of breast cancer specifically, relatively little is known of the links to the gut microbiota. Recently published studies have shown that ablation of the gut microbiota through antibiotics can cause a poor prognosis in humans(*358, 525*) and pre-clinically(*355, 356*), particularly through activity of mast cells(*357*). However, protective associations between gut microbial communities and breast cancer are largely undefined. With so little known of how to modulate the microbiota positively in breast cancer, *Bifidobacterium* represent the ideal platform for identification of novel live biotherapeutics to improve breast cancer patient outcomes.

Possibly the key finding from this work is that *Bifidobacterium*, as a genus, have broad anti-tumour potential in the context of breast cancer. We have shown this in the context of a four-strain consortium and observed similar growth inhibitions from administrations of single strains. The beneficial effects of *Bifidobacterium* can carry across breast cancer subtypes, which is vital for clinical translation, but in some contexts are also limited by subtype. This is exemplified by the efficacy of the *Bif* cocktail in the BRPKp110 model compared to the PyMT-BO1 model, which mirrors a common clinic situation whereby therapeutics are effective in some subtypes of breast cancer, but not others(*14*). The role of *Bifidobacterium* here is clearly nuanced and strain specific, as *B. pseudocatenulatum* LH663 efficacy is comparatively effective across all the major models tested. These data show that whilst looking at tumour inhibition, two different treatments of *Bifidobacterium* can appear equivalent, the mechanisms driving these effects are clearly unique. Further evidence to this came from the deconstruction of the *Bif* cocktail, whereby three individual single strains where effective in inhibiting tumour progression compared to control and *Bif* cocktail tumours, but only LH663 was significantly upregulated anti-tumourigenic $CD8^+$ T effector memory polarisation. This again highlights the breadth of mechanisms likely behind the anti-tumourigenic effects we observed, and broadly supports evidence from the literature showing a highly varied array of mechanisms from *Bifidobacterium* in the inhibition of tumours. For example, *Bifidobacterium* production of metabolites(*363*), cell wall structural

components(*387*), and direct bacterial cell transit(*526*) have all been implicated in protective effects against cancer. A departure from the majority existing research, however, is that *B. bifidum* LH80 and *B. animalis* LH506 may be operating through a non-$CD8^+$-dependent pathway. There has been some evidence for this in other tumour indications, for example Ma et al.(*343*), have shown that commensal *Clostridium* species can modify bile acid production in the gut and thus alter downstream chemokine production by liver endothelial cells, which in turn increases protective NKT cell recruitment to liver tumours and suppression of tumour outgrowth In other work, Pal et al.(*527*), have also demonstrated a dual T helper and NK cell protective response from the microbiome against metastatic bone tumours, which is lost upon antibiotic ablation of the commensal microbiota. Our exciting finding of non-$CD8^+$ T cell mechanisms offers future potential for *Bifidobacterium* cocktail rationally targeting different synergistic pathways.

Whilst using a combination approach with *Bifidobacterium* is potentially the optimal route to maximum therapeutic efficacy, our data do show the use of bacterial consortia must be carefully considered. Notably, the presence of three individually effective strains, which appear to operate through different mechanisms, did not result in a synergistic or additive reduction in tumour progression. It is perhaps possible that even uniquely effective strains can operate in ways which are non-obviously competitive and are thus difficult to predict or control. Likewise, it is also plausible that the reasons for the absence of additional benefit between the three individually efficacious strains was due to the presence of a strain which was not beneficial (*B. longum subsp. longum* NCIMB 8809). We know from observation in culture that '8809' grows at a much faster rate to much higher CFU than the other *Bifidobacterium* strains within the *Bif* cocktail, so we hypothesise that the ineffective 8809 strain was potentially outcompeting the other beneficial species. These findings ultimately show that complex communities of microbes are difficult to control and can interact with each other in unpredictable ways, potentially altering the desired therapeutic outcome. Such complex interaction also dramatically increases the difficulty with a detailed mechanism of action can be identified, as using multiple bacterial candidates can initiate several, potentially competing, mechanistic pathways, which are themselves triggered by different bacterial functional effector components (e.g., metabolites, structural components etc.) secreted by the different microbes administered. As a final consideration for the use of consortia, commercial translation and Chemistry, Manufacturing, and Controls (CMC) processes become exponentially more difficult with more strains incorporated into the same product. Considerations of different bacterial growth conditions and mediums,

consistent CFU dosing, viability, stability, carrier compounds and how these interact across different types of bacterial poses a significant challenge. To mitigate against the risks of consortia, and to ensure the difficultly of CMC is justified, it is vital to only develop rationally designed consortia based on bacteria with different, complementary mechanisms, which can operate together non-competitively *in vivo*.

Another key consideration from the data generated was the clinical relevance of potential *Bifidobacterium*-based therapy against breast cancer. As previously mentioned, part of this consideration informed our use of multiple subtypes of disease, allowing assessment of breadth of potential of our therapeutic candidates and potentially inform patient stratification. Another key aspect of clinical relevancy was testing of our lead candidate, LH663, in combination with clinically relevant chemotherapy and immunotherapy across our various subtypes. These data highlighted yet more nuance for the use of *Bifidobacterium*, showing an exciting ability to enhance therapeutic response to cancer therapeutics, but only in specific models/subtypes. To our knowledge, this level of depth within breast cancer has not been attempted, but the concept of trialling therapeutics across different subtypes of a given indication is clearly key for other cancer indications. Importantly, we also showed that therapeutic success is not limited to breast cancer, as LH663 was also effective in inhibition of B16F10 melanoma primary tumour burden. This is likely due to the mechanism of LH663 seemingly involving enhanced $CD8^+$ T cell immunity, as activation of this pathway is beneficial across most solid tumour types(*528*). These combined factors again highlight clear translational potential of *Bifidobacterium*-based cancer therapy. In addition to effects at the primary tumour, *Bifidobacterium* treatment (from the *Bif* cocktail and LH663) displayed anti-metastatic properties. This factor is highly relevant for patients, as metastasis is the major cause of mortality in the clinic. Indeed, recent research is also suggesting that metastasis at the very earliest stages of tumour progression could be the major determinant of clinical outcome and metastatic severity(*529*). Because our experiments focused on metastases at the micro-metastatic or even single cell level, we were excitingly able to show that *Bifidobacterium* can inhibit such early events of tumour cell dissemination and seeding (shown by fewer tumour cells in the lungs and fewer macromolecular metastatic legions). By revealing inhibitory effects both at the primary tumour and against metastasis, our data suggest that *Bifidobacterium* could be useful both in the neoadjuvant setting, in a combination approach to shrink a primary tumour to operable size for a mastectomy, or in the adjuvant setting post-mastectomy to shrink secondary tumours and inhibit primary regrowth.

Overall, our results suggest that the potential for the use of *Bifidobacterium* as a breast cancer therapeutic is broad, mechanistically varied, and completely untapped clinically. We have demonstrated that these bacteria can inhibit primary tumour growth and metastasis across several breast cancer subtypes and cancer indications and shown an ability to enhance response to standard of care therapeutics. Notably, we have also highlighted the complexity of these bacterial mechanisms of action and shown that *Bifidobacterium* act in a strain-, species-, and disease-specific manner. This highlights that a deep mechanistic understanding will be essential for therapeutic translation to be successful, highlighting that more bacteria does not necessarily equate to strong therapeutic response. This key mechanistic information will likely inform types of appropriate combination approaches (e.g., chemotherapy, immunotherapy etc.) and patient stratification.

4. Mechanistic studies reveal *B. pseudocatenulatum* LH663 induces a potent anti-tumour immune response

Since the translation of ICI immunotherapy to the clinic began in 2011, development of existing and new cancer immunotherapies has become one of the single largest priorities within cancer research(*243*). The opportunity represented by cancer immunotherapy is huge, being that successful induction of host anti-tumour immunity potentially offers the only tangible route to both complete tumour destruction and prevention of recurrence. This prevention of recurrence is a key advantage over other types of cancer therapies, as engagement of the adaptive immune system and the associated memory function for tumour-associated antigens means that the immune system can continue surveillance for recurrent tumours, potentially for years, after regression of the primary cancer(*530, 531*). This type of memory function is not comparably engaged by other therapeutics, and so immunotherapy may represent the closest concept to achieving a 'cure' for cancer. However, this idealistic view of immunotherapy is unfortunately far removed from the current clinical reality. Clinically approved immunotherapy is predominantly limited to depleting antibody treatments targeting immune checkpoints, such as CTLA-4 and the PD-1/PD-L1 axis, which mechanistically inhibit inflammatory cell exhaustion to enhance cytotoxic effector function and tumour cell death(*532*). Presently, melanoma represents the most responsive cancer indication to immunotherapy, yet 40-50% (depending on regime) still do not respond(*533*). Likewise, 50% renal cell carcinoma patients(*534*) and 50-60% of non-small cell lung cancer patients(*535*) are unresponsive to approved immunotherapy options. To improve the clinical outcome, it will be necessary to identify the key mechanisms of therapy resistance which exist for a significant portion of patients, as well as developing new types of complementary approaches which target synergistic immunomodulatory pathways.

Within the context of immunotherapy, the gut microbiome has received a significant amount of attention over the last decade. Keystone studies have illustrated that gut bacteria can drive response or resistance to ICI immunotherapy in humans(*361, 373, 397*) and animal models(*356, 362, 429*). Early trial data in humans has previously demonstrated the therapeutic potential of this concept in the clinic, as Baruch et al., showed that faecal microbiota transfer from immunotherapy responsive to non-

responsive metastatic melanoma patients was able to rescue therapeutic response in a subset of patients(*375*)**.** The use of *Bifidobacterium* as a novel immunotherapy agent, both as a monotherapy and co-therapy with ICIs, has shown promise(*362, 363, 387*), with Dizman et al., even demonstrating promising phase I clinical trial results using a 'bifidogenic' live bacterial product in renal cell carcinoma patients(*377*). That *Bifidobacterium* are highly immune modulatory is not surprising when the functions of these bacteria are considered. Principally dominant within the infant microbiome, *Bifidobacterium* perform a range of vital functions symbiotically with the infant host. Here, *Bifidobacterium* are key in programming the developing immune system in infants and secrete a range of immunomodulatory and anti-microbial metabolites, many as by-products of the degradation of their human milk oligosaccharide (HMO) nutrient source(*536*). The abundance of *Bifidobacterium* in infants can be significantly stunted through antibiotic exposure, dietary intake of formula milk rather than breast, and caesarean compared to vaginal birth route(*537*). These factors are particularly prevalent in pre-term infants, and human studies have shown that supplementation of these deficient pre-term infants with *Bifidobacterium* was able to dramatically reduce the incidence of severe infection (necrotising enterocolitis), as well as an overall 50% reduction in all-cause mortality(*538*). Under this context, an appealing rationale for the therapeutic use of *Bifidobacterium* is to translate the immune stimulatory activity of the genus from developing infants into adults harbouring immunological disease (e.g., cancer).

Although the use of *Bifidobacterium* has already shown promise therapeutically, defining a comprehensive mechanism of action for microbial therapeutics will be essential to their clinical translation. These types of studies are difficult for several reasons, including the difficultly of working with several vast biological systems (gut bacteria, host gastrointestinal tract, systemic immunity, and a cancer) at the boundary of a range of specialist disciplines (microbiology, immunology, bioinformatics, cancer biology). Additionally, our work in chapter 3 has demonstrated that the mechanisms of action of *Bifidobacterium* are likely very broad, whilst also being context dependent within the host. Proper understanding of these mechanisms will provide the only useful informants for optimal therapeutic combination approaches and future patient stratification. To achieve this ambitious level of mechanistic depth, we decided to study our candidates individually to reduce experimental variables and confounders, focusing mechanism studies on our most advanced candidate *B. pseudocatenulatum* LH663. We conducted extensive immunological assessment of the tumour and systemic immune system to definitively show that LH663 operates through a $CD8^+$ T cell specific

and dependent mechanism. LH663 activates local and systemic $CD8^+$ T cell responses (causing inflammatory polarisation and activation), whilst therapeutic efficacy was lost in $CD8^+$ deficient tumours. Upstream, we found that LH663 activated key $CD8^+$-promoting macrophage and dendritic cell pathways, but through mechanisms which were not dependent on systemic metabolite release or bacterial cell translocation to tumours.

4.1. Basal-like E0771 breast tumours do not respond to *B. pseudocatenulatum* LH663 administration

To assess the therapeutic potential of LH663 even more broadly and gain potential clues to mechanism of action, we supplemented LH663 to animals bearing basal-like E0771 tumours (Figure 4.1A). In contrast to the positive results from other luminal and triple negative breast cancer models, LH663 supplementation did not significantly alter primary tumour burden (Figure 4.1B). In accordance, assessment of the primary tumour immune microenvironment also revealed that LH663 did not induce the characteristic polarisation of naïve $CD8^+$ T cells to effector memory cells, and in fact, induced a reverse of this trend to increase the percentage of tumour infiltrating naïve $CD8^+$ cells (Figure 4.1C). Further assessment of the expression of activation (Granzyme B, Ki67) and exhaustion (PD-1) markers further confirmed that $CD8^+$ T cells were not more active in E0771 tumours following LH663 administration (Figure 4.1C). Outside of the primary tumour, there was also an absence of any systemic changes to $CD8^+$ T cells in the spleen (Figure 4.1D), suggesting a mechanism specific to E0771 primary tumours was driving resistance to LH663 efficacy.

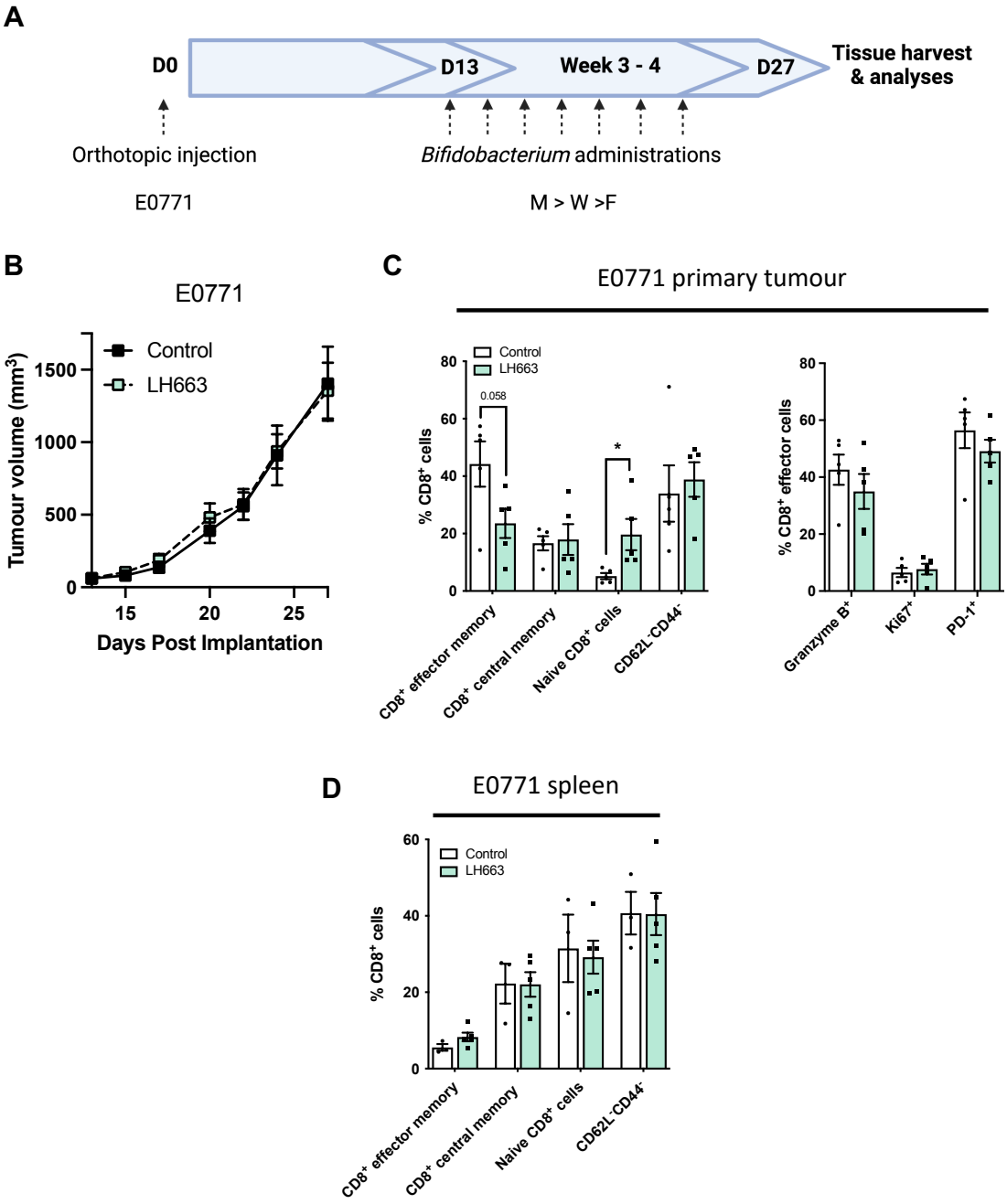

Figure 4.1. *B. pseudocatenulatum* LH663 does not inhibit the growth of basal-like E0771 breast tumours. (A) Experimental outline of E0771 tumour growth experiments. (B) Mean (± SEM) E0771 tumour growth over time following administration of *B. pseudocatenulatum* LH663, n=9-10. (C) Quantification of mean (± SEM) intra-tumoural $CD8^+$ T cell effector memory polarisation (left) and markers of immune activity (right), n=5. (D) Quantification of mean (± SEM) $CD8^+$ T cell effector memory polarisation in the spleen of E0771 tumour-bearing animals, n=5. Statistical comparisons were calculated by two-tailed unpaired *t* test. $^*P < 0.05$.

4.2. Intrinsic immunological differences between luminal, 4T1 and E0771 breast tumours provide insights into *B. pseudocatenulatum* LH663 anti-tumour mechanism

Whilst the finding of a LH663-resistant tumour model was unfortunate for the translational prospects of the therapy, the observation did provide a platform for further definition of the mechanism of action. Given we had observed previously that LH663 had activated $CD8^+$ T cells in the PyMT-BO1 model and successfully inhibited the growth of BRPKp110, PyMT-BO1 and 4T1 breast tumours, we hypothesised that a unique, tumour-intrinsic, immunological mechanism was driving E0771 therapeutic resistance. Defining the tumour immune microenvironment in E0771 model compared with the immune microenvironment of the tumour models which did respond to LH663 treatment may highlight likely mechanistic determinants of LH663 efficacy.

Comparison of the microenvironment between the relevant breast cancer models clearly indicated in E0771 displayed highly necrotic primary tumours, displaying an average of around 40% live intra-tumoural cells compared with more than 80% in each of the other models (Figure 4.2A-B). This suggested a more suppressive environment within E0771 tumours, corresponding with significant reduction in the infiltration of $CD8^+$ T cells as a percentage of the total live immune compartment (Figure 4.2C). Given that cell death was so elevated within E0771, we also decided to account for differences between tumour models by quantifying the infiltration of live $CD8^+$ T cells as a percentage of (live and dead) total cells within the tumour. This revealed an even greater reduction in $CD8^+$ T cells between E0771 tumours and the other models (Figure 4.1D), likely owing to an increased percentage of E0771 immune cell death, highlighting that E0771 tumours were approaching relative $CD8^+$ T cell deficiency. This $CD8^+$ deficiency was further demonstrated from comparison of the polarisation of tumour infiltrating lymphoid cells, which showed an increased percentage of T helper cells and reduced percentage of $CD8^+$ T cells (i.e., a lower $CD8^+$/T helper ratio) in E0771 primary tumours compared to the other tumour models (Figure 4.2E and 4.2G).

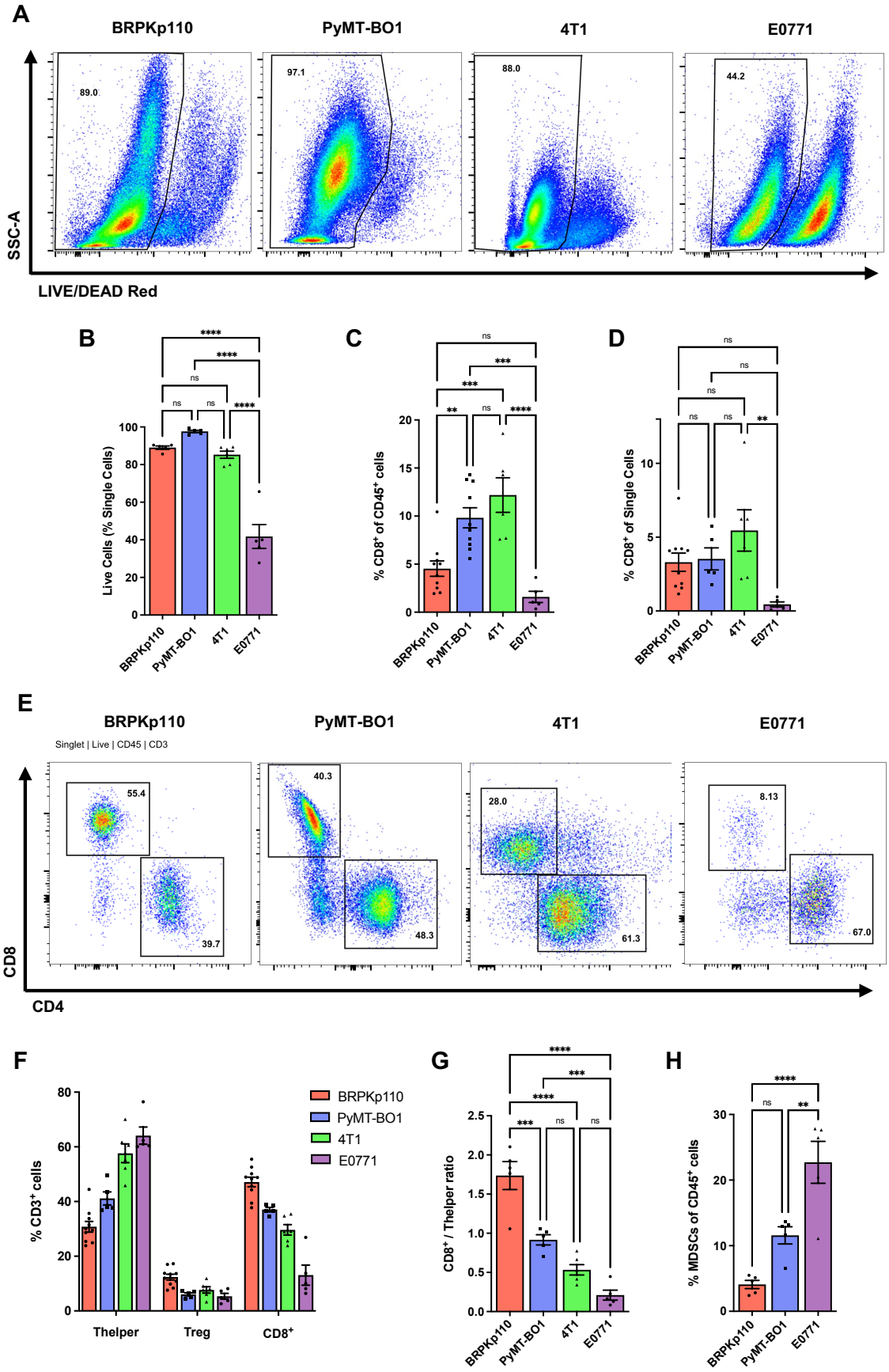
A
BRPKp110
PyMT-BO1
4T1
E0771
89.0
97.1
88.0
44.2
SSC-A
LIVE/DEAD Red
B
Live Cells (% Single Cells)
C
% CD8+ of CD45+ cells
D
% CD8+ of Single Cells
E
Singlet | Live | CD45 | CD3
55.4
39.7
40.3
48.3
28.0
61.3
8.13
67.0
CD8
CD4
F
% CD3+ cells
BRPKp110
PyMT-BO1
4T1
E0771
Thelper
Treg
CD8+
G
CD8+ / Thelper ratio
H
% MDSCs of CD45+ cells

Figure 4.2. E0771 primary tumours have a more immunosuppressive tumour microenvironment than the BRPKp110, PyMT-BO1 or 4T1 cancer models. (A) Representative flow cytometry plots with (B) Quantification showing the abundance of live cells in the indicated breast tumour models. (C) Quantification of the percentage of $CD8^+$ T cells as a percentage of live $CD45^+$ or of (D) total single cells. (E) Representative flow cytometry plots showing the polarisation of $CD3^+$ lymphocytes towards $CD4^+$ or $CD8^+$ T cells. (F) Quantification of the polarisation of $CD3^+$ lymphocytes, (G) the ratio of $CD8^+$ to $CD4^+$ T cells and the (H) infiltration of myeloid derived suppressor cells within the indicated primary tumour models. (A-H) Values represent the mean (±SEM), n=5-10, with statistical significance being calculated using a one-way ANOVA with Tukey's multiple comparisons test. ****$P < 0.0001$, ***$P < 0.001$, **$P < 0.01$, *$P < 0.05$.

One of the most well-defined mechanisms of adaptive immunotherapy resistance is the abundance and activity of immune suppressive cells, which we suspected to be a key feature of E0771 tumours. Whilst we did not observe any increase in the abundance of Treg cells (Figure 4.2F), we did see a highly significant increase in the infiltration of myeloid-derived suppressor cells (MDSCs) in E0771 tumours compared to BRPKp110 and PyMT-BO1 tumours (Figure 4.2H). Mechanistically, it is likely that infiltration of these suppressive cells is at least partly responsible for the $CD8^+$ T cell deficiency of E0771 primary tumours and provides evidence that this $CD8^+$ population is required for LH663 efficacy.

4.3. *B. pseudocatenulatum* LH663 induces systemic anti-tumour immunity through a $CD8^+$ T cell-dependent mechanism

With our prior data from section 3.2. highlighting LH663-induced $CD8^+$ T cell inflammatory polarisation, alongside LH663 resistance in poorly $CD8^+$-infiltrated tumours, we concentrated on defining the functional changes to local and systemic $CD8^+$ cells following efficacious LH663 administration. Focusing on the BRPKp110 luminal A model, we observed the same characteristic trend of an increased polarisation of tumour-infiltrating $CD8^+$ effector memory T cells (Figure 4.3A-B). In addition to immunological changes at the primary tumour, systemic changes in cancer immunity are also vital, particularly for immunosurveillance of distal metastases(*92*). Our data show that $CD8^+$ cells within key systemic lymphoid organs, the spleen and tumour draining lymph node, are significantly polarised to the central memory cell subtype (Figure 4.3C-D). This suggests LH663 may induce an enhanced ability to

immunologically respond to future tumour recurrence of systemic metastasis. For cancer targeting $CD8^+$ T cells to induce tumour cell death, the secretion of cytolytic effectors from intracellular cytotoxic granules is essential(*539, 540*). Enhanced expression of CD107a (LAMP-1) on the cell surface of tumour infiltrating $CD8^+$ cells highlighted an increase in effector degranulation (Figure 4.3E), which was also mirrored with an increase in the production of cytolytic granzyme B (Figure 4.3F) following LH663 administration. These data show that LH663 induces both inflammatory polarisation and enhanced anti-tumour cytotoxin release from tumour infiltrating $CD8^+$ cells, following a classical anti-tumour immune mechanism.

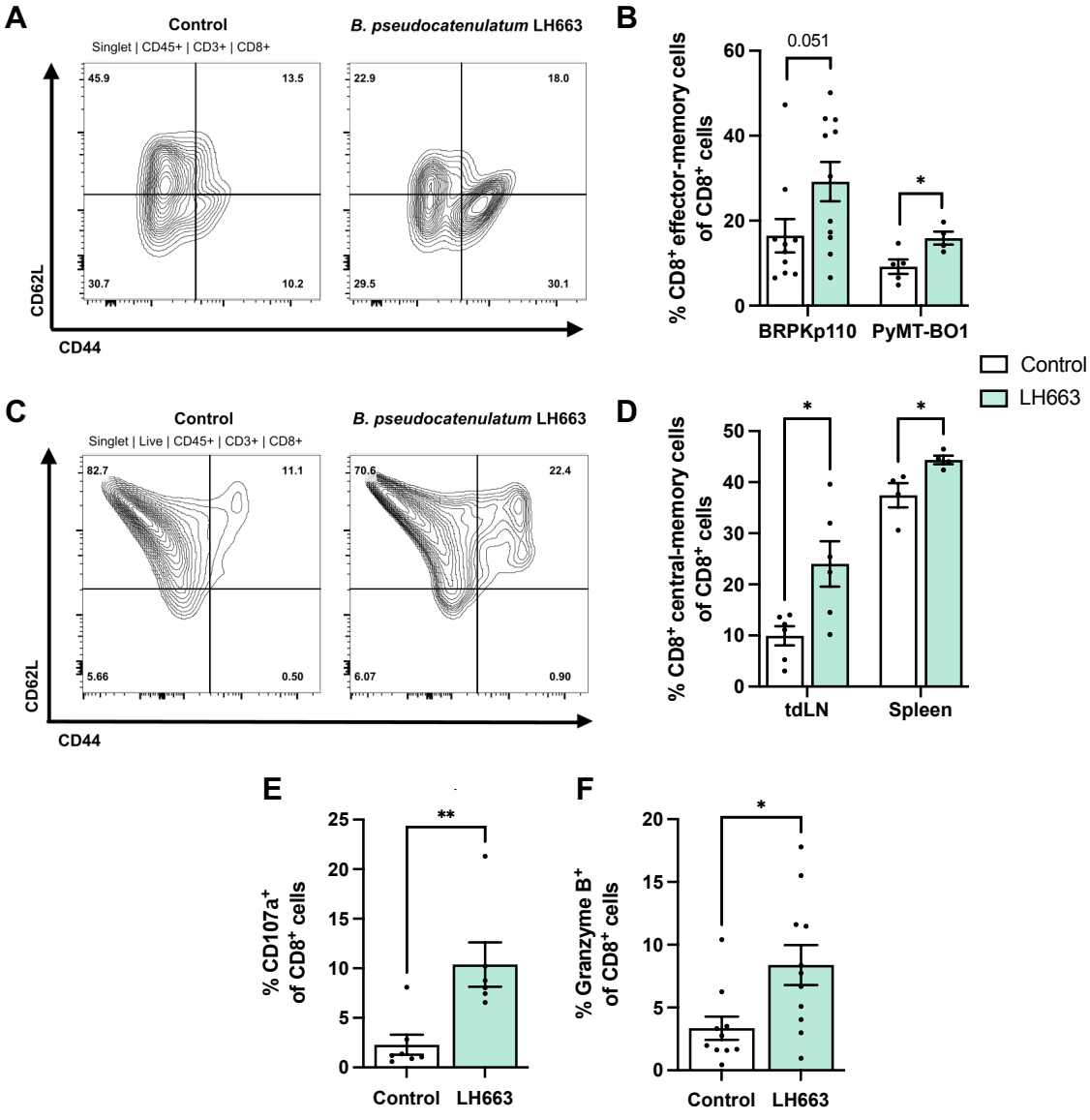

Figure 4.3. *B. pseudocatenulatum* LH663 administration increases pro-inflammatory CD8$^+$ T cell polarisation and activation in primary tumours and systemic lymphoid sites. (A) Representative flow cytometry plot with quantification showing the effector memory polarisation of BRPKp110 primary tumour CD8$^+$ T cells. (B) Quantification of CD8$^+$ T effector memory cell polarisation within BRPkp110 (n=11) and PyMT-BO1 (n=4-5) primary tumours. (C) Representative flow cytometry plots showing CD8$^+$ central memory polarisation in the BRPKp110 tumour-draining lymph node. (D) Quantification of the percentage of CD8$^+$ central memory-polarised T cells within tumour-draining lymph nodes (n=6) and spleens (n=4) of BRPKp110 tumour-bearing animals. (E) Quantification of the CD8$^+$ T cell expression of CD107a (n=5-6) and (F) granzyme B (n=10-11) within BRPKp110 primary tumours. Plots show mean values (± SEM) with statistical significance calculated by (B-D) two-tailed unpaired *t* test and (E-F) Mann-Whitney U test. $^{**}P < 0.01$, $^{*}P < 0.05$.

Alongside the production of cytotoxic effectors. The release of pro-inflammatory cytokines, such as IFNγ and TNFα, are essential markers for immune activation(*541*). These factors enhance the inflammatory response through a variety of mechanisms, including increasing tumour antigen presentation(*542*), co-stimulating CD8$^+$ anti-tumour effector release(*543*), and recruitment of other inflammatory cells through induction of localised production of chemokines(*544*). Probing changes to these key cytokines, we demonstrated that LH663 administration induces a systemic increase in IFNγ levels in the serum (Figure 4.4A), again highlighting a positive induction of systemic tumour immunity. Concordantly, we also observed an increase in primary tumour levels of IFNγ (non-statistically significant increased trend) and TNFα. A key consideration for contextualising these changes is defining the cell populations responsible for the increased cytokine release. We show that BRPKp110 tumour infiltrating CD8$^+$ T cells display an enhanced expression of both IFNγ and TNFα (Figure 4.4C), as well as similarly pro-inflammatory IL-2 (Figure 4.4D), following LH663 administration. We also demonstrate that these changes to CD8$^+$ cytokine release are not limited to the BRPKp110 tumours, as the same findings were observed within 4T1 triple negative primary tumours (Figure 4.4E). Taken together, these results demonstrate that LH663 enhances the inflammatory polarisation, cytokine release, and cytolytic effector secretion of anti-tumour CD8$^+$ T cells.

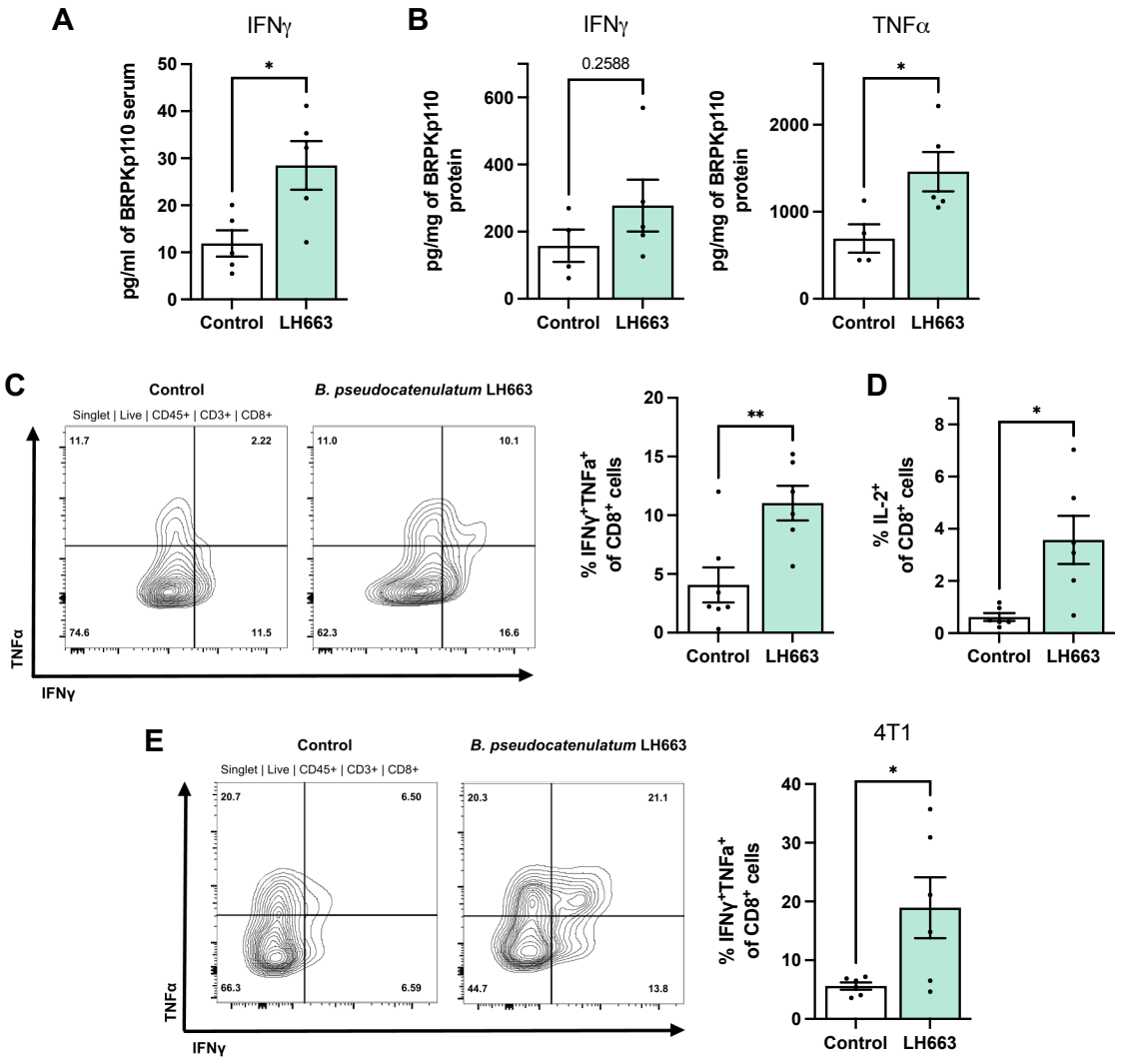

Figure 4.4. *B. pseudocatenulatum* LH663 induces the production of IFNγ and TNFα by tumour infiltrating CD8⁺ T cells. (A) Quantification of IFNγ in the serum (n=5) and (B) IFNγ (n=4-5) and TNFα (n=4-5) in the primary tumour of BRPKp110-bearing animals measured by MSD multiplex cytokine analysis. (C) Representative flow cytometry plots with quantification showing co-expression of IFNγ and TNFα and (D) IL-2 by BRPKp110-infiltrating CD8⁺ T cells following administration of *B. pseudocatenulatum* LH663, n=6-7. (D) Representative flow cytometry plots with quantification of co-expression of IFNγ and TNFα by 4T1-infiltrating CD8⁺ T cells, n=6. Plots show mean values (± SEM) with statistical significance calculated by two-tailed unpaired *t* test. $^{**}P < 0.01$, $^{*}P < 0.05$.

Although we had previously demonstrated that LH663 was ineffective in poorly CD8⁺-infiltrated E0771 tumours, it is vital to also validate the relevance of CD8⁺ T cells in a tumour model which is responsive to LH663 intervention. Focusing on BRPKp110 tumours, as the most well characterised in the context of the LH663-induced CD8⁺ T

cell response, we conducted CD8 antibody depletion to induce *in vivo* loss of function. Our results demonstrate that depletion of $CD8^+$ T cells in BRPKp110 primary tumours rescues the tumour growth inhibition of LH663 compared with the isotype control arm (Figure 4.5A). Efficient knock down of intratumoural $CD8^+$ T cells was demonstrated following αCD-8 antibody administration (Figure 4.5B), and the data show that the anti-tumour mechanism of LH663 is dependent on the $CD8^+$ T cell population.

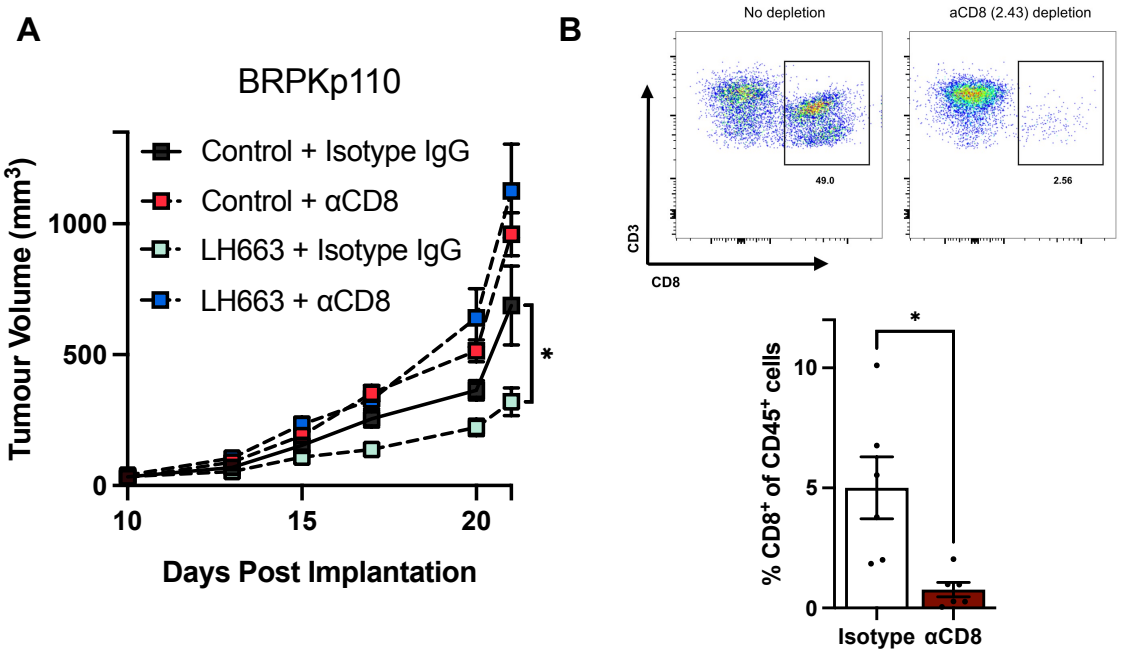

Figure 4.5. The anti-tumour activity of *B. pseudocatenulatum* LH663 is dependent on $CD8^+$ T cells. (A) BRPKp110 mean (± SEM) tumour growth over time following administration of vehicle control or *B. pseudocatenulatum* LH663 in combination with either αCD8-depleting antibody or IgG isotype control, n=9. (B) Flow cytometry plot with associated quantification showing depletion of $CD8^+$ T cells within the BRPKp110 primary tumour following treatment with αCD8-depleting antibody, n=6. Plots show mean values (± SEM) with statistical significance calculated by two-tailed unpaired *t* test. **P* < 0.05.

4.4. *B. pseudocatenulatum* LH663 does not signal through pro-inflammatory T helper or NK cell pathways

Whilst we have effectively shown the necessity of $CD8^+$ T cells for LH663 efficacy, it is also possible that other immune cells contribute to the anti-tumour mechanism. Indeed,

subsets of T helper cells, as well as NK cells, could be responsible for tumour inhibition and some of the increases in IFNγ and TNFα levels observed in tumour tissue and serum. To initially characterise the potential for other lymphocytes to be contributing to LH663-mediated tumour inhibition, we quantified infiltration of adaptive immune cells in BRPKp110 and 4T1 tumours (Figure 4.6). We did not observe any major changes in BRPkp110 tumours, although we did measure an upward trend in all lymphoid populations assessed in the 4T1. Although statistical significance was reached for the infiltration of Treg cells, the overall polarisation of lymphoid cells did not change following LH63 administration, suggesting that the increase in Treg infiltration was caused by a gross increase in lymphoid cells rather than a Treg-specific change. It is possible that enhanced lymphoid infiltration could be contributing to LH663 efficacy in the 4T1 model, although the mechanism is not conserved across the BRPKp110 model, which suggests a potential decrease in mechanistic relevancy compared to the $CD8^+$ effector activity which was observed in multiple tumour types.

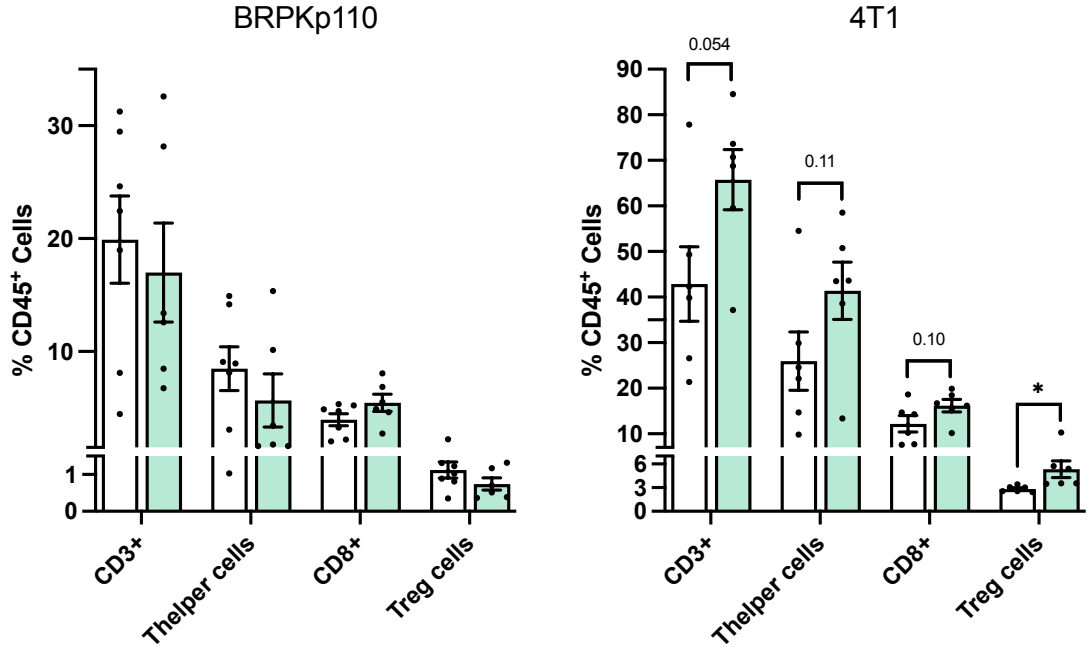

Figure 4.6. *B. pseudocatenulatum* LH663 administration does not significantly alter the infiltration of adaptive immune cells. Data shows mean infiltration (± SEM) of the indicated immune populations in either BRPKp110 (n=6-7) or 4T1 (n=6) primary tumours. Statistical comparison was conducted using two-tailed unpaired *t* test. **P* < 0.05.

Immunological mechanisms of immunotherapy commonly involve T helper activity alongside that of the $CD8^+$ population(*545, 546*). This is partly due to the activity of immune checkpoint inhibitors acting on many types of immune cells (including T helpers), but is also translated across many studies of microbiome based immunotherapy which incorporate dual $CD8^+$ and T helper cell mechanisms(*354, 363*). To test this, we probed the several outputs of T helper activity within LH663-treated primary tumours. Within BRPKp110 tumour bearing animals, we did not observe any inflammatory effector memory polarisation or IL-2 production in T helper cells, which would be expected during T helper engagement (Figure 4.7A). Similarly, there was no increase in T helper production of IFNγ, suggesting that T helper cells were not contributing to the LH663-induced increase in gross levels of IFNγ we had observed previously. We did show a statistically significant increase in IL-4 production in BRPKp110 infiltrating T helper cells, a defining feature of the Th2 subset, but we did not see this increase conserved in the 4T1 model, whereby no changes in IFNγ or IL-4 production were seen (Figure 4.7B). This suggested that the increase in IL-4 was unlikely to be a key mechanistic feature of LH663 efficacy, and that T helper activity is unlikely to be a major contributor to the LH663 therapeutic response.

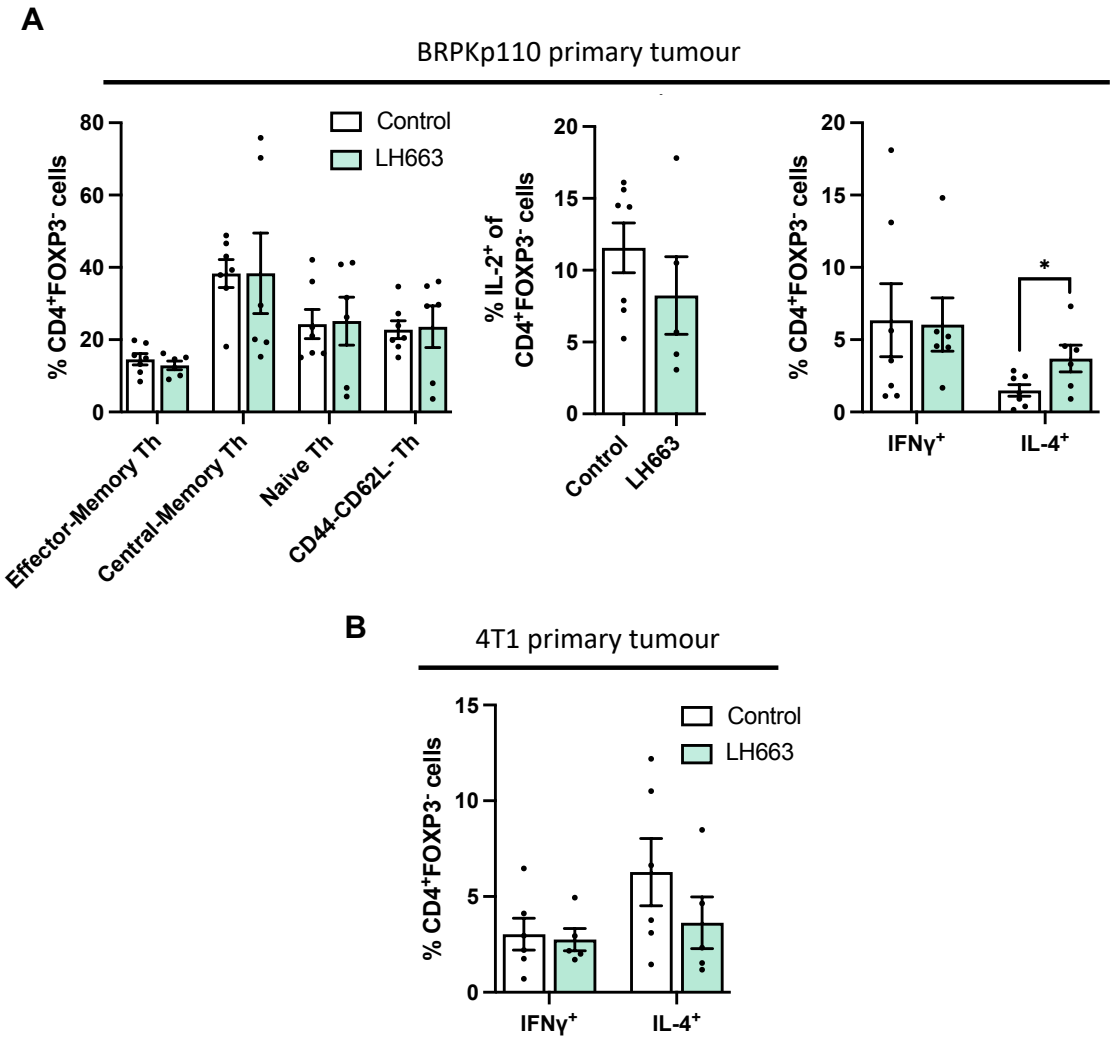

Figure 4.7. Inflammatory T helper responses are not increased following treatment with *B. pseudocatenulatum* LH663. (A) Quantifications showing T helper effector memory polarisation (left, n=6-7), IL-2 production (center, n=6-7) and IFNγ and IL-4 production (right, n=6-7) within BRPKp110 primary tumours. (B) Quantification of T helper IFNγ and IL-4 within 4T1 primary tumours. Quantifications show mean values (± SEM) and statistical significance was measured by two-tailed unpaired *t* test. **P* < 0.05.

In addition to T helper cells, NK cells can also secrete the key cytokines and effectors produced by tumour targeting $CD8^+$ T cells, such as IFNγ, TNFα, and cytolytic enzymes(*169*). To assess the potential mechanistic relevancy of NK cells, we initially quantified their infiltration to show that LH663 did not alter the abundance of NK cells, or their effector release within BRPKp110 primary tumours (Figure 4.8A). This absence of enhanced NK cell activity was also observed in the 4T1 model (Figure 4.8B), with NK cell TNFα production even decreasing in this model. Complementing the T helper findings, the absence of enhanced NK production of IFNγ (or TNFα) following LH663

administration suggests that NK cells do not contribute to the increased gross levels of these cytokines, reinforcing the hypothesis that $CD8^+$ T cells are specifically responsible for anti-tumour immune effector activity and overall therapeutic efficacy.

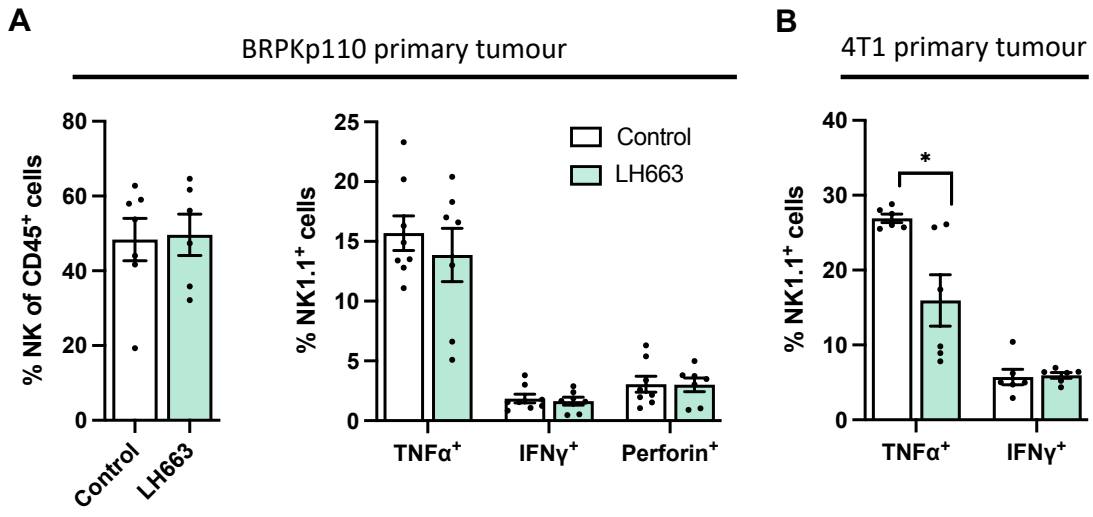

Figure 4.8. NK cell infiltration and activity is not significantly altered by administration of *B. pseudocatenulatum* LH663. (A) NK cell infiltration (left, n=6-7) and effector production (right, n=7-8) within BRPKp110 primary tumours. (B) NK cell inflammatory cytokine production within 4T1 primary tumours (n=8). Quantifications show mean values (± SEM) and statistical significance was measured by two-tailed unpaired *t* test. **P* < 0.05.

4.5. *B. pseudocatenulatum* LH663 administration induces CD8-permissive tumour microenvironment through repolarisation of tumour associated macrophages

With our data strongly suggesting that the downstream effector mechanism of LH663 is specifically mediated by $CD8^+$ T cells, we next sought to define the upstream mechanisms which may be driving the enhanced $CD8^+$ activity. Given $CD8^+$ cells are adaptive, antigen dependent immune cells, there are several upstream processes which dictate their infiltration and activation. Within the immediate tumour microenvironment, the balance of pro- and anti-inflammatory immune cells (e.g., macrophages, MDSCs, Tregs, DCs) is crucial for an optimal $CD8^+$ T cell response(*547*). Whilst we did not observe any major changes in MDSCs, DCs or non-

CD8 lymphoid cells within the primary tumour (Figure 4.9A), our immune profiling did highlight a significant reduction in the infiltration of CD206^{+} macrophages in BRPKp110 and PyMT-BO1 primary tumours (Figure 4.9B-C). This reduction of 'M2-like' immunosuppressive macrophages causes an overall repolarisation of the macrophage compartments towards the 'M1-like' MHCII^{+} macrophage subtype, which is classically considered more pro-inflammatory and CD8-permissive(*197*). It is possible that this type of alteration to the primary tumour macrophage compartment contributes to the enhance CD8^{+} T cell response we see *in vivo*, as activated CD8^{+} cells receive fewer inhibitory signals from within the tumour milieu and can thus kill tumour cells more efficiently.

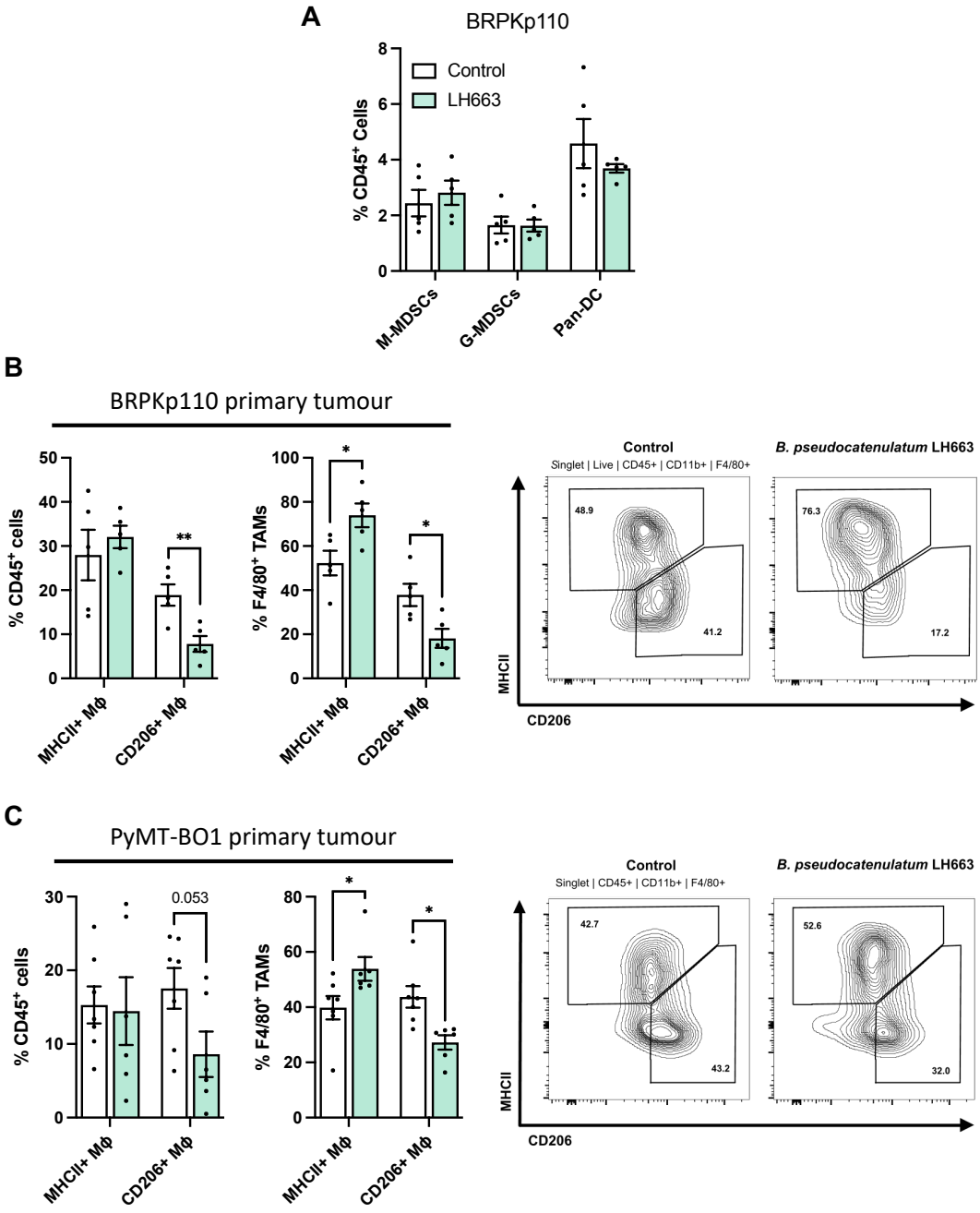

Figure 4.9. *B. pseudocatenulatum* LH663 administration reduce the infiltration of CD206$^+$ macrophages within luminal primary tumours. (A) Quantification and representative flow cytometry plot showing the infiltration and polarisation of MHCII$^+$ and CD206$^+$ macrophages within BRPKp110 (n=5) and (B) PyMT-BO1 (n=6-7) primary tumours. Quantifications show mean values (± SEM) and statistical significance was measured by two-tailed unpaired *t* test. $^{**}P < 0.01$, $^{*}P < 0.05$.

4.6. CD8-specific dendritic cell pathways are induced following administration of *B. pseudocatenulatum* LH663

At an earlier stage of the adaptive immune response, the recognition of tumour associated antigens (TAAs) by DCs and the subsequent process of antigen presentation to naïve CD8$^+$ T cells is vital for a strong and durable anti-tumour immune response. Our existing data on CD8$^+$ T cell inflammatory polarisation, particularly at the tumour draining lymph node and spleen, suggested this process was enhanced due to the increased expression of CD44, which occurs after successful antigen priming and activation of the T cell receptor(*548*). Additionally, an enhancement in systemic (rather than tumour-restricted) anti-cancer immunity further suggested that the CD8$^+$-driven response may not have been initiated simply by factors localised to the primary tumour (e.g., TAM polarisation). Working from this hypothesis, we show that LH663 increases (to near statistically significant levels) the systemic pool of circulating DCs in the blood (Figure 4.10A). In addition, we observe that the increase in circulating DCs appears to be primarily driving a specific increase in the cDC1 subset rather than cDC2 subset (Figure 4.10B), with these cells priming CD8$^+$ T cells and T helper cells respectively(*130, 549*). These data comply with our findings that CD8$^+$ T cell specifically, and not T helper cells, are more activated following LH663 administration. The increase in systemic, CD8$^+$-specific cDC1 cells was also translated in the tumour-draining lymph node, the primary site of tumour specific antigen priming (Figure 4.10C). Notably, DCs localised within the tumour-draining lymph node were also more mature, suggesting an enhanced ability to present TAAs efficiently (Figure 4.10D). Taken together, these data suggest that LH663 administration causes an increase in circulating levels of CD8$^+$-specific cDC1 cells, which display a potentially increased ability to present antigen due to increased maturity and correlate with a systemic increase in activated antigen-primed CD8$^+$ central memory and tumour effector memory cells.

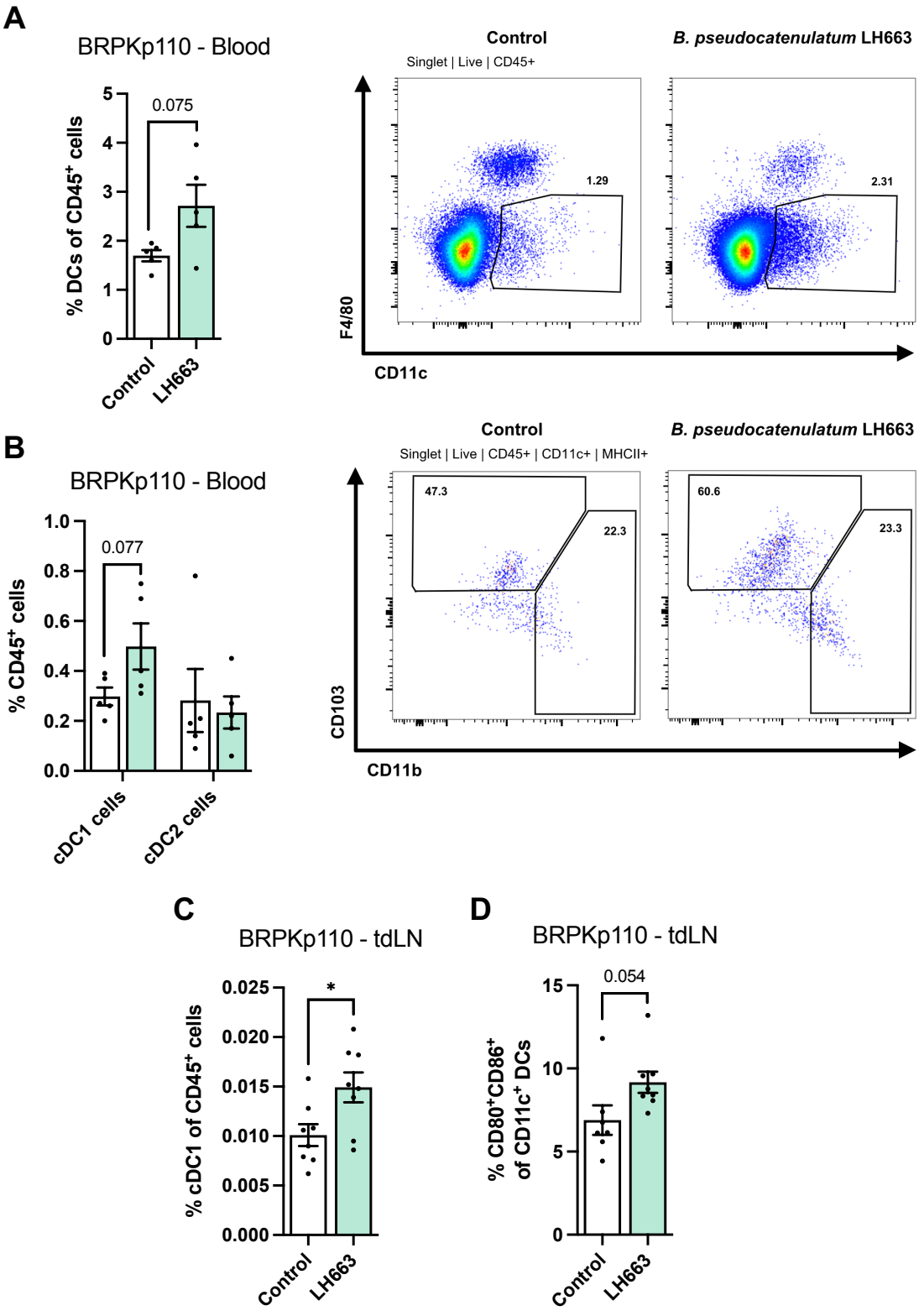
A
BRPKp110 - Blood
% DCs of CD45+ cells
0.075
Control
LH663
Control
B. pseudocatenulatum LH663
Singlet | Live | CD45+
1.29
2.31
F4/80
CD11c
B
BRPKp110 - Blood
% CD45+ cells
0.077
cDC1 cells
cDC2 cells
Control
B. pseudocatenulatum LH663
Singlet | Live | CD45+ | CD11c+ | MHCII+
47.3
22.3
60.6
23.3
CD103
CD11b
C
BRPKp110 - tdLN
% cDC1 of CD45+ cells
*
Control
LH663
D
BRPKp110 - tdLN
0.054
% CD80+CD86+ of CD11c+ DCs
Control
LH663

Figure 4.10. Administration of *B. pseudocatenulatum* LH663 increases the abundance of systemic and tumour-draining lymph node cDC1 cells. (A) Quantification and representative flow cytometry plots showing the infiltration of dendritic cells and (B) cDC cells in the blood of BRPKp110-bearing animals (n=5). (C) Quantification of the infiltration of cDC1 cells within BRPKp110 tumour-draining lymph nodes, n=8. (D) Quantification of the percentage of $CD80^+CD86^+$ mature dendritic cells within BRPKp110 tumour-draining lymph nodes, n=7-8. Data shows mean values (± SEM) with statistical significance calculated using two-tailed unpaired *t* test. $*P < 0.05$.

4.7. Untargeted metabolomics reveals that *B. pseudocatenulatum* LH663 does not significantly alter levels of 500 circulating metabolites

With key $CD8^+$ T cell mechanism identified, alongside evidence of $CD8^+$-promoting upstream pathways, we were next interested in defining the LH663-induced functional output from the gut. Across the broader field, the functional outputs from the gut induced by therapeutic bacteria have been poorly defined. Recent research is beginning to prioritise this mechanistic information, and the most evidenced bacteria-induced functional outputs are metabolic in nature(*363, 423, 429*). The general premise here, is that the bacteria enter the gut, produce a bioactivate metabolite which crosses the gastrointestinal epithelium and circulated systemically to bind and activate target immune cells.

To discover whether the mechanism of LH663 was initiated by the production of a microbial metabolite, or through induction of secondary metabolites from other sources, we conducted untargeted metabolomics of 500 metabolites in the serum of tumour-bearing animals. In BRPKp110-bearing serum, there was no significant change to the overall metabolome signature following LH663 administration (Figure 4.11A). With exception of tetradecanedioic acid. It was notable that the most significant alterations were reductions in metabolite levels rather than increases following LH663 administration (Figure 4.11B), although no individual metabolite abundance changed significantly after control for the FDR (Figure 4.11C).

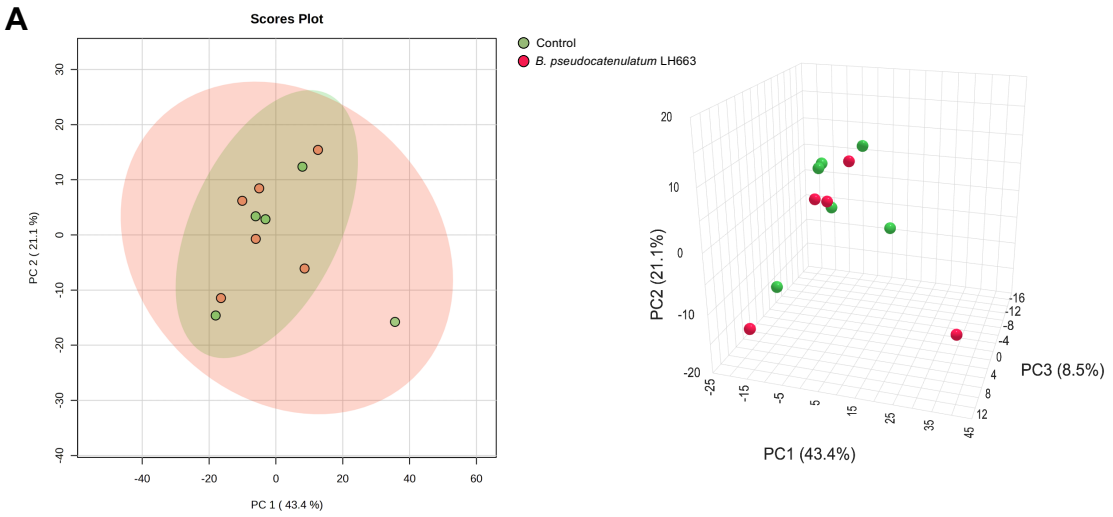
A
Scores Plot
Control
B. pseudocatenulatum LH663
PC 2 (21.1 %)
PC 1 (43.4 %)
PC2 (21.1%)
PC3 (8.5%)
PC1 (43.4%)

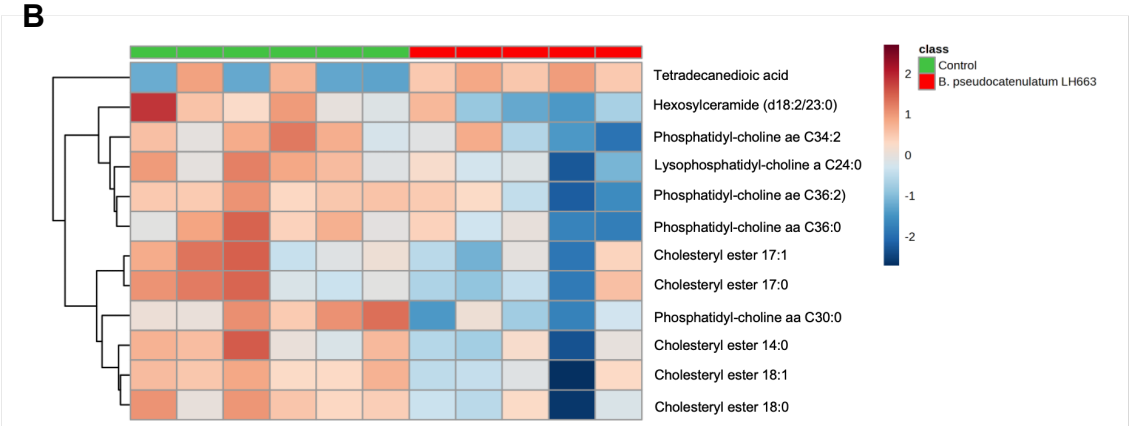
B
Tetradecanedioic acid
Hexosylceramide (d18:2/23:0)
Phosphatidyl-choline ae C34:2
Lysophosphatidyl-choline a C24:0
Phosphatidyl-choline ae C36:2)
Phosphatidyl-choline aa C36:0
Cholesteryl ester 17:1
Cholesteryl ester 17:0
Phosphatidyl-choline aa C30:0
Cholesteryl ester 14:0
Cholesteryl ester 18:1
Cholesteryl ester 18:0
class
Control
B. pseudocatenulatum LH663

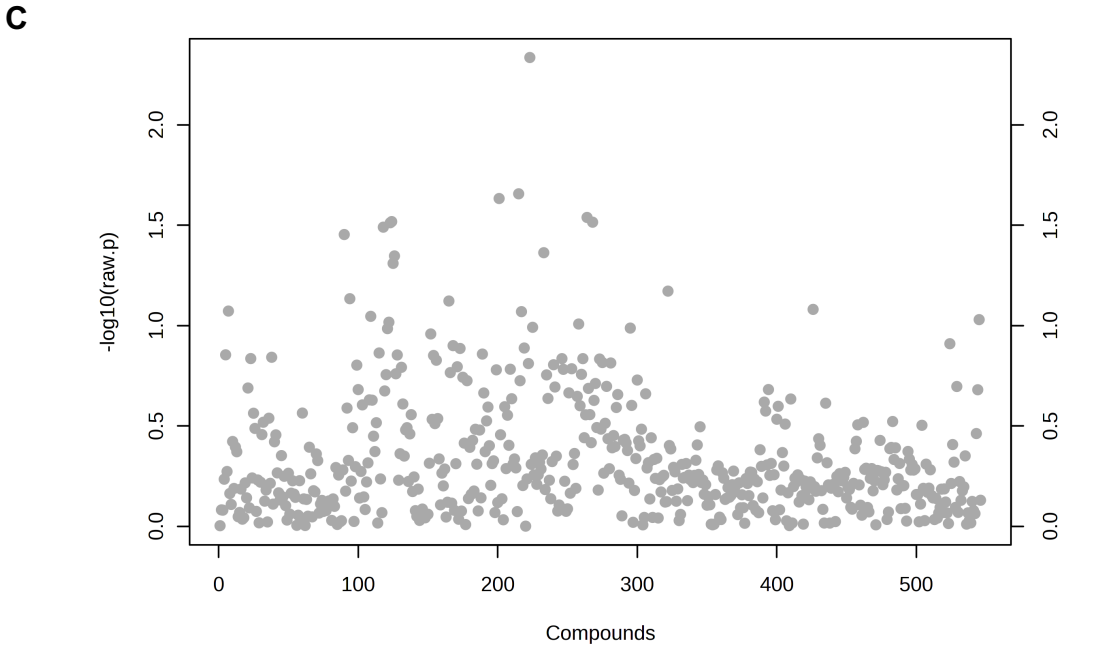
C
-log10(raw.p)
Compounds

Figure 4.11. Administration of *B. pseudocatenulatum* LH663 does not significantly alter major serum metabolite levels in BRPKp110 tumour-bearing animals. (A) 2D and 3D PCA score plots of serum metabolite profiles of BRPKp110-bearing animals; shaded circles indicate 95% confidence intervals. (B) Heatmap showing the top 12 differentially expressed serum metabolites between vehicle control and *B. pseudocatenulatum* LH663 treated animals. (C) Plot showing significance scores for the differential expression of 500 serum metabolites following therapeutic intervention, n=5. Statistical differences were assessed by two-tailed unpaired *t* test with an FDR applied at $P < 0.05$.

Because the existing literature and evidence for the induction of immune modulatory metabolites, specifically by *Bifidobacterium*, is so strong(*289, 536, 550*), we also undertook the untargeted metabolomics in the serum of PyMT-BO1 tumour bearing animals. Our rationale was that metabolite-dependent drivers of the LH663 mechanism should be conserved across tumour models and reproduce in our analyses. In accordance with the BRPKp110 model, the PyMT-BO1 metabolome (modelled by our 500-analyte panel) was not significantly altered following LH663 administration (Figure 4.12A). The most significantly altered metabolites in PyMT-BO1 sera were again mostly reduced rather than increased following therapeutic intervention, with the only increases being hexosylceramide, trihexosylceramide and dodecanoyl-carnitine (Figure 4.12B). As in the BRPKp110 model, none of these alterations in individual metabolites were statistically significant (Figure 4.12C) and none of the most significantly changing metabolites were consistent across both tumour models, further suggesting that the effects of LH663 are not mediated by secretion of metabolites.

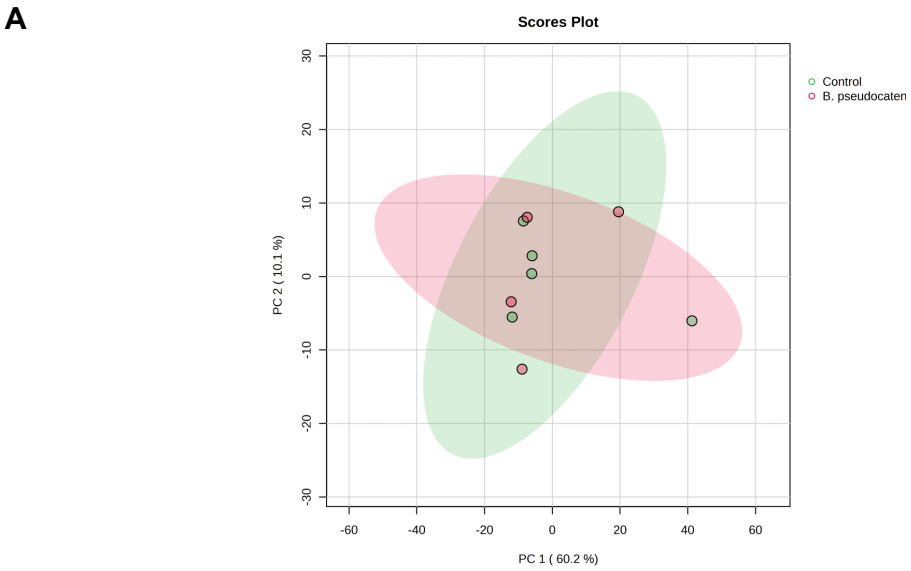
A
Scores Plot
Control
B. pseudocaten
PC 2 (10.1 %)
PC 1 (60.2 %)
30
20
10
0
-10
-20
-30
-60
-40
-20
0
20
40
60

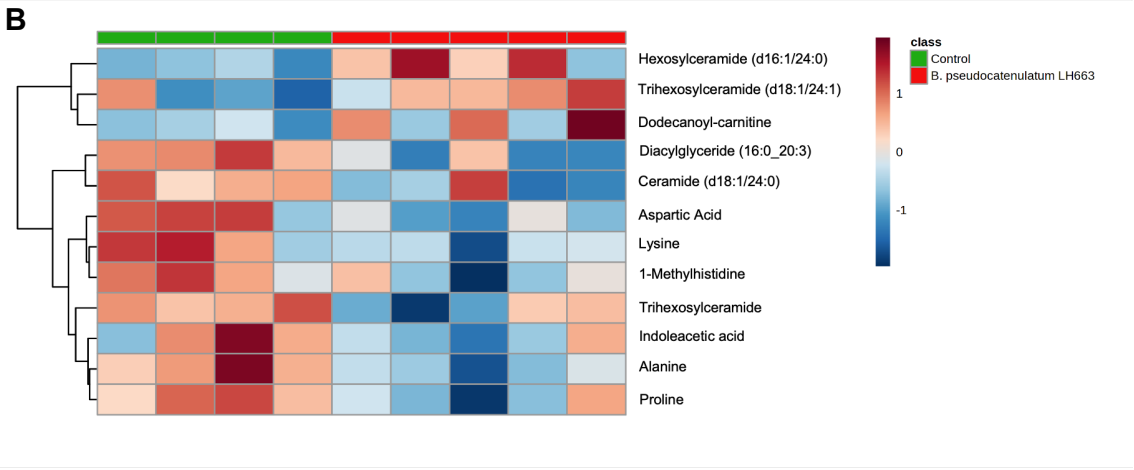
B
class
Control
B. pseudocatenulatum LH663
1
0
-1
Hexosylceramide (d16:1/24:0)
Trihexosylceramide (d18:1/24:1)
Dodecanoyl-carnitine
Diacylglyceride (16:0_20:3)
Ceramide (d18:1/24:0)
Aspartic Acid
Lysine
1-Methylhistidine
Trihexosylceramide
Indoleacetic acid
Alanine
Proline

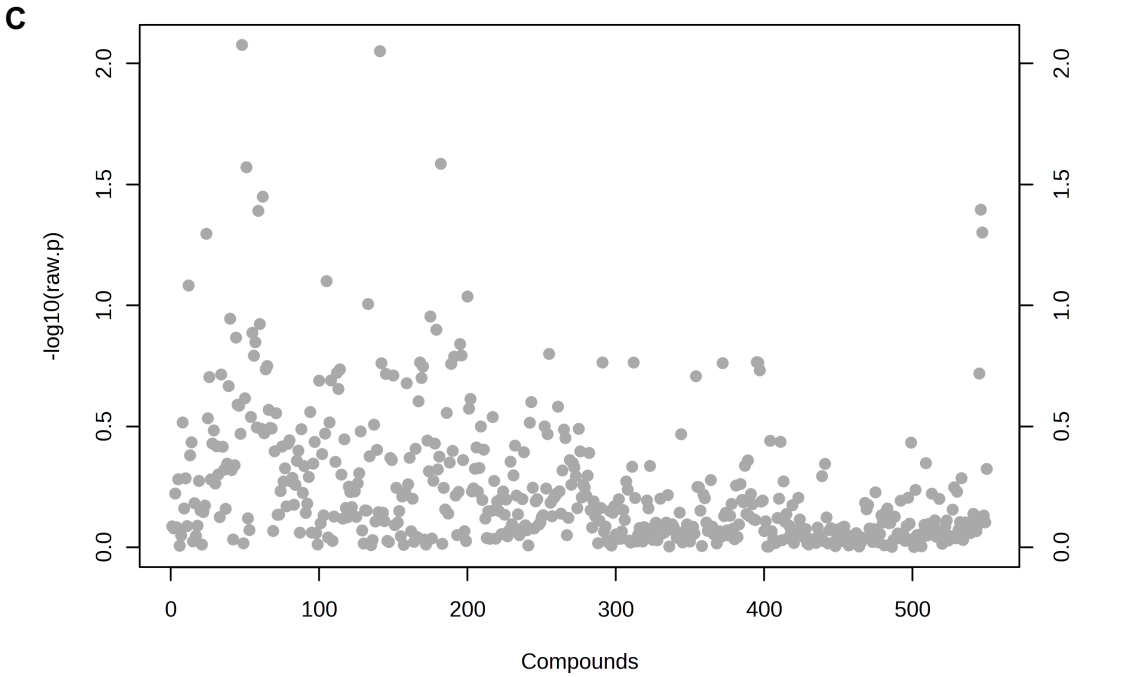
C
-log10(raw.p)
0.0
0.5
1.0
1.5
2.0
0
100
200
300
400
500
Compounds

Figure 4.12. Administration of *B. pseudocatenulatum* LH663 does not significantly alter major serum metabolite levels in PyMT-BO1 tumour-bearing animals. (A) 2D PCA score plot of serum metabolite profiles of PyMT-BO1 tumour-bearing animals; shaded circles indicate 95% confidence intervals. (B) Heatmap showing the top 12 differentially expressed serum metabolites between vehicle control and *B. pseudocatenulatum* LH663 treated animals. (C) Plot showing significance scores for the differential expression of 500 serum metabolites following therapeutic intervention, n=5. Statistical differences were assessed by two-tailed unpaired *t* test with an FDR applied at $P < 0.05$.

Although our untargeted metabolomics did not show any changes in individual circulating metabolites, we wanted to understand whether a combination of trending changes in metabolite levels may cooperate to significantly alter a metabolic pathway. Analysing both the BRPKp110 and PyMT-BO1 serum metabolome, we did not observe any significant alterations to metabolic pathways (Figure 4.13). In a similar fashion to the prior analysis, we also did not observe any consistency between tumour models, as the most significantly altered pathways were different between PyMT-BO1 and BRPKp110-bearing animals. Generally, the most significant changes were also associated with a low pathway impact score, suggesting that only a small component of the total pathway changed considerably, generally suggesting that the activity of the larger pathway was unlikely to be meaningfully disrupted or enhanced.

A

BRPKp110

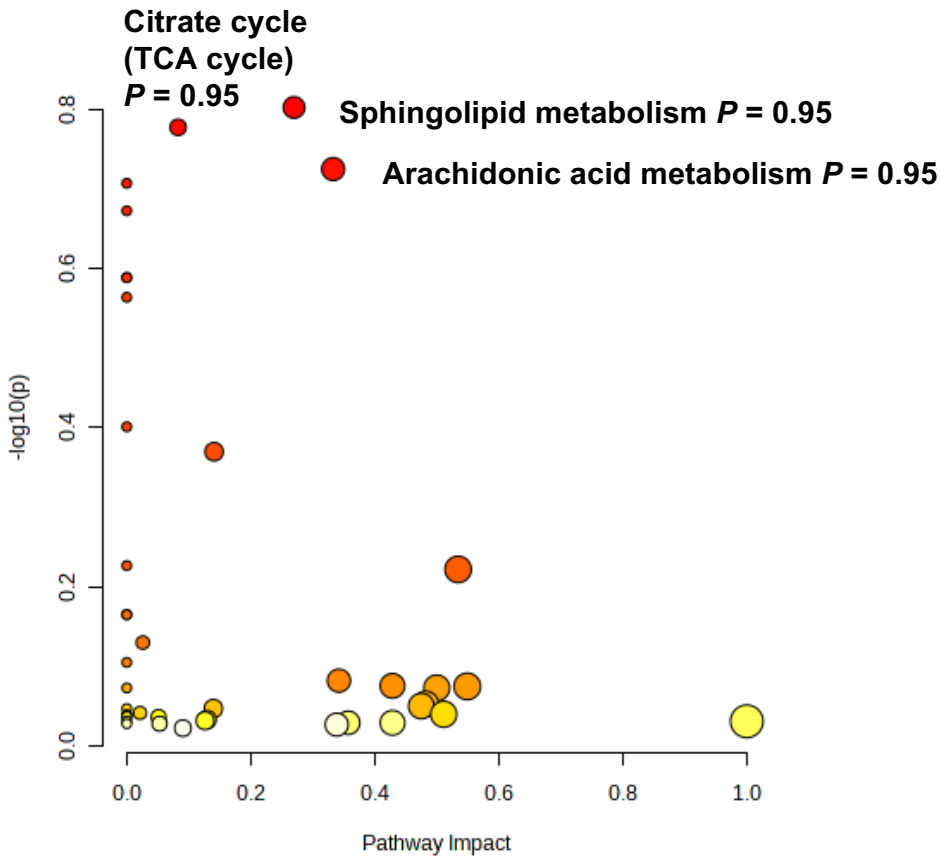

B

PyMT-BO1

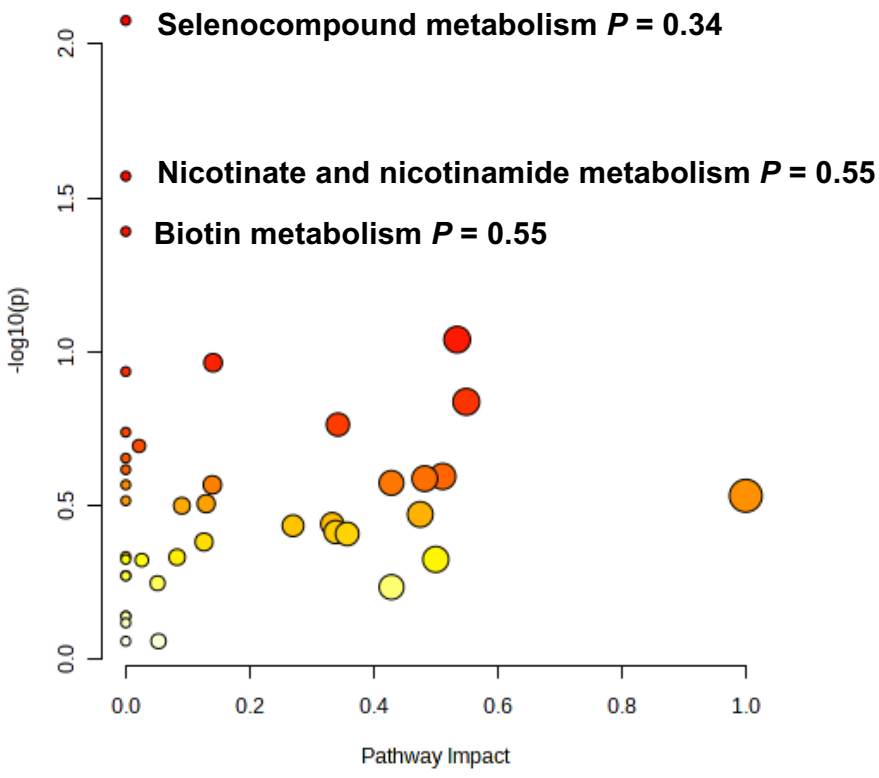

Figure 4.13. Serum metabolic pathways are not significantly altered following *B. pseudocatenulatum* LH663 administration. Metabolic pathway analysis plots created using MetaboAnalyst 5.0. from animals bearing (A) BRPKp110 and (B) PyMT-BO1 primary tumours. Plots show the most significantly altered metabolic pathways from changes in serum metabolites following *B. pseudocatenulatum* LH663 treatment. The *x*-axis represents the topologically computed pathway impact analysis, the *y*-axis shows the –log10(*p*) enrichment score. Highly impacted pathways are characterised by a high pathway impact and high –log10(*p*) enrichment score (top right region).

4.8. Assessment of the 'tumour microbiome' reveals *B. pseudocatenulatum* LH663 does not directly traffic to tumours to induce anti-cancer immunity

Although our untargeted metabolomics was relatively conclusive in suggesting an absence of a metabolic mechanism of action, we surmised that there must remain a key functional output from the gut following administration of LH663 to drive anti-tumour immunity. The idea of the 'tumour microbiome', the presence of a distinct community of microbes which reside within primary tumours, has received a vast amount of attention over recent years(*402, 415, 511, 551*). The tumour microbiome has been postulated as a potential therapeutic target(*408*), diagnostic biomarker(*415*), and a mechanism of action for therapeutic gut bacteria(*413*). Even in the context of *Bifidobacterium*, research has shown that the genus can be therapeutic if administered directly to the primary tumour(*526, 552*), whilst other research has offered some evidence for the direct translocation of *Bifidobacterium* from the gut to distal primary tumours(*409*).

To answer the question of whether a direct translocation of LH663 to the primary tumour could be responsible for inducing tumour immunity, and to assess whether a breast tumour microbiome could represent an experimental confounder, we used a culture-based method to assess the potential microbial habitation BRPKp110 tumours (Figure 4.14A). Bacterial culture did reveal some selective bacterial growth from BRPKp110 tumour homogenate (Figure 4.14B), though bacterial growth appeared visually to be highly variable in total CFU, colony morphology, oxygen tolerance. This variability is reflected in the subsequent shotgun metagenomic sequencing data, which highlights a highly variable abundance of bacteria between individual tumours within the same experimental conditions (Figure 4.14C). Although there is some diversity

within the bacterial species identified, relative abundance analysis reveals that the BRPKp110 are largely dominated by aerobic species associated with environmental contamination (*Staphylococcus xylosus*, *S. aureus*, *S. nepalensis*, etc.) in the air and on the skin (Figure 4.14D). Where more anaerobic bacteria dominate, they are typically related to various Clostridial species (*Lachnoclostridium*, *Enterocloster* etc.), which are known to be endospore-forming and thus persist in open environments for prolonged periods. A subset of lactic acid bacteria which were detected and are not readily associated with environment contamination, and thus could represent more probable tumour microbiome candidates, are the lactobacillus-type species (*Lactobacillus johnsonii*, *Limosillactbacillus reuteri*, *Ligilactobacillus animalis* etc.). However, where these anaerobic bacteria are present, they are only very lowly abundant and so their biological relevance is questionable. Additionally, heatmap comparison between tumour homogenates reveal that these bacteria are all sourced from the same tumour, and not present in significant abundances in any of the other tumours sampled, regardless of experimental condition (Figure 4.15A). Moreover, heatmap analysis highlights a distinct absence of a consistent microbial signature across BRPKp110 tumours, strongly implying that there is not a commensal breast tumour microbiome (at least in the recently proposed sense) in our animal models. The microbial signatures detected therefore more likely represent environment contaminants or individual animal variation (perhaps due to an atypically leaky gut). Notably, there were no significant differences between control and LH663-treated groups and no *Bifidobacterium* were identified in any of the tumours (Figure 4.15A), suggesting an alternative mechanism of action driving LH663 efficacy.

Though the identification of bacteria through selective culture is one of the most powerful and definitive methods of tumour microbiome assessment, the approach is clearly susceptible to introduction of contaminants. The method also requires live culturable bacteria, whilst It is possible that some bacteria residing in tumours may be live but not culturable, or even no longer alive due to a short lifespan. To account for this possibility, we performed selective qPCR analysis of primary tumours for the *Bifidobacterium pseudocatenulatum*-specific GroEL gene, but we again did not see any evidence for LH663 cells residing in the primary tumour, with no positive signal in any group tested (Figure 4.15B)

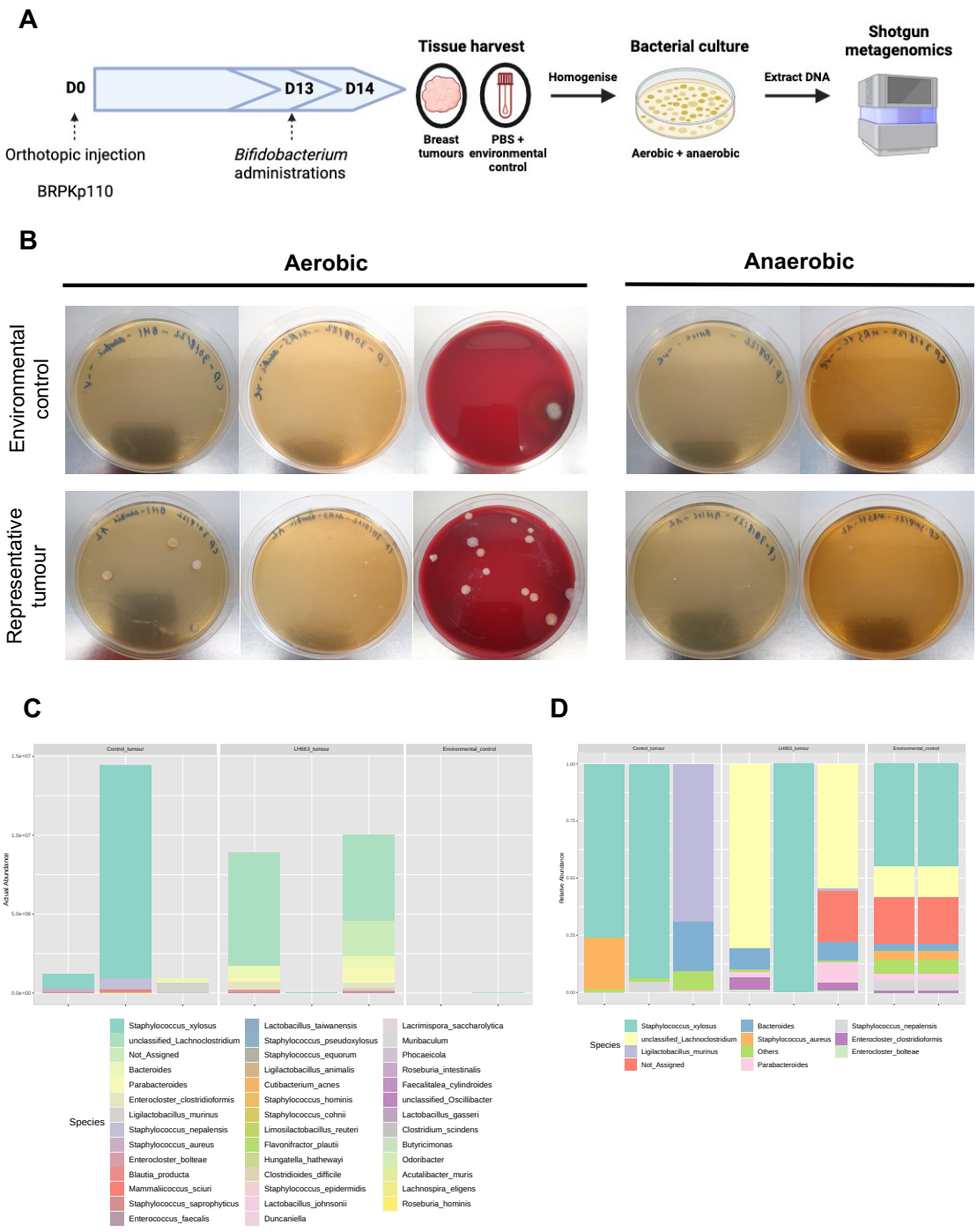

Figure 4.14. A culture-based method for the assessment of a commensal breast tumour microbiome within BRPKp110 primary tumours. (A) Experimental outline of tumour microbiome studies, BRPKp110 tumours were established for 13 days and animals were administered dosages *Bifidobacterium pseudocatenulatum* LH663 or corresponding vehicle control. Tumours were extracted, homogenised and cultured. DNA was extracted from the resulting bacterial colonies and sequenced. (B) Images of bacterial culture plates from the environmental control solution and a representative BRPKp110 tumour homogenate. (C) Bar plot showing the actual, and (D) relative abundances of detected bacterial species within tumours (treated with the indicated interventions) and environmental control solution.

A

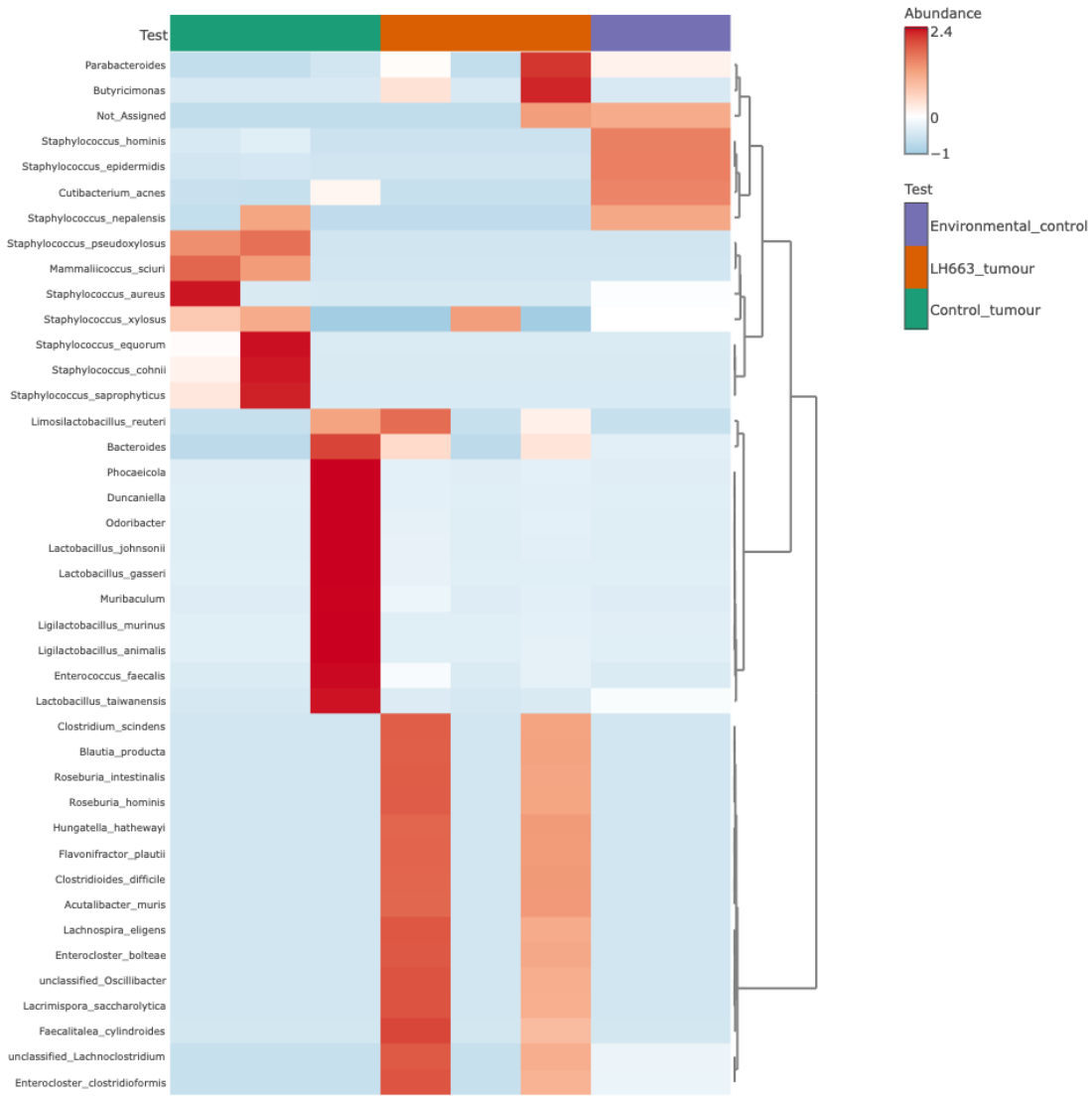
Test
Parabacteroides
Butyricimonas
Not_Assigned
Staphylococcus_hominis
Staphylococcus_epidermidis
Cutibacterium_acnes
Staphylococcus_nepalensis
Staphylococcus_pseudoxylosus
Mammaliicoccus_sciuri
Staphylococcus_aureus
Staphylococcus_xylosus
Staphylococcus_equorum
Staphylococcus_cohnii
Staphylococcus_saprophyticus
Limosilactobacillus_reuteri
Bacteroides
Phocaeicola
Duncaniella
Odoribacter
Lactobacillus_johnsonii
Lactobacillus_gasseri
Muribaculum
Ligilactobacillus_murinus
Ligilactobacillus_animalis
Enterococcus_faecalis
Lactobacillus_taiwanensis
Clostridium_scindens
Blautia_producta
Roseburia_intestinalis
Roseburia_hominis
Hungatella_hathewayi
Flavonifractor_plautii
Clostridioides_difficile
Acutalibacter_muris
Lachnospira_eligens
Enterocloster_bolteae
unclassified_Oscillibacter
Lacrimispora_saccharolytica
Faecalitalea_cylindroides
unclassified_Lachnoclostridium
Enterocloster_clostridioformis
Abundance
2.4
0
−1
Test
Environmental_control
LH663_tumour
Control_tumour

B

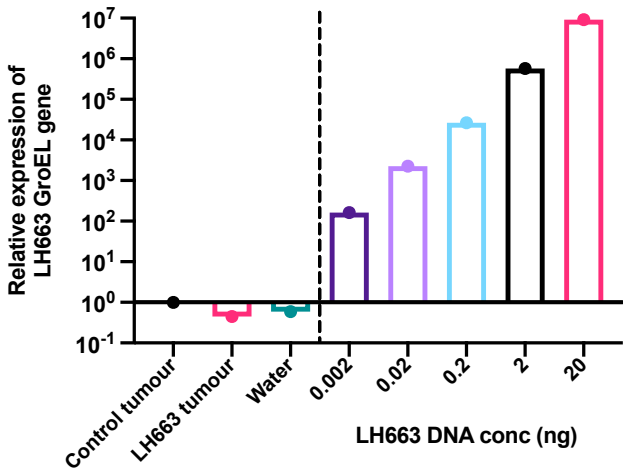
Relative expression of LH663 GroEL gene
10^7
10^6
10^5
10^4
10^3
10^2
10^1
10^0
10^{-1}
Control tumour
LH663 tumour
Water
0.002
0.02
0.2
2
20
LH663 DNA conc (ng)

Figure 4.15. The anti-cancer mechanism of *B. pseudocatenulatum* LH663 are not driven by a direct translocation of bacterial cells to the tumour. (A) Heatmap showing the differential abundances of all detected intra-tumoural bacterial strains across individual tumours and experimental conditions. (B) Quantification by qPCR of the presence of the *B. pseudocatenulatum* GroEL gene within endpoint BRPKp110 primary tumours, with LH663-DNA-spiked controls.

4.9. *B. pseudocatenulatum* LH663 does not cause inflammatory pathway activation in the colonic mucosal immune system

Given our data largely dismissed the possibility of the key functional output of the gut being either a metabolite or direct bacterial cell translocation, we next hypothesised that a direct translocation of immune cells from the gut may be responsible for the LH663 anti-tumour mechanism. Although this possibility is difficult to model, with the only validated experimental approach involving the use of kaede mice to track fluorescently labelled cells(*527, 553*), we assayed the gut mucosal immune system for possible signs of immune activation and infer potential downstream mechanisms. Through work from other members of the lab, we have confirmed via selective *Bifidobacterium* culture from LH663-monocolonised germ free mice, that LH663 cells are most abundant (colonised) in the upper colon (data not shown). We therefore chose to focus our immunological assessment of the gut immune system within the colon, initially focusing on colonic DCs. We speculate that the increased pool of DCs we observed in the blood may have originated from and been programmed in the gut before travelling systemically via the mesenteric lymph node(s) and portal vein. Assessment of DC infiltration into the colonic mesenteric lymph node did not reveal any changes however (Figure 4.16A), where we might expect a concurrent decrease in mesenteric DCs following LH663 administration to account for increased systemic DC export. To probe for changes which may have been occurring at the gastrointestinal epithelium (including the lamina propria layer), multiplex cytokine analysis of BRPKp110 tumour-bearing intestinal epithelium was performed but did not highlight any significant differences in inflammatory pathways (Figure 4.16B). We conducted the same analyses on PyMT-BO1 tumour-bearing colons, observing a slight anti-inflammatory reduction in TNFα and near significant reduction in IFNγ (Figure 4.16C). The finding of these cytokines only being affected in a single model does cast doubt over their biological relevance to LH663 mechanism, but they are nonetheless the precise cytokines which are induced systemically and within the primary tumour and

could be suggestive of IFNγ^{+}TNFα^{+} immune cells translocating from the colon to systemic sites.

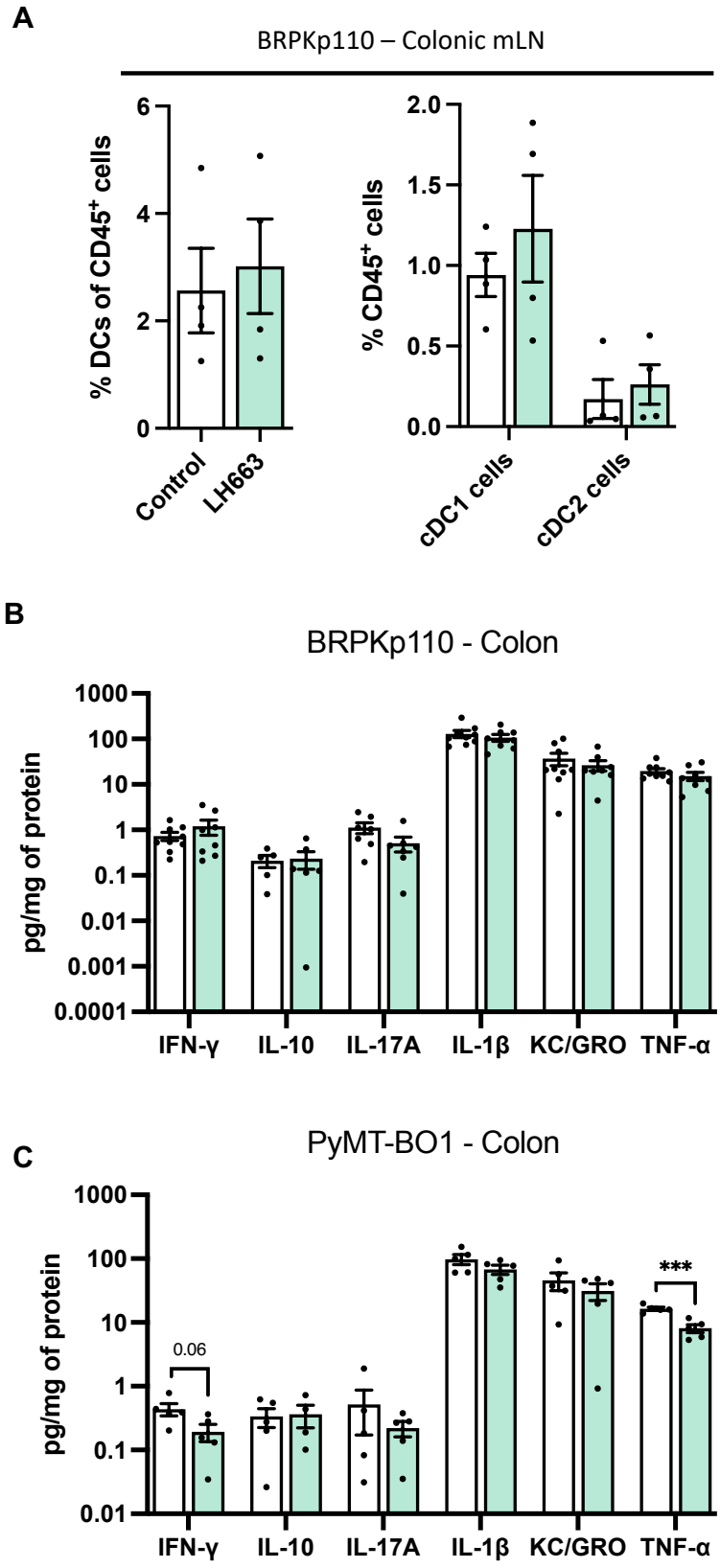

Figure 4.16. *B. pseudocatenulatum* LH663 administration does not cause major changes to the colonic mucosal immune system. (A) Quantification of the infiltration of total DCs and cDC subsets into the colonic mesenteric lymph node of BRPKp110-bearing animals (n=5). (B) Cytokine production in the colonic tissue of BRPKp110 (n=8-9) and (C) PyMT-BO1 (n=5) tumour-bearing animals quantified by a custom MSD U-PLEX assay, normalised to the levels of extracted tissue protein. Bars indicate mean values (± SEM) and statistical differences were measured by two-tailed unpaired *t* test. ***$P < 0.001$

4.10. Discussion

Following fundamental advancements in genomics in the early 2000's, the microbiome field has moved on from culturomic-limited methodologies to assessment of complete microbial communities across disease and intervention cohorts(*554*). This step change within the field quickly sparked a huge increase in the associations of gut bacteria with health and disease outcomes(*328*), shifting the perception of gut bacteria from relative homeostatic bystanders to targetable therapeutic pathways. Despite the weight of evidence of the therapeutic potential of gut bacteria, particularly within cancer(*555*), microbe-based therapies (outside of *C. difficile* infection(*556*)) have not been successfully translated to the clinic. There have been several unsuccessful clinic trials attempting the translation of microbiome therapeutics, which has increased skepticism across the broader pharmaceutical landscape. There are a range of reasons for this, but a key factor is most certainly a poor understanding of the mechanisms of action underlying complex local and systemic outputs from such huge microbial communities. Many of the first therapeutic approaches have utilised faecal microbiota transplant (FMT) therapy, whereby the complete microbiota of two individuals is merged. A more popular trend in recent years is a refinement of this idea, by developing defined bacterial consortia of key strains supposed to be responsible for therapeutic efficacy in a smaller cocktail(*367*). Although this approach changes fewer experimental variables than FMT, both suffer from introducing a huge number of mechanistic confounders simultaneously, which makes defining the discrete mechanisms of action a major challenge. The result of the mechanistic uncertainty underlying these popular approaches has meant that patient-specific pathways required for treatment efficacy and resistance are largely unknown, making proper patient stratification near impossible and impeding clinical translation. Given the vital importance of mechanism for these therapeutics, we built on our findings from chapter 3 to fully define and validate the downstream immunological pathways driving therapeutic efficacy of *B.*

pseudocatenulatum LH663 administration. To further understand the key host-specific pathways driving response, we also identified other key upstream immunological pathways which may drive efficacy and sought to characterise the systemic functional outputs from the gut following LH663 administration.

Our platform for later mechanism studies originated from the finding that LH663 was not therapeutically efficacious in basal-like E0771 tumours. LH663 administration did not induce anti-tumour immune activation within the primary tumour or systemically, indicating a key mechanism of resistance specific to the E0771 tumour model. Comparison of the immune microenvironment of the resistant E0771 tumours, with the non-resistant BRPKp110, PyMT-BO1 and 4T1 tumours, revealed a specific reduction in $CD8^+$ T cells and increase in MDSCs within resistant tumours. This key finding not only provides key evidence for the mechanism of action of LH663, but also highlights a potential patient relevant pathway of resistance in the abundance of immunosuppressive MDSCs. The amplification of MDSCs is a hallmark of many human tumour types including pancreatic ductal adenocarcinoma (PDAC), ovarian and luminal breast cancer(*557, 558*). These findings have potential implications for patient stratification, suggesting LH663 would be a poor candidate within PDAC, for example, or for tumours with high expression of PD-L1 or immunosuppressive cell types. These results also demonstrate a potential discrepancy between our mouse models and human luminal breast cancer, as we may not expect LH663 to be effective in the BRPKp110 and PyMT-BO1 models given the immunosuppressive nature of human luminal tumours. It is important to note that more mechanistic work would be required to prove this putative resistance mechanism, and there may be uncharacterised pathways that would allow for LH663 efficacy in humans, which will only be conclusively revealed following a clinical trial. In contrast to luminal breast cancer, human melanoma and triple negative breast cancer are considered more responsive to $CD8^+$ T cell therapy(*528, 559*), which is replicated in the LH663-response of the B16F10 and 4T1 tumour models. Although the discovery of an LH663-resistant tumour model was disappointing on a surface level, the finding does provide crucial mechanistic information and a basis for vital patient stratification, highlighting the value of using several unique pre-clinical cancer models when developing new therapeutics.

Building on the association of LH663 efficacy with $CD8^+$ T cell infiltration, we sought to deeply characterise and validate the LH663 effector mechanism. We demonstrated that LH663 induces inflammatory $CD8^+$ T cell effector memory polarisation and cytotoxic granzyme B degranulation within the primary tumour, as well as central

memory polarisation at the tumour draining lymph node and spleen. These results demonstrate that transient anti-cancer immunity at the primary tumour is also coupled with more durable systemic cancer immunity, which is crucial for prevention of tumour recurrence and treatment of metastasis(*560*). Indeed, the induction of systemic immunity may represent a mechanism through which LH663 is able to reduce the lung metastatic nodule seeding and outgrowth shown in chapter 3, and further highlights the potential for LH663 to be used as either a neoadjuvant or adjuvant breast cancer therapeutic pre- or post-mastectomy. Induction of central memory cells is further beneficial for the primary tumour, as recent research suggests that these cells have an enhanced ability to kill tumour cells compared with effector memory cells due to a reduced propensity for exhaustion(*561, 562*), and other studies also suggest that it may be the central memory subset of T cells which mediate response to checkpoint immunotherapy(*562, 563*). When focused again on the primary tumour immune response, we observed that the increase $CD8^+$ T cell cytotoxic degranulation is also coupled with expression of inflammatory cytokines such as IFNγ, TNFα and IL-2. The co-expression of both IFNγ and TNFα in this context highlights that LH663 induces enhanced $CD8^+$ polyfunctionality, whereby the same individual cell(s) produce higher levels of different immunological effectors simultaneously, likely inducing an exponential, rather than linear, increase in immune activation and tumour cell death. The expansion of $CD8^+$ T cell IFNγ and TNFα production was reflected by gross increases in these cytokines systemically (IFNγ) and in the primary tumour (TNFα), whilst other major producers of these cytokines (T helper and NK cells) did not contribute to increased secretion, showing that the LH663 mechanism is both $CD8^+$ dependent and specific.

The potential of E0771 resistance to LH663 being due to a high infiltration of $CD8^+$-inhibitory MDSCs highlights the potential importance of the tumour immune microenvironment to the efficacy of LH663. These association are further demonstrated in clinical cohorts, as tumour types and patients with highly immunosuppressive microenvironments display an enhanced resistance to checkpoint immunotherapy(*564*). Whilst tumour microenvironment-determinants of therapeutic resistance are vital considerations for clinical translation, equally important are potential factors in tumours that may be directly required for therapeutic mechanism of action. The fact that $CD8^+$ T cells are antigen-restricted adaptive immune cells inherently prescribes that their activity relies on the activity of other local and systemic immune cells(*565*), and we hypothesised that the LH663 mechanism of action was likely to depend on intermediary cell types upstream on the $CD8^+$ T cell immune

response. Profiling the wider immune compartment of LH663-treated primary tumours, we revealed discrete changes to tumour infiltrating macrophages (TAMs) rather than changes to MDSCs or intratumoural DCs. LH663-treated tumour displayed a specific decrease in $CD206^+$ macrophage infiltration, without affecting the infiltration of the $MHCII^+$ subtype. These subtypes reflect the classical 'M2' and 'M1' subtypes of macrophages respectively, with M2-like macrophages considered $CD8^+$ T cell-suppressive and associated with poor clinical outcomes, and $MHCII^+$ macrophages associated with better outcomes and a more functional $CD8^+$ response(*566, 567*). These data thus suggested that LH663 could be acting on $CD206^+$ macrophages to cause a reduction in their abundance within the primary tumour and an overall repolarisation of macrophages to an $MHCII^+$ rich and $CD8^+$-permissive subtype, releasing the brakes on the $CD8^+$ downstream response which was upregulated following LH663 treatment. Importantly, these findings were replicated across two separate tumour models (BRPKp110 and PyMT-BO1, myeloid analyses were not performed in 4T1 tumours), which strongly supports their mechanistic relevance as a conserved feature of LH663 efficacy. This contrasts with other immunological findings which were enhanced in one tumour model only, such as increase lymphoid infiltrate to 4T1 tumours or increased T helper IL-4 production in BRPKp110 tumours, which exemplify non-conserved features that are less relevant to the LH663 mechanism. The gut microbiome is known to have strong interactions with TAMs in both protective and pro-tumourigenic contexts, with the commensal microbiome having previously been linked to enhanced anti-tumour immunity and $MHCII^+$ macrophage polarisation in response to CpG immunotherapy and oxaliplatin chemotherapy across various solid tumour types(*353*).

As well as factors within the tumour microenvironment, systemic immunology is also required for the anti-tumour activity of $CD8^+$ T cells. Crucial for this, is the activity of dendritic cells (DCs), which are the immune population responsible for most of the priming of $CD8^+$ T cells with TAAs(*131*). Mechanistically, immature classical dendritic cells (cDC) travel from the tumour draining lymph node (tdLN) to the tumour, phagocytose tumour debris, undergo cell maturation, and present TAA(*568*). Antigen loaded DCs then travel back to the tdLN and cross present TAA to naïve T cells, which differentiate into central memory and effector memory subsets and exert immunity against the tumour(*568*). The cDC cells are split into the cDC1 and cDC2 subsets, which programme $CD8^+$ and T helper cells respectively(*99*). Functionality of this multi-step process is essential for anti-tumour immunity, and activation of these pathways particularly corresponds with our findings of enhanced central memory $CD8^+$ cells in

the tdLN. Systemically, we observed an (near significant) increase in the circulating pool of DCs which appeared to be correlated with an increase in cDC1 but not cDC2 cells. The $CD8^+$-specific cDC1 cells were also increased in the tumour-draining lymph node, showing the relevance of the change to the tumour and a direct spatial correlation with our $CD8^+$ cell data. Taken together, these data suggest that the mechanism of LH663 may be dependent on one of, or both, DC activation and $CD206^+$ macrophage inhibition. Interactions between the gut microbiome, and particularly *Bifidobacterium*, and DCs are well documented in literature(*456, 569, 570*). The seminal work from Sivan et al.(*362*), which first described a link between *Bifidobacterium* and cancer outcomes, demonstrated a mechanism based on the activation DCs and $CD8^+$ T cells. More broadly, activation of DCs and downstream induction of anti-tumour immunity is perhaps the most described effector pathway for *Bifidobacterium* and microbiome-based therapies(*363, 367, 571*), and thus activation of DCs is a strong candidate LH663 mechanism of action.

To provide the mechanistic clarity required for future LH663 clinical translation, our final major aim for the chapter was to define the LH663-induced functional output from the gut which was mediating systemic immunological responses. Understanding this, may also provide an alternative to using live bacteria therapeutically, and could present the option of using the direct functional output as the anti-cancer therapeutic. Defining microbe-induced functional outputs from the gut is a major gap in the field, potentially representing the single largest pool of novel biological understanding missing from mechanistic research into gut bacteria. There are, however, several commonly defined mechanisms proposed: systemic metabolite secretion, direct microbial translocation, and gut-derived immune cell translocation. The secretion of microbial metabolites which induce systemic anti-cancer responses is the most well defined and supported in current literature, for example Mager et al.(*363*), showed that several species of bacteria (including *B. pseudolongum*) produced the metabolite inosine, which circulated systemically following administration of ICI immunotherapy and enhanced cytotoxic T helper and $CD8^+$ immunity. Another recent example from Zhang et al.(*429*), demonstrated that a strain of *L. plantarum* and its indole-3-lactic acid metabolite crossed the gastrointestinal epithelium and enhanced the function of dendritic cells and $CD8^+$ T cells against colorectal cancer through transcriptional enhancement of IL-12 and epigenetic rewriting of cholesterol metabolism respectively. To provide the broadest possible picture on systemic metabolite release following LH663 administration, we used untargeted metabolomics to show no significant changes in the abundance of 500 metabolites in the serum of BRPKp110 or PyMT-BO1 tumours.

This finding expectedly extended to analysis of functional pathways, revealing no major changes. Of note within these results, was that the most significantly altered metabolites between control and LH663 groups was not consistent between the two models tested, suggesting any non-significant trends were not mechanistically relevant. Although these data relatively conclusively showed an absence of metabolic changes, more targeted approaches in metabolites not tested in our untargeted approach may have revealed differences. For example, the untargeted panel did not test for abundances of short chain fatty acids (SCFAs) known to be produced and augmented by *Bifidobacterium(572-574)*, which have been linked to cancer outcomes. For example, Liuu et al.(*428*), have demonstrated that microbial SCFAs (butyrate and pentanoate) can enhance anti-tumour $CD8^+$ effector activity in models of CAR-T cell immunotherapy.

Although evidence for a residential tumour microbiome is fiercely debated(*419, 420, 575*), there is a significant amount of literature and interest in this potential biological phenomenon both as a diagnostic/prognostic biomarker and targetable therapeutic axis(*576-578*). Although this is a recently emerging field, this is some evidence for *Bifidobacterium* cell translocation to systemic tumours, with Rizvi et al.(*409*), showing an enhanced qPCR signature for *Bifidobacterium* following high-salt diet induced anti-tumour immunity. Accordingly, another approach by Abdolalipour et al.(*552*), involving the direct intravenous administration of *Bifidobacterium* results in accumulation within primary tumours and inhibition of tumour outgrowth, suggesting that if LH663 could cross the intestinal epithelium and travel systemically, it is probable that we may see a *Bifidobacterium* signature within the primary tumour. During assessment of potential functional output of the gut, selective culture from LH663-treated tumours did not reveal the presence of *B. pseudocatenulatum* LH663, or any other member of the *Bifidobacterium* genus, suggesting that LH663 does not travel systemically to exert anti-tumour immunity. To further confirm our findings, we also used a qPCR approach specific to the *B. pseudocatenulatum* GroEL gene to show no LH663 within primary tumours. We do however recognise that the large abundance of host DNA increases the difficulty of identifying such low biomass signatures of bacteria, and more resolving approaches used in recent literature have performed biotin/streptavidin-based bacterial DNA enrichments to increase qPCR sensitivity(*408*). Culturomics did reveal the dominance of many species of *Staphylococcus*, but such bacteria are common environmental contaminants largely found in the air or on the skin(*579, 580*), so are questionable constituents of a resident tumour microbiome community (or experimental confounder). Contaminants may have arisen during tissue harvest, or earlier in the

experimental process during orthoptic surgery (which inherently exposes internal tissues to airborne contaminants). Further to the unlikely bacterial signatures which were identified, analysis of individual tumours did not show any consistency in the bacterial signatures discovered which would be indicative of a residential tumour microbiome, strongly suggesting the absence of this debated phenomenon in our model. We do however note that a breast tumour microbiome may be more likely to establish in a slow growing spontaneous tumour model, whereby bacteria have more time to translocate, colonise and establish, compared to our 21-day BRPKp110 orthotopic tumour model.

A final attempt to characterise the LH663-induced functional output from the gut built on the hypothesis of direct immune cell programming by LH663 within the mucosal immune system before systemic cell translocation and induction of anti-tumour immunity. Proving these mechanisms are difficult, but breakthrough studies are now beginning to demonstrate these direct immune cell translocations following microbiome interventions. Pal et al.(*527*), showed that perturbation of the microbiome through antibiotics prevented a mechanism of NK and Th1 cell traffic from the intestinal epithelium to the bone which would usually act to restrain melanoma bone legion outgrowth. With our previous results suggesting an increase in the total circulating pool of DCs and cDC1 cells, we hypothesised that LH663 could be programming intestinal DCs which then circulate systemically to induce enhanced tumour immunity. Due to other work in the lab revealing that LH663 primarily colonises the upper colon, we focused on characterising the colonic mucosa, but did not observe any changes in DC infiltration into the major colonic mesenteric lymph node. If enhanced translocation of gut DCs was responsible for the enhanced pool of systemic DCs, we would likely expect less DCs within the colonic lymph node, suggesting that colon resident DCs were not preferentially migrating systemically following LH663 treatment. For our hypothesis to hold true, it may therefore be more likely that LH663 programmes gut DCs from the small intestine, which is more typically associated with systemic immune programming via the network of Peyer's patches(*294*). Another explanation for these findings could be that LH663 encourages sustained differentiation or proliferation of local colonic DCs, or their precursors, to maintain the local pool of DCs even following an enhanced systemic translocation. Whilst multiplex cytokine analysis of adaptive immune analytes in the colonic intestinal tissue revealed a reduction in TNFα and near significant reduction in IFNγ levels in PyMT-BO1-bearing animals, this finding was not replicated in the BRPKp110-bearing animals, leaving questions over the biological relevance of the finding. Notwithstanding the inconsistency between models, these

inflammatory analytes are the exact cytokines in which we see changes systemically and at the primary tumour, so could reflect a translocation of $CD8^+$ T cells expressing IFNγ and TNFα from the colon to the tumour.

Overall, our data provide experimentally validated findings for the downstream $CD8^+$ T cell-dependent mechanism of action of therapeutic LH663 administration across several models of breast cancer. We couple this with concrete associations to $CD8^+$-promoting macrophage and DC pathways, which could represent the upstream determinants of the observed $CD8^+$ activity. In contrast to most of the existing literature(*363, 413, 429*), we have shown the key functional output from the gut is neither metabolite-based nor dependent on direct translocation of bacterial cells. Whilst our gut mucosal immunology is not conclusive, we speculate that direct programming and systemic translocation of gut immune cells represents the most likely LH663-induced functional output. Experimentally validating these mechanisms are difficult however and may rely on identification of the key effector produced by LH663 cells, enabling *in vitro*/*ex vivo* experiments highlighting potential interactions with and functional changes to candidate immune cells.

5. *B. pseudocatenulatum* LH663 produces a unique exopolysaccharide with potential as a novel anti-cancer therapeutic

For a microbe to be therapeutic, it must produce an active compound. Despite the simplicity of this statement, characterisation of the active compounds produced by therapeutic gut microbes in complex disease is remarkably poor, with relatively few studies successfully obtaining such a level of mechanistic depth. The active compound may represent a solitary determinant or be one of many active compounds to initiate a biological effect in the host. Likewise, this active compound may directly interact with the host, or it may induce the activity of secondary commensals as part of a more complex therapeutic network. Key examples of these active compounds, as introduced in chapter 4, include microbial produced metabolites(*422*), cell structural components (e.g., peptidoglycan, flagellin)(*581*) and sugars(*434*). Importantly, the production of these functional active compounds can be variable and context dependent, with host-specific conditions within the gut (e.g., pH, nutrient availability, abundance of competing microbes) all converging to impact bacterial viability and function(*582*). For example, a bacterium which does not survive well in a particular host may be impeded in the ability to secrete bioactive metabolites or to sustain key physical interactions. The differential availability of nutrients between different hosts can have an impact on the constituents of bacterial cell walls and sugars(*583, 584*), potentially changing their physical confirmation and altering binding affinity and biological activity. This range of host-intrinsic factors, which are variable between individuals, may represent a key reason why the efficacy of therapeutic bacteria has been inconsistent in human clinical trials thus far. We speculate that some patients will have conditions conducive to the production and activity of microbial active compounds and respond to therapy, whilst others do not.

With these key factors considered, defining microorganism-produced active compounds represents a huge advance within the field of microbiome therapeutics. By identifying these therapeutic agents, we gain the ability to use either live bacteria or their active compound(s) as the active pharmaceutical ingredient (API), which we can tune depending on disease indication and mechanism of action to determine the approach most likely to induce patient benefit. In most cases, the isolation and use of the active compound(s) of microbes will likely represent an advantage over using live

bacteria by avoiding the confounder of individual-specific conditions disrupting live bacterial cells, which may alter *in vivo* active compound production. Thus, by using microbe-derived active compounds as therapeutics, the issues of inconsistent clinical efficacy may be overcome. Even where live bacteria are chosen as the API, knowledge of the active compounds determining efficacy will allow clinicians to stratify patients based on their specific conditions (e.g., microbiota profile, diet, nutrient composition), to ensure successful active compound activity and more consistent clinical responses.

An unfortunate reality of microbiome biology is that definition of microbial active compounds is difficult. This is due to the scale and complexity of gut microbiota, with so many interlinking and changing variables (i.e., gut microorganisms), it is challenging to work backward from a gut community-based approaches to define individually relevant compounds produced by an individual microbial strain. To gain this level of clarity, it is essential to study potential bacterial candidates individually to ascertain which bioactive compounds a strain can produce, in what quantities, and defining the potential impact of these compounds on other microbes and the host. Finally, a clear and detailed definition of the *in vivo* impact of the whole bacteria is also required, to validate a candidate active compound can recapitulate the fundamental mechanism(s) of action of the live bacterium. Although we endeavoured to identify the complete systemic (outside the gut) effector mechanism driving *B. pseudocatenulatum* LH663 anti-cancer efficacy in chapter 4, some key pathways were not completely validated. We successfully showed the downstream effector pathway driving response was dependent on the activity of $CD8^+$ T cells, whilst also identifying key candidate upstream immunological pathways (macrophages and dendritic cells) which may be driving the $CD8^+$ response. However, we were unable to validate the key functional outputs from the gut driving the response and link them to a specific immune effector pathway. We were able to show the effect was not driven by systemic release of bioactive metabolites, or through direct translocation of live LH663 cells, but our immune profiling of the gut was incomplete (only focused on the colon) and inconclusive.

Our aims for this chapter were to characterise the key functional interactions and active compounds within the host gastrointestinal tract following LH663 administration. Our intention was to leverage these findings to infer the likely systemic functional output outside the gut, through testing the identified active compound against the immunological pathways we have shown to be important ($CD8^+$ T cells, macrophages, and dendritic cells). Our data show that the therapeutic effect of LH663 is not

dependent on other bacteria within the gut and rather is due to direct effect of bacterial exopolysaccharide (EPS) on the cell surface. EPS analysis revealed a glucose- and galactose-rich structure, which specifically activated dendritic cells rather than $CD8^+$ T cells or monocytes/macrophages, through a TLR-independent mechanism.

5.1. Administration of *B. pseudocatenulatum* LH663 does not alter the commensal microbiota

To initially characterise the potential effects of *B. pseudocatenulatum* LH663 within the gut, we sought to define whether other commensal bacteria may be impacted by determinants of LH663 therapeutic efficacy. To gain view into the effect of LH663 on commensal microbiota dynamics, we conducted shotgun whole genome sequencing (WGS) of the caecum of BRPKp110 tumour bearing animals. Analysis of the wider microbiome profile revealed that there were no significant differences in bacterial phyla and species relative abundances following LH663 administration (Figure 5.1A). As expected, administration of LH663 did not significantly impact α-diversity (Figure 5.1B) or β-diversity (Figure 5.1C), highlighting an absence of difference to individual species or to the wider microbiome profile between groups. As with our metabolomics approaches, we also profiled PyMT-BO1 tumour-bearing animals to identify notable changes conserved across tumour models, thus boosting reliability of the interpretation of such large datasets. Our data in PyMT-BO1 animals showed the same results, no changes to individual phyla (Figure 5.2A) or species, as well as no changes to α-diversity (Figure 5.2B) or β-diversity (Figure 5.2C). Taken together these data show that LH663 does not significantly alter the abundance of other commensal within the host gut, indicating that the anti-tumour effects of LH663 are not due to the amplification or inhibition of other biologically active bacteria.

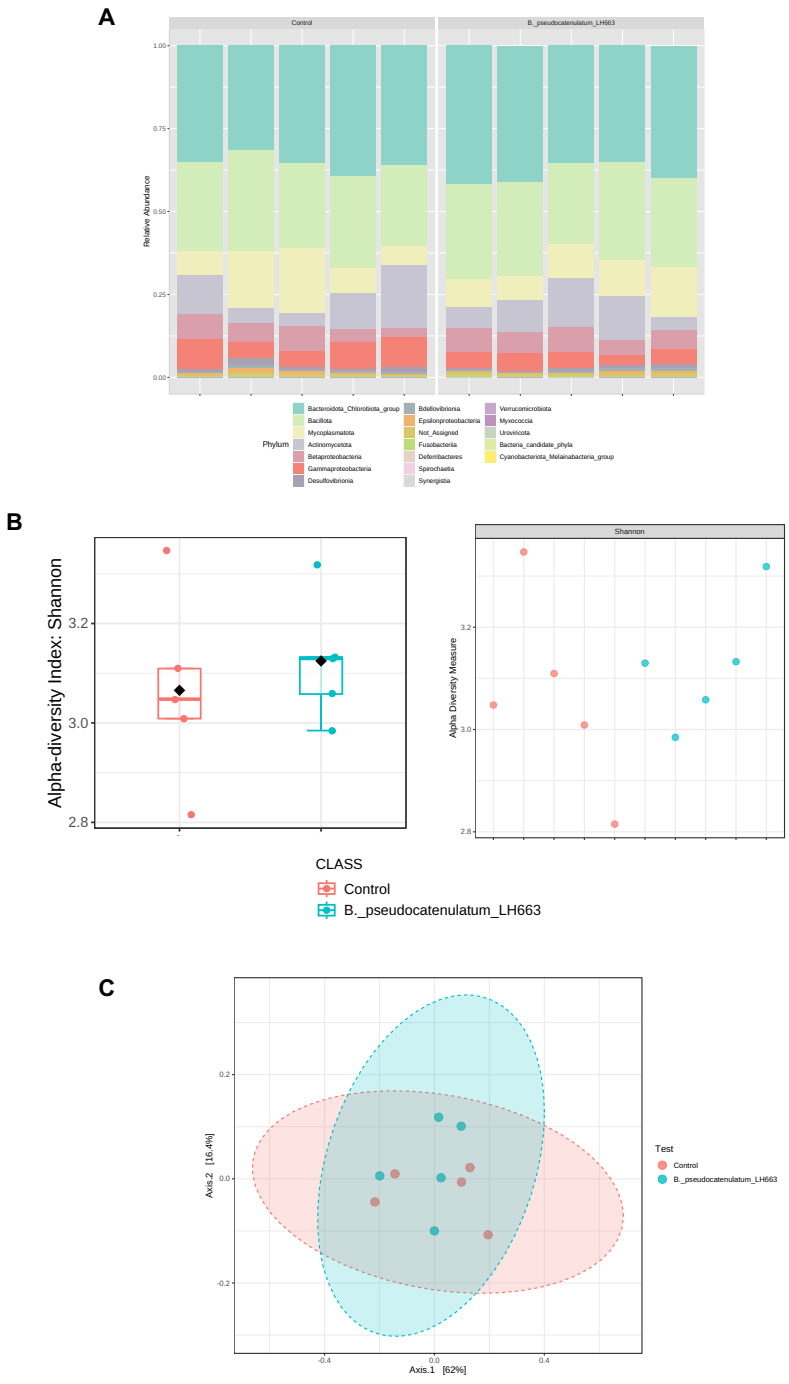

Figure 5.1. *B. pseudocatenulatum* LH663 administration does not significantly alter the balance of the commensal gut microbiome in BRPKp110 tumour-bearing animals. (A) Stacked bar plots showing relative abundance of bacterial phyla following administration with *B. pseudocatenulatum* LH663. (B) Boxplots showing the α-diversity of control or *B. pseudocatenulatum* LH663 treated animals measured via the Shannon index. (C) β-diversity of endpoint caecal microbiomes visualised using principal coordinate analysis (PCoA) with the Bray–Curtis index. (A-C) n=5.

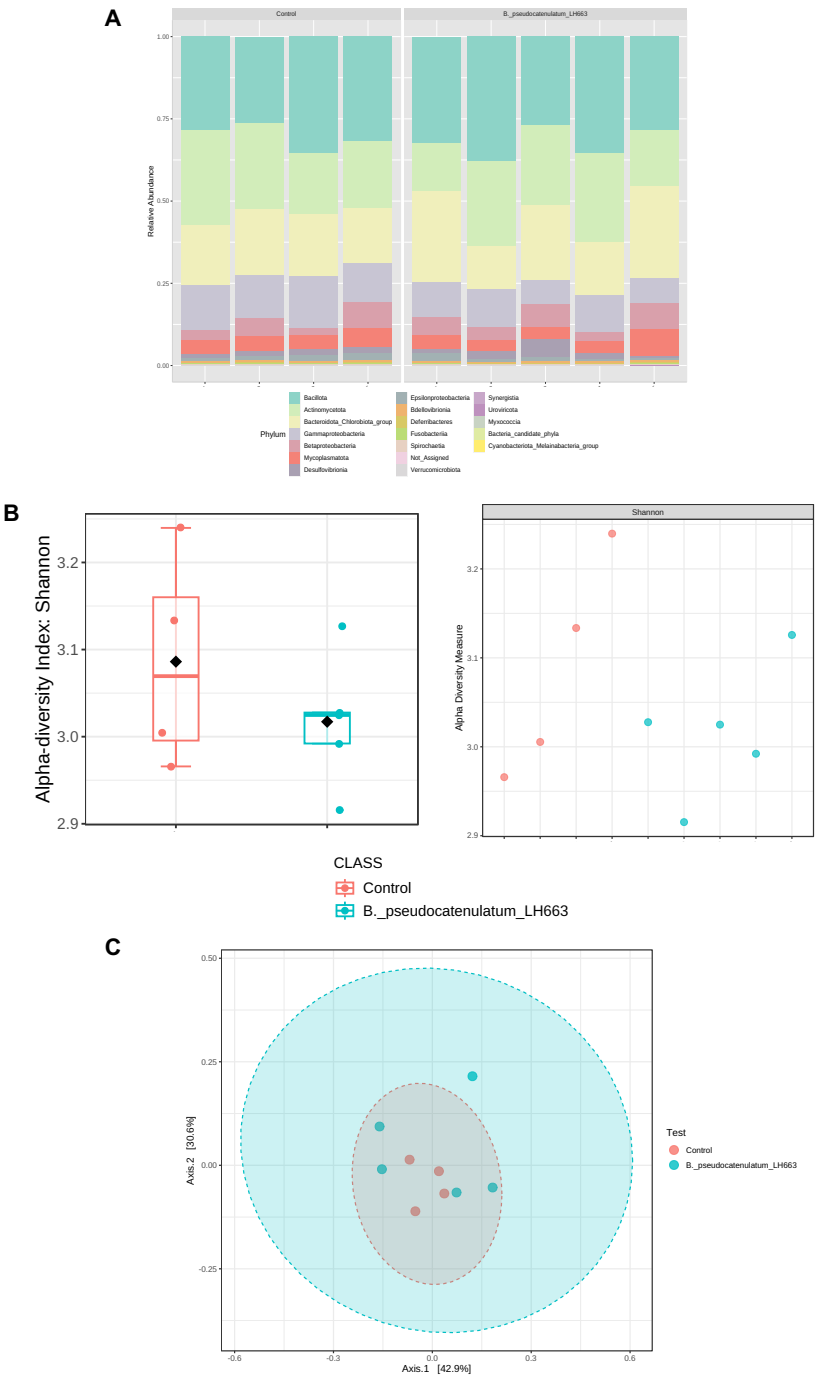

Figure 5.2. *B. pseudocatenulatum* LH663 administration does not significantly alter the balance of the commensal gut microbiome in PyMT-BO1 tumour-bearing animals. (A) Stacked bar plots showing relative abundance of bacterial phyla following administration with *B. pseudocatenulatum* LH663. (B) Boxplots showing the α-diversity of control or *B. pseudocatenulatum* LH663 treated animals measured via the Shannon index. (C) β-diversity of endpoint caecal microbiomes visualised using principal coordinate analysis (PCoA) with the Bray–Curtis dissimilarity index. (A-C) n=5.

In addition to diminishing the relevance of other commensal bacteria to the LH663 mechanism, the absence of any effects of LH663 on other bacteria indicated an absence of biological processes from LH663 capable of modulating other bacteria (e.g., production of commensal nutrient sources or anti-microbial bacteriocins). This is perhaps surprising, given that the presence of *Bifidobacterium* is associated with enhanced activity and prevalence of other commensals(*379*), and that *Bifidobacterium* have also been shown to produce anti-microbial bacteriocins(*585-587*). Notably, analysis of the genomic reads for both the *Bifidobacterium* genus and *B. pseudocatenulatum* revealed no significant alterations following LH663 administration (Figure 5.3). This is surprising, given a relatively high dose of LH663 ($1x10^{10}$ CFU) was administered only 24 hours prior to caecum harvest for DNA isolation. Given the lack of an increase in *Bifidobacterium* signature, the data suggest that LH663 cells are flushed through the gut quickly (within 24 hours) and thus do not effectively colonise the murine host. This may be due to the human strain not being adapted to effectively embed within a murine host, or may be due to a fundamental lack of viability of LH663 cells following arrival to the gut. Mechanistically, these findings infer that the *in vivo* action of LH663 is likely transient, with only a short window for active processes such as metabolite production and cross feeding to occur (if they occur at all due to poor viability), potentially explaining why the administration of LH663 does not alter the abundance of other commensals.

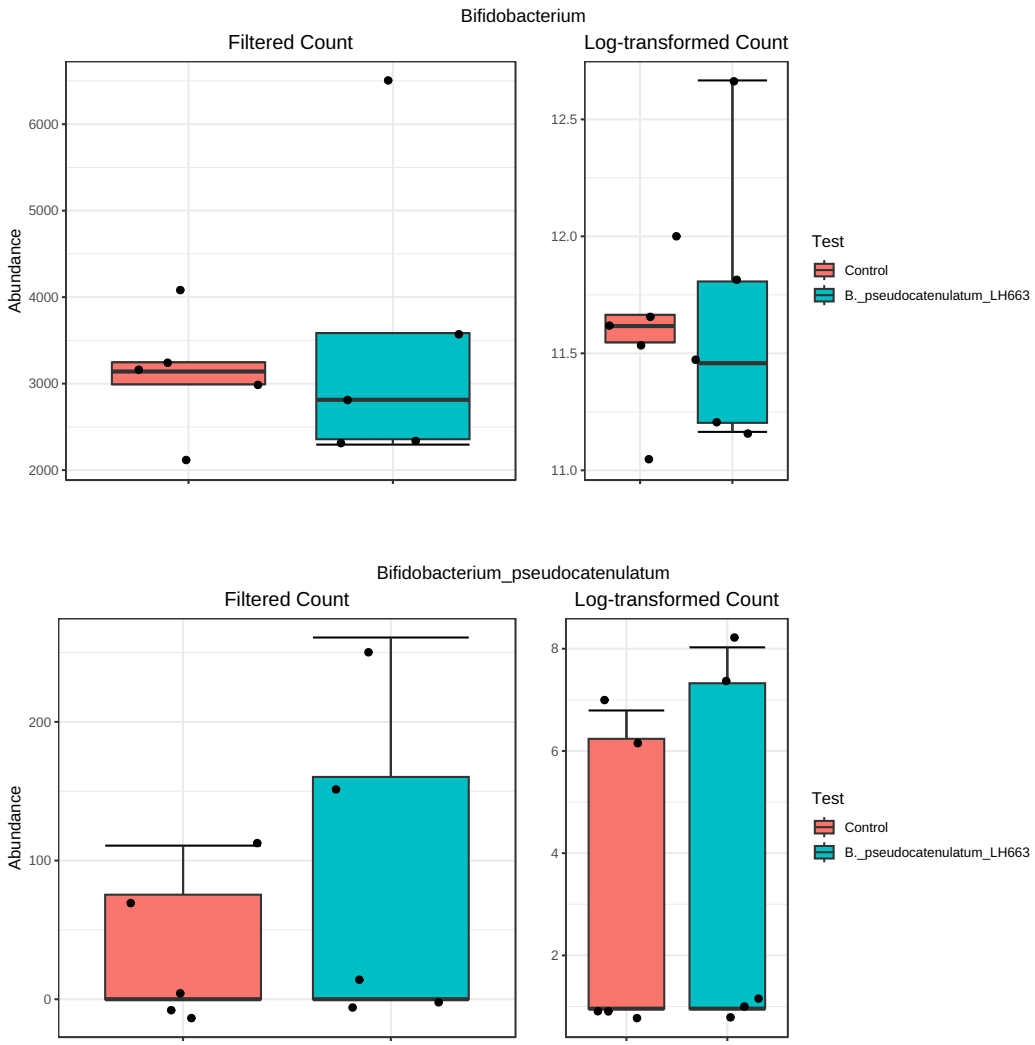

Figure 5.3. *B. pseudocatenulatum* LH663 treatment does not significantly increase the abundance of *Bifidobacterium* genomic reads in the caecum 24 hours post-administration. Bar plots showing the filtered and log-transformed counts of *Bifidobacterium* (top) and *B. pseudocatenulatum* (bottom) genomic reads in the caecum 24 hours after LH663 administration in BRPKp110 tumour-bearing animals, n=5.

5.2. *B. pseudocatenulatum* LH663 appears to inhibit tumour growth independently of other commensal bacteria

Although our shotgun WGS data had inferred a limited potential for other commensals to be mediating the LH663 mechanism of action, we validated this theory through an antibiotic-based knockdown of the commensal gut microbiota prior to LH663 therapy against BRPKp110 tumours (Figure 5.4A). The VNMAA antibiotic cocktail is a well defined model for whole microbiota depletion(*355, 356, 588*) and we have previously

validated successful microbiota ablation after just three treatments(*355*). As expected, the cancer-protective effects of LH663 administration were not reversed following gut microbiota clearing with antibiotics, with the tumour volumes of non-cleared and antibiotic-cleared microbiota groups being equivalent in size (Figure 5.4B). It is however notable that antibiotic only control tumours were smaller (non-statistically significant trend) than the non-antibiotic controls, which is in contrast to the weight of literature suggesting microbiota ablation would likely cause enhanced tumour progression(*354-356*) and is associated with worse clinical outcomes(*589*). The result of this slight decrease in antibiotic-treated controls was that the reduction of tumour volumes compared to antibiotic + LH663-treated animals was not statistically significant (*P*=0.24). However, given that there was no difference between either of the LH663-treated tumour groups, and our metagenomics data showing no changes in other commensal species, we concluded that commensal bacteria are most likely dispensible for LH663 efficacy.

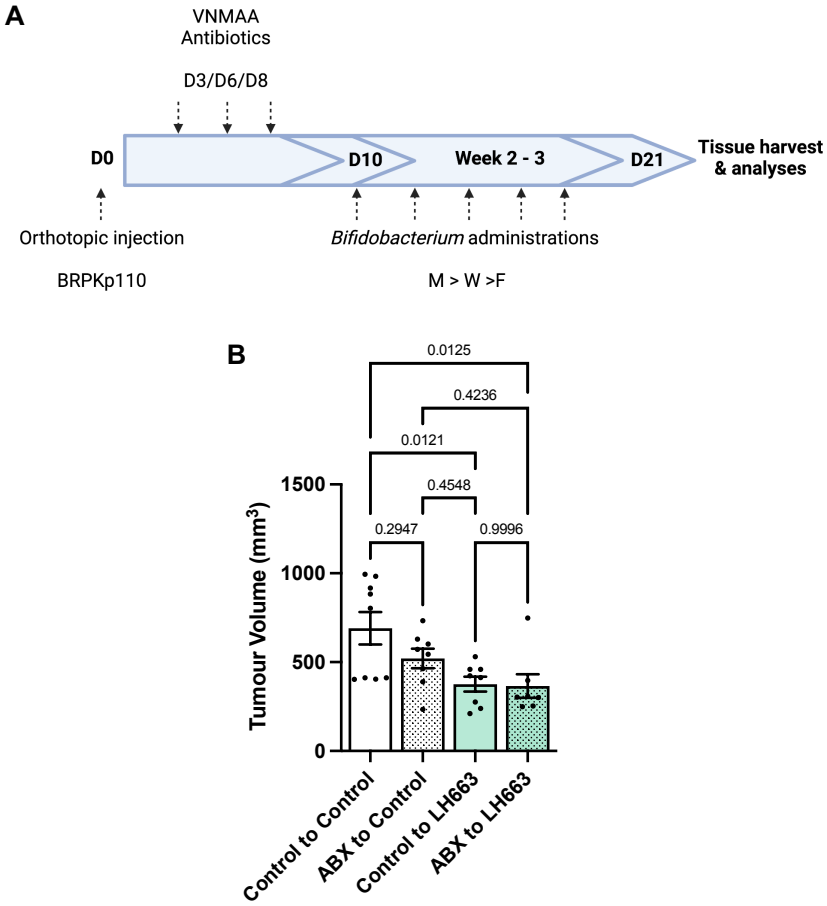

Figure 5.4. Antibiotic-induced depletion of the commensal gut microbiota does not diminish the anti-tumour efficacy of *B. pseudocatenulatum* LH663. (A) Experimental outline of antibiotic depletion experiment, three treatments of VNMAA cocktail were administered to the animals before the onset of a palpable tumour and administration of *Bifidobacterium*. (B) Endpoint BRPKp110 tumour volumes of control or antibiotic pre-treated animals supplemented with either *B. pseudocatenulatum* LH663 or vehicle control, n=7-9. Bars represent mean values (± SEM) and statistical significance was calculated by one-way ANOVA with Tukey's multiple comparison test. *P* values represented within the figure.

5.3. *B. pseudocatenulatum* LH663 exopolysaccharide (EPS) is sufficient for anti-tumour immunity independent of viable bacteria

Building on the finding that LH663 administration did not signficiantly enhance the amount of caecal *B. pseudocatenulatum* genomic reads 24 hours post-treatment, we hypothesised that a physical interaction between LH663 cells and the host was more probable than an active functional process due to the extremely short window within which LH663 is present in the gut. Our proof of concept for this was to test the neccesity for viable LH663 cells for anti-cancer efficacy, whereby any active processes would be inhibited and only physical interactions (e.g., from cell structural componants) would be possible. Although the most common technique for these experiments is usually to heat-kill bacteria, this approach is likely to degrade and alter the delecate structual components of the bacterial cell wall. As such, we utilised an approach developed by Moor et al.(*489*), using peracetic acid treatment to simulataneously kill the bacteria and preserve the outer structural components. Using this appraoch, we successfully demonstrate anti-tumour effiacy of peracetic acid-killed LH663 to equivalent levels shown from the live LH663 control arm (Figure 5.5A). These data concusively validate the neccesity of a non-active physical interaction for LH663 therapeutic effiacy, supporting our previous data refuting a mechanism based on metabolite release or active LH663 cell translocation.

Although little is known of the physical *Bifidobacterium* components which drive systemic immunity, primarily due to the weight of literature focused on the release of microbial metabolites, there is evidence to suggest that structural peptidogylcan(*387*) and exopolysaccharide (EPS)(*456*) can act as key stimulators of host immunity. EPS, in particular, has been associated with the modulation of both macrophages(*455*) and dendritic cells(*456*), so formed the intial focus of our investigation. To test the potential

relevance of EPS to the LH663 mechanism, we enzymatically isolated EPS from the host LH663 cells to over 95% purity of carbohydrates (data not shown) and delivered the exogenous sugar orally to BRPKp110 tumour bearing animals. BRPKp110 tumour growth was significantly inhibited by exogenous LH663-EPS administration, to equivalent levels observed from administration of live, intact, LH663 cells (Figure 5.5B). Analysis of the serum of LH663-EPS treated animals highlighted the same elevated levels of IFNγ (Figure 5.5C) as we had previously shown from live LH663 in section 4.3. Within BRPKp110 primary tumours, LH663-EPS treated animals showed an increase in IFNγ and TNFα co-expressing $CD8^+$ T cells (Figure 5.5D), with this $CD8^+$ population also being more heavily polarised to the activated effector-memory subtype (Figure 5.5E).

The promotion of the characteristic LH663 $CD8^+$ T cell response following exogenous LH663-EPS treatment solidifies the hypothesis that EPS is the LH663 active compound, and further analysis demonstrated LH663-EPS recapitulation of upstream $CD8^+$-promoting pathways stimulated by live LH663. Treatment with LH663-EPS induced a significant reduction in $CD206^+$ macrophage infiltration into BRPKp110 primary tumours (Figure 5.5G), whilst also increasing the pool of circulating dendritic cells (Figure 5.6A). As seen in live LH663 treated animals, the increase in total systemic dendritic cells was specifically mirrored in enhanced levels of the $CD8^+$-specific cDC1 population, but not the T helper-specific cDC2 population (Figure 5.6B). Notably, use of exogenous EPS appeared to induce systemic dendritic cells much more significantly than live LH663 (Figure 4.10). Taken together, these data demonstrate that LH663-EPS treatment completely recapitulates the BRPKp110 tumour inhibition and immunological mechanism observed from live LH663, with the biology of this (likely) physical interaction supporting our prior data suggesting a mechanism not dependent on viable LH663 cells or active processes (e.g., metabolite release or active cell translocation).

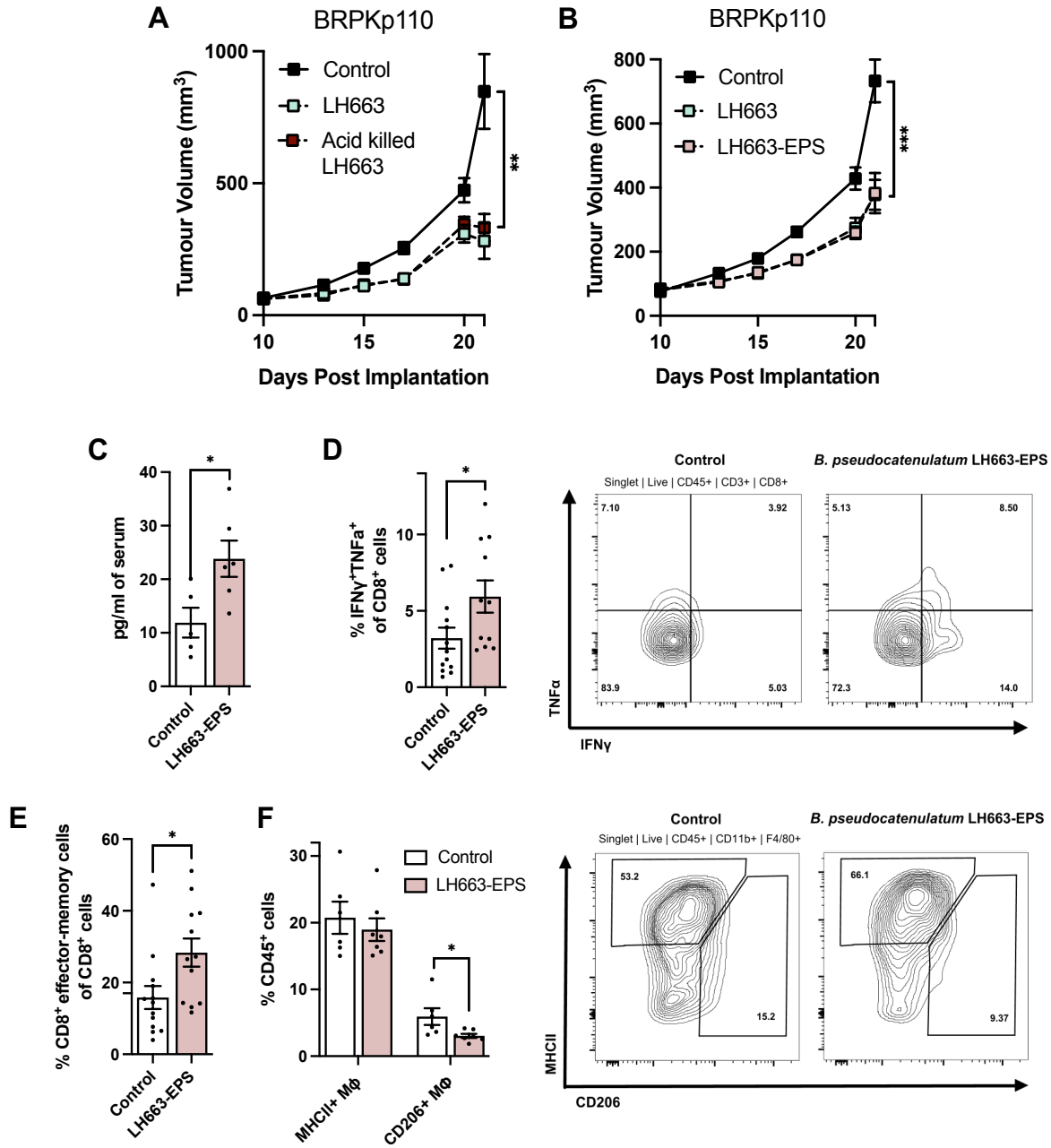
A
BRPKp110
Tumour Volume (mm3)
Control
LH663
Acid killed LH663
Days Post Implantation
**
B
BRPKp110
Tumour Volume (mm3)
Control
LH663
LH663-EPS
Days Post Implantation
***
C
pg/ml of serum
Control
LH663-EPS
*
D
% IFNγ+TNFa+ of CD8+ cells
Control
LH663-EPS
*
Control
B. pseudocatenulatum LH663-EPS
Singlet | Live | CD45+ | CD3+ | CD8+
7.10
3.92
83.9
5.03
5.13
8.50
72.3
14.0
TNFα
IFNγ
E
% CD8+ effector-memory cells of CD8+ cells
Control
LH663-EPS
*
F
% CD45+ cells
Control
LH663-EPS
MHCII+ Mφ
CD206+ Mφ
*
Control
B. pseudocatenulatum LH663-EPS
Singlet | Live | CD45+ | CD11b+ | F4/80+
53.2
15.2
66.1
9.37
MHCII
CD206

Figure 5.5. *B. pseudocatenulatum* LH663 exopolysaccharide (EPS) mediates BRPKp110 anti-tumour immunity independent of viable bacterial cells. (A) BRPKp110 mean (± SEM) tumour growth over time following administration of vehicle control, live LH663 or an equivalent dose of peracetic acid-killed LH663, n=8-9. (B) BRPKp110 mean (± SEM) tumour growth over time following administration vehicle control, live LH663, or isolated LH663-EPS, n=20-23, N=3. (C) Quantification of IFNγ in the serum of BRPKp110-bearing animals measured by MSD multiplex cytokine analysis, n=5-6. (D) Quantification with representative flow cytometry plots showing co-expression of IFNγ and TNFα by BRPKp110 tumour-infiltrating $CD8^+$ T cells following administration with isolated LH663-EPS, n=11-13. (E) Quantification of primary tumour $CD8^+$ effector memory T cell polarisation following LH663 administration, n=11-13. (F) Quantification and representative flow cytometry plot showing the infiltration of $MHCII^+$ and $CD206^+$ macrophages within BRPKp110 primary tumours following LH663-EPS administration, n=7. (C-F) Bars represent mean values ± SEM. (A-F) Statistical comparisons were calculated by two-tailed unpaired t test. ***P < 0.001, **P < 0.01, *P < 0.05.

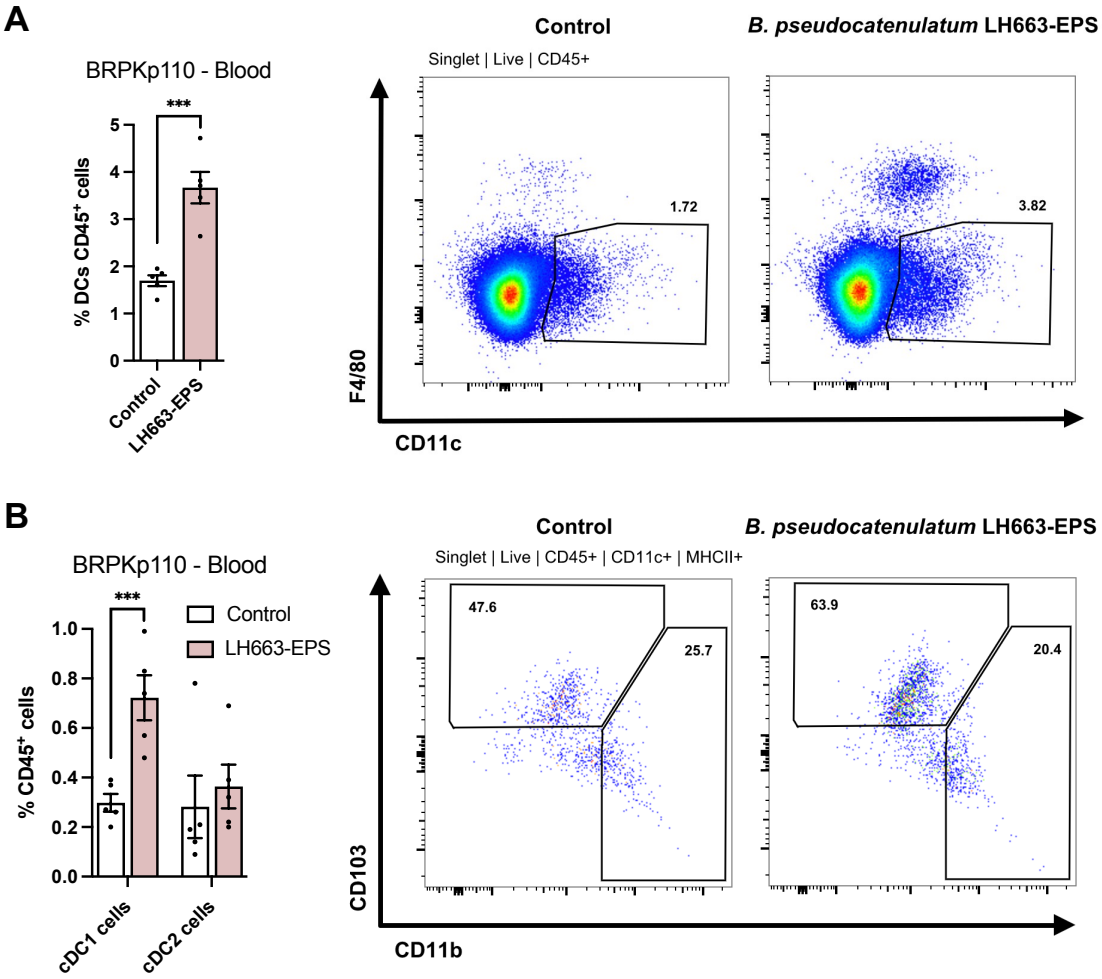

Figure 5.6. Administration of *B. pseudocatenulatum* LH663 EPS increases the circulating pool of DCs and cDC1 cells in the blood of BRPKp110 tumour-bearing animals. (A) Quantification and representative flow cytometry plots showing the infiltration of DCs and (B) cDC cells in the blood of BRPKp110-bearing animals following LH663-EPS treatment, n=5. Bars represent mean values (± SEM) and statistical comparisons were calculated by two-tailed unpaired *t* test. ***$P < 0.001$.

5.4. *B. pseudocatenulatum* LH663-EPS anti-tumour immunity does not depend on the activity of T helper or NK cells

In addition to the complete recapitulation of the live LH663 immunological mechanism activating $CD8^+$ T cells, macrophages, and dendritic cells, we also wanted to confirm that LH663-EPS was not signalling through any other potentially inflammatory pathways which could be contributing to anti-tumour immunity. As seen from live LH663 treatment, LH663-EPS did not alter the infiltration of major adaptive immune cell populations to BRPKp110 primary tumours (Figure 5.7A) and thus relies on alterations to immune cell activity. Immune activity, or indeed the systemic increases in IFNγ following LH663-EPS administration, is not caused by enhanced T helper cell or NK cell effector release (Figure 5.7B-C). These data highlight that the LH663-EPS mechanism of action, just as observed from live LH663, is both dependent on and specific to enhanced $CD8^+$ T cell effector activity, likely mediated by amplification of $CD8^+$-promoting macrophages and dendritic cells.

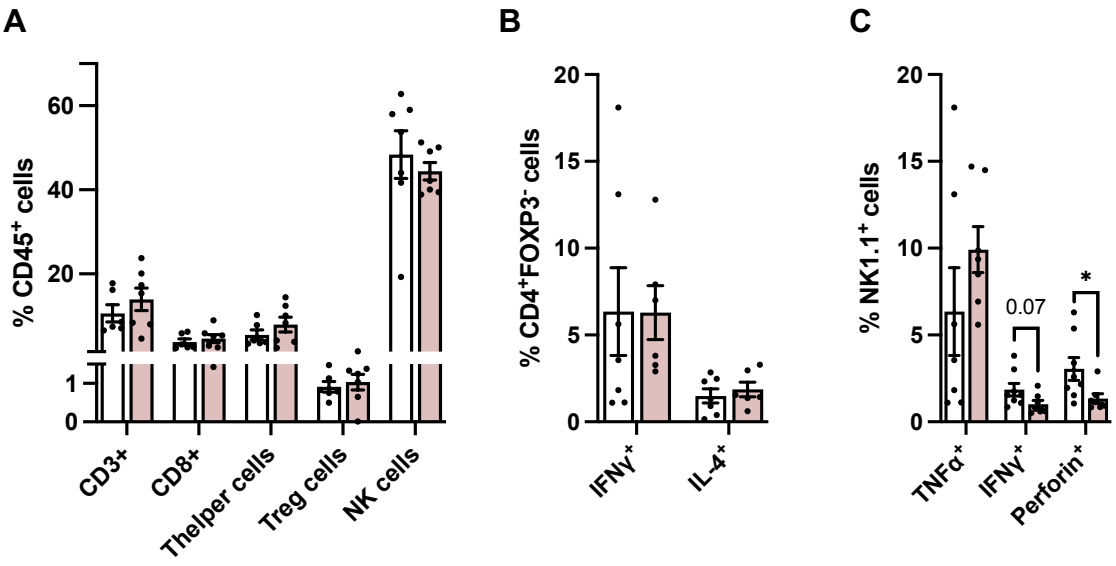

Figure 5.7. BRPKp110 primary tumour immune cell infiltrate or inflammatory T helper and NK cell responses are not enhanced by *B. pseudocatenulatum* LH663-EPS administration. (A) Infiltration of adaptive immune cells and NK cells into BRPKp110 primary tumours following LH663-EPS administration, n=7. (B) Quantification of intratumoural T helper cell IFNγ and IL-4 expression (n=6-7), and (C) NK cell IFNγ, TNFα and perforin expression following LH663-EPS administration, n=7-8. Bars represent mean values (± SEM) and statistical significance was calculated by two-tailed unpaired *t* test. **P* < 0.05.

5.5. Structural analysis of *B. pseudocatenulatum LH663* EPS reveals a galactose and glucose-rich structure

A major factor in the *in vivo* mechanisms of microbial EPS action is the composition and structure of the polysaccharide. EPS confirmation can vary widely between different types of bacteria, even different strains of the same species(*436*). Indeed, specific host immune receptors have different affinities for different sugar residues in different structural combinations, which can in turn generate significantly different immunological responses(*314, 449, 450*).

Using a gas chromatography mass spectrometry (GC-MS) approach to glycosyl analysis (based on depolymerisation of polysaccharides to monosaccharides with alditol acetate), we show that LH663-EPS is largely dominated by glucose and galactose sugar residues (Figure 5.8). Analysis of the precise molar ratios show a slightly enhance prevalence of galactose, alongside a negligible (and likely

mechanistically irrelevant) signal for mannose (Table 5.1). To infer structural details of how the sugar monomers link together, it is crucial to understand the location of the location of glycosidic bonds linking individual sugar monomers, as different carbon-carbon bond locations on different sugar monomers will specifically alter the 3D structure of the complete polysaccharide. Analysis of the most common linkage positions on each sugar monomer show a dominance of the 3-Linked galactopyranosyl residues, 4-Linked galactopyranosyl residues, and 4-Linked glucopyranosyl residues (Figure 5.9). Quantitative comparisons demonstrate these linkage residues are present in roughly equal ratios within the LH663-EPS sugar backbone and make up nearly 80% of the total linkage positions (Table 5.2). Overall, the linkage analysis showed mostly the presence of 3- and 4-linked galactose, along with 4- and 6-linked glucose residues. To complete the assessment of the EPS structure, 2D NMR analysis will be required to identify which sugar monomers link to each other through specific linkage points, as well as how polysaccharide chains may branch from the main backbone. Thus, more NMR-based experiments are required to establish a complete LH663-EPS structure.

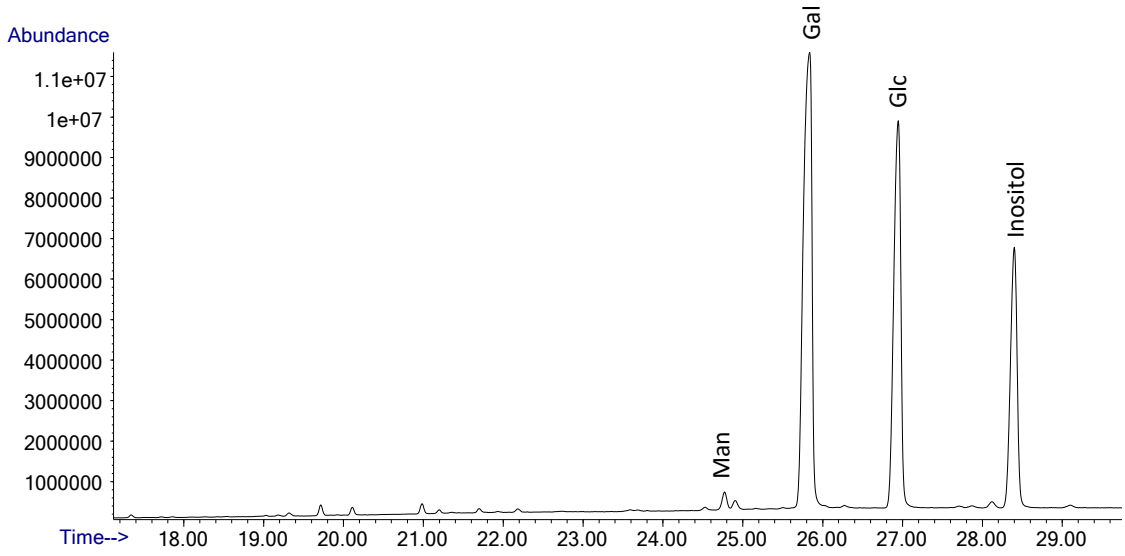

Figure 5.8. B. pseudocatenulatum LH663 EPS is dominated by galactose and glucose sugars. GC chromatogram of the monosaccharides generated by alditol acetate analysis of LH663 EPS. Inositol acted as the internal standard.

Table 5.1. Calculated molar ratios of LH663-EPS monosaccharides residues

B. pseudocatenulatum LH663 EPS	
Monosaccharide	**Mol %**
Mannose (Man)	1.4
Galactose (Gal)	57.8
Glucose (Glc)	40.7

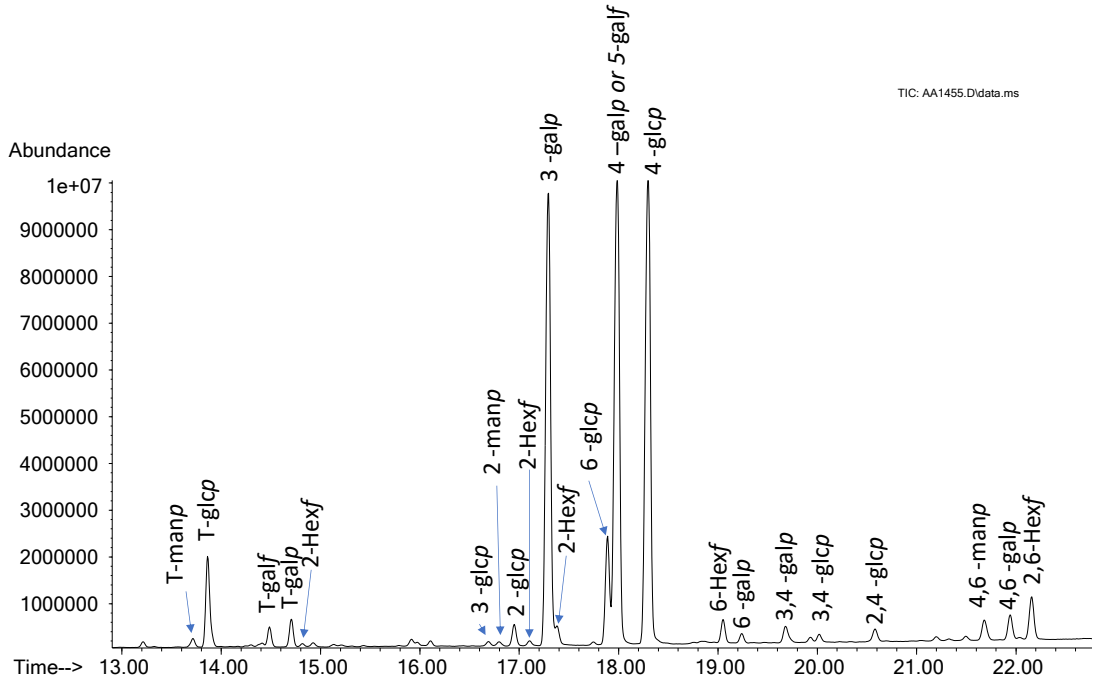

Figure 5.9. Glycosyl linkage types of *B. pseudocatenulatum* LH663 EPS. GC chromatogram of the partially methylated alditol acetates (PMAAs) labelling glycosyl linkage residues.

Table 5.2. Ratios of the peak areas corresponding to specific LH663-EPS glycosyl linkage residues

Mode of Linkage	LH663 EPS
Terminal mannopyranosyl residue (t-Man*p*)	0.4%
Terminal glucopyranosy| residue (t-Glc*p*)	4.1%
Terminal galactofuranosy| residue (t-Gal*f*)	0.8%
Terminal galactopyranosyl residue (t-Gal*p*)	1.2%
2-Linked hexofuranosy| residue (2-Hex*f*)	1.2%
3-Linked glucopyranosyl residue (3-Glc*p*)	0.3%
2-Linked mannopyranosyl residue (2-Man*p*)	0.3%
2-Linked glucopyranosyl residue (2-Glc*p*)	1.0%
3-Linked galactopyranosyl residue (3-Gal*p*)	25%
6-Linked glucopyranosyl residue (6-Glc*p*)	5%
4-Linked galactopyranosyl residue or 5 Linked galactofuranose residue (4-Gal*p* or 5-Gal*f*)*	26.5%
4-Linked glucopyranosyl residue (4-Glc*p*)*	27%
6-Linked hexofuranosy| residue (6-Hex*f*)	1%
6-Linked galactopyranosyl residue (6-Gal*p*)	0.4%
3,4-Linked galactopyranosyl or 3,5-linked galactofuranosyl residue (3,4-Gal*p* or 3,5-Gal*f*)*	0.9%
3,4-Linked glucopyranosyl residue (3,4-Glc*p*)*	0.4%
2,4-Linked glucopyranosyl residue (2,4-Glc*p*)*	0.6%
4,6-Linked mannopyranosyl residue (4,6-Man*p*)*	1.1%
4,6-Linked galactopyranosyl or 5,6-linked galactofuranosyl residue (4,6-Gal*p* or 5,6-Gal*f*)*	1.2%
2,6-Linked hexofuranosy| residue (2,6-Hex*f*)	2.2%

* The PMAAs of a 4-linked hexopyranose is identical to that of the 5-linked hexofuranose of the same sugar. Mannose and glucose are rarely seen in the furanose form, but galactofuranose is quite common. Therefore, and because three hexofuranose residues (2-Hex*f*, 6-Hex*f*, and 2,6-Hex*f*) were detected, we mentioned the possibility of furanose ring form only for the Gal residues, although it is theoretically also possible for Man and Glc residues.

5.6. Comparison of *B. pseudocatenulatum* LH663 with other strains of *B. pseudocatenulatum* demonstrate strain-specific EPS activity

A key question which arises from the discovery of an EPS-dependent mechanism of action, is how widespread is this biology across the *B. pseudocatenulatum* species, or

even across the *Bifidobacterium* genus more broadly? To gain insight over this, we administered several unique strains of *B. pseudocatenulatum* (LH13, LH14, alongside LH663) to test their ability to inhibit growth of BRPKp110 primary tumours. Alongside LH663 treatment, which inhibited tumour progression as expected, LH13 was successful in stunting tumour outgrowth whilst LH14 was not (Figure 5.11A). Analysis of the $CD8^+$ T cell response in primary tumours did not show any statistically significant differences between any of the groups tested, although we did observe a unusually high level of variation which likely combined with a low number of repeats to produce this data. Notwithstanding, we observed a non-statistically significant increase in polyfunctional $CD8^+$ T cells expressing IFNγ and TNFα following treatment with either LH663 or LH13, but not with LH14, correlating immune response with tumour inhibition (Figure 5.11B). Building on this, we wanted to understand whether the anti-tumour response we observed following both LH663 and LH13 administration was potentially due to an expression of similarly functioning EPS. Surprisingly, comparative genomics between the strains tested revealed that LH13 and LH14 had near identical EPS genomic clusters, which contrasted significantly with the EPS genomic clusters in the LH663 strain. Further analysis of the LH663 genome revealed a very similar combination of EPS clusters to another *B. pseudocatenulatum* type strain 'DSM 20438', which suggests that this strain may produce very similar EPS as LH663 and potentially show similar effects.

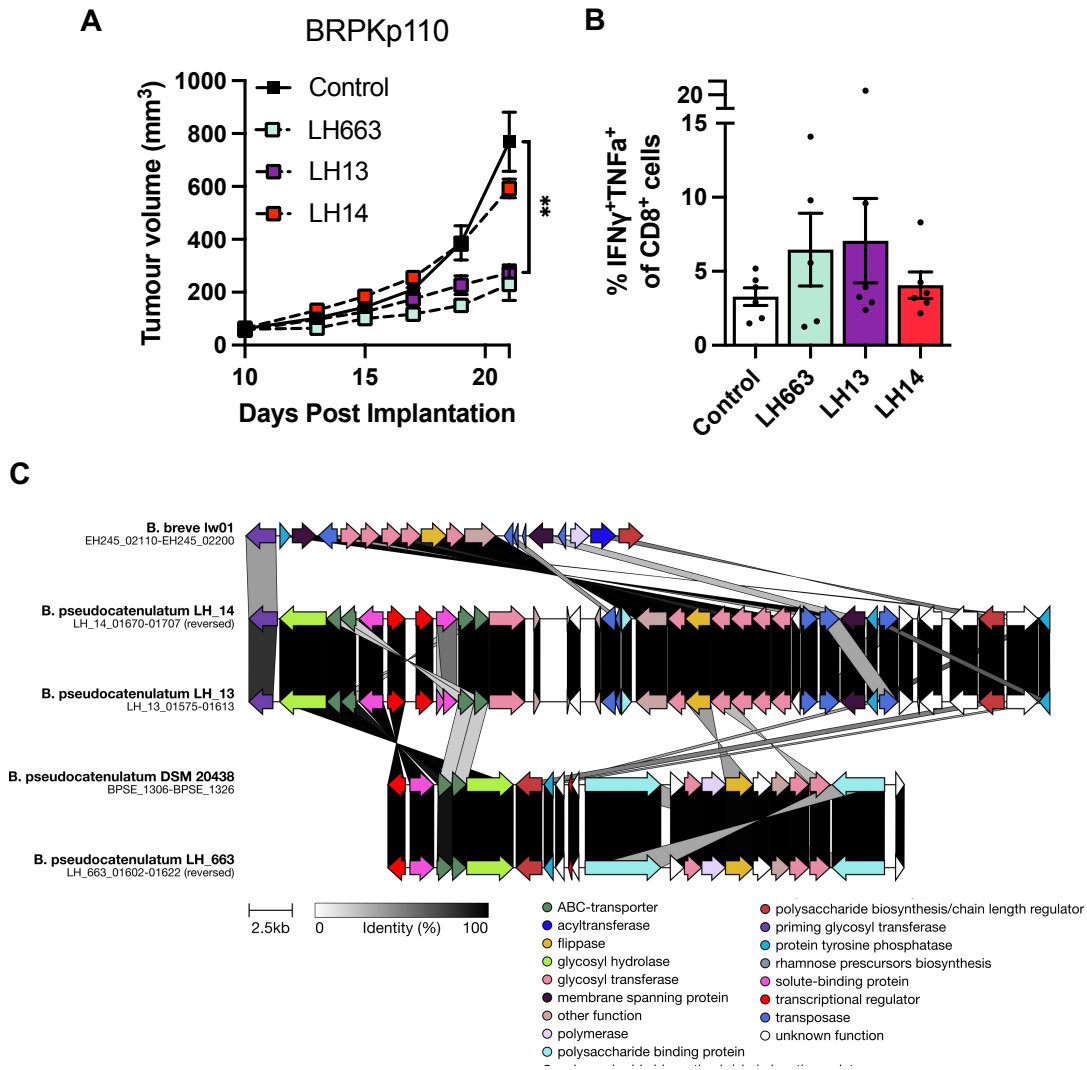

Figure 5.11. *B. pseudocatenulatum* produce unique strain-specific exopolysaccharides which have different functional effects. (A) BRPKp110 mean (± SEM) tumour growth over time following administration of the indicated strains of *B. pseudocatenulatum*, n=5-7. (B) Quantification of co-expression of IFNγ and TNFα by BRPKp110 tumour-infiltrating $CD8^+$ T cells following administration with strains of *B. pseudocatenulatum*, n=6-7. Bars indicate mean values (± SEM). (C) Proposed architecture of putative EPS clusters predicted in the genomes of the strains used in this study, and their homology to previously reported bifidobacterial EPS gene clusters based on Ferrario et al., 2016*(436)* and Wang et al., 2019*(503)*. Homology maps show amino acid identity above 30% (blastp E-value = 1e-50). Gene functions were predicted based on blastp searches against bifidobacterial EPS cluster sequences from the above-mentioned publications, the NCBI reference protein database (refseq_protein, default settings) and results generated with dbCAN3 server (hmmer E-value < 1e-15, coverage > 0.35). Statistical differences were calculated by (A) one-way ANOVA with Tukey's multiple comparisons test, or (B) Kruskal-Wallis with Dunn's multiple comparisons test. $^{**}P < 0.01$.

The finding that efficacious LH13 likely produces a similar EPS to the non-efficacious LH14, both of which probably being distinct from the tumour immunity-inducing LH663 EPS, suggested that LH13 may inhibit BRPKp110 tumour growth through an EPS-independent mechanism. Comparison of the average nucleotide identity (ANI) score across the whole genome of the strains shows that LH13 and LH14 are more similar to each other than to LH663 (Figure 5.12). Further analysis revealed a relatively small number of single nucleotide polymorphisms (SNPs) between both LH13 and LH14 relative to LH663 (Table 5.3), with further analysis of the nature of these SNPs potentially representing a platform for identification of why LH13 is efficacious when LH14 is not. The data overall highlight that there is significant variation between EPS genomic clusters, and likely physical structures, between different strains of the same species of *Bifidobacterium*, which in turn cause strain-specific effects on host (anti-tumour) immunity.

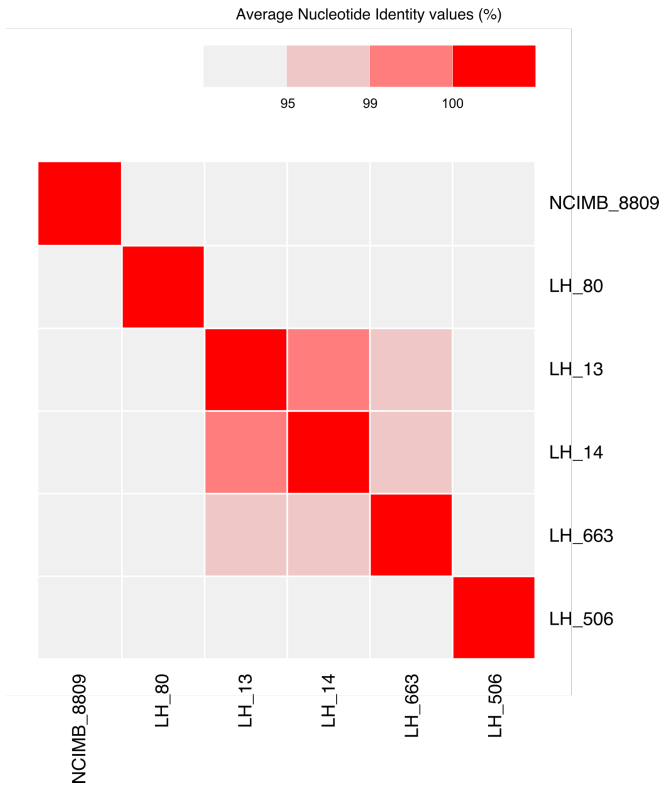

Figure 5.12. Average nucleotide identity (ANI) between *Bifidobacterium* strains used in this study. ANI value > 95% was considered for species delineation.

Table 5.3. Single nucleotide polymorphism (SNP) distance matrix between *Bifidobacterium pseudocatenulatum* isolates used in this study.

Strain	LH_663	LH_13	LH_14
LH_663	0	18,424	18,682
LH_13	18,424	0	1,414
LH_14	18,682	1,414	0

5.7. *B. pseudocatenulatum* EPS specifically activates dendritic cells *in vitro*

Given we have identified that the EPS produced by LH663 is the key active compound mediating anti-cancer efficacy of LH663, we sought to identify how the EPS likely interacts with the host and how this could fit in to the wider LH663 mechanism of action. In literature, one of the most described effects of microbial EPS on the host is the induction of immunity(*590*), which is an obvious link to the downstream immunological mechanism of action we have identified. Additionally, we hypothesised from our work in chapter 4 that the most likely gut functional output was a direct LH663 programming of gut immune cells causing a systemic cell translocation, which hypothetically could be mediated by LH663-EPS. Returning to this hypothesis, we undertook characterisation of the immunological effects on LH663-EPS on candidate immune cells *in vitro*. Focusing on the key pathways previously shown as important to the LH663 mechanism, we reveal that whilst live LH663 strongly stimulated pro-inflammatory cytokines (e.g., TNF, KC/GRO, IL-6) in $CD8^+$ T cells *in vitro*, LH663-EPS did not induce any obvious responses (Figure 5.13A). This finding was not unexpected, given that $CD8^+$ T cells are antigen restricted adaptive cells and require upstream activation, and so we moved our analysis towards monocyte and toll-like receptor (TLR) reporter lines. Initial focusing on live bacteria and comparison between LH663, LH13 and LH14, we found that LH663 was far more immunologically potent than either LH13 or LH14 as measured through NF-kB stimulation in THP1-blue monocytes (Figure 5.13B). Use of TLR reporter lines subsequently demonstrated that this increase

was due to a markedly greater stimulation of TLR2 (Figure 5.13C), which some literature suggests can be activated by bacterial EPS(*444, 591*). Due to the TLR4 and TLR5 sensitivity to LPS and flagellin respectively, none of the strains signalled through either of these other inflammatory receptors. However, testing of our myeloid reporter lines with LH663-EPS revealed an absence of general myeloid inflammatory response (measured by NF-kB stimulation in THP1-blue monocytes), or TLR activation (Figure 5.13D-E). These findings strongly suggests that LH663-EPS does not, in the initial phases of the anti-tumour immune mechanism, signal through monocytes, macrophages or the major extracellular TLRs.

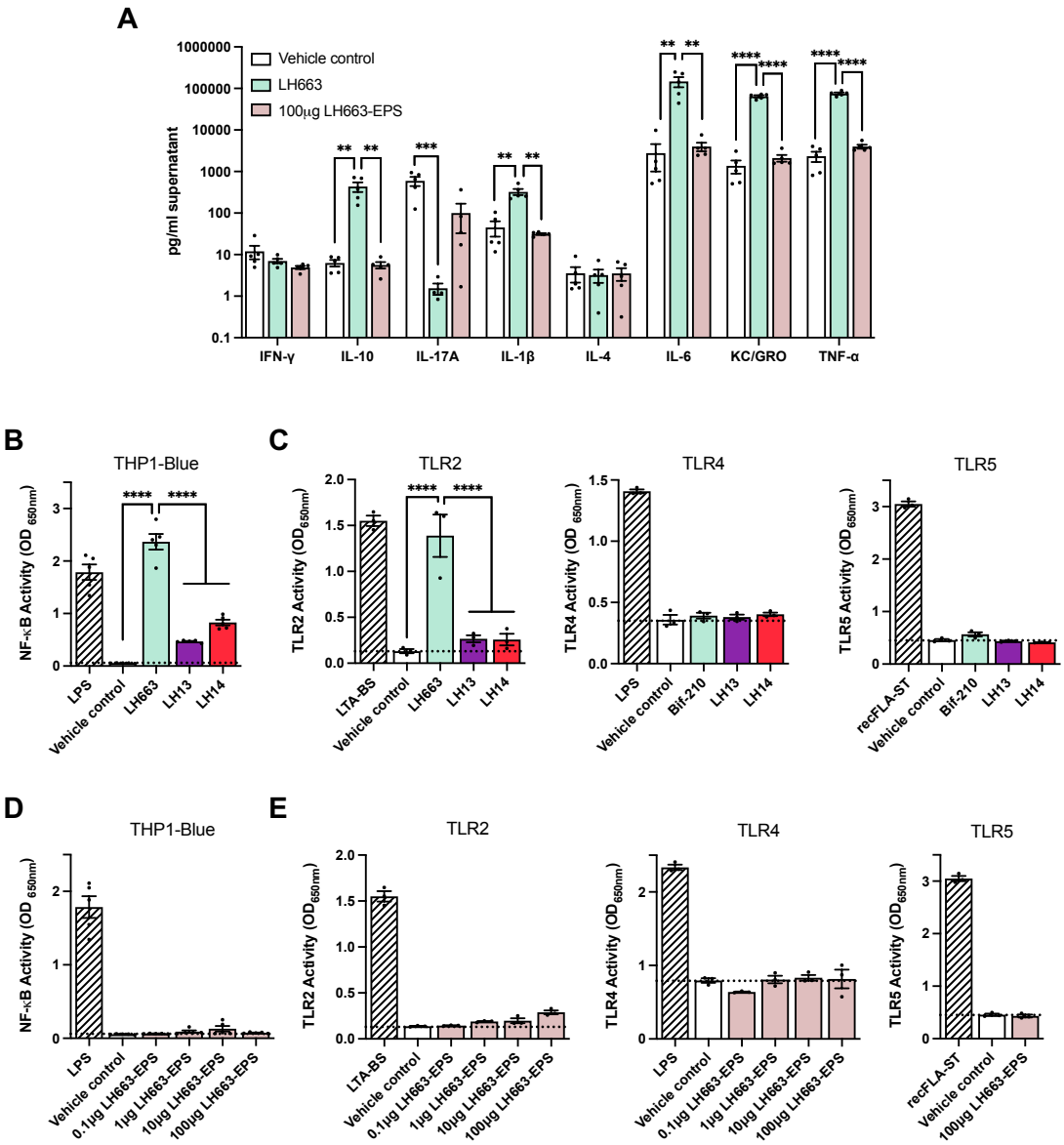

Figure 5.13. *B. pseudocatenulatum* LH663-EPS is not immunogenic to CD8⁺ T cells or monocytes *in vitro*. (A) Pro-inflammatory cytokine release from CD8⁺ T cells treated with either live LH663 cells or LH663-EPS *in vitro*, n=5 (B) Levels of NF-kB activity in THP1-blue monocytes following treatment with the indicated strains of *B. pseudocatenulatum*, n=5. (C) Activation of toll-like receptors by HEK-Blue-hTLR2, HEK-Blue-hTLR4, and HEK-Blue-hTLR5 cells following stimulation with strains of *B. pseudocatenulatum* measured by detection of the SEAP reporter, n=3. (D) Levels of NF-kB activity in THP1-blue monocytes following treatment with the indicated dosages of *B. pseudocatenulatum* LH663 EPS, n=5. (E) Activation of toll-like receptors by HEK-Blue-hTLR2, HEK-Blue-hTLR4, and HEK-Blue-hTLR5 cells following stimulation with dosages of *B. pseudocatenulatum* EPS, n=3. Bars represent mean values (± SEM) and statistical differences were calculated using one-way ANOVA with Tukey's multiple comparisons test. ****$P < 0.0001$.

With our *in vitro* data suggesting limited stimulation of either $CD8^+$ T cells or monocytes by LH663-EPS, the final mechanism-relevant immune population to probe was DCs. LH663-EPS modulation of this population would be logical given that bacterial EPS is known to be reactive to DCs through C-type lectin receptors to induce both pro-inflammatory and anti-inflammatory responses(*450, 592*). Additionally, the increase in systemic DCs with enhanced maturity we have observed previously could be explained by a direct translocation from the gut following LH663-EPS programming, fitting in with the broader increase we observe in anti-tumour $CD8^+$ T cell immunity. In contrast to the other immune populations tested, analysis of the effects of LH663-EPS on bone marrow-derived DCs (BMDCs) *in vitro* showed enhanced inflammatory responses. LH663-EPS treatment, even at a low dose of 1μg, increased BMDC maturation and suggests an enhanced potential to express antigen, correlating with our findings from *in vivo* DCs following LH663 treatment (Figure 5.14A). This conclusion is supported by an enhanced expression of MHCII in BMDCs following LH663-EPS treatment, which is another key marker for DC maturation and antigen presentation capability (Figure 5.14B-C). Overall, these data show that LH663-EPS directly activates DCs, but not $CD8^+$ T cells or monocytes, and could support a hypothesis of LH663-EPS causing a systemic translocation of gut resident DCs to induce anti-tumour immunity.

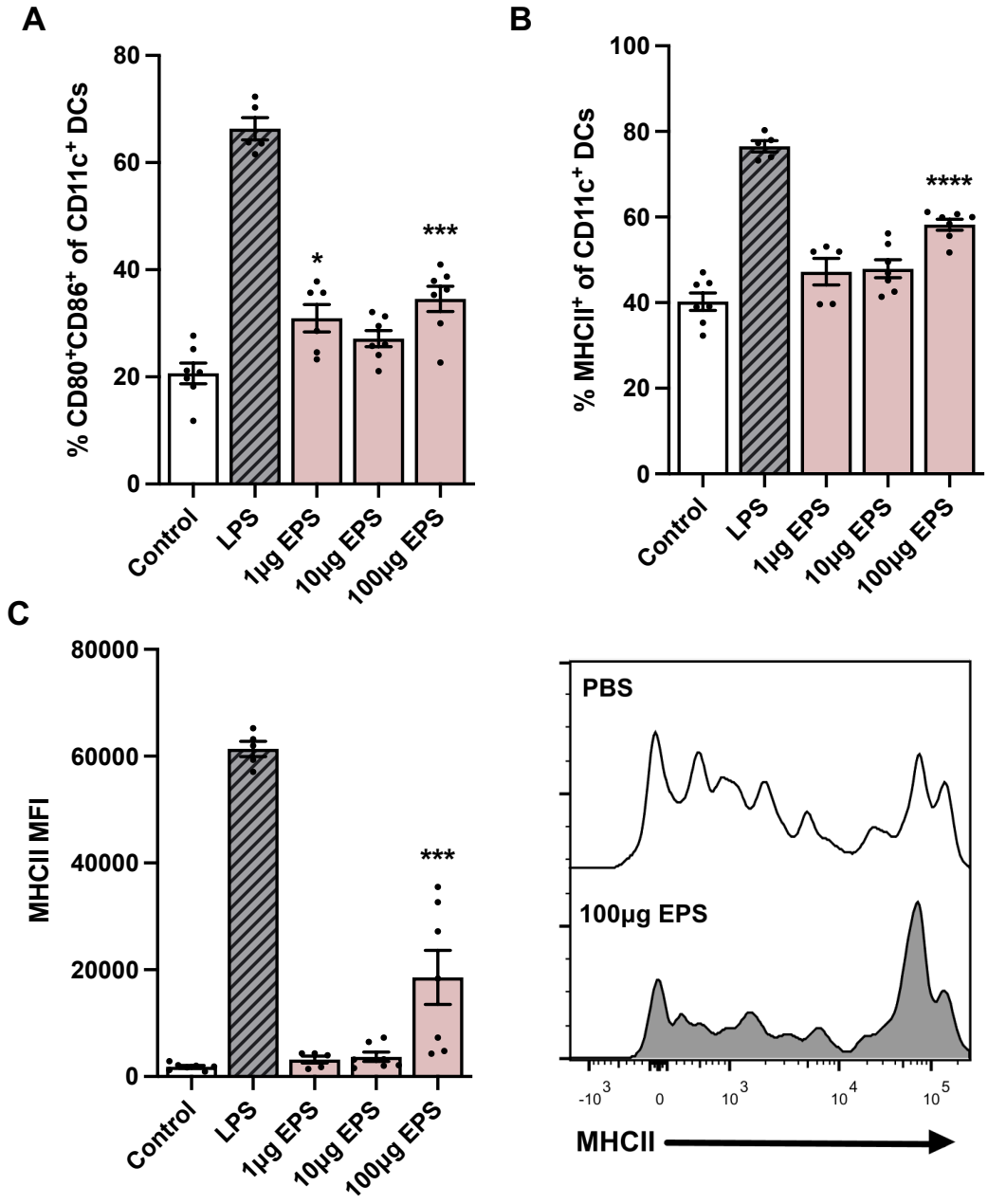

Figure 5.14. Exopolysaccharide isolated from *B. pseudocatenulatum* LH663 enhances dendritic cell maturation *in vitro*. Quantification of (A) $CD80^{+}CD86^{+}$ mature dendritic cells and (B) $MHCII^{+}$ dendritic cells following exposure to doses of LH663 EPS. (C) Quantification with representative histogram plots of dendritic cell MHCII expression measured by median fluorescence intensity. Bars represent mean values (± SEM), n=6-7, statistical significance was calculated by one-way ANOVA with Tukey's multiple comparisons test. ****$P < 0.0001$, ***$P < 0.001$, *$P < 0.05$.

5.8. Discussion

The search for the active compounds produced by therapeutic bacteria is a major challenge in the field of microbiome therapeutics. The relative youth of microbiome research and the difficulty with working on such complex biology has caused a paucity of knowledge in this space, although research compiled over the last few years is beginning to reveal novel facets of the driving host-microbe interactions. Actively produced microbial metabolites have thus far received most attention(*430, 593*), although more research is now revealing roles for active compounds not continually produced and excreted by active processes, such as cell wall peptidoglycan(*387*). An important factor which unifies most microbial active compounds, is that their production can be dictated and disrupted by the conditions of the host, such as differential nutrient availability and presence of competitive strains, which we hypothesise to be a major driver of inconsistency between responsive and non-responsive patients from unsuccessful clinical trials using bacteria. Additionally, the absence of such key knowledge about the active compounds produced by therapeutic bacteria impedes the ability to biochemically improve on therapeutic progress (e.g., by development of small molecule alternatives) because the key ligand-receptor interactions are not defined. Because of the biological importance of identifying microbial active compounds to the translation of bacterial therapeutics, and the potential for such knowledge to shed light on the downstream host-microbe interactions important for LH663 efficacy, the work in this chapter aimed to identify the key functional compound produced by LH663 for induction of anti-cancer immunity.

A major concept within microbiome research is the idea of biological networks between large diverse communities of bacteria. The principal of the one microbe, increasing or decreasing the activity or prevalence of another, which in turn mediates a functional effect on the host. Such secondary effects are commonly observed across metabolic pathways during nutrient biodegradation, whereby a primary metaboliser provides a nutrient source for a secondary metaboliser, which can continue sequentially until a nutrient is converted into its bioavailable form(*594*). A key hallmark of this process in action would be an altered microbiota profile following administration of LH663, although we did not see any such changes in the caecum of either BRPKp110 or PyMT-BO1 tumour models. The finding that there was not a significant increase in the

abundance of *B. pseudocatenulatum* genomic reads 24 hours-post administration was particularly surprising in this dataset, suggesting that LH663 cells were largely flushed out of the gut in less than this timeframe. The likely transient nature of LH663 within the commensal gut put the wider microbiome analysis into context because there is such a short window for LH663 to conduct active processes which may influence the activity of other microbes, increasingly the likelihood of a direct interaction with the host mediating LH663 efficacy. This hypothesis was substantiated by antibiotic-clearing of the commensal gut microbiome prior to LH663 administration, which though not quite statistically significant, did not reverse the rescue of LH663-treated tumour volume and suggested a mechanism not dependent on other bacteria.

With our shotgun metagenomic and antibiotic pre-treatment data suggesting a direct mechanism of action of LH663, we were able to focus more directly on LH663 host-microbe interactions as the likely mediator of anti-cancer efficacy. The next big question to answer here was whether the active compound of LH663 was produced by active or inactive processes within the gut. Given that LH663 appears to pass through the gut within 24 hours, we speculated that this was most likely an inactive process which did not rely on viable bacterial cells. Indeed, killing of LH663 cells with peracetic acid prior to administration showed that viability, and thus continually active bacterial cell processes, are not required for the mechanism of action, allowing us to focus on the physical antigenic structures intrinsically expressed by LH663 cells. Although peptidoglycan has been implicated as one such immunogenic structure expressed by *Bifidobacterium(387)*, another relevant structure which has been strongly associated with host immune activation is EPS(*595*). Although microbial EPS production in the gut has never been shown to induce systemic anti-tumour immune response, many studies have shown *Bifidobacterium* EPS to induce both pro- and anti-inflammatory immune responses in dendritic cells(*456, 592, 595*), monocytes/macrophages(*457*), and adaptive T cells(*456, 596*). The characterised interactions between EPS and these key immune populations, all of which we had previously identified as relevant to the LH663 downstream mechanism of action, focused our attention on EPS as a candidate for the active compound produced by LH663. Enzymatic isolation of EPS from LH663 allowed us to test this hypothesis *in vivo*, highlighting that administration of LH663-EPS alone recapitulated the tumour reduction and anti-cancer immune activation associated with the efficacy of live LH663 treatment. Notably, we were able to achieve this using a relatively low dose of EPS, 80μg per administration, which is roughly isolated from ~$1x10^8$ CFU. This is despite previous data generated in the lab (not shown) which demonstrated that administration of $1x10^8$ CFU of live LH663 was not sufficient to

inhibit tumour growth, implying that isolated EPS may be more potent than EPS delivered on a bacterial cell vehicle.

Although our structural conclusions are incomplete due to the absence of NMR analyses, characterisation of the LH663-EPS did reveal a dominance of galactose and glucose sugar monomers within the structure. Although there is huge variation in EPS composition between different species and strains of *Bifidobacterium(436)*, this type of composition is relatively typical and species of *B. longum(597)* and *B. bifidum(592)* has also be shown to also be dominated by galactose and glucose residues (albeit in different confirmations). Interestingly, study by Speciale et al.(*592*), highlighted several polysaccharide fractions isolated from the EPS of *B. bifidum* displaying markedly different immunological activities, highlighting the possibility of LH663 EPS being comprised of more than one polysaccharide structure.

With our data concretely showing the mediation of anti-tumour immunity by LH663-EPS, a key point to understand is how broadly the benefits of LH663 may apply to other strains of *B. pseudocatenulatum*. This research question, the variability of EPS between different strains of the same species of *Bifidobacterium*, is completely open; most literature to date has only compared EPS from different species of *Bifidobacterium(597-599)* with very little work shown from *B. pseudocatenulatum*. Our use of three strains of *B. pseudocatenulatum*, LH663, LH13 and LH14, highlighted that there is strain level differences and variability, as LH14 was ineffective in inhibiting tumour growth whilst the other strains were effective. Due to an unusual amount of variability in the data and a relatively low number of repeats, we were unable to confirm statistically whether both LH663 and LH13 produced the same characteristic $CD8^+$ T cell immune response, with these data being key for drawing more reliable conclusions. Genomic comparisons of the EPS clusters of the *B. pseudocatenulatum* strains tested did however highlight a near identical genetic similarity between LH13 and LH14 EPS, which in turn was highly distinct from the EPS of LH663. This not only suggested any tumour inhibition induced by LH13 was likely mechanistically distinct from the LH663-EPS, but also that there appears to be significant strain level differences in *Bifidobacterium* EPS composition. Ultimately, we believe this to be an ideal phenomenon, as there is potential for many types of unique EPS structures to perform a wide variety of therapeutic functions. Use of comparative genomics in this way could ultimately provide a scalable platform for the identification of more active compounds from other therapeutic bacteria, by comparing the genomic differences between similar strains which are and are not therapeutically efficacious and focusing

on the core areas of genomic difference, wherein the production of the active compound must be mediated. The data we collected again highlight the varied mechanisms through which *Bifidobacterium* can be protective against cancer.

The identification of EPS mediating the mechanism of LH663 therapy provides a strong platform for the identification of the initial host response which induces anti-tumour immunity. *In vitro* co-cultures with LH663-EPS and immune cells implicated a limited interaction between LH663-EPS and $CD8^+$ T cells or monocytes, whereas there was significant activity induced by LH663-EPS in BMDCs. Although an absence of stimulation of $CD8^+$ T cells was expected, given their antigen restricted nature, it was surprising to see no inflammatory stimulation within monocytes. This is particularly striking because *Bifidobacterium* EPS, and EPS more broadly, has been associated with activation of TLR2 and stimulation of downstream immunity(*444, 600*). Contrastingly, LH663-EPS did not stimulate TLR2 to any detectable level, despite live LH663 cells stimulating TLR2 very strongly compared with either LH13 or LH14. This again highlights significant differences between different strains of the same species and may have been mediated by cell wall peptidoglycan associated with TLR2 activation(*601*). Although it appears that the action of LH663-EPS is TLR-independent, based on the lack of stimulation of THP1-Blue monocytes or TLR reporter lines, it is possible that other TLRs (which were not tested) are highly expressed on monocytes could recognise the LH663-EPS. Additionally, the lack of antigen exposure to the $CD8^+$ T cells may have caused a differential expression of cell surface receptors, so it is possible that EPS may still interact directly with $CD8^+$ T cells during states of antigenic challenge.

Importantly, we showed that LH663-EPS does induce activation of BMDCs *in vitro*, stimulating the expression of maturation markers CD80, CD86 and MHCII. Given that DCs are the only population which contribute to the *in vivo* mechanism and respond to LH663-EPS, these data suggest that DCs may represent the first step in the host response to the LH663-induced anti-tumour immunity. There is evidence in the literature describing EPS interactions with DCs(*592*), but the precise receptor activities responsible for these changes are not well characterised. Though better described in the context of fungal pathogenesis(*446, 602, 603*), C-type lectin receptors (CLRs) are prime candidates for dendritic cell receptor sensing of microbial EPS. Although individual CLRs can recognise a variety of sugar residues, different CLRs have different glucosyl affinities. For instance, the CLR dectin-1 has strong affinity for glucose(*604*), dectin-2 for mannose(*605*), and DC-SIGN for mannose and

glucose(*450*). With our structural data highlighting a high abundance of glucose residues, Dectin-1 is a strong candidate binding receptor for LH663-EPS, with interrogation of the key receptors mediating LH663-EPS interaction with DCs representing a key future direction. Overall, we hypothesise that LH663 interacts with gut DCs via the surface EPS through a CLR, inducing DC activation, maturation, and systemic translocation, thus increasing the uptake and cross presentation of tumour antigens to $CD8^+$ T cells, enhancing systemic $CD8^+$ immunity against tumours.

6. Developing microbial outer membrane vesicles (OMVs) from *Bacteroides thetaiotaomicron* (Bt) as a novel anti-cancer therapeutic

Use of bacteria to treat cancer has remerged in the past decades and acknowledged as a piece of 'forgotten knowledge', which can be traced back to the 1890's where 'Coley's Toxin' (a heat killed mixture of *Streptococcus pyogenes* and *Serratia marcescens*) was utilised as a remedy against cancer(*606*). Though the primitive therapy was poorly standardised and induced often severe side effects, the approach was relatively successful in many patients compared with the alternative standard of care approaches at the time(*607*). Though the mechanism of action was not understood at the time, we now appreciate the approach to be the earliest attempt of immunotherapy, using bacteria to stimulate an enhanced immune response against tumours(*608*). Modern standards of medicine demand more nuanced and targeted therapeutics, but the rationale of using bacteria in this way is sound. The key considerations then, are how we can stimulate the strongest anti-cancer immune responses with bacteria whilst minimising severe side effects associated with infection.

A recently popularised approach, which has also been explored in this thesis, is the use of commensal gut microbes as effectors for cancer therapy. Use of commensal (non-pathogenic) bacteria in a physiologically appropriate environment (the gut) has significant benefits in safety and has also been shown to be effective in stimulating local and systemic anti-cancer immune responses(*292*). A key reason for the safety of these approaches is the gastrointestinal tract providing a natural barrier to limit direct translocation of bacterial components and interactions with the host, preventing runaway infection and thus treatment rejection(*609*). However, this limit to direct host-microbe interactions by the gut also means only a fraction of immunomodulatory effects of the gut microbiota are fully realised. With a direct systemic exposure of the host to the right types of bacterial components, we might enhance anti-cancer immune responses even more strongly than approaches merely localised to the gut.

Attempts have already been made in this regard, beginning with Coley's Toxin, and more recent research has explored direct administration of live and attenuated/killed bacteria into the blood stream(*610, 611*). Though this can have obvious benefits, these approaches usually use strains with pathogenic potential, thus posing significant

danger in causing infection and/or significant adverse side-effects(*612*), particularly in immunocompromised cancer patients undergoing chemo- or radiotherapy(*613*). There is therefore an unmet clinical opportunity for therapeutics which can harness the full immunomodulatory power of microbes, without posing significant risk of infection (by retaining a replicative cell) or side effects (caused by using pathogenic bacterium). Bacterial outer membrane vesicles (OMVs) represent excellent candidates for filling this niche, as they generally contain or present the major immunomodulatory antigens of the parental bacterium without having the ability to proliferative or actively potentiate pathogenesis(*614*). OMVs are also amenable to genetic and biochemical manipulation, and so can also be used as a drug delivery platform for other anti-cancer agents (e.g., chemotherapeutics)(*614*). Isolation and purification of OMVs allows them to be administered directly into the blood stream and bypass the relatively impermeable intestinal epithelium, which allows for a more potent and controlled method of administration compared to ingestion of live bacteria.

The work in this chapter explores the potential for OMVs derived from the gut commensal *Bacteroides thetaiotaomicron* (Bt) to inhibit tumour progression in mouse models of cancer. Bt OMVs were chosen due to extensive research by our collaborators, who have shown their ability to safely stimulate immune pathways (e.g., dendritic cells, macrophages, and natural killer cells) *in vitro*(*393*) and *in vivo(394)*, whilst also providing therapeutic benefit in the context of mucosal vaccines(*615, 616*). In the context of cancer, we show that Bt OMVs are well tolerated in tumour bearing animals but display hugely variable anti-tumour efficacy depending on bacterial culture conditions, administration route, dose, and tumour type, highlighting key considerations for their potential clinical translation. Bt OMVs are effective in stimulating various arms of the immune system and are most efficacious when generated from a minimal media (absent of animal products) under intravenous (IV) administration at a high dose. IV-administered OMVs efficiently accumulate in primary tumours, inhibiting primary and metastatic melanoma outgrowth. Our work on Bt OMVs couples with our research on administration of *Bifidobacterium* to demonstrate the broad potential of bacterial therapy against cancer.

6.1. Bt OMVs generated in 'brain-heart infusion' media do not have linear dosage effects on mammary tumour volume

Over the course of the project, the conditions of Bt culture underwent several optimisations. For initial experiments, Bt was grown in a brain heart infusion (BHI) growth medium and OMVs isolated and quantified as outlined in section 2.3.4. To initially pilot the anti-tumour effects of Bt OMVs, we administered various doses through an intraperitoneal (IP) injection to animals bearing orthotopic luminal B-like PyMT-BO1 breast tumours (Figure 6.1A). Following OMV administration, we observed a notable dosage effect on tumour growth, where 'low' ($1x10^4$) and 'high' ($1x10^{10}$) OMV doses did not significantly alter tumour volume, compared with 'medium' doses ($1x10^6$ and $1x10^8$) which caused a notable trend reduction (non-significant due to low replicates) (Figure 6.1B).

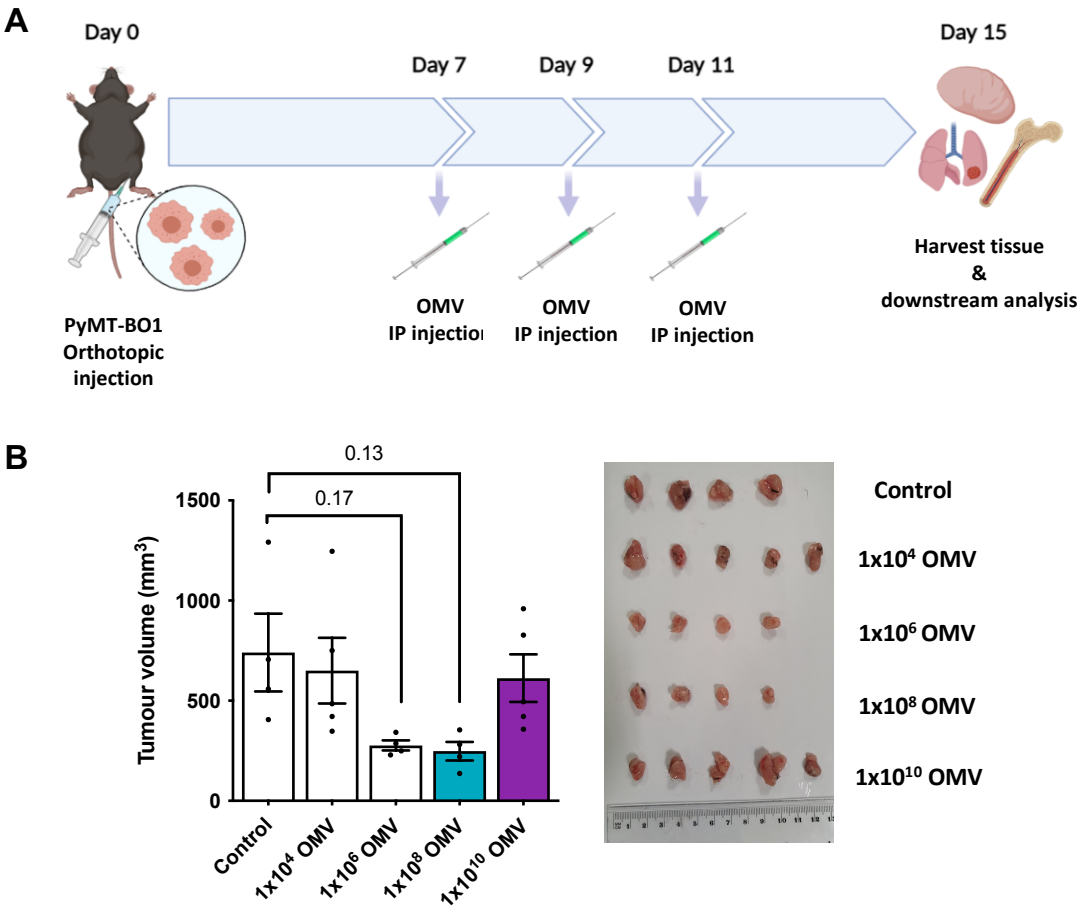

Figure 6.1. Administration of *B. thetaiotaomicron* OMVs generated in BHI media cause dose dependent effects on PyMT-BO1 mammary tumour growth. (A) Experimental outline of PyMT-BO1 OMV tumour growth experiments, OMVs were administered 3x intraperitoneally from the onset of a palpable tumour. (B) Endpoint PyMT-BO1 tumour volumes with representative tumour image following OMV administration at the indicated dosages, n=4-5. Bars represent mean values (± SEM) and statistical significance was calculated by one-way ANOVA with Tukey's multiple comparisons test.

To further elucidate how Bt OMVs may affect cancer progression, we took forward two OMV dosages: one at $1x10^8$ to model the 'effective' dosage, and one dose at $1x10^{10}$ to model an ineffective high dose. This experimental setup served the dual purpose of further defining the therapeutic potential of the effective Bt OMV dose and modelling why we might see a loss of efficacy at high doses. The finding of a loss of effectiveness at high OMV dose may have suggested that some bioactive component on the OMVs caused adverse immunological effects at high (but not medium) doses. To broadly assess for signs of infection and general host tolerance to OMVs, we measured animal body weight following OMV administration. Our data indicated that OMV administration did not induce any bodyweight changes, where we might see a reduction in cases of severe adverse side therapy effects or runaway inflammation (Figure 6.2A).

Using the PyMT-BO1 tumour model, we successfully replicated the dosage effects seen in the pilot, with administration $1x10^8$ OMVs causing a significant decrease in tumour volume and $1x10^{10}$ OMV administration having no protective impact (Figure 6.2B). Due to breast cancer being such a heterogenous disease with several molecular subtypes, a therapeutic with success in one is not necessarily successful in another(*617*). There is a severe need for new treatments which are effective across different breast cancer subtypes, which may complement and overcome resistance to existing therapies. To assess the translational potential of OMV treatment more broadly, we tested OMV administration in the 'basal-like' E0771 breast tumour model (Figure 6.2C). Though differences between groups were not statistically significant, the trend in tumour volume was the same as in the PyMT-BO1 model, reinforcing the presence of a dosage effect and suggesting Bt OMVs may have promise as a multi-subtype breast cancer therapeutic.

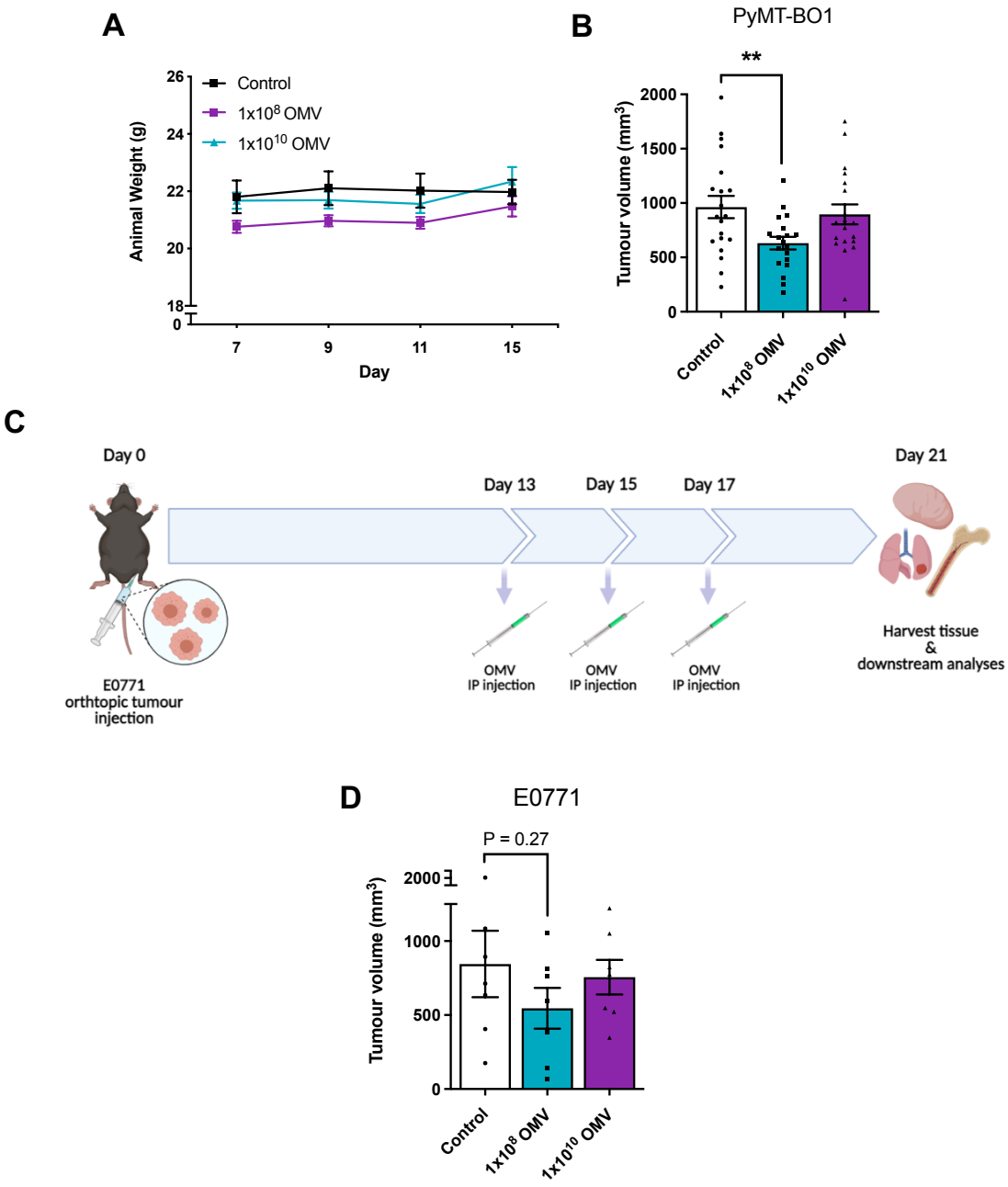

Figure 6.2. OMVs generated in BHI media reduce mammary tumour growth at a medium but not high dosage. (A) Animal weights following OMV administration in PyMT-BO1 tumour bearing animals, n=12 N=2. (B) Endpoint PyMT-BO1 tumour volumes following OMV administration, n=20 N=2. (C) Experimental outline of E0771 tumour experiments. (D) Endpoint E0771 tumour volumes following OMV administration, n=7. Bars represent mean value (± SEM) and statistical significance was calculated by two-tailed unpaired *t* test. $^{**}P < 0.01$.

6.1.1. OMVs do not alter breast cancer cell proliferation or apoptosis *in vitro*

Following our finding that Bt OMVs can reduce breast tumour burden at specific dosages, we next sought to identify whether the effects seen were caused by a direct interaction between the OMVs and tumour cells. To gain a broad overview of any gross changes, we conducted high-throughput colorimetric testing of PyMT-BO1 cell viability using the Alamar Blue cell viability reagent, which produces fluorescent resorufin in the presence of living cells(*618*). This revealed no significant changes to cell viability however, even across a wide spectrum of OMV dosages, suggesting Bt OMVs were not directly impacting PyMT-BO1 cell growth (Figure 6.3A). This finding was supported by propidium iodide cell cycle analysis, which did not appear to show any major OMV-induced changes to PyMT-BO1 cell cycle arrest (G0/G1) or progression to active cell division phases (S-G2-M phase) (Figure 6.3B-C). It is important to note that there was just a single biological repeat for this however, so it is possible more data would show differences between treatments. Analysis of Ki67 expression by flow cytometry may have shown some slight changes at the lowest ($1x10^4$) and highest ($1x10^{10}$) doses, though no treatment causes a dramatic change in Ki67 which might explain difference in *in vivo* tumour volumes (Figure 6.3D). Nevertheless, more repeats are again required to substantiate any conclusive findings. Although OMV treatment did not show any obvious impact on tumour cell proliferation, it is possible that OMV-induced apoptosis could have been responsible for a reduction in tumour volume. Using flow cytometric staining of PyMT-BO1 expression Annexin V following OMV treatment, we did not see any consistent or dramatic effects on cell apoptosis, suggesting the direct interactions between Bt OMVs and BrCa cells are not, in isolation, responsible for changes to breast tumour volume (Figure 6.3E). Though some of the experiments require more replicates, the data taken together suggest that OMVs do not directly contribute to PyMT-BO1 tumour cell viability, indicating that other mediators, such as the immune cells or secondary metabolites, are required for OMV-induced changes in tumour burden.

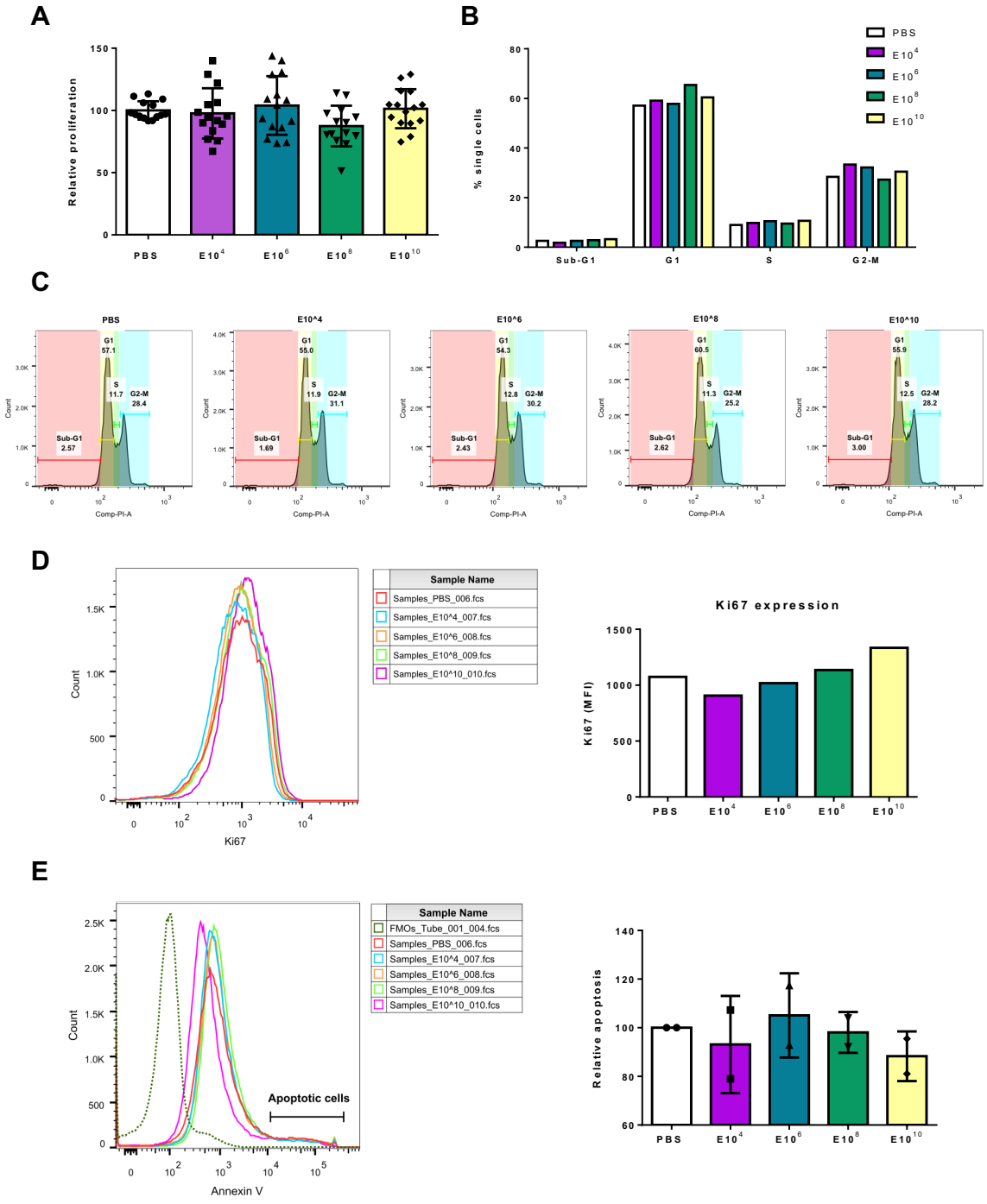

Figure 6.3. BHI-OMVs do not directly influence PyMT-BO1 proliferation or apoptosis in vitro. (A) Relative proliferative activity measured by Alamar Blue assay, cells were cultured for 48h and OMVs administered into culture medium 24h before endpoint. Fluorescence values were measured at 590nm, n=15 N=3. (B) Quantification of cell cycle progression of PyMT-BO1 cells measured through PI staining following the treatment indicated OMV dosages, bars represent respective cell cycle stages and (C) histograms show gating strategy, n=1. (D) Histogram and associated quantification of PyMT-BO1 cell expression of Ki67 following the indicated treatments by flow cytometry, n=1 (E) Histogram and associated quantification of PyMT-BO1 apoptosis following OMV treatment quantified by Annexin V staining, n= 2.

6.1.2. The tumour histopathological response to Bt OMV administration

Tumour histopathology, which can be used to assess common 'hallmarks of cancer', is an essential tool used to understand the fundamental mechanisms underpinning cancer biology(*619*). Often representing the overall effect of a given effector mechanism on tumours, cancer hallmarks (e.g., tumour proliferation, apoptosis, and angiogenesis) can be an underpinning explanation for changes to tumour burden(*4*). To ascertain how Bt OMV administration might affect these hallmarks, we undertook immunofluorescent and histological tumour staining to visualise changes to tumour pathology. Using TUNEL staining as a measure of tumour apoptosis, we observed the expected apoptotic trend which correlated with the tumour volume (more apoptotic cells in the effective $1x10^8$ treatment), although the differences were not statistically significant and may reflect the effect rather than cause of smaller tumours (Figure 5.4A).

Whilst Ki67 staining for proliferative cells did not show the expected decrease following the $1x10^8$ OMV dose, the results did highlight that tumours receiving the highest dose were significantly more proliferative than either of the other groups (Figure 6.4B). This data suggests that some component of the Bt OMVs induces a proliferative effect on PyMT-BO1 tumour cells which is not observed at a lower dose, potentially explaining the observed difference in tumour volume between the groups. Immunofluorescent staining indicated that smaller tumours in the $1x10^8$ group may have had fewer blood vessels, with differences approaching statistical significance despite a low number of replicates (Figure 6.4C)). Tumour angiogenesis is a cancer hallmark inextricably linked to tumour pathology, and so reduced angiogenesis could be a downstream mechanism through which the effective $1x10^8$ dose of OMVs reduces breast tumour volume.

Though not a 'classical' cancer hallmark, tumour extracellular matrix deposition is a histopathological feature which is consistently tied to tumour growth and metastasis. To quantify whether this could be a feature of differential OMV effects on tumours, we performed Picro Sirius Red staining for collagen. Staining intensity was quantified by thresholding analysis, although no differences between groups was observed (Figure 6.5).

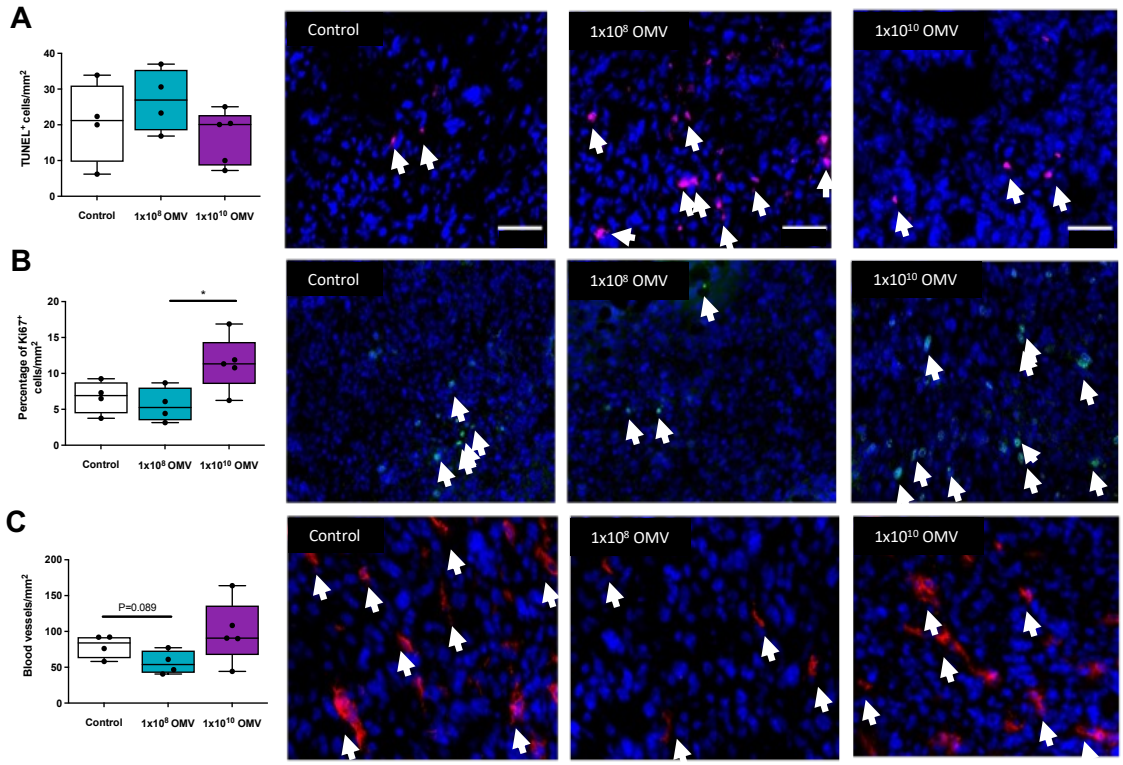

Figure 6.4. BHI-generated OMV administration may cause alterations to classical cancer hallmarks in PyMT-BO1 tumours. (A) Quantification with representative images showing apoptosis within PyMT-BO1 tumours following OMV treatment, visualised by TUNEL immunofluorescent staining. The number of TUNEL$^+$ cells (red) was quantified in whole tumour sections. (B) Quantification and representative images showing PyMT-BO1 tumour proliferation after OMV treatment, quantified by average percentage of dual Ki67$^+$(green)/DAPI$^+$ (blue) cells in a single field of view at three distinct regions of interest per tumour. (C) Quantification and representative images showing tumour angiogenesis after OMV treatment, visualised by endomucin staining (red) and quantified as total number of vessels across whole tumour sections. n=4-5 N=1. Statistical significance was calculated by two-tailed unpaired *t* test. $^{**}P < 0.01$.

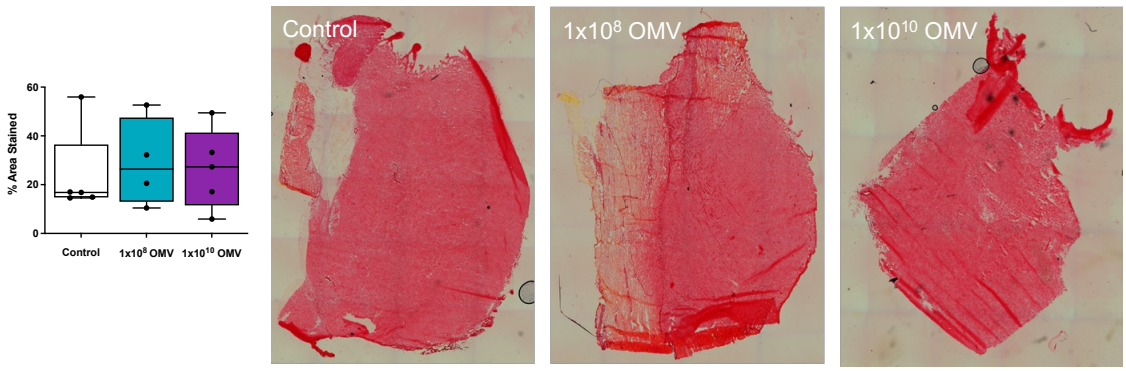

Figure 6.5. OMVs generated in BHI do not alter PyMT-BO1 tumour collagen deposition. Tumours from the denoted groups were sectioned and stained with Picro-Sirius Red and staining intensity was quantified using ImageJ. Statistical significance was calculated by Mann-Whitney U test.

6.1.3. Assessment of the tumour immune microenvironment following BHI-OMV administration

As OMVs usually contain the immunostimulatory proteins of their parental bacterium, we hypothesised that a likely mechanism for Bt OMV-induced tumour reduction was through activation of the immune system. Previous studies have shown the effectiveness of Bt OMVs in stimulating the immune system, as they have been shown to interact with macrophages and dendritic cells (DCs) and stimulate release of IL-6 and IL-10(*393, 394*).

Using flow cytometry, we conducted detailed immune profiling of the both PyMT-BO1 and E0771 primary tumours following OMV administration, hypothesising that mechanistically important mechanisms should be conserved across tumour models given the apparently consistent OMV-induced changes to *in vivo* tumour growth. Analysis of major myeloid and lymphoid populations in PyMT-BO1 tumours only revealed a slight increase in macrophages at the highest dose of OMVs (Figure 6.6A). Whilst macrophages are generally considered anti-inflammatory in the context of tumours and thus could explain why $1x10^{10}$ OMV-treated tumours are larger than $1x10^{8}$ OMV-treated, the tumourigenic effects of macrophages here are subtype specific (often delineated based on expression of MHCII and CD206). Additionally, this trend is not replicated in E0771 tumours, which alternatively display changes in infiltration to lymphoid and NK cells (Figure 6.6B). The efficacious $1x10^{8}$ OMV-treated E0771 tumours do display an enhanced infiltration of lymphoid cells and reduction in NK cells, which is rescued in the $1x10^{10}$ OMV treated group, which may contribute to the observed difference in tumour volume. There is an additional trend of increased infiltration of B-cells in $1x10^{8}$ OMV-treated group, despite this population generally being associated with negative outcomes (depending on cell subtype)(*620*). Importantly however, these E0771 immune infiltrate results are again not replicated across both tumour models, casting doubt over their mechanistic relevance and reliability.

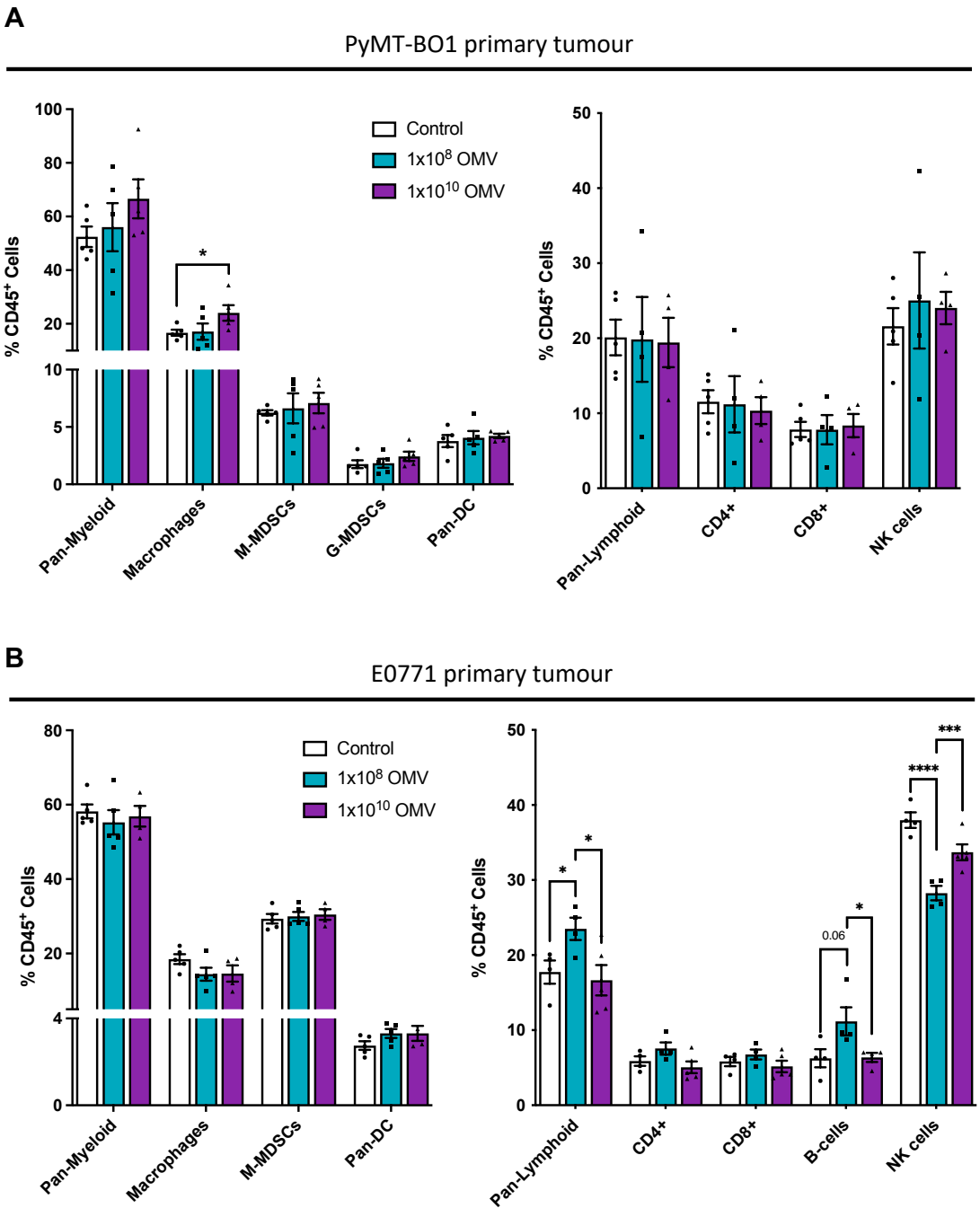

Figure 6.6. BHI-generated OMV treatment induces tumour model-specific alterations in immune cell infiltration. Mean (± SEM) infiltration of the indicated immune populations within (A) PyMT-BO1 and (B) E0771 primary tumours following OMV administration, n=4-5. Statistical significance was calculated by two-tailed unpaired *t* test. ****$P < 0.0001$, ***$P < 0.001$, *$P < 0.05$.

The infiltration of immune populations is an important component in any assessment of the immune response, although it is a limited measure of overall immune activity. As well as increase immune infiltration, the immune system can also manipulate the properties of immune cells already present in an area of inflammation, generally through the expression of cytokines to enable cell polarisation and activation. As such, immune cell infiltration and cytokine production go together for assessment of immune activity.

Using a multiplex Meso-Scale Delivery (MSD) assay for simultaneous cytokine analysis, we identified changes in some key cytokines in both the primary tumour and serum. Although previous literature has indicated the ability of Bt OMVs to stimulate IL-10 signalling(*393*), we observed a (non-statistically significant) trend of decreased IL-10 in the effective group, before a return to control IL-10 levels at the highest dose (Figure 6.7A). This pattern correlates with overall tumour volumes between the groups and suggests OMV-induced reduction of BrCa tumours may occur through lower IL-10, a (context-dependent) anti-inflammatory and pro-tumourigenic cytokine(*621*). Another difference in primary tumour cytokine profile is the reduction in levels of IL-1ß, which is trending downwards in each OMV dosage, reaching statistical significance at the highest $1x10^{10}$ OMV dose (Figure 6.7A). Like IL-10, IL-1ß is typically associated with poor outcome in cancer, inducing an anti-inflammatory pro-tumourigenic response(*622*). With the lowest levels of IL-1ß being observed in the $1x10^{10}$ group, this classical association does not correlate expectedly with tumour volume, which we might expect to be smaller rather than larger due to lower OMV-induced IL-1ß expression, casting doubt over the biological relevance of the trend with respect to OMV-induce tumour volume changes.

Though we mostly focus on the response of the primary tumour, late-stage cancer is a systemic disease, and systemic tumour dissemination (metastasis) is the major cause of death among patients(*623*). As such, changes in systemic immunity are relevant to understanding the potential impact of OMV administration on the development and outgrowth of metastatic legions. To probe the effects of Bt OMV administration on systemic immunity, we conducted cytokine profiling of serum, which again revealed changes in some key mediators. Interestingly, control serum did not have detectable levels of IFNγ whilst serum from OMV-treated animals did (Figure 6.7B). Though not possible to assess the true scale of any differences here, these data do suggest that OMV administration, regardless of dosage, stimulates systemic IFNγ release. This is likely a beneficial response in the context of control over tumour metastasis, as IFN-γ is

the major stimulator of the anti-tumourigenic response of $CD8^+$ T cells, T-helper cells and NK cells(*624*). Contrasting with the pro-inflammatory properties of IFN-γ, OMV administration also significantly increased systemic levels of anti-inflammatory IL-10. This contrasts with the primary tumour, where IL-10 levels decreased in the $1x10^8$ OMV group, though without complementary circulatory immune cell profiling it is difficult to draw concrete conclusions. In accordance with these changes, KC/GRO (CXCL1) levels were also decreased following OMV administration, which may be important given an association with a poor prognosis in breast cancer. KC/GRO is the major chemokine released by TAMs and is purported to promote BrCa metastasis through activation of NF-κB signalling and increasing tumour cell migration and invasion(*625*). A caveat here is the systemic decrease in KC/GRO caused by the highest OMV dosage is not replicated in the primary tumour, so may not be relevant to this physiological site. Overall, broad spectrum cytokine analysis of the primary tumour and serum has identified several potential cytokine effectors for OMV-mediated effects, although a lack of synergy between tumour and systemic expression makes more concrete mechanistic conclusions more difficult. Taken together, the data suggest a nuanced balance between pro- and anti-tumourigenic cytokine effectors, which appear to change dynamically following different dosages of Bt OMVs, offering some potential explanations for the sensitivity in tumour volume response.

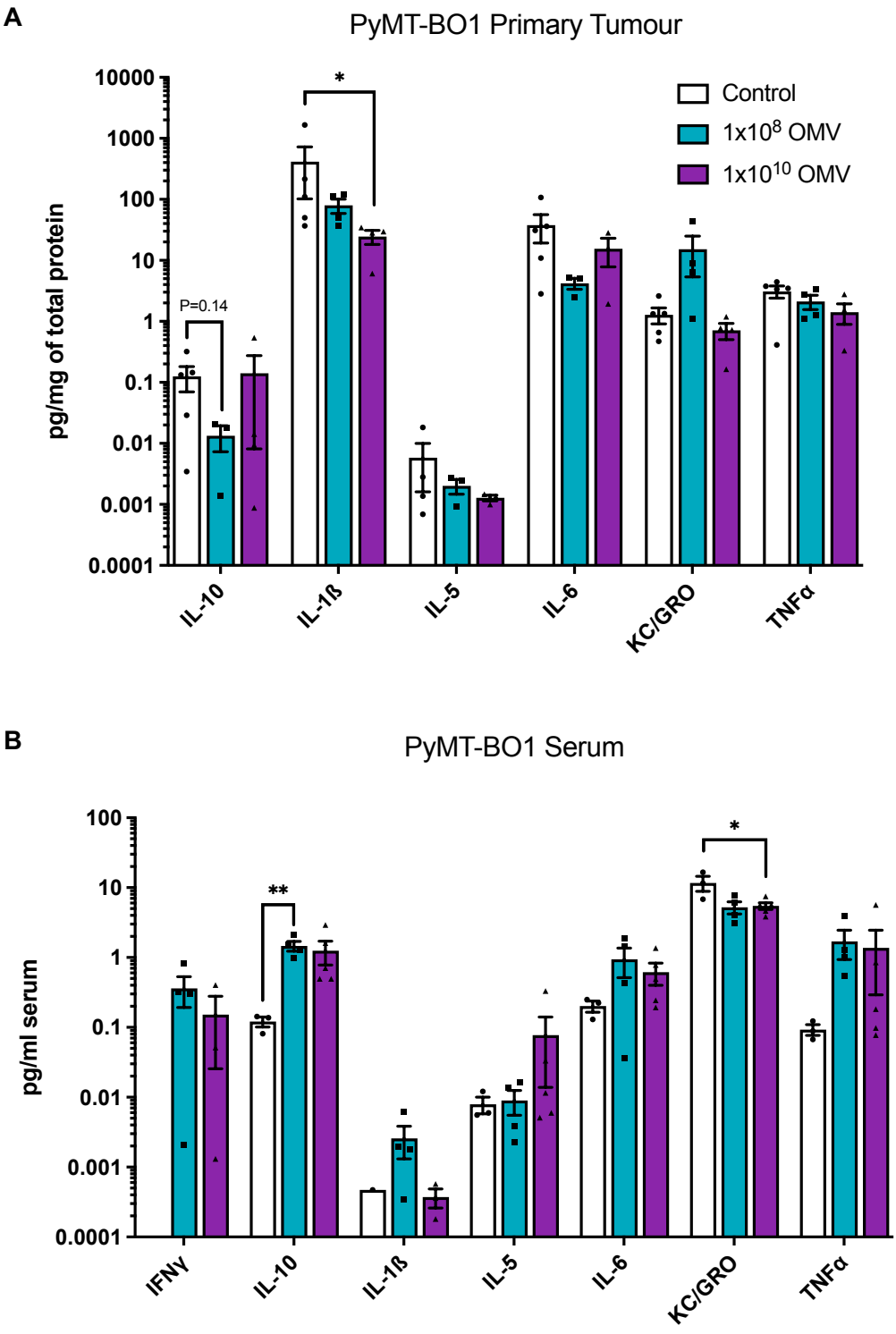

Figure 6.7. BHI-generated OMV administration induces changes to specific cytokines. Cytokine production in the (A) primary tumour and (B) serum of PyMT-BO1 tumour-bearing animals following administration of the indicated doses of OMVs, quantified by a custom MSD U-PLEX assay and normalised to the levels of extract tissue protein. n=3-5. Bars indicate mean values (± SEM) and statistical differences were measured by two-tailed unpaired t test. **P < 0.01, *P < 0.05.

6.1.4. The lung pre-metastatic niche undergoes discrete lymphoid changes following BHI-OMV treatment

As tumour metastasis is responsible for the majority of deaths among breast cancer patients(*626*), consideration of the potential anti-metastatic properties of a prospective therapeutic is vital. As OMV administration was shown to influence the immune microenvironment of primary tumours, as well as systemic cytokine release, we analysed the immune landscape of the primary metastatic niche (lungs) for changes which may influence metastatic outgrowth. As the OMVs have previously been associated with interactions with macrophages and induction of IL-10(*393*), we were particularly interested in potential changes in this major immune population. The role of lung macrophages during breast cancer metastasis is not as well characterised as in the primary tumour, but they are similarly thought to be a negative prognostic marker(*627*) and a potentially targetable therapeutic axis(*628*). Indeed, recent work has identified and characterised a population of 'metastasis-associated macrophages' (MAMs) and their precursor population (MAMPCs) (Figure 6.8A), which undergo mass expansion upon outgrowth of metastatic legions and function to supress $CD8^+$ T cell anti-tumour responses(*629*).

In accordance with our findings of limited OMV-induced changes to myeloid populations at the primary tumour, we again observed no significant changes in the lung to cancer-relevant macrophages, MDSCs and DCs (Figure 6.8B). Contrastingly, we did observe decreases in several lymphoid populations, such as $CD4^+$ and $CD8^+$ T cells. Each of these populations are broadly considered anti-tumourigenic(*630*), so their decreased infiltration into the pre-metastatic niche is not likely beneficial, although we would require concrete data on associated changes in metastatic dissemination to corroborate these findings.

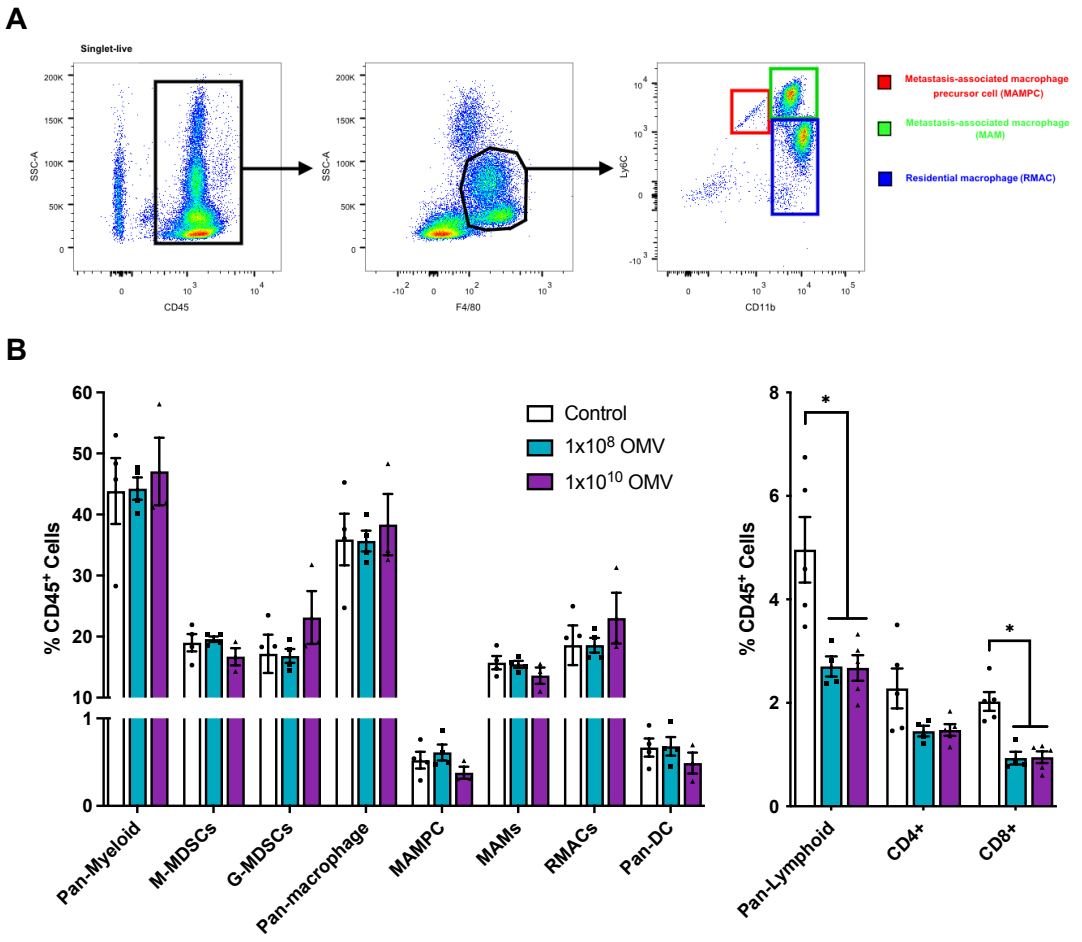

Figure 6.8. BHI-generated OMVs change the lymphoid but not the myeloid profile of the pre-metastatic niche. (A) Example gating strategy for the identification of residential and metastasis-associated macrophages in the lung, (B) assessment of major myeloid and lymphoid populations in the lung following OMV treatment, n=5. Bars represent mean values (± SEM) and statistical differences were measured by two-tailed unpaired *t* test. **P* < 0.05.

6.2. Administration of OMVs generated in a minimal 'BDM' media causes a linear tumour volume dosage response

During the development of microbial therapeutics, extensive optimisation is vital to improve quality and yield. One issue we initially faced was the culture of Bt in BHI media, which contains high levels of animal (and potentially biologically active) contaminants. This causes an 'impure' final OMV product (with similar-sized biological contaminants), which may have the potential to cause undesirable effects. Indeed,

there is current focus in the pharmaceutical industry on reducing the presence of animal-contaminants in therapeutic preparations to decrease potential off-target effects and increase access to patients (e.g., with dietary or religious restrictions)(*631, 632*). We speculate that animal contaminants may partly account for the unusual tumour volume response to Bt OMVs, as increased OMV dosages also delivers an increased number of BHI-derived contaminants, which may have a pro-tumourigenic influence. Recent research has also shown that Bt OMVs are indeed responsive to their local environment, with a significantly different proteome profile of *in vivo* gastro-intestinal tract-challenged OMVs compared with OMVs isolated from bacterial culture media alone(*633*). In addition to harmful off-target effects, the presence of OMV-sized contaminants could cause OMV counts from our nano-particle tracker to be inaccurate, with no way of controlling variability in contaminant numbers between experiments. To address these weaknesses and improve the prospects of eventual pharmaceutical translation, we sought to use a Bt defined growth medium ('BDM') free of animal products (and therefore, biological contaminants). During this process, we also decided to use a $1x10^7$ rather than $1x10^8$ OMV dose, as we hypothesised a larger difference in OMV number between our medium and high doses would make dissecting mechanistic differences in tumour response easier.

OMVs generated in this new 'minimal' media, named *Bacteroides*-defined media ('BDM'), exhibited different effects on PyMT-BO1 breast tumour volume compared with BHI-generated OMVs. Following the change in growth media, the U-shaped dosage curve observed following BHI-generated OMV administration was not present, resulting in a more conventional(*634*) linear relationship between BDM-OMV dose and tumour volume (Figure 6.9). Here, the highest $1x10^{10}$ OMV dose was most effective, suggesting that either BHI contaminants or BHI-induced changes to the OMV contents were responsible for the dosage response previously seen.

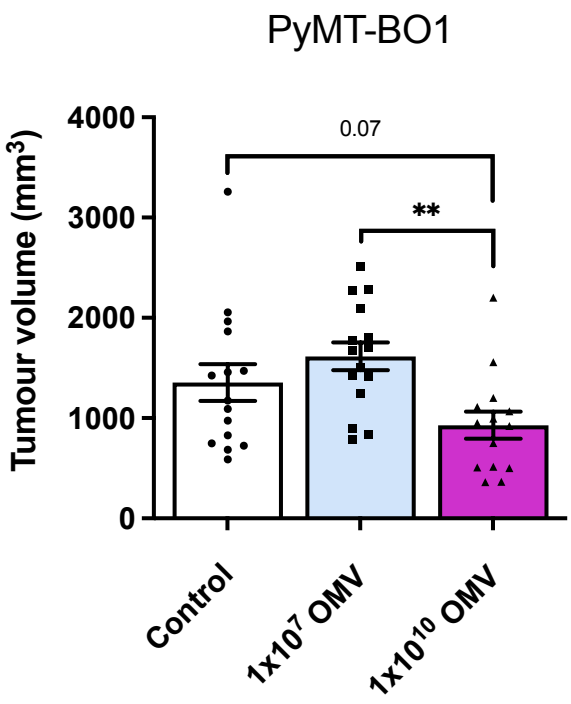

Figure 6.9. Administration of *B. thetaiotaomicron* OMVs generated in minimal BDM media cause dose dependent effects on PyMT-BO1 mammary tumour growth. Endpoint PyMT-BO1 tumour volumes following OMV administration at the indicated dosages, n=15-16. Bars represent mean values (± SEM) and statistical significance was measured by two-tailed unpaired *t* test. ***P* < 0.01.

6.2.1. *B. thetaiotaomicron* OMVs induce changes in immune infiltrate regardless of bacterial growth medium

With a different tumour volume dosage response to OMVs generated in BDM medium (BDM-OMVs) compared with BHI-generated OMVs, we speculated that the OMV-induced immunological associations may be altered. Changes in infiltration of immune populations between BHI and BDM preparations may also highlight mechanistic pathways induced by potential BHI contaminants.

Contrasting with the immunological effects induced by BHI-OMVs in PyMT-BO1 tumours, the infiltration of many more myeloid populations was significantly altered by OMV administration. At the highest $1x10^{10}$ OMV dose, which previously increased total macrophage infiltrate, BDM-OMVs at the equivalent dose decreased macrophage infiltration, although trends in the major subpopulations of macrophages were not statistically significant (Figure 6.10A). Additionally, BDM-OMV administration increased

the infiltration of MDSCs in the primary tumour, a negative prognostic marker due to their strong anti-inflammatory properties(*635*). Analysis of lymphoid and NK populations in the primary tumour also revealed inverse results following BDM-OMV administration, whereby the medium $1x10^7$ OMV dose decreased lymphoid and increased NK cell infiltrate (the opposite to the results in BHI-OMV experiments), with this effect rescued at the higher $1x10^{10}$ OMV dose (Figure 6.10A). Whilst the exact biological and mechanistic relevance of these pathway changes to PyMT-BO1 tumourigenesis are difficult to dissect, alteration of the culture conditions of Bt OMV generation causes significant differences to both the therapeutic efficacy and functional immune responses generated *in vivo*.

This conclusion is supported by analysis of the pre-metastatic lung, whereby we observe changes in MDSCs and DCs following $1x10^7$ BDM-OMV administration which were not present following BHI-OMV administration. Although there was a slight significant reduction in infiltration of $CD8^+$ T cells in the lung at the medium dose, this was not replicated at the high $1x10^{10}$ dose and is again inconsistent with a large reduction across lung lymphoid populations following BHI-OMV treatment.

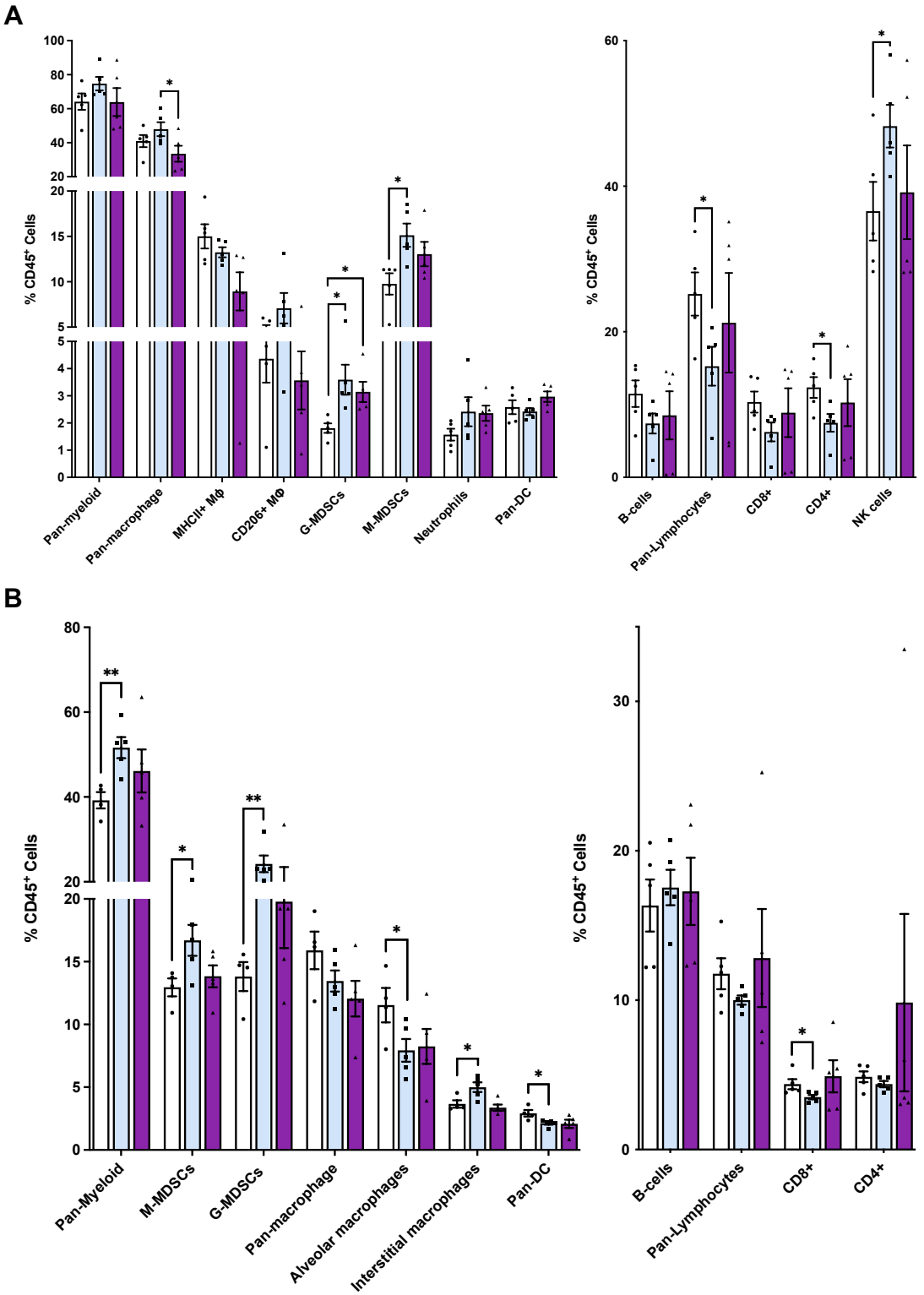
A
% CD45+ Cells
Pan-myeloid
Pan-macrophage
MHCII+ Mϕ
CD206+ Mϕ
G-MDSCs
M-MDSCs
Neutrophils
Pan-DC
B-cells
Pan-Lymphocytes
CD8+
CD4+
NK cells
B
% CD45+ Cells
Pan-Myeloid
M-MDSCs
G-MDSCs
Pan-macrophage
Alveolar macrophages
Interstitial macrophages
Pan-DC
B-cells
Pan-Lymphocytes
CD8+
CD4+

Figure 6.10. BDM-generated OMVs alter infiltration of several immune populations in the primary tumour and lung dose-dependently. Mean (± SEM) infiltration of the indicated immune populations within PyMT-BO1 (A) primary tumours and (B) pre-metastatic lungs following OMV administration, n=4-5. Statistical significance was calculated by two-tailed unpaired *t* test. $^{**}P < 0.01$, $^{*}P < 0.05$.

6.2.2. Assessment of the impact of BDM-OMVs on early-stage tumour dissemination

Continuing with a systemic view of breast cancer disease progression and to complement our immune profiling of the metastatic niche, we used flow cytometry to quantify the luciferase and GFP-expressing PyMT-BO1 tumour cells in PyMT-BO1 primary tumour-bearing endpoint lungs following BDM-OMV administration. Use of non-tumour bearing lungs, tumour-spiked control lungs and FMO controls (Figure 6.11A) validated the sensitivity of the method for the detection of early metastases, which is increasingly understood be vital for later stage metastatic burden and overall prognosis(*529*).

BDM-OMV administration at the efficacious $1x10^{10}$ dose results in a correlative decrease in early metastatic spread to near-statistically significant levels (more repeats are likely required to conclusively power the statistical findings) (Figure 6.11B-C). As we might expect given the primary tumour volume response, this effect was not seen to the same extent at the medium $1x10^{7}$ OMV dosage. As we did not observe any changes in immune infiltration in the lungs at the $1x10^{10}$ dose and this experimental timepoint represents a very early stage of metastasis prior to legion formation, we can conclude that these changes to metastatic spread are likely due to anti-metastatic effects at the primary tumour rather than lung. As we do see smaller tumours at the $1x10^{10}$ dose, it is possible that changes to early dissemination could be due to altered primary tumour burden alone. Overall, more work is required to further elucidate how OMV administration influences metastasis, although the apparent overall reduction in early tumour dissemination highlights promise for future OMV-based breast cancer therapeutics.

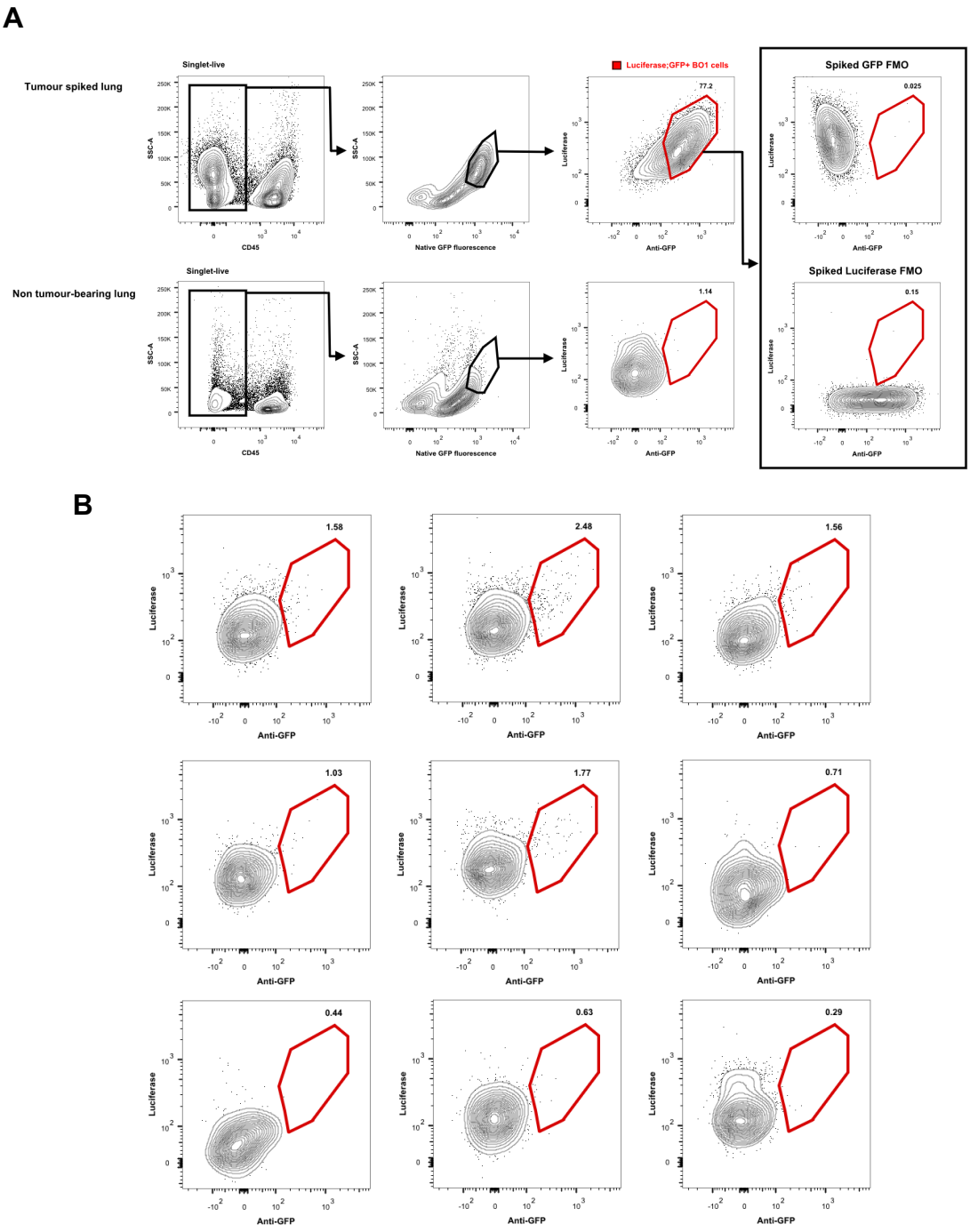
A
Tumour spiked lung
Non tumour-bearing lung
Singlet-live
Luciferase;GFP+ BO1 cells
Spiked GFP FMO
Spiked Luciferase FMO
SSC-A
CD45
Native GFP fluorescence
Luciferase
Anti-GFP
77.2
0.025
1.14
0.15
B
1.58
2.48
1.56
1.03
1.77
0.71
0.44
0.63
0.29
C
P=0.10
% lung metastatic B6BO1 cells
0.10
0.08
0.06
0.04
0.02
0.00
Control
1x10^7 OMV
1x10^10 OMV

Figure 6.11. Administration of BDM-generated OMVs causes a trend of reduced early metastatic dissemination with increasing dose. (A) Gating strategy for the identification of metastatic GFP$^+$Luciferase$^+$ PyMT-BO1 cells within the lungs of tumour-spiked and non-tumour-bearing control lungs. (B) Representative contour plots showing the identification of metastatic PyMT-BO1 cells in the lung following the indicated treatments. (C) Quantification of the percentage of PyMT-BO1 metastatic cells in the lung at experimental day 15, n=3-5. Statistical significance was calculated by two-tailed unpaired *t* test with Welch's correction.

6.3. Intravenous administration of OMVs is more effective than intraperitoneal administration in reducing B16F10 melanoma tumour burden

Though the tumour experiments presented previously highlight the potential of a prospective OMV-based therapy, previous studies have shown more dramatic reductions in tumour burden following delivery of OMVs derived from other bacteria(*634, 636*). A key difference separating our work from these studies is our use of an IP delivery route, which likely reduces OMV-accumulation at the tumour and other systemic sites compared with an IV injection. Additionally, IV administration is the most standard method for administrations in human patients, so use of this route is also more clinically relevant. In addition to the administration route, another unanswered question from our existing studies was whether Bt OMVs might have protective effects in other cancer types.

To address each of these questions, we probed the effects of an $1x10^{10}$ BDM-OMV dose (previously characterised as most effective) administered through IP and IV routes on growth of B16F10 melanoma tumours. Whilst our existing method of IP-delivered $1x10^{10}$ BDM-OMVs did not significantly alter tumour growth, IV administration caused a dramatic reduction to primary tumour volume (Figure 6.12). Comparatively, IV delivery increased the efficacy of OMV administration by three times (~20% reduction IP vs. ~60% IV). These findings not only indicate Bt OMVs may be effective in reducing tumour burden across several cancer types, but also that IV delivery can significantly increase treatment efficacy.

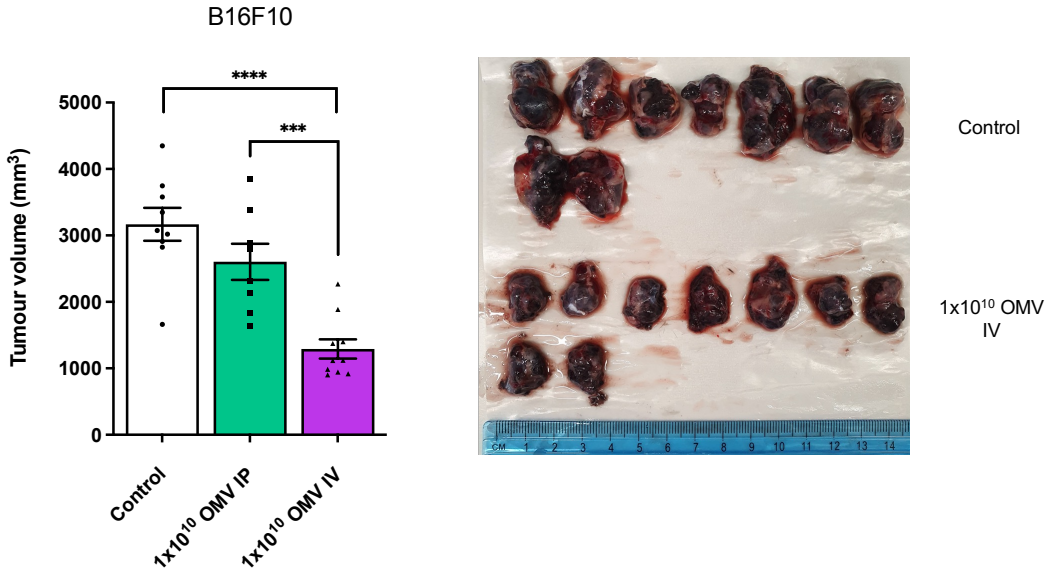

Figure 6.12. Administration of BDM-generated OMVs significantly reduce B16F10 melanoma tumour burden when delivered intravenously, but not intraperitoneally. Quantification with representative image of endpoint B16F10 tumour volume following intravenous and intraperitoneal OMV administrations at experimental days 7, 9 and 11, n=8-10. Statistical significance was calculated by two-tailed unpaired *t* test. ****$P < 0.0001$, ***$P < 0.001$.

6.4. IV-administered OMVs show promise as a novel anti-cancer therapeutic against primary and secondary tumour growth

With critical improvements to therapy efficacy following IV delivery, we wanted to bolster our data to highlight the potential of IV-administered OMVs for the treatment of cancer. We altered the OMV administration regime to every third day from the onset of palpable tumours, so to distribute OMV-treatment more evenly throughout the course of the experiments (Figure 6.13A). Given such clear differences between IP and IV OMV administration efficacy, it is possible that the fundamental mechanism of action may be different and thus the effective dose may also be altered. As with our BDM-OMV IP administrations however, IV administration resulted in a linear inverse relationship between BDM-OMV dose and tumour growth and highlighted the highest $1x10^{10}$ dose to be most effective (Figure 6.13B-C). To gain further insight to the translational potential of this OMV therapy, we utilised the same experimental outline in the CMT19T lung carcinoma tumour model (Figure 6.13D). Though not statistically

significant, endpoint CMT19T tumours trended smaller than control and indicated that OMV therapy could be efficacious across multiple cancer types, although seemingly most effective in melanoma treatment.

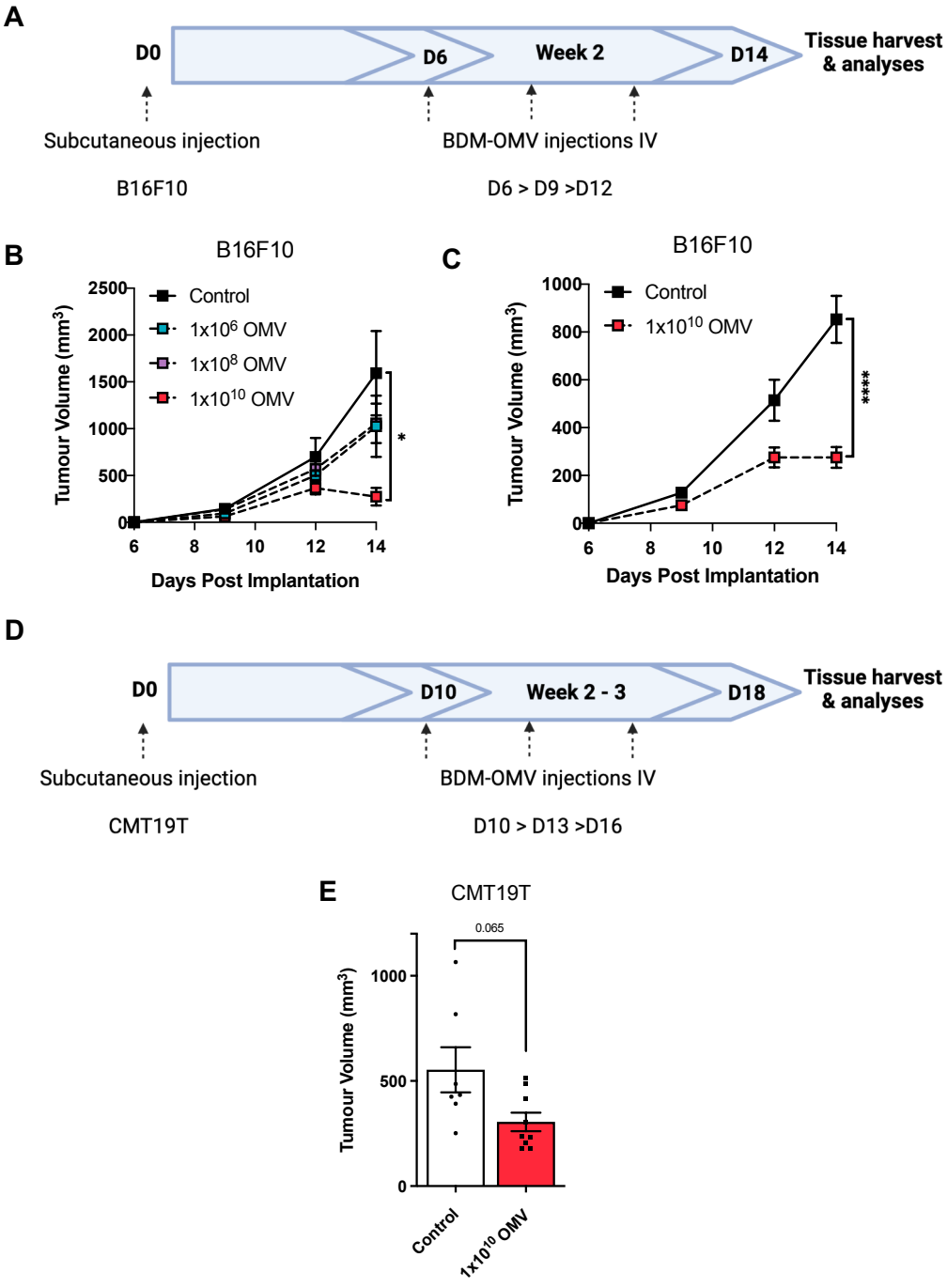

Figure 6.13. OMVs inhibit primary tumour growth at a high dose following intravenous administration. (A) Experimental outline of B16F10 melanoma primary tumour experiments with intravenous administrations of OMVs at 3-day intervals following onset of a palpable tumour. (B) Mean (± SEM) primary B16F10 tumour growth over time following increasing OMV dosages (n=5) and (C) following a defined $1x10^{10}$ OMV dose delivered intravenously (n=24). (D) Experimental outline of CMT19T lung carcinoma primary tumour experiments with intravenous administrations of OMVs at 3-day intervals following onset of a palpable tumour. (E) Mean (± SEM) endpoint CMT19T tumour volumes following administration of $1x10^{10}$ OMVs intravenously (n=7-9). Statistical significance was calculated by two-tailed unpaired *t* test. ****$P < 0.0001$, *$P < 0.05$.

As mentioned previously through this chapter, assessment of tumour metastasis is vital for the development of novel cancer therapeutics. This is particularly relevant in the context of melanoma; whereby surface skin legions are easily surgically removed and metastasis to distal organs represents the major cause of death. Due to the rapid growth B16F10 primary tumours, animals reach experimental endpoint long before the natural dissemination and metastatic outgrowth of secondary tumours can meaningfully occur. As such, we used an experimentally induced model of melanoma metastasis involving direct IV administration of B16F10 cells to the tail vein. Tumour cells were allowed to circulate and seed at metastatic sites for three days before OMV therapy onset (Figure 6.14A). Visual inspection of endpoint lungs revealed that OMV treatment induced a near significant reduction to the number of observable metastatic nodules (Figure 6.14B). Histological analysis revealed that lung legions treated with OMVs were also significantly smaller than controls, demonstrating that OMV administration effectively inhibited secondary tumour outgrowth (Figure 6.14C).

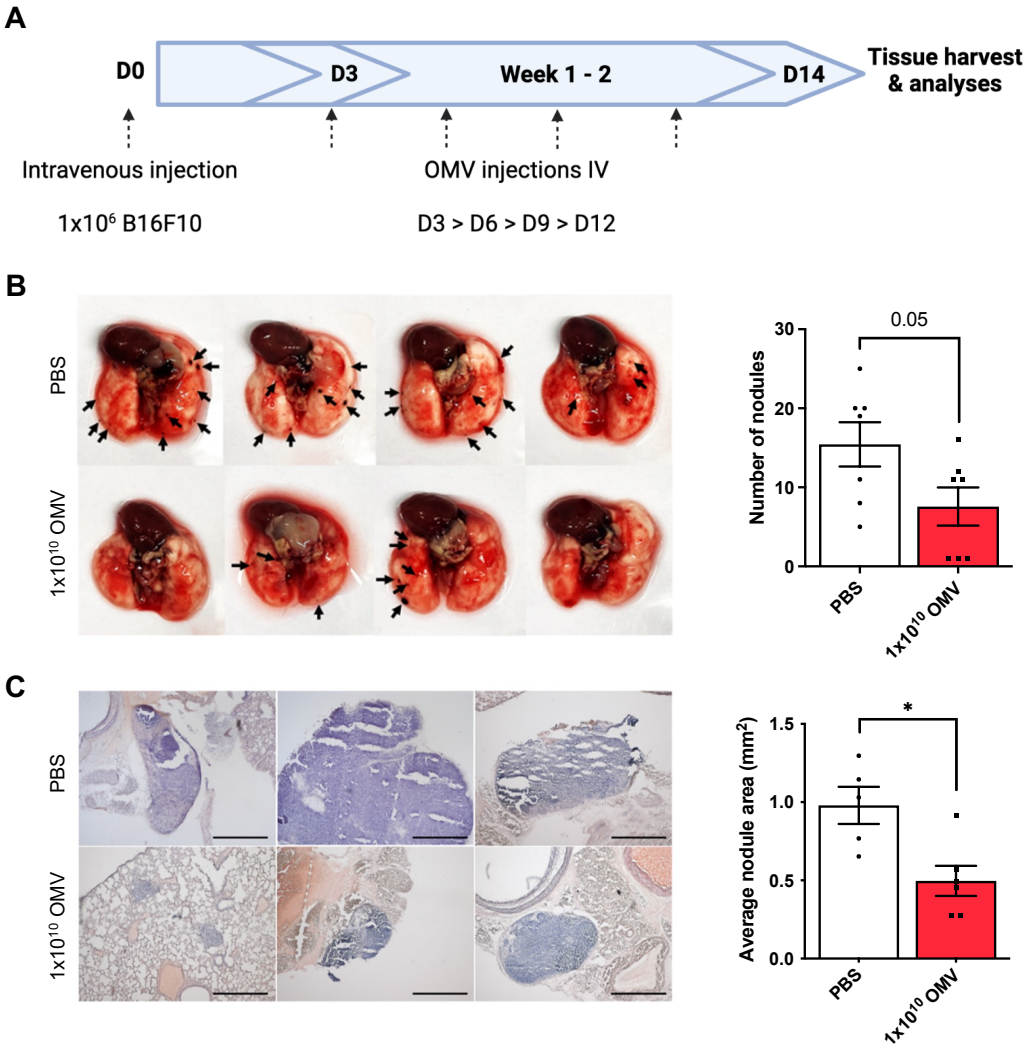

Figure 6.14. IV-administered OMVs inhibit the outgrowth of B16F10 lung legions. (A) Outline of B16F10 experimental metastasis experiment: $1x10^6$ B16F10 cells were injected intravenously and allowed to seed in the lungs for 3 days before administration of $1x10^{10}$ OMVs or vehicle control. (B) Representative images (left) and quantification (right) of the number of visible B16F10 lung nodules following OMV treatment, n=7. (C) Representative images (left) and quantification (right) of the average lung nodule size in animals treated with vehicle control or $1x10^{10}$ OMVs, legions were visualised following H&E staining and size quantified using ImageJ software, n=5-6. Bars represent mean (± SEM) and statistical differences were quantified using two-tailed unpaired *t* test. **P* < 0.05.

6.5. IV-administered OMVs do not cause significant host weight change or altered organ histopathology

Due to our continued optimisation of the OMV therapeutic, we undertook reassessment of treatment tolerability to ensure the altered OMV preparation (BDM rather than BHI) and administration route (IV rather than IP) did not induce any major adverse side effects. Measurement of animal body weight following OMV administration showed no significant changes in weight across multiple OMV dosages (Figure 6.15A). Additionally, histological examination of major organs of animals did not show any major signs of inflammation or tissue damage following the highest $1x10^{10}$ dose of OMVs (Figure 6.15B). Although a complete assessment of drug tolerability is challenging in animals, these data do indicate that IV administered OMVs do not induce major adverse effects which would be noticeable by weight change, histopathology, or animal behaviour (normal behaviour was observed across all treatment groups.

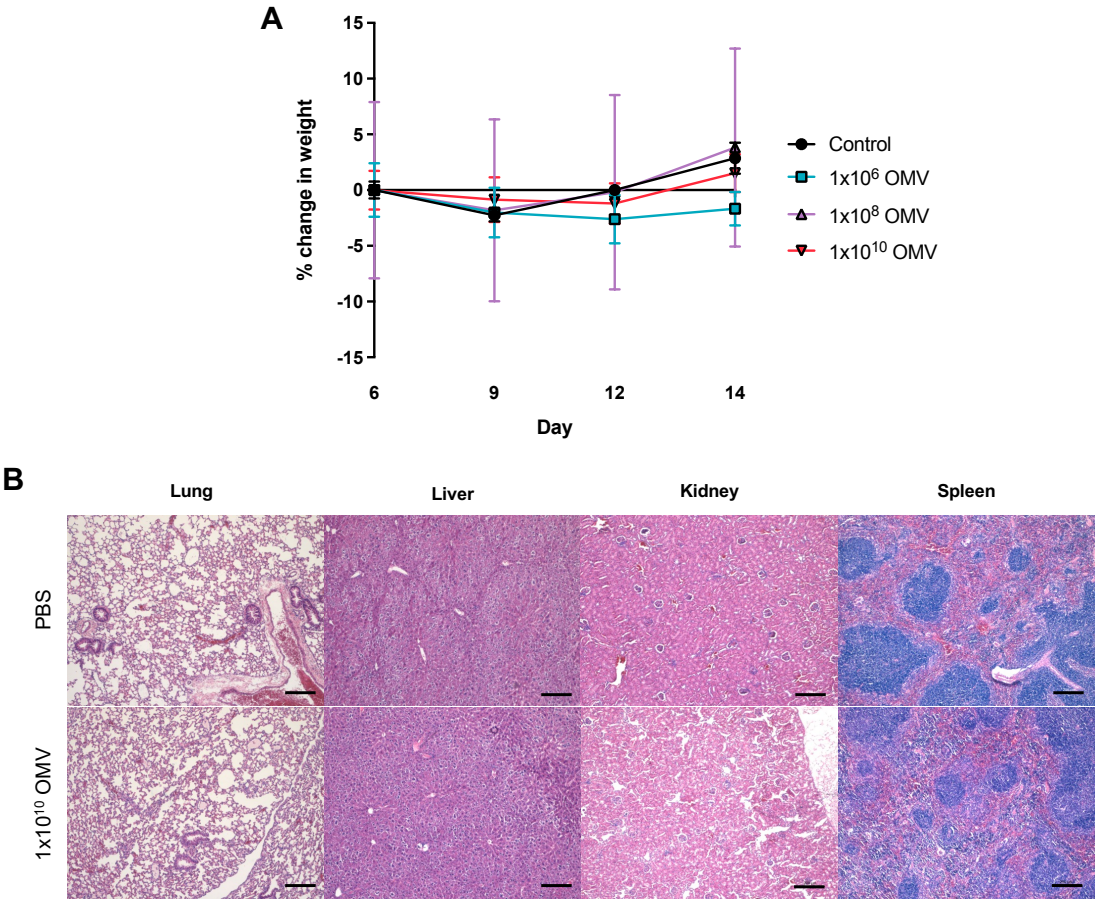

Figure 6.15. Effect of OMV treatment on animal body weight and major organ histology
(A) Mean (± SEM) B16F10 tumour-bearing animal weight change over time following administration of OMVs at the indicated dosages, n=5. (B) Representative images showing H&E histological staining of vehicle control or $1x10^{10}$ OMV treated organs (lung, liver, kidney, and spleen).

6.6. IV-administered OMVs efficiently translocate to the primary tumour

A key consideration for the identification of mechanism of action of OMV therapy is the physical localisation of the OMVs after administration. More OMVs localised to the primary tumour, for instance, increases the probability of key functional interactions occurring locally within the tumour rather than systemically. Likewise, significant accumulation of OMVs within the spleen may implicate this organ as the site of key functional interactions. To assess this, we generated and administered Bt OMVs containing a nano-luciferase tag (OMV^{NLuc}), which emit bioluminescence in the presence of the furimazine substrate(*637*). Three hours following IV administration of $1x10^{10}$ OMV^{NLuc}, or vehicle control, day 10 B16F10 tumour-bearing, or non-tumour-bearing control animals had major organs and tumours excised and bathed in a furimazine solution *ex vivo* before assessment of bioluminescent signal (Figure 6.16A). As expected, IV administration of vehicle control solution did not induce any bioluminescent signal, highlighted a lack of background signal, whereas OMV^{NLuc} administration results in detectable bioluminescent signal across major organs (Figure 6.16B). Analysis of non-tumour bearing animals demonstrated accumulation of OMVs predominantly in the lung, kidney, spleen, and liver (in descending order of signal), although one animal did not demonstrate any positive bioluminescent signal. Analysis of tumour bearing animals demonstrated OMV accumulation of OMVs within the primary tumour at levels roughly comparable to the spleen, although there was an unexpectedly greater signal of OMVs across all the major organs tested (Figure 6.16C). Overall, these data demonstrate that IV administration of $1x10^{10}$ OMVs results in efficient accumulation in the primary tumour, although not at levels which exceed many other major organs. OMVs also accumulate in the lung, liver, kidney, and spleen, with each of these sites relevant for tumour metastasises or orchestration of the anti-tumour immune response, suggesting OMVs may be effective in initiating systemic cancer inhibition and key mechanistic interactions may occur outside of the primary tumour.

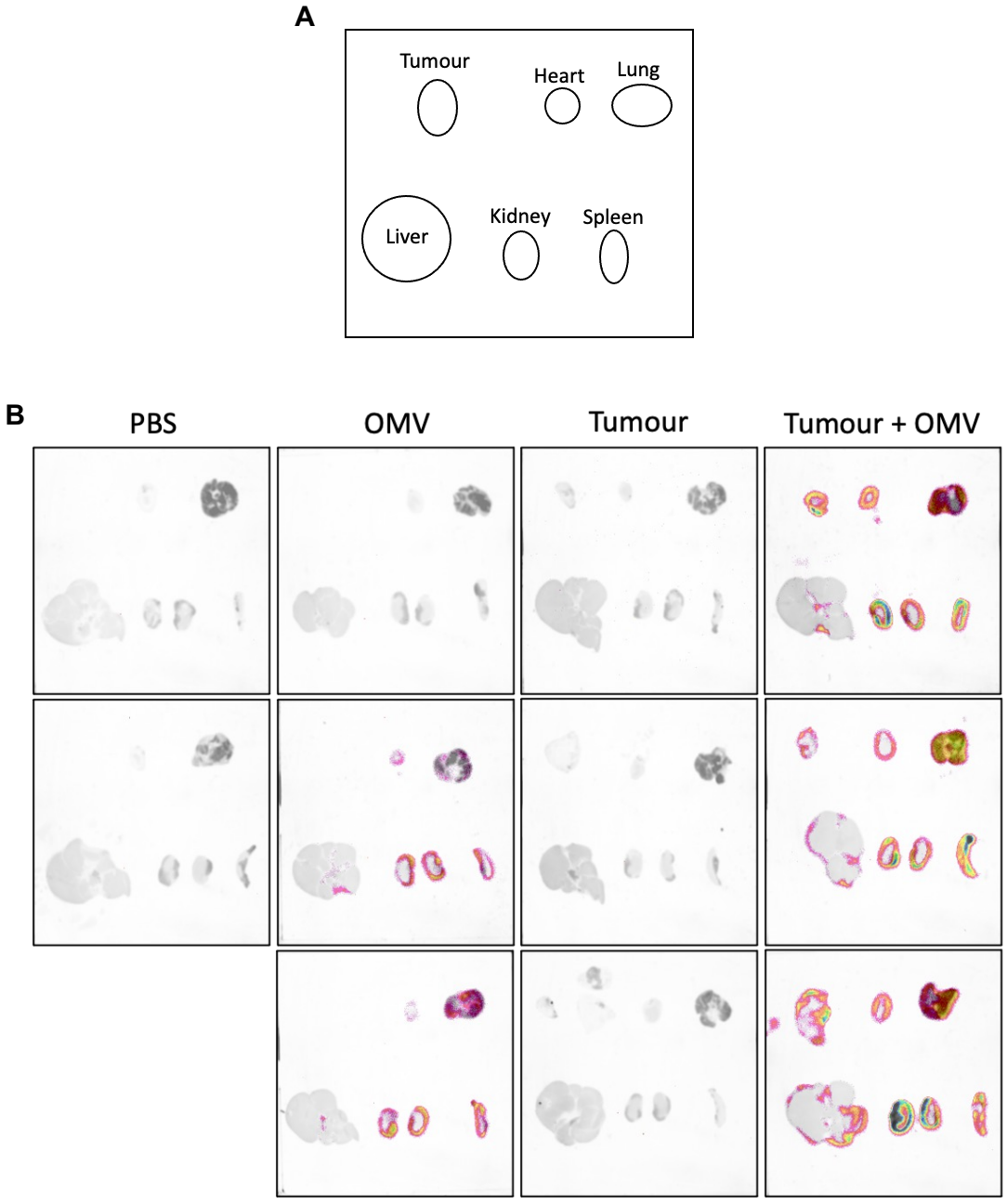
A
Tumour
Heart
Lung
Liver
Kidney
Spleen
B
PBS
OMV
Tumour
Tumour + OMV
C
Luminescence (AU)
2.0×10^10
1.5×10^10
1.0×10^10
5.0×10^09
0
PBS
Tumour
OMV
Tumour + OMV
Tumour
Heart
Lung
Liver
Kidney
Spleen

Figure 6.16. Nano-luciferase-tagged OMVs administered intravenously accumulate in B16F10 primary tumours. (A) WT mice or mice bearing day 10 B16F10 tumours were orally administered with luciferase-tagged OMVs (OMV^{NLuc}, 1×10^{10}) or vehicle control, individual organs were excised 4 hours post-administration for imaging according to the indicated layout using a Bruker *in vivo* Xtreme. (B) Representative images of non-tumour bearing (left) or tumour bearing (right) mouse organs following administration with vehicle control ('PBS', 'Tumour') or $1x10^{10}$ OMV^{NLuc} ('OMV', 'Tumour + OMV'). (C) Quantification of the absolute amount of bioluminescent signal in control or OMV^{NLuc} –treated animal organs, n=3.

6.7. OMVs stimulate NF-kB *in vitro* through TLR2 and TLR4 activation

The most defined(*638*) and intuitive mechanism for OMV-induced cancer inhibition is activation of the host immune system. To understand the broad anti-cancer and immunological effects of OMVs, we undertook *in vitro* immunological co-culture experiments. As we had confirmed from our work with PyMT-BO1 breast cancer, we initially validated that OMV treatment (at any dosage) did not alter B16F10 tumour cell viability (Figure 6.17A), implicating the mechanism of action of tumour cell death to occur via an intermediatory (e.g., immune) system component. Conversely, treatment of THP1-Blue monocytes with increasing concentration of OMVs highlighted a dose dependent and potent stimulation of NF-kB inflammatory response, highlighting the strong immunogenic potential of the OMVs within the host (Figure 6.17B). Activation of NF-kB in monocytes and macrophages has varying roles in cancer due to the ubiquitous nature of system(*639*), though is more typically associated with enhanced cancer onset and progression(*640*). Analysis of specific TLR activation demonstrated that BDM-OMVs stimulated both TLR2 and TLR4, although stimulating TLR2 much more strongly with a half maximal effective concentration (EC_{50}) of $1.85x10^8$ OMVs compared with $2.28x10^9$ OMVs for TLR4, representing a more than 10-fold increase in potency (Figure 6.17C-D).

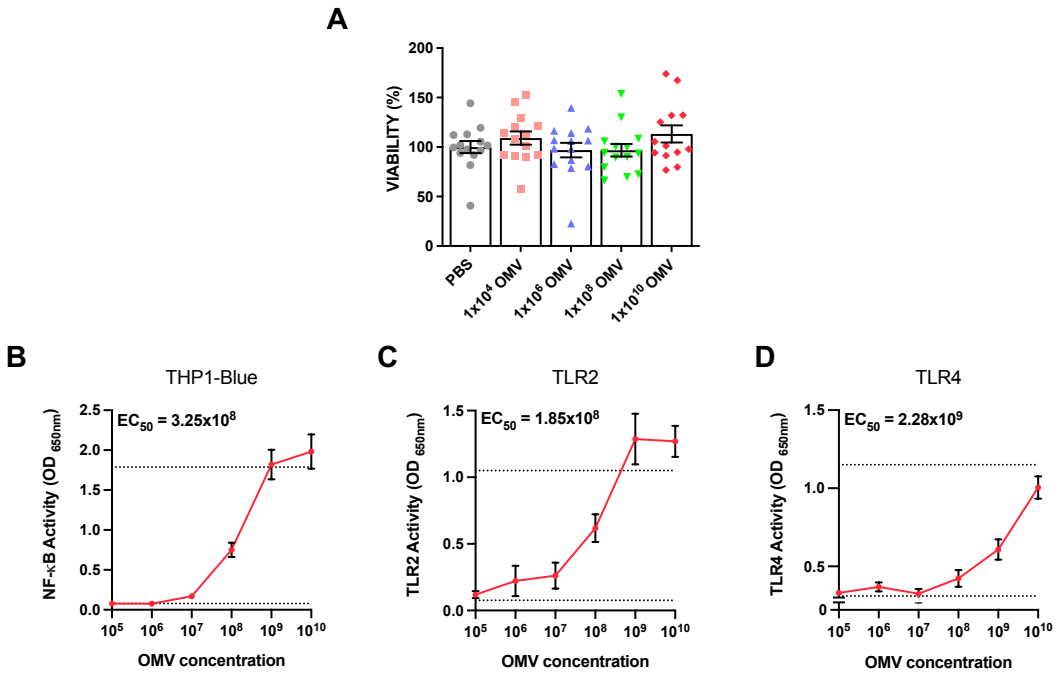

Figure 6.17. OMVs induce immune activation through TLR activation *in vitro*. (A) Relative proliferation of B16F10 cells treated *in vitro* with the indicated doses of OMVs, proliferation was quantified through Alamar Blue fluorescence, n=15 N=3. (B) Quantification of NF-kB activity in THP1-Blue monocytes in response to escalating dosages of OMVs, activity was measured through QUANTI-blue visualisation of the SEAP reporter, n=5. (C) Quantification of TLR2 activity in HEK-Blue hTLR2 cells and (D) TLR4 activity in HEK-Blue hTLR4 cells via detection of the SEAP reporter with HEK-Blue detection solution, n=3. (B-D) Lower dotted line indicates the mean signal induced by the negative vehicle (PBS) control and the upper dotted line indicates the mean signal induced by the relevant positive control.

6.8. IV-administered OMVs do not induce major changes to pro-inflammatory pathways *in vivo*

Given that OMV administration is highly effective in stimulating immunological responses *in vitro*, we next analysed cytokine release in OMV-treated primary tumours and sera to understand how OMVs may be controlling cancer immune responses *in vivo*. Multiplex analysis of proinflammatory cytokines in endpoint B16F10 primary tumours revealed that OMV administration did not cause statistically significant changes in any of the analytes tested, with the only notable change being a near-significant increase in TNFα levels (Figure 6.18A). TNFα is a key proinflammatory

cytokine associated with the activation of $CD8^+$ T cells, NK cells and macrophages(*641*), with its role being considered anti- or pro-tumourigenic depending on context(*642*). In the case of protective responses involving $CD8^+$ T cells, release of other inflammatory cytokines (e.g., IFNγ) typically occurs concurrently, although we do not observe such changes in OMV-treated animals. Comparing these results to cytokine levels in the serum of the same endpoint animals reveals that the potential increase in TNFα occurs locally within the tumour, whilst systemic levels of IFNγ decrease following OMV administration (Figure 6.18B). This reduction in IFNγ is matched by an increased level of systemic IL-10, which is known to be induced by Bt OMV exposure to monocytes(*393*) and canonically functions to supress inflammatory (IFNγ) release(*643*). The cytokine data together do not provide the concrete (pro-inflammatory) associations expected for our hypothesised OMV-mediated tumour inhibition, leaving the *in vivo* anti-cancer mechanism of action as an open question for future exploration.

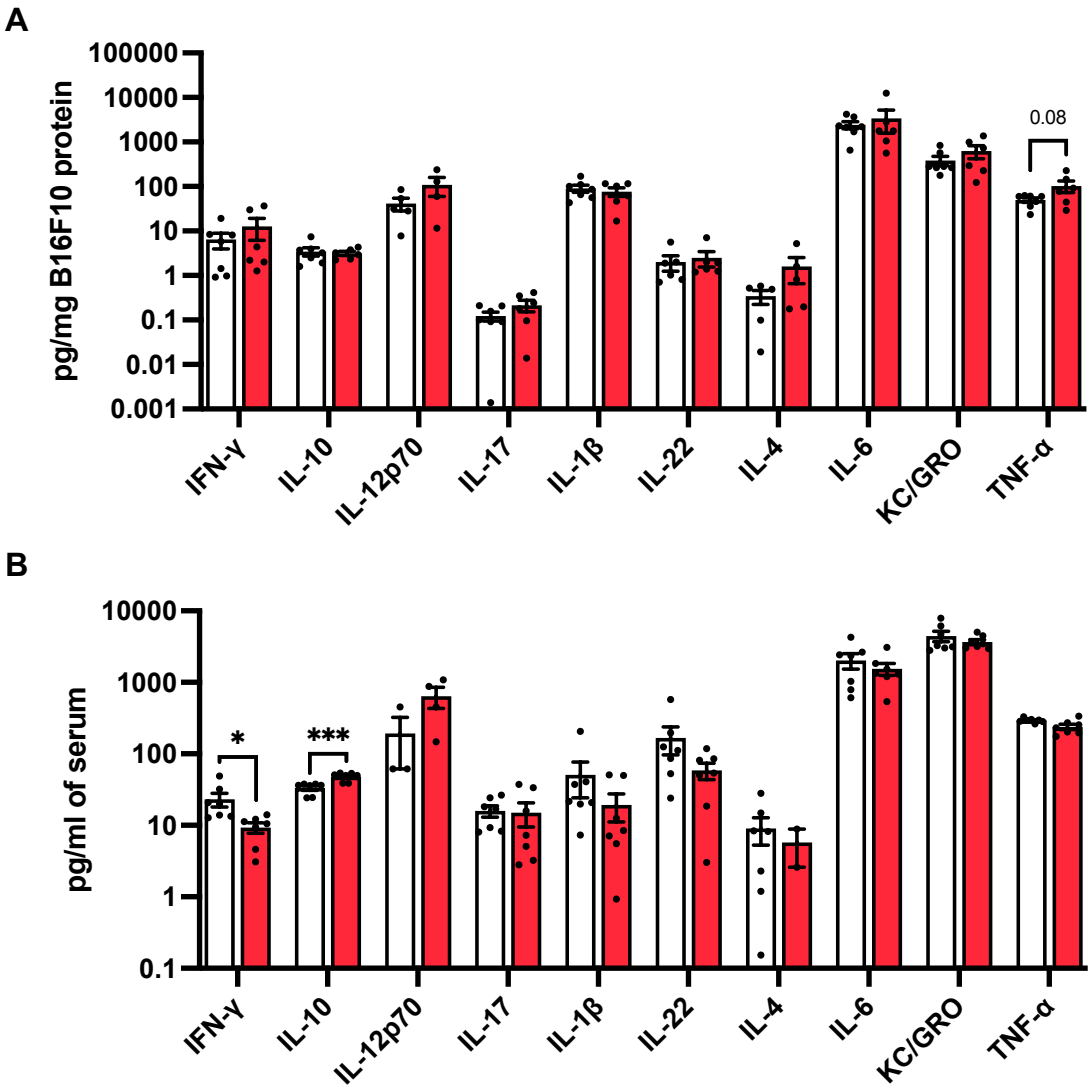

Figure 6.18. Intravenous OMV administration does not significantly alter inflammatory cytokine release *in vivo*. (A) Mean (± SEM) cytokine production in B16F10 primary tumours (n=5-7) and (B) serum (n=5-6) following OMV administration, quantified by a custom MSD U-PLEX assay and normalised to the levels of extract tissue protein. Statistical differences were calculated by two-tailed unpaired *t* test.

6.9. Discussion

Weaponising the full power of bacteria to modulate the immune system represents an exciting overarching goal for microbiome therapeutics development. Deadly diseases such as cancer, IBD, and liver disease all have immunologically driven aetiology, so represent ideal therapeutic targets(*644*). Direct systemic delivery of bacterial antigens bypasses the natural barrier of the intestinal epithelium, allowing host-microbe interactions at a scale and intensity not possible from conventional gut microbiota supplementation. The challenge here, is the balance between beneficial and non-beneficial stimulation of the immune system, which may provide therapeutic benefit or induce toxic side effects. This point has been exemplified through the early attempts at bacterial cancer therapy at the dawn of the 20th century, whereby the use of heat-killed and systemically administered pathogens resulted in major adverse side effects(*608*). In more recent times, the translation of attenuated salmonella as a tumour colonising and inhibiting therapeutic ultimately failed phase I trials due to limited efficacy and dose-dependent side effects(*645*), highlighting the safety challenge of using systemic live bacterial approaches. Through our focus on bacterial OMVs as novel therapeutics, we present an inert therapeutic which lacks infectious replicative capacity, yet also potently stimulates the immune system in a similar fashion to complete bacterial cells. By using OMVs derived from the non-pathogenic commensal *Bacteroides thetaiotaomicron* (Bt), we implement OMVs with an inherently limited potential for major adverse side effects (compared with pathogen-based approaches) and explore their potential in the context of cancer therapy.

Our initial experiments utilising OMVs involved Bt growth in BHI growth media. The OMVs generated from these preparations (BHI-OMVs), administered through an IP injection, caused an ‘U-shaped’ tumour reduction dosage response, whereby only the medium doses appeared to reduce tumour burden whilst the low and high doses did not. Histological examination of PyMT-BO1 primary tumours revealed a higher level of

proliferation within high $1x10^{10}$ dose primary tumours compared to control or $1x10^{8}$ OMV groups, whilst *in vitro* tumour cell-OMV co-cultures did not highlight any obvious direct interactions. Immunological analyses of the effects of the BHI-OMVs revealed alterations in immune cell infiltration at the primary tumour and in the pre-metastatic lung at both the efficacious medium dose and non-efficacious high dose. Implicated cell pathways included macrophages, lymphoid cells ($CD8^{+}$ T cells, T helper cells etc.) and NK cells, although none of the correlative immunological associations were consistent between different tumour models (PyMT-BO1 vs. E0771) or physiological site (primary tumour vs. lung), making concrete mechanistic conclusions unclear. More broadly, the data highlighted the immunogenic nature of the BHI-OMVs without any reliable indication of mechanism, with the observed dose curve highlighting a delicate dosage balance dictating therapy response. This dosage trend is quite atypical in comparison to other literature looking at anti-tumour effects of OMVs(*634*), implying a tumour-protective mechanism which is stimulated at a medium dose ($1x10^{6}$-$1x10^{8}$ OMVs), alongside a pro-tumourigenic mechanism which only occurs at a high dosage. Ultimately, the observed response curve represents a problematic issue for potential clinical translation, which would likely require delicate tuning of OMV dosage to prospective patients (based on patient size, weight etc.) to achieve therapeutic response. Additionally, the long-term implications of a sustained ineffective (high) dose are unclear. If there is a pro-tumourigenic mechanism occurring at the ineffective dose, the tumours may proceed to grow larger than controls over time, potentially worsening clinical outcomes. With the lack of clear mechanism, problematic dosage response, and relatively unimpressive pre-clinical efficacy (30-40% tumour reduction), we recognised the necessity for therapeutic optimisation.

A consideration for OMV therapeutic translation is advantage of a pharmaceutical preparation free from animal products and potential contaminants. Our generation of Bt OMVs in BHI growth medium is problematic in this regard, with BHI media using bovine and porcine organs and thus likely containing OMV-sized animal contaminants which may be bioactive. To address this, our collaborators within the Carding Lab at the Quadram Institute developed an animal product-free Bacteroides Defined Media (BDM), which we used for subsequent OMV (BDM-OMV) generation. Use of BDM-OMVs in place of BHI-OMVs resulted in the loss of the BHI-OMV dosage effect, with a medium dose now ineffective and a high dose ($1x10^{10}$) most efficacious. BDM-OMV administration also resulted in the dose dependent modulation of different immune cells compared to BHI-OMVs, increasing levels of MDSCs in the primary tumour and pre-metastatic lung. These data suggest that a function of the Bt growth conditions in

BHI media caused a significant functional difference to the effect of the OMV preparation. This could be due to bioactive BHI contaminants within the final OMV preparation or could be components in the BHI media altering the proteomic constituents of the OMVs themselves, as shown previously(*633*). The latter of these theories derives from the biology of bacteria being highly responsive and adaptable to the local growth environment, with cellular machinery and functional outputs which change dependent on availability of nutrients, oxygen levels, pH, and bacterial competitors, ultimately impacting the production of active compounds. Whichever the precise mechanism, the loss of the U-shaped dose response and the replacement with a linear response curve with increasing BDM-OMV dose, highlights that the use of BHI was dictating both the anti- and pro-tumourigenic effects of the BHI-OMVs depending on dose. Notably, there is a lack of literature characterising the effects of bacterial derived culture media (such as BHI) on mammalian immune responses, with these data indicating such common microbiology culture conditions may be significant experimental confounders in other studies. Overall, these data caution the use of BHI and other animal product-based growth media on therapeutic bacterial preparations, and further highlight the importance of bacterial environmental conditions to cellular functional outputs.

Although the use of BDM-OMVs improved the translational prospects of OMV therapy through removal of the problematic U-shaped dose curve, key issues including absence of a clear anti-tumour mechanism and poor overall anti-tumour efficacy remained. A general theme in pre-clinical cancer research is that therapeutics are usually more effective in pre-clinical mouse models than in humans, likely owing to the enhanced complexity of human tumours(*646*). As such, a 30-40% reduction in tumour volume in mice following BDM-OMV treatment may not translate to a similar reduction in human tumours, making the prospects of industry support for clinical trials slim. Other research studies in the space have also demonstrated better efficacy, with the landmark study by Kim et al.(*634*), demonstrating complete CT26 colon tumour regression and immunological memory function from OMVs derived from a range of attenuated pathogens (e.g., *E. coli*). Although using OMVs from attenuated bacteria has inherent risks as discussed above, the proven potential of anti-tumour OMVs highlighted the need for further BDM-OMV treatment optimisation to improve therapeutic response. A key difference between our regime and existing approaches is the use of an IP (rather than IV) route of administration, as well as the use of different types of cancer. Comparison of the most efficacious BDM-OMV dose, $1x10^{10}$, delivered through IP or IV injections to B16F10 melanoma-bearing animals, demonstrated a

markedly greater response to the IV administration route. In addition to IV administration being more clinically relevant to current cancer therapeutic treatment in humans(*647, 648*), IV administration likely results in enhanced accumulation of OMVs in key systemic sites (primary tumour, spleen, lymph nodes, lungs), potentially stimulating stronger anti-tumour responses in the locations they are required. Further validation of BDM-OMV IV-administration highlighted the same linear inverse tumour volume dose response as identified from IP administration in PyMT-BO1 breast cancer, showing that the BDM-OMV dose response is driven by the OMVs themselves rather than the administration route. IV-administered BDM-OMVs reduced primary and metastatic tumour inhibition in B16F10 melanoma and near-significant primary tumour reduction in CMT19T lung carcinoma, demonstrating more promising efficacy for potential clinical translation. IV administration of BDM-OMVs also improved efficacy without inducing changes to animal bodyweight or major organ histopathology, indicating the absence of severe adverse side-effects.

Although much of the literature using bacterial vesicles in cancer therapy describes immunological mechanisms of action(*634, 649, 650*), studies are emerging which suggest directly apoptotic mechanisms are possible(*651*). A recent example from Jiang et al.(*652*), use *Bifidobacterium*-derived extracellular vesicles to reduce tumour burden in triple negative breast cancer xenograph models by the induction of apoptosis. Assessment of OMV biodistribution is relevant to mechanism, as a higher dosage of OMVs to the tumour (e.g., from an IV compared to IP injection) may increase the likelihood of a directly apoptotic mechanism. Using nano-luciferase-tagged OMV^{NLuc} treatment, we demonstrated the *in vivo* distribution of IV-administered OMV to include multiple tumour relevant sites, including the lungs, primary tumour, and spleen. However, *in vitro* Alamar Blue assays established that BDM-OMVs, as shown previously with BHI-OMVs, did not directly impact tumour (B16F10) cell viability regardless of dose. These data suggest that the BDM-OMV mechanism is more likely immunologically driven, particularly given the strong *in vitro* induction of NF-κB in monocytes by BDM-OMVs, which appears to be driven through a similarly potent TLR2 response. The findings are consistent with Fonseca et al.(*393*), who had previously demonstrated Bt OMVs to be strong inducers of monocytes *in vitro* and to cause enhanced IL-10 secretion through TLR2 activation. It is further notable that the EC_{50} values for NF-κB, TLR2, and TLR4 activity are all above an $1x10^8$ dose of BDM-OMVs, which we had demonstrated through our tumour dose response experiments, to not significantly reduce tumour volume. Given a higher dose of OMVs is required to both

stimulate a strong immunological response *in vitro* and reduce tumour volume *in vivo*, the data add further weight to the potential OMV-induced mechanism of action being immunological (through the induction of myeloid TLRs).

A significant caveat to the immunological hypotheses, is that assessment of endpoint B16F10 primary tumours did not reveal alterations to pro-inflammatory cytokines typically relevant for immune mediated tumour destruction (e.g., TNFα, IFNγ, IL-12p70). In contrast, systemic cytokine analysis showed an anti-inflammatory IL-10 release and concurrent IFNγ inhibition, which whilst supporting previous research demonstrating Bt OMV IL-10 induction(*393*), is generally considered to be a pro-tumourigenic response(*653*) and thus is not a clear explanation for the *in vivo* OMV-induced tumour reduction. A possible explanation for these data could be that the key tumour-inhibitory interactions may be occurring in another tumour relevant site, such as the spleen, as we have validated from the tracking experiments that the BDM-OMVs accumulate in this tissue at comparable levels to the primary tumour. Another insight from the OMV^{NLuc} tracking data is the accumulation of OMVs in the outer regions of major organs and the primary tumour rather than through the core of the entire structures, which may implicate that the key immunological interactions are spatially localised to these regions and are not as obvious when measured alongside the entire tissue (as seen from protein analysis or flow cytometry preparation). It is further possible, and potentially likely, that the elapsed time (2 days) between OMV administration and endpoint tissue harvest causes the key immunological pathways induced by OMVs to be missed. If the key mechanisms driving OMV response are indeed transient and potent, it may be necessary to assess OMV responses at much shorter timepoints, at hours rather than days post-administration. Certainly, more work is required to identify the key pathways and physiological sites mediating the tumour-protective mechanism of BDM-OMV treatment, employing broader (immunological) assessments of key tumour-relevant sites for anti-tumour pathway induction.

Overall, the work in this chapter demonstrates the great potential, and risk, associated with systemic administration of bacterial therapeutic products. Our data highlight that use of Bt OMVs offers therapeutic potential, depending on growth conditions and administration route, without inducing noticeable side effects. The stark difference in functional effect of Bt-OMVs depending on the growth media used, highlights the reoccurring theme of bacterial active compound production being adaptable to the environmental growth conditions, whilst differences in efficacy depending on administration route demonstrates further considerations for potential clinical

translation. With the correct OMV generation and administration protocols, Bt OMVs have strong potential as novel anti-cancer therapeutics.

7. Final discussion

Cancer is one of the single greatest threats to human health in the modern world, ranking alongside cardiovascular disease as the most common cause of premature death in the world(*1*). There is a great unmet need for new and improved cancer treatments to bolster current approaches, which suffer from inconsistent efficacy across different indications and individuals(*654*). A particular aim within this, is to develop treatments which target both primary and secondary disease, as well as inhibiting tumour recurrence following successful treatment. The shortest realistic route to this aim of a 'cure' for cancer, capable of targeting each of the tranches of disease, is likely through harnessing the power of immune system (i.e., cancer immunotherapy). Cancer immunotherapy, in the form of immune checkpoint inhibition, has already landed in the clinic for several indications, although efficacy is highly variable, and most patients will not respond(*655*). It is thus clear, that to fully unlock the power of the immune system against tumours, novel and complementary immunomodulatory approaches are required. Gut bacteria have strong potential for immune modulation, as they help programme our immune system in infancy (through to adulthood)(*656*) and have been shown to induce pro- or anti-cancer immunity depending on context(*657*). Though this new field of using bacteria for immunotherapy has gained large interest, the underlying mechanisms and host-microbe interactions which drive responses remain largely unknown. This lack of understanding has made microbial therapies difficult to translate as patients are harder to stratify, therapeutics are difficult to rationally improve, and synergistic approaches are not easily identified, resulting in failed clinical trials(*658, 659*).

The broad aims of this thesis were to undertake systematic microbial drug development in the context of cancer. Specifically, we aimed to identify novel therapeutic approaches, assess their translational potential (across different cancer types and potential standard of care synergy), and define key mechanistic determinants and host-microbe interactions which dictated therapy response. We used multiple approaches, including live bacteria supplementation, isolated bacterial active compounds, and bacterial mimicry with OMVs. We also tested distinct routes of supplementation, orally to the gut or systemically to the blood stream, to optimise different types of approaches targeting different mechanistic pathways. Our drug development processes combined with our focus on mechanism, served the overall

goal of bringing new microbial therapeutic approaches closer to effective clinical translation.

Most of the work conducted for this thesis concentrated on the beneficial genera *Bifidobacterium*. We chose to focus here because *Bifidobacterium* have been shown to be strongly immunomodulatory, particularly in early life immune programming(*381, 660*), whilst also being linked to beneficial outcomes pre-clinically(*362, 386, 387, 661*) and clinically(*352, 377*) in cancer. Although the positive associations have been previously identified, the distinct mechanistic knowledge required for clinical translation is poorly defined, and the broader potential for *Bifidobacterium*-based therapy from different species in different cancer types has not been thoroughly assessed. Our initial approaches utilised several strains from different species of *Bifidobacterium* to highlight that the genus of bacteria is broadly protective in breast cancer; a disease indication without previously published beneficial associations. Importantly, our data also demonstrated that different types of *Bifidobacterium* utilise different anti-tumour mechanisms of action, opening the exciting possibility of combining different strains/species with unique and synergistic anti-tumour mechanisms to increase efficacy. A cautionary finding, however, is that blind combination of several strains does not guarantee successful outcomes. More bacteria, even those shown to be beneficial, is not always better (and can be worse) likely due to competitive interactions between strains, which speak to the consequences of a lack of detailed mechanistic understanding. Further demonstrating strong translational potential, we show that *Bifidobacterium* therapy can be combined with standard of care chemotherapy and immunotherapy to enhance treatment response, with this approach the most likely clinical utilisation of well tolerated microbial therapeutics.

Although strong translational potential for *Bifidobacterium* was demonstrated, our key aim was to go to a much deeper level of mechanistic depth than most previous literature. To enable this, we focused on one key strain, *B. pseudocatenulatum* LH663, because preliminary data indicated an enhanced $CD8^+$ T cell response in primary tumours. Further experimentation across multiple pre-clinical models of breast cancer confirmed this finding, showing LH663 to induce anti-tumour $CD8^+$ T cell activation in the primary breast tumour, tumour-draining lymph node, and spleen. LH663-treated $CD8^+$ T cells showed traits of both transient and long lived (memory) immunity against breast tumours, suggesting both neoadjuvant and adjuvant applications against primary and recurrent disease. LH663 treatment was not effective in $CD8^+$-deficient E0771 tumours or in $CD8^+$-depleted BRPKp110 tumours, showing the mechanism to

be $CD8^+$-dependent. We did not detect enhanced activation of any other anti-tumour effector pathways following LH663 treatment, suggesting a $CD8^+$-specific mechanism, which was further associated with changes in $CD8^+$-modulating macrophages and dendritic cells. With the discrete systemic immunology of LH663-efficacy uncovered, we wanted to identify the key functional output from the gut driving systemic responses. Going against dogma in the field(*363*), our untargeted metabolomics of sera demonstrated no detectable changes to systemic metabolites, suggesting that a microbial metabolite from the gut was not mediating the observed responses. Additionally, analysis of primary tumours showed no direct translocation of LH663 cells to the primary tumour, removing another possible functional output. Given these data, we hypothesised that the most likely functional output from the gut was systemic translocation of gut immune cells locally activated following LH663 treatment. Although our colon immune profiling did not demonstrate any concrete answers to this question, it is possible that LH663-induced immune activation occurs in other anatomical compartments of the gut, such as the small intestine.

To further define the mechanism of action, we concluded that identifying the active compound produced within the gut following LH663 administration would improve the likelihood of defining the host-microbe interactions which dictate response, and thus enable easier identification of the functional output from the gut to complete the mechanism. In service of these studies, we first wanted to establish whether the active compound interacting with the host to dictate response was produced by LH663 direct, or whether it was produced by another commensal which was stimulated by LH663 administration. Shotgun metagenomic assessment of commensal microbiota dynamics did not reveal any changes to individual species or the wider microbial population following LH663 treatment, suggesting a limited potential for the involvement of other commensal bacteria in the mechanism. This conclusion is bolstered by the finding that antibiotic depletion of commensal bacteria prior to LH663 administration did not rescue tumour volume, again suggesting a direct mechanism linking LH663 to the host. A secondary outcome from our metagenomic sequencing was a surprising finding that the number of *Bifidobacterium* and specific *Bifidobacterium pseudocatenulatum* genomic reads in the caecum of LH663-treated animals was not increased 24 hours post-administration. This finding suggested a highly transient exposure of the host to LH663, with the bacterial cells not appearing to colonise effectively and having a short period of time to conduct active biological processes (such as metabolite release). These associations and the reduced likelihood of active processes mediating anti-tumour immunity, suggested a non-active physical interaction may be mediating the

functional effect. We confirmed this hypothesis through pre-killing of LH663 cells with peracetic acid(*489*), as acid-killed LH663 remained efficacious against breast tumours to levels near-identical to live LH663 supplementation. Further experiments demonstrated that exopolysaccharide (EPS), one of the key immunomodulatory antigens produced by *Bifidobacterium*, was the key active compound produced by LH663 in mediating anti-tumour immunity. Isolated oral administration of EPS again reduced primary tumour volume to levels identical to live LH663 supplementation, whilst also inducing the same characteristic $CD8^+$ T cell activation and macrophage/dendritic cell infiltration. Structural analyses showed the LH663 EPS to be a glucose and galactose-rich structure, and *in vitro* assays did not demonstrate any noticeable direct activation of either $CD8^+$ T cells or monocytes. Comparatively, *in vitro* supplementation of BMDCs with EPS did induce a notable increase in dendritic cell maturation, mirroring our *in vivo* findings and suggesting that the starting point for the immune mechanism could be LH663 EPS activation of dendritic cells.

Although the bulk of our work focused on the oral supplementation of live *Bifidobacterium* or isolated microorganism-derived active compounds to the gut, we recognise that this represents only one type of approach to microbial cancer therapy. We were further interested in how microbial therapies may benefit from breaking the physiological confine of the gastrointestinal tract if administered systemically into the blood stream. Our initial hypothesis was that direct injection of a bacterial therapeutic would enable a higher quantity and potency of host-microbe interactions at distal tumour relevant sites to enable enhanced anti-tumour immunity. A key consideration for this approach is safety, as an increased potency of bacterial therapy could enhance the onset of serious adverse side effects (e.g., infection). To minimise these risks whilst simultaneously capturing the immune stimulating potential of bacteria, we utilised bacterial OMVs as systemically administered therapeutics, as these structures generally contain most of the bioactive compounds from the parental bacterium whilst lacking the ability to replicate(*638*). We chose to isolate OMVs from *Bacteroides thetaiotaomicron* (Bt), as this species is a well-tolerated commensal with an excellent safety record(*662*), which has been previously associated with positive outcomes in human cancer(*397*).

The bulk of our work using OMVs highlights the considerable challenges faced during microbial drug development and application, as our therapeutic outline underwent several optimisations and alterations, which resulted in considerably different outcomes. This is exemplified by the finding of two distinct dose responses to Bt OMVs

generated either in BHI media, which contains contaminating animal products, or a minimal vegan media (BDM), which did not. These data highlight the relevance of potential contaminants and the adaptability of bacteria to different growth conditions, which can in turn influence active compound expression and therapeutic effects. The data suggest that some bioactive contaminant from the BHI media was causing a pro-tumourigenic response at high OMV doses, whilst causing an anti-tumourigenic response at lower doses. The results of tumour immune profiling for OMVs from either condition were inconclusive and inconsistent, limiting downstream mechanistic insights, but did demonstrate the strong immunomodulatory capacity of the OMVs. Further optimisations of the therapeutic included adaptation of the administration route and type of cancer indication, with each of these factors again significantly modulating therapy efficacy. Utilisation of an effective dose of IP-administered OMVs validated in breast cancer did not induce a similarly protective response in melanoma, whilst administration of the same OMV dose via IV injection markedly enhanced tumour inhibition (again in melanoma) compared with an IP administration route. The relevance of administration route is particularly interesting, as the dosage response curve remained the same regardless of injection method, but the efficacy was dramatically different. This phenomenon could be caused either by an extension to the same mechanistic action (due to enhanced OMV delivery to active systemic sites) or could be due to an entirely different mechanism (due to delivery to previously inactive, tumour-relevant sites). Through this series of drug development cycles and therapy optimisations, we developed an effective therapeutic routine of high OMV dose ($1x10^{10}$ OMVs) administered intravenously to B16F10 melanoma-bearing animals. This therapy was effective in reducing primary tumour volume by ~60%, as well as reducing metastatic legion outgrowth, through a mechanism independent of direct tumour cell killing. The therapy appeared to be well tolerated, not inducing noticeable changes to animal behaviour, changes to body weight, or major organ histopathology. Whilst *in vitro* studies showed OMVs to be highly immunostimulatory in monocytes, particularly through TLR2 activation, *in vivo* cytokine production in the primary tumour did not demonstrate any major changes indicative of a pro-inflammatory anti-tumour immunity. Concurrently, analysis of serum cytokines showed a reduction in IFNγ and increase in IL-10, normally indicative of a pro-tumourigenic anti-inflammatory immune response. These findings did not correlate with the observed tumour volume reduction, so it is evident more work is required to define the *in vivo* mechanism of action mediating protective OMV induced responses.

With the work in this thesis taken together, we present a broad outline of various approaches to microbial drug development utilising different bacteria, bacterial products, growth conditions, and administration methodologies, which all contribute to varying levels of anti-cancer efficacy. With particular focus on *Bifidobacterium* and *B. pseudocatenulatum* LH663 therapy in breast cancer, we define a detailed mechanism of action across multiple biological systems, displaying novel biology of gut microbial EPS mediating systemic anti-cancer immune responses. Overall, we believe our approach to drug development and focus on detailed mechanisms of action provide a lens to the future of microbial therapeutic development and translation to the clinic.

7.2. Future work

Although we have already demonstrated multiple key steps of the LH663 mechanism against breast cancer, there remains some important outstanding questions. Key among these questions, is the definition of the LH663 functional output from the gut. We have demonstrated the systemic immunological mechanisms dictating LH663-induced tumour inhibition, as well as showing that the EPS produced by LH663 is mediating the response. However, it is still unclear how LH663 EPS in the gut induces an anti-tumour immune cascade outside the gut. We hypothesise the most likely link between these findings is that the immune cascade begins from local immune cells (specifically, dendritic cells) within the gut, which are primed and activated locally by LH663 EPS prior to a systemic cell translocation and induction of tumour immunity. This type of biology has been demonstrated in other contexts in cancer(*527*) but is a relatively unexplored element of human physiology. For us to properly assess whether systemic DC release following LH663 administration originated from the gut, we would need to employ longitudinal cell tracing experiments across the length of the gastrointestinal tract. The only experimentally validated method to do this would employ the Kaede mouse model(*663-665*). These mice contain photoconvertible cells, which under steady state emit green fluorescence, but in the presence of violet light become converted to red fluorescence(*666*). To track cells from the gut, we would perform a laparotomy and expose the length of the gut to low intensity violet light, converting all the cells of the gut from green to red. Following completion of surgery, LH663 would be administered to the animals, and we would then harvest blood and tumour tissues for cytometric analyses to look for the presence of red fluorescent cells (i.e., originating from the gut) in systemic sites. We could then assess the cell surface

marker profile of these cells by flow cytometry for the purposes of immune phenotyping (e.g., to confirm whether these are dendritic cells), as well as FACS isolating the cells *ex vivo* for purposes of RNA-Seq to enable a deeper insight into functional changes. To enable assessment of the specific origin of LH663-host interactions in the gut, we could simultaneously undertake profiling of gut lymph nodes and lamina propria to assess whether there is a concurrent reduction in red fluorescent cells (matching the specific marker profile identified systemically) in each gut location, which would be indicative of a source for the systemic cells. These types of experiments would not only reveal whether the LH663 mechanism involves a systemic translocation of gut programmed immune cells but could also reveal the specific location at which these key interactions occur.

Demonstrating the mechanistic relevance of any gut programmed immune cell is also vital. We would undertake this through an adoptive transfer approach, whereby LH663 EPS treated (dendritic) cells (implicated for the experiments above) would be adoptively transferred into naïve tumour-bearing animals. We would then observe the impact of these cells on tumour growth, expecting an inhibition of tumour progression and induction of $CD8^+$ T cell immunity. If we do indeed show that (dendritic) cell translocation from the gut mediates the LH663 mechanism, another key insight to gather would be definition of how LH663 EPS interacts with the DCs. We have shown that EPS exposure increases BMDC maturation *in vitro* through non-TLR2, TLR4 or TLR5 interactions, although we have not defined the specific receptors mediating the response. The most likely receptor family, we speculate, are the C-type lectin receptors (CLRs), which have been shown to recognise a wide array of bacterial and fungal exopolysaccharides(*602, 667*) and induce DC activation and maturation. Given the EPS produced by LH663 is dominated by glucose and galactose residues, it likely that the CLR responsible has a high affinity for these residues, such as the CLR DC-SIGN(*668*) or macrophage-galactose type lectin (MGL)(*669*). We would gain clues to this using reporter lines similar to the TLR lines, highlighting specific CLR activity in response to LH663. We would then seek to confirm the mechanistic relevance of our findings with an *in vivo* depletion experiment, perhaps using a knockout animal model or antibody-mediated functional block.

Compared with our *Bifidobacterium* and LH663 research, the OMV drug development work requires far more fundamental mechanistic characterisation. The bulk of the progress in this project was optimisation of OMV isolation, administration, and tumour model selection. We have shown concrete efficacy of our finalised treatment regime

against primary and metastatic tumours, although the *in vivo* mechanism of action remains unknown. Our *in vitro* experiments have shown both that OMVs do not directly impact tumour cell viability and are strongly immunogenic, although *in vivo* cytokine release in the primary tumour and serum does not indicate induction of anti-tumour immunity. Although the results of the *in vivo* cytokine arrays are certainly valid, they may not present the full picture. It may be possible, for example, that the strong immunogenic changes following OMV administration occur more transiently and rapidly than detectable from endpoint sample collection, which had not been exposed to OMVs for two days. An additional approach, then, would be to undertake *in vivo* immune profiling more rapidly following OMV administration, perhaps in sequential timepoints leading up to 24 hours. In addition to altered timing of sample collection, the immune profiling of OMV treated animals would need to be conducted to a similar depth as shown in our LH663 work. Alongside assessment of gross levels of cytokines within tissues, we would perform concurrent flow cytometry to assess immune cell infiltration, polarisation, and effector secretion (activation). These experiments would converge to identify immune cells and pathways of interest, which could be taken forward for downstream *ex vivo*/*in vitro* co-culture experiments with OMVs. More complete assessment of systemic tissues would also be a priority for future OMV work, as our OMV^{NLuc} tracking experiments demonstrated accumulation in other tumour relevant tissues such as the lungs and spleen. Mechanistically, the spleen and systemic lymph nodes are important pools of systemic immune cells, so would be assessed for potential immunological changes with high priority.

Translationally, there is also more research to be conducted to show whether OMV treatment may enhance response to standard of care. A combination of OMV therapy with αPD-1 immune checkpoint inhibitors would be particularly valuable, given these therapeutics are clinically approved for melanoma patients but experience a high proportion of non-responders(*533*). A key benefit of OMVs, alongside their enhanced safety compared to live bacteria, is their ability to be genetically and biophysically manipulated. New approaches emerging from OMV therapeutic research are using OMVs as drug delivery vectors to encapsulate cytotoxic cancer drugs(*636, 649*). This type of extension to our research could provide significant value, as chemotherapeutic drug bioavailability toward target tumour cells is a major cause of poor efficacy and severe side effects, whilst we have shown naïve OMVs to specifically accumulate in primary tumours and inhibit cancer progression. It is a possibility that encapsulating cytotoxic drugs within our OMVs may increase the risk of adverse side effects, so we would also explore alternative approaches with could be better tolerated, such as the

encapsulation of other immune stimulatory drugs (e.g., STING agonists) to further enhance tumour immunity. The fundamental workflow for generating these OMV-drug complexes has been explored previously(*649*), first involving encapsulation of the desired exogenous compound within lipid nanovesicles, which would then be coextruded through 0.22nm filters alongside the isolated Bt OMVs, with this processing allowing the formation of OMV-nanovesicle-drug complexes.

A final translational exercise which we would be interested in conducting would be a combination approach of using LH663 (or LH663 EPS) alongside OMV treatment. This could begin in B16F10 melanoma, given we have shown each of these therapies to work independently in the model, but could also be trialled in breast cancer (although we have not used IV administered OMVs in this context). Although these experiments would be combining two largely unrelated projects academically, the industrial and commercial need for more effective microbial drug candidates is significant. The prospect of translating these therapeutics into a clinical trial would become much greater if they could behave synergistically to inhibit tumour progression. If this was observed in future work, we could again return to a combination approach with standard of care immunotherapy. Given it is rare to see microbial therapeutics achieve more than a 50% pre-clinical tumour inhibition, it is perhaps likely that clinically approved therapeutics may rely on a combination of individually effective microbial therapeutics within one drug preparation, prescribed in combination with the most appropriate standard of care regime. A key consideration, however, would be the potential for stacking side effects, so markers for animal welfare would need to be closely monitored for such experiments.

8. Abbreviations

$A_{2A}R$: Adenosine 2A receptor
AA: Alditol acetates
ANI: Average nucleotide identity
AMP: Anti-microbial protein
APC: Antigen present cell
API: Active pharmaceutical ingredient
ARG1: Arginase 1
BDM: Bacteroides defined media
BEV: Bacterial extracellular vesicle
BHI: Brain heart infusion
Bif cocktail: *Bifidobacterium* cocktail
BMDC: Bone marrow-derived dendritic cell
BrCa: Breast cancer
Bt: *Bacteroides thetaiotaomicron*
CAF: Cancer-associated fibroblast
CAR: Chimeric antigen receptor
CAZymes: Carbohydrate-Active Enzymes
CDP: Common dendritic progenitor
cDCs: Convention dendritic cell
CFU: Colony forming unit
CLP: Common lymphoid progenitor
CLR: C-type lectin receptor
CMC: Chemistry, Manufacturing, and Controls
CMP: Common myeloid progenitor
CoA: Coenzyme A
CRC: Colorectal cancer
C-section: Caesarian section
CTLA-4: Cytotoxic T-lymphocyte-associated protein 4
CVD: Cardiovascular disease
CXCL: C-X-C motif chemokine ligand
CXCR: C-X-C motif chemokine receptor
DAMP: Damage associated molecular pattern
DC: Dendritic cell
DCIS: Ductal carcinoma in situ

ECM: Extracellular matrix

ER: Oestrogen receptor

EPS: Exopolysaccharide

EV: Extracellular vesicle

FAE: Follicle-associated epithelium

FFPE: Formaldehyde fixed paraffin embedded

FITC: Fluorescein isothiocyanate

FMT: Faecal microbiota transplant

FMO: Fluorescence minus one

FOXP3: Forkhead box protein P3

GABA: Glutamate into γ-amino butyric acid

GALT: Gut-associated lymphoid tissue

GC-MS: Gas chromatography mass spectrometry

GFP: Green fluorescent protein

GIT: Gastrointestinal tract

GM-CSF: Granulocyte-macrophage colony stimulating factor

G-MDSC: Granulocytic myeloid derived suppressor cell

GPCR: G-protein coupled receptor

GRAS: Generally recognised as safe

H&E: Haematoxylin & eosin

HER2: human epidermal growth factor receptor

HMO: Human milk oligosaccharide

HR: Hormone receptor

HSC: Haematopoietic stem cell

IBD: Inflammatory bowel disease

IBS: Irritable bowel syndrome

ICI: Immune checkpoint inhibitor

IDO: indoleamine 2, 3-dioxygenase

IFN: Interferon

Ig: Immunoglobulin

IL: Interleukin

ILA: Indole-3-lactic acid

iNOS: Inducible nitric oxide synthase

IP: Intraperitoneal

IV: Intravenous

LCIS: Lobular carcinoma in situ

LPS: Lipopolysaccharide

LTA: Lipoteichoic acid

LTA-BS: *B. subtilis* lipoteichoic acid

M-cells: Microfold cells

MAMP: Microbe-associated molecular pattern

MAPK: Mitogen-activated protein kinase

MAM: Metastasis-associated macrophage

MAMPC: Metastasis-associated macrophage precursor cell

MDSC: Myeloid-derived suppressor cell

MHC: Major histocompatibility complex

MLN: Mesenteric lymph node

M-MDSC: Monocytic myeloid derived suppressor cell

MMP: Matrix metalloproteinase

MRS: Man Rogosa Sharpe

NEC: Necrotising enterocolitis

NF-κB: Nuclear factor kappa-light-chain-enhancer of activated B cells

NK: Natural killer (cell)

NKG2D: NK cell activating receptor

NMR: Nuclear magnetic resonance

NO: Nitric oxide

NOD: Nucleotide-binding oligomerization domain-containing protein

NSCLC: Non-small cell lung cancer

OMV: Outer membrane vesicle

PAMP: Pathogen associated molecular pattern

PBMC: Peripheral blood mononuclear cell

PBS: Phosphate-buffered saline

PCR: Polymerase chain reaction

PD-1: Programmed death receptor

PDGF: Platelet-derived growth factor

PD-L1: Programmed death receptor ligand

PD: Parkinson's disease

PG: Peptidoglycan

PGRP: peptidoglycan recognition protein

PI: Propidium iodide

PMAA: Partially methylated alditol acetate

PP: Peyer's patch

PR: Progesterone receptor

PRR: Pattern recognition receptor

PSA: Polysaccharide A

recFLA-ST: Recombinant flagellin *Salmonella typhimurium*

ROS: Reactive oxygen species

SCFA: Short chain fatty acid

SED: Sub-epithelial dome

Siglec: Immunoglobulin-type lectin

SNPs: Single nucleotide polymorphisms

TAA: Tumour-associated antigen

TAM: Tumour-associated macrophage

TAD: Tight-adherence (Pili)

Tcm: T central memory cells

TCR: T cell receptor

tdLN: Tumour-draining lymph node

Tem: T effector memory

TGFβ: Transforming growth factor beta

Th1: T helper 1 cell

Th2: T helper 2 cell

Th17: T helper 17 cell

TLR: Toil-like receptor

TMAO: Trimethylamine-N-oxide

TME: Tumour microenviroment

TNM: Tumour, Node, Metastasis

TRAIL: TNF-related apoptosis ligand

Treg: T regulatory cell

TSG: Tumour suppressor gene

TUNEL: Terminal deoxynucleotidyl transferase dUTP nick end labeling

VEGF: Vascular endothelial growth factor

VNMAA: Vancomycin, neomycin, metronidazole, amphotericin, and ampicillin

WHO: World health organisation

WTA: Wall teichoic acid

9. References

1. F. Bray, M. Laversanne, E. Weiderpass, I. Soerjomataram, The ever-increasing importance of cancer as a leading cause of premature death worldwide. *Cancer* **127**, 3029-3030 (2021).
2. H. Sung *et al.*, Global Cancer Statistics 2020: GLOBOCAN Estimates of Incidence and Mortality Worldwide for 36 Cancers in 185 Countries. *CA Cancer J Clin* **71**, 209-249 (2021).
3. S. Chen *et al.*, Estimates and Projections of the Global Economic Cost of 29 Cancers in 204 Countries and Territories From 2020 to 2050. *JAMA Oncol* **9**, 465-472 (2023).
4. D. Hanahan, R. A. Weinberg, The hallmarks of cancer. *Cell* **100**, 57-70 (2000).
5. D. Hanahan, R. A. Weinberg, Hallmarks of cancer: the next generation. *Cell* **144**, 646-674 (2011).
6. D. Hanahan, Hallmarks of Cancer: New Dimensions. *Cancer Discov* **12**, 31-46 (2022).
7. V. Beral, R. Peto, UK cancer survival statistics. *BMJ* **341**, c4112 (2010).
8. L. Wilkinson, T. Gathani, Understanding breast cancer as a global health concern. *Br J Radiol* **95**, 20211033 (2022).
9. C. Allemani *et al.*, Global surveillance of trends in cancer survival 2000-14 (CONCORD-3): analysis of individual records for 37 513 025 patients diagnosed with one of 18 cancers from 322 population-based registries in 71 countries. *Lancet* **391**, 1023-1075 (2018).
10. C. R. UK. (2023).
11. P. L. Welcsh, M. C. King, BRCA1 and BRCA2 and the genetics of breast and ovarian cancer. *Hum. Mol. Genet.* **10**, 705-713 (2001).
12. C. X. Deng, F. Scott, Role of the tumor suppressor gene Brca1 in genetic stability and mammary gland tumor formation. *Oncogene* **19**, 1059-1064 (2000).
13. P. J. Stephens *et al.*, The landscape of cancer genes and mutational processes in breast cancer. *Nature* **486**, 400-404 (2012).
14. E. S. McDonald, A. S. Clark, J. Tchou, P. Zhang, G. M. Freedman, Clinical Diagnosis and Management of Breast Cancer. *J Nucl Med* **57 Suppl 1**, 9s-16s (2016).
15. A. Taherian-Fard, S. Srihari, M. A. Ragan, Breast cancer classification: linking molecular mechanisms to disease prognosis. *Briefings in Bioinformatics* **16**, 461-474 (2014).
16. P. Clauser, M. A. Marino, P. A. Baltzer, M. Bazzocchi, C. Zuiani, Management of atypical lobular hyperplasia, atypical ductal hyperplasia, and lobular carcinoma in situ. *Expert Rev Anticancer Ther* **16**, 335-346 (2016).
17. F. Nakhlis, M. Morrow, Ductal carcinoma in situ. *Surg Clin North Am* **83**, 821-839 (2003).
18. M. Inoue *et al.*, Specific sites of metastases in invasive lobular carcinoma: a retrospective cohort study of metastatic breast cancer. *Breast Cancer* **24**, 667-672 (2017).
19. R. I. Somiari *et al.*, High-throughput proteomic analysis of human infiltrating ductal carcinoma of the breast. *Proteomics* **3**, 1863-1873 (2003).

20. C. M. Perou *et al.*, Molecular portraits of human breast tumours. *Nature* **406**, 747-752 (2000).
21. G. Bianchini *et al.*, Molecular anatomy of breast cancer stroma and its prognostic value in estrogen receptor-positive and -negative cancers. *J Clin Oncol* **28**, 4316-4323 (2010).
22. M. Ayers *et al.*, Gene expression profiles predict complete pathologic response to neoadjuvant paclitaxel and fluorouracil, doxorubicin, and cyclophosphamide chemotherapy in breast cancer. *J Clin Oncol* **22**, 2284-2293 (2004).
23. L. J. van 't Veer *et al.*, Gene expression profiling predicts clinical outcome of breast cancer. *Nature* **415**, 530-536 (2002).
24. J. S. Reis-Filho, L. Pusztai, Gene expression profiling in breast cancer: classification, prognostication, and prediction. *The Lancet* **378**, 1812-1823 (2011).
25. A. Prat *et al.*, Clinical implications of the intrinsic molecular subtypes of breast cancer. *The Breast* **24**, S26-S35 (2015).
26. K. Sato *et al.*, Prognostic significance of the progesterone receptor status in Ki67-high and -low Luminal B-like HER2-negative breast cancers. *Breast Cancer* **23**, 310-317 (2016).
27. L. T. Yao *et al.*, Neoadjuvant endocrine therapy: A potential strategy for ER-positive breast cancer. *World J Clin Cases* **7**, 1937-1953 (2019).
28. H. G. Russnes, O. C. Lingjærde, A.-L. Børresen-Dale, C. Caldas, Breast Cancer Molecular Stratification: From Intrinsic Subtypes to Integrative Clusters. *The American Journal of Pathology* **187**, 2152-2162 (2017).
29. M. M. Moasser, The oncogene HER2: its signaling and transforming functions and its role in human cancer pathogenesis. *Oncogene* **26**, 6469-6487 (2007).
30. A. Davoli, B. A. Hocevar, T. L. Brown, Progression and treatment of HER2-positive breast cancer. *Cancer Chemotherapy and Pharmacology* **65**, 611-623 (2010).
31. F. Schettini *et al.*, Hormone Receptor/Human Epidermal Growth Factor Receptor 2-positive breast cancer: Where we are now and where we are going. *Cancer Treatment Reviews* **46**, 20-26 (2016).
32. M. D. Valentin, S. D. da Silva, M. Privat, M. Alaoui-Jamali, Y.-J. Bignon, Molecular insights on basal-like breast cancer. *Breast Cancer Research and Treatment* **134**, 21-30 (2012).
33. H. Kuroda, F. Ishida, M. Nakai, K. Ohnisi, S. Itoyama, Basal cytokeratin expression in relation to biological factors in breast cancer. *Hum Pathol* **39**, 1744-1750 (2008).
34. E. A. Rakha *et al.*, Prognostic markers in triple-negative breast cancer. *Cancer* **109**, 25-32 (2007).
35. S. Alexandrou *et al.*, The Proliferative and Apoptotic Landscape of Basal-like Breast Cancer. *Int J Mol Sci* **20**, 667 (2019).
36. R. Ribeiro, M. J. Carvalho, J. Goncalves, J. N. Moreira, Immunotherapy in triple-negative breast cancer: Insights into tumor immune landscape and therapeutic opportunities. *Front Mol Biosci* **9**, 903065 (2022).
37. H. A. Wahba, H. A. El-Hadaad, Current approaches in treatment of triple-negative breast cancer. *Cancer Biol Med* **12**, 106-116 (2015).

38. T. A. Moo, R. Sanford, C. Dang, M. Morrow, Overview of Breast Cancer Therapy. *PET Clin* **13**, 339-354 (2018).
39. C. Denkert, C. Liedtke, A. Tutt, G. von Minckwitz, Molecular alterations in triple-negative breast cancer-the road to new treatment strategies. *Lancet* **389**, 2430-2442 (2017).
40. N. England. (2020).
41. S. A. McLaughlin, Surgical management of the breast: breast conservation therapy and mastectomy. *Surg Clin North Am* **93**, 411-428 (2013).
42. A. A. Onitilo, J. M. Engel, R. V. Stankowski, S. A. Doi, Survival Comparisons for Breast Conserving Surgery and Mastectomy Revisited: Community Experience and the Role of Radiation Therapy. *Clin Med Res* **13**, 65-73 (2015).
43. P. Cortazar *et al.*, Pathological complete response and long-term clinical benefit in breast cancer: the CTNeoBC pooled analysis. *Lancet* **384**, 164-172 (2014).
44. A. Downing, C. Twelves, D. Forman, G. Lawrence, M. S. Gilthorpe, Time to begin adjuvant chemotherapy and survival in breast cancer patients: a retrospective observational study using latent class analysis. *Breast J* **20**, 29-36 (2014).
45. E. B. C. T. C. G. E. E. a. bc.overview@ctsu.ox.ac.uk, E. B. C. T. C. G. (EBCTCG), Anthracycline-containing and taxane-containing chemotherapy for early-stage operable breast cancer: a patient-level meta-analysis of 100 000 women from 86 randomised trials. *Lancet* **401**, 1277-1292 (2023).
46. S. Jones *et al.*, Docetaxel With Cyclophosphamide Is Associated With an Overall Survival Benefit Compared With Doxorubicin and Cyclophosphamide: 7-Year Follow-Up of US Oncology Research Trial 9735. *J Clin Oncol* **27**, 1177-1183 (2009).
47. G. von Minckwitz *et al.*, Neoadjuvant carboplatin in patients with triple-negative and HER2-positive early breast cancer (GeparSixto; GBG 66): a randomised phase 2 trial. *Lancet Oncol* **15**, 747-756 (2014).
48. M. Ando *et al.*, Randomized phase II study of weekly paclitaxel with and without carboplatin followed by cyclophosphamide/epirubicin/5-fluorouracil as neoadjuvant chemotherapy for stage II/IIIA breast cancer without HER2 overexpression. *Breast Cancer Res Treat* **145**, 401-409 (2014).
49. W. M. Sikov *et al.*, Impact of the addition of carboplatin and/or bevacizumab to neoadjuvant once-per-week paclitaxel followed by dose-dense doxorubicin and cyclophosphamide on pathologic complete response rates in stage II to III triple-negative breast cancer: CALGB 40603 (Alliance). *J Clin Oncol* **33**, 13-21 (2015).
50. E. Alba *et al.*, A randomized phase II trial of platinum salts in basal-like breast cancer patients in the neoadjuvant setting. Results from the GEICAM/2006-03, multicenter study. *Breast Cancer Res Treat* **136**, 487-493 (2012).
51. R. Peto *et al.*, Comparisons between different polychemotherapy regimens for early breast cancer: meta-analyses of long-term outcome among 100,000 women in 123 randomised trials. *Lancet* **379**, 432-444 (2012).
52. C. Davies *et al.*, Relevance of breast cancer hormone receptors and other factors to the efficacy of adjuvant tamoxifen: patient-level meta-analysis of randomised trials. *Lancet* **378**, 771-784 (2011).
53. S. A. Nazarali, S. A. Narod, Tamoxifen for women at high risk of breast cancer. *Breast Cancer (Dove Med Press)* **6**, 29-36 (2014).

54. J. Blakemore, F. Naftolin, Aromatase: Contributions to Physiology and Disease in Women and Men. *Physiology (Bethesda)* **31**, 258-269 (2016).
55. P. E. Goss *et al.*, Randomized trial of letrozole following tamoxifen as extended adjuvant therapy in receptor-positive breast cancer: updated findings from NCIC CTG MA.17. *J Natl Cancer Inst* **97**, 1262-1271 (2005).
56. D. Cameron *et al.*, 11 years' follow-up of trastuzumab after adjuvant chemotherapy in HER2-positive early breast cancer: final analysis of the HERceptin Adjuvant (HERA) trial. *Lancet* **389**, 1195-1205 (2017).
57. G. von Minckwitz *et al.*, Adjuvant Pertuzumab and Trastuzumab in Early HER2-Positive Breast Cancer. *N Engl J Med* **377**, 122-131 (2017).
58. P. J. Medina, S. Goodin, Lapatinib: a dual inhibitor of human epidermal growth factor receptor tyrosine kinases. *Clin Ther* **30**, 1426-1447 (2008).
59. M. J. O'Connor, Targeting the DNA Damage Response in Cancer. *Mol Cell* **60**, 547-560 (2015).
60. C. S. Walsh, Two decades beyond BRCA1/2: Homologous recombination, hereditary cancer risk and a target for ovarian cancer therapy. *Gynecol Oncol* **137**, 343-350 (2015).
61. C. J. Lord, A. Ashworth, PARP inhibitors: Synthetic lethality in the clinic. *Science* **355**, 1152-1158 (2017).
62. M. E. Robson *et al.*, OlympiAD extended follow-up for overall survival and safety: Olaparib versus chemotherapy treatment of physician's choice in patients with a germline BRCA mutation and HER2-negative metastatic breast cancer. *Eur J Cancer* **184**, 39-47 (2023).
63. J. K. Litton *et al.*, Talazoparib in Patients with Advanced Breast Cancer and a Germline BRCA Mutation. *N Engl J Med* **379**, 753-763 (2018).
64. A. Grinshpun, S. M. Tolaney, H. J. Burstein, R. Jeselsohn, E. L. Mayer, The dilemma of selecting a first line CDK4/6 inhibitor for hormone receptor-positive/HER2-negative metastatic breast cancer. *NPJ Breast Cancer* **9**, 15 (2023).
65. V. Debien *et al.*, Immunotherapy in breast cancer: an overview of current strategies and perspectives. *NPJ Breast Cancer* **9**, 7 (2023).
66. P. Schmid *et al.*, Event-free Survival with Pembrolizumab in Early Triple-Negative Breast Cancer. *N Engl J Med* **386**, 556-567 (2022).
67. S. M. Tolaney *et al.*, Effect of Eribulin With or Without Pembrolizumab on Progression-Free Survival for Patients With Hormone Receptor-Positive, ERBB2-Negative Metastatic Breast Cancer: A Randomized Clinical Trial. *JAMA Oncol* **6**, 1598-1605 (2020).
68. B. Sikandar, M. A. Qureshi, S. Naseem, S. Khan, T. Mirza, Increased Tumour Infiltration of CD4+ and CD8+ T-Lymphocytes in Patients with Triple Negative Breast Cancer Suggests Susceptibility to Immune Therapy. *Asian Pac J Cancer Prev* **18**, 1827-1832 (2017).
69. N. C. I. (NCI). (2019).
70. C. Garbe, U. Leiter, Melanoma epidemiology and trends. *Clin Dermatol* **27**, 3-9 (2009).
71. J. Berk-Krauss, J. A. Stein, J. Weber, D. Polsky, A. C. Geller, New Systematic Therapies and Trends in Cutaneous Melanoma Deaths Among US Whites, 1986-2016. *Am J Public Health* **110**, 731-733 (2020).

72. E. Hodis *et al.*, A landscape of driver mutations in melanoma. *Cell* **150**, 251-263 (2012).
73. J. M. Mehnert, H. M. Kluger, Driver mutations in melanoma: lessons learned from bench-to-bedside studies. *Curr Oncol Rep* **14**, 449-457 (2012).
74. K. Eddy, R. Shah, S. Chen, Decoding Melanoma Development and Progression: Identification of Therapeutic Vulnerabilities. *Front Oncol* **10**, 626129 (2020).
75. R. A. Scolyer, G. V. Long, J. F. Thompson, Evolving concepts in melanoma classification and their relevance to multidisciplinary melanoma patient care. *Mol Oncol* **5**, 124-136 (2011).
76. W. E. Damsky, L. E. Rosenbaum, M. Bosenberg, Decoding melanoma metastasis. *Cancers (Basel)* **3**, 126-163 (2010).
77. C. Lee, F. Collichio, D. Ollila, S. Moschos, Historical review of melanoma treatment and outcomes. *Clin Dermatol* **31**, 141-147 (2013).
78. L. E. Davis, S. C. Shalin, A. J. Tackett, Current state of melanoma diagnosis and treatment. *Cancer Biol Ther* **20**, 1366-1379 (2019).
79. V. W. Rebecca, V. K. Sondak, K. S. Smalley, A brief history of melanoma: from mummies to mutations. *Melanoma Res* **22**, 114-122 (2012).
80. P. B. Chapman *et al.*, Improved survival with vemurafenib in melanoma with BRAF V600E mutation. *N Engl J Med* **364**, 2507-2516 (2011).
81. A. Hauschild *et al.*, Dabrafenib in BRAF-mutated metastatic melanoma: a multicentre, open-label, phase 3 randomised controlled trial. *Lancet* **380**, 358-365 (2012).
82. J. L. Manzano *et al.*, Resistant mechanisms to BRAF inhibitors in melanoma. *Ann Transl Med* **4**, 237 (2016).
83. I. Arozarena, C. Wellbrock, Overcoming resistance to BRAF inhibitors. *Ann Transl Med* **5**, 387 (2017).
84. F. S. Hodi *et al.*, Improved survival with ipilimumab in patients with metastatic melanoma. *N Engl J Med* **363**, 711-723 (2010).
85. C. Robert *et al.*, Nivolumab in previously untreated melanoma without BRAF mutation. *N Engl J Med* **372**, 320-330 (2015).
86. J. Schachter *et al.*, Pembrolizumab versus ipilimumab for advanced melanoma: final overall survival results of a multicentre, randomised, open-label phase 3 study (KEYNOTE-006). *Lancet* **390**, 1853-1862 (2017).
87. H. A. Tawbi *et al.*, Relatlimab and Nivolumab versus Nivolumab in Untreated Advanced Melanoma. *N Engl J Med* **386**, 24-34 (2022).
88. C. Fellner, Ipilimumab (yervoy) prolongs survival in advanced melanoma: serious side effects and a hefty price tag may limit its use. *P T* **37**, 503-530 (2012).
89. A. Botticelli *et al.*, The role of immune profile in predicting outcomes in cancer patients treated with immunotherapy. *Front Immunol* **13**, 974087 (2022).
90. D. G. DeNardo *et al.*, Leukocyte complexity predicts breast cancer survival and functionally regulates response to chemotherapy. *Cancer Discov* **1**, 54-67 (2011).
91. Y. Z. Zhang, Y. Y. Li, Inflammatory bowel disease: pathogenesis. *World J Gastroenterol* **20**, 91-99 (2014).
92. D. S. Vinay *et al.*, Immune evasion in cancer: Mechanistic basis and therapeutic strategies. *Semin Cancer Biol* **35 Suppl**, S185-S198 (2015).

93. L. Ferrucci, E. Fabbri, Inflammageing: chronic inflammation in ageing, cardiovascular disease, and frailty. *Nat Rev Cardiol* **15**, 505-522 (2018).
94. D. Li, M. Wu, Pattern recognition receptors in health and diseases. *Signal Transduct Target Ther* **6**, 291 (2021).
95. E. Hardy, H. Sarker, C. Fernandez-Patron, Could a Non-Cellular Molecular Interactome in the Blood Circulation Influence Pathogens' Infectivity? *Cells* **12**, (2023).
96. S. C. A. Nielsen, S. D. Boyd, Human adaptive immune receptor repertoire analysis-Past, present, and future. *Immunol Rev* **284**, 9-23 (2018).
97. J. S. Marshall, R. Warrington, W. Watson, H. L. Kim, An introduction to immunology and immunopathology. *Allergy Asthma Clin Immunol* **14**, 49 (2018).
98. N. D. Pennock *et al.*, T cell responses: naive to memory and everything in between. *Adv Physiol Educ* **37**, 273-283 (2013).
99. A. R. Sánchez-Paulete *et al.*, Antigen cross-presentation and T-cell cross-priming in cancer immunology and immunotherapy. *Ann Oncol* **28**, xii44-xii55 (2017).
100. L. Sun *et al.*, Innate-adaptive immunity interplay and redox regulation in immune response. *Redox Biol* **37**, 101759 (2020).
101. G. Altan-Bonnet, R. Mukherjee, Cytokine-mediated communication: a quantitative appraisal of immune complexity. *Nat Rev Immunol* **19**, 205-217 (2019).
102. D. Shevyrev, V. Tereshchenko, T. N. Berezina, S. Rybtsov, Hematopoietic Stem Cells and the Immune System in Development and Aging. *Int J Mol Sci* **24**, (2023).
103. H. Cheng, Z. Zheng, T. Cheng, New paradigms on hematopoietic stem cell differentiation. *Protein Cell* **11**, 34-44 (2020).
104. Y. Wang, J. Liu, P. D. Burrows, J. Y. Wang, B Cell Development and Maturation. *Adv Exp Med Biol* **1254**, 1-22 (2020).
105. F. Cichocki, B. Grzywacz, J. S. Miller, Human NK Cell Development: One Road or Many? *Front Immunol* **10**, 2078 (2019).
106. C. C. Winterbourn, A. J. Kettle, M. B. Hampton, Reactive Oxygen Species and Neutrophil Function. *Annu Rev Biochem* **85**, 765-792 (2016).
107. T. A. Wilgus, S. Roy, J. C. McDaniel, Neutrophils and Wound Repair: Positive Actions and Negative Reactions. *Adv Wound Care (New Rochelle)* **2**, 379-388 (2013).
108. K. Prame Kumar, A. J. Nicholls, C. H. Y. Wong, Partners in crime: neutrophils and monocytes/macrophages in inflammation and disease. *Cell Tissue Res* **371**, 551-565 (2018).
109. F. Ginhoux *et al.*, Fate mapping analysis reveals that adult microglia derive from primitive macrophages. *Science* **330**, 841-845 (2010).
110. G. Arango Duque, A. Descoteaux, Macrophage cytokines: involvement in immunity and infectious diseases. *Front Immunol* **5**, 491 (2014).
111. C. V. Jakubzick, G. J. Randolph, P. M. Henson, Monocyte differentiation and antigen-presenting functions. *Nat Rev Immunol* **17**, 349-362 (2017).
112. D. D. Metcalfe *et al.*, Biomarkers of the involvement of mast cells, basophils and eosinophils in asthma and allergic diseases. *World Allergy Organ J* **9**, 7 (2016).

113. D. J. Jackson, P. Akuthota, F. Roufosse, Eosinophils and eosinophilic immune dysfunction in health and disease. *Eur Respir Rev* **31**, (2022).
114. S. H. He, H. Y. Zhang, X. N. Zeng, D. Chen, P. C. Yang, Mast cells and basophils are essential for allergies: mechanisms of allergic inflammation and a proposed procedure for diagnosis. *Acta Pharmacol Sin* **34**, 1270-1283 (2013).
115. S. C. Eisenbarth, Dendritic cell subsets in T cell programming: location dictates function. *Nat Rev Immunol* **19**, 89-103 (2019).
116. A. Gardner, B. Ruffell, Dendritic Cells and Cancer Immunity. *Trends Immunol* **37**, 855-865 (2016).
117. M. Y. Zanna *et al.*, Review of Dendritic Cells, Their Role in Clinical Immunology, and Distribution in Various Animal Species. *Int J Mol Sci* **22**, (2021).
118. B. Reizis, Plasmacytoid Dendritic Cells: Development, Regulation, and Function. *Immunity* **50**, 37-50 (2019).
119. D. Schaue *et al.*, Radiation and inflammation. *Semin Radiat Oncol* **25**, 4-10 (2015).
120. M. J. Proctor *et al.*, A derived neutrophil to lymphocyte ratio predicts survival in patients with cancer. *Br J Cancer* **107**, 695-699 (2012).
121. R. Weber *et al.*, Myeloid-Derived Suppressor Cells Hinder the Anti-Cancer Activity of Immune Checkpoint Inhibitors. *Front Immunol* **9**, 1310 (2018).
122. R. Bai *et al.*, Mechanisms of Cancer Resistance to Immunotherapy. *Front Oncol* **10**, 1290 (2020).
123. M. Nahrendorf, F. K. Swirski, Abandoning M1/M2 for a Network Model of Macrophage Function. *Circ Res* **119**, 414-417 (2016).
124. P. J. Murray *et al.*, Macrophage activation and polarization: nomenclature and experimental guidelines. *Immunity* **41**, 14-20 (2014).
125. J. Xue *et al.*, Transcriptome-based network analysis reveals a spectrum model of human macrophage activation. *Immunity* **40**, 274-288 (2014).
126. Y. Pan, Y. Yu, X. Wang, T. Zhang, Tumor-Associated Macrophages in Tumor Immunity. *Front Immunol* **11**, 583084 (2020).
127. S. B. Willingham *et al.*, The CD47-signal regulatory protein alpha (SIRPa) interaction is a therapeutic target for human solid tumors. *Proc Natl Acad Sci U S A* **109**, 6662-6667 (2012).
128. S. Zanganeh *et al.*, Iron oxide nanoparticles inhibit tumour growth by inducing pro-inflammatory macrophage polarization in tumour tissues. *Nat Nanotechnol* **11**, 986-994 (2016).
129. A. Del Prete *et al.*, Dendritic cell subsets in cancer immunity and tumor antigen sensing. *Cell Mol Immunol* **20**, 432-447 (2023).
130. D. Dudziak *et al.*, Differential antigen processing by dendritic cell subsets in vivo. *Science* **315**, 107-111 (2007).
131. C. Fu, A. Jiang, Dendritic Cells and CD8 T Cell Immunity in Tumor Microenvironment. *Front Immunol* **9**, 3059 (2018).
132. E. W. Roberts *et al.*, Critical Role for CD103(+)/CD141(+) Dendritic Cells Bearing CCR7 for Tumor Antigen Trafficking and Priming of T Cell Immunity in Melanoma. *Cancer Cell* **30**, 324-336 (2016).
133. M. Thiel *et al.*, Efficiency of T-cell costimulation by CD80 and CD86 cross-linking correlates with calcium entry. *Immunology* **129**, 28-40 (2010).

134. K. E. Foreman, T. Wrone-Smith, A. E. Krueger, B. J. Nickoloff, Expression of costimulatory molecules CD80 and/or CD86 by a Kaposi's sarcoma tumor cell line induces differential T-cell activation and proliferation. *Clin Immunol* **91**, 345-353 (1999).
135. S. Iborra *et al.*, Optimal Generation of Tissue-Resident but Not Circulating Memory T Cells during Viral Infection Requires Crosspriming by DNGR-1. *Immunity* **45**, 847-860 (2016).
136. B. Ruffell *et al.*, Macrophage IL-10 blocks CD8+ T cell-dependent responses to chemotherapy by suppressing IL-12 expression in intratumoral dendritic cells. *Cancer Cell* **26**, 623-637 (2014).
137. M. Martínez-López, S. Iborra, R. Conde-Garrosa, D. Sancho, Batf3-dependent CD103+ dendritic cells are major producers of IL-12 that drive local Th1 immunity against Leishmania major infection in mice. *Eur J Immunol* **45**, 119-129 (2015).
138. M. L. Broz *et al.*, Dissecting the tumor myeloid compartment reveals rare activating antigen-presenting cells critical for T cell immunity. *Cancer Cell* **26**, 638-652 (2014).
139. M. Binnewies *et al.*, Unleashing Type-2 Dendritic Cells to Drive Protective Antitumor CD4. *Cell* **177**, 556-571.e516 (2019).
140. D. J. Theisen *et al.*, WDFY4 is required for cross-presentation in response to viral and tumor antigens. *Science* **362**, 694-699 (2018).
141. A. M. van der Leun, D. S. Thommen, T. N. Schumacher, CD8 + T cell states in human cancer: insights from single-cell analysis. *Nat Rev Cancer* **20**, 218-232 (2020).
142. J. C. Nolz, G. R. Starbeck-Miller, J. T. Harty, Naive, effector and memory CD8 T-cell trafficking: parallels and distinctions. *Immunotherapy* **3**, 1223-1233 (2011).
143. A. Ivetic, H. L. Hoskins Green, S. J. Hart, L-selectin: A Major Regulator of Leukocyte Adhesion, Migration and Signaling. *Front Immunol* **10**, 1068 (2019).
144. T. Samji, K. M. Khanna, Understanding memory CD8. *Immunol Lett* **185**, 32-39 (2017).
145. C. Gordy, Y. W. He, Endocytosis by target cells: an essential means for perforin- and granzyme-mediated killing. *Cell Mol Immunol* **9**, 5-6 (2012).
146. Q. Fu *et al.*, Structural Basis and Functional Role of Intramembrane Trimerization of the Fas/CD95 Death Receptor. *Mol Cell* **61**, 602-613 (2016).
147. A. Vermare, M. V. Guérin, E. Peranzoni, N. Bercovici, Dynamic CD8 + T Cell Cooperation with Macrophages and Monocytes for Successful Cancer Immunotherapy. *Cancers (Basel)* **14**, (2022).
148. W. Jiang *et al.*, Exhausted CD8+T Cells in the Tumor Immune Microenvironment: New Pathways to Therapy. *Front Immunol* **11**, 622509 (2020).
149. M. F. Krummel, J. P. Allison, CD28 and CTLA-4 have opposing effects on the response of T cells to stimulation. *J Exp Med* **182**, 459-465 (1995).
150. Y. Agata *et al.*, Expression of the PD-1 antigen on the surface of stimulated mouse T and B lymphocytes. *Int Immunol* **8**, 765-772 (1996).
151. Y. Iwai *et al.*, Involvement of PD-L1 on tumor cells in the escape from host immune system and tumor immunotherapy by PD-L1 blockade. *Proc Natl Acad Sci U S A* **99**, 12293-12297 (2002).

152. N. Joller, V. K. Kuchroo, Tim-3, Lag-3, and TIGIT. *Curr Top Microbiol Immunol* **410**, 127-156 (2017).
153. J. Saravia, N. M. Chapman, H. Chi, Helper T cell differentiation. *Cell Mol Immunol* **16**, 634-643 (2019).
154. R. E. Tay, E. K. Richardson, H. C. Toh, Revisiting the role of CD4 + T cells in cancer immunotherapy—new insights into old paradigms. *Cancer Gene Ther* **28**, 5-17 (2021).
155. J. Borst, T. Ahrends, N. Bąbała, C. J. M. Melief, W. Kastenmüller, CD4 (+) T cell help in cancer immunology and immunotherapy. *Nat Rev Immunol* **18**, 635-647 (2018).
156. C. M. Smith *et al.*, Cognate CD4(+) T cell licensing of dendritic cells in CD8(+) T cell immunity. *Nat Immunol* **5**, 1143-1148 (2004).
157. C. M. Reed, N. D. Cresce, I. S. Mauldin, C. L. Slingluff, W. C. Olson, Vaccination with Melanoma Helper Peptides Induces Antibody Responses Associated with Improved Overall Survival. *Clin Cancer Res* **21**, 3879-3887 (2015).
158. S. Gnjatic *et al.*, Survey of naturally occurring CD4+ T cell responses against NY-ESO-1 in cancer patients: correlation with antibody responses. *Proc Natl Acad Sci U S A* **100**, 8862-8867 (2003).
159. R. Kennedy, E. Celis, Multiple roles for CD4+ T cells in anti-tumor immune responses. *Immunol Rev* **222**, 129-144 (2008).
160. A. Basu *et al.*, Differentiation and Regulation of T H Cells: A Balancing Act for Cancer Immunotherapy. *Front Immunol* **12**, 669474 (2021).
161. K. Chen, J. K. Kolls, Interluekin-17A (IL17A). *Gene* **614**, 8-14 (2017).
162. C. Fu *et al.*, Activation of the IL-4/STAT6 Signaling Pathway Promotes Lung Cancer Progression by Increasing M2 Myeloid Cells. *Front Immunol* **10**, 2638 (2019).
163. C. C. Hong *et al.*, Pretreatment levels of circulating Th1 and Th2 cytokines, and their ratios, are associated with ER-negative and triple negative breast cancers. *Breast Cancer Res Treat* **139**, 477-488 (2013).
164. M. Liu *et al.*, TGF-β suppresses type 2 immunity to cancer. *Nature* **587**, 115-120 (2020).
165. J. Lee *et al.*, An Antibody Designed to Improve Adoptive NK-Cell Therapy Inhibits Pancreatic Cancer Progression in a Murine Model. *Cancer Immunol Res* **7**, 219-229 (2019).
166. A. R. Mistry, C. A. O'Callaghan, Regulation of ligands for the activating receptor NKG2D. *Immunology* **121**, 439-447 (2007).
167. L. Moretta *et al.*, Human NK cells and their receptors. *Microbes Infect* **4**, 1539-1544 (2002).
168. O. Mandelboim *et al.*, Recognition of haemagglutinins on virus-infected cells by NKp46 activates lysis by human NK cells. *Nature* **409**, 1055-1060 (2001).
169. G. Habif, A. Crinier, P. André, E. Vivier, E. Narni-Mancinelli, Targeting natural killer cells in solid tumors. *Cell Mol Immunol* **16**, 415-422 (2019).
170. A. Martín-Fontecha *et al.*, Induced recruitment of NK cells to lymph nodes provides IFN-gamma for T(H)1 priming. *Nat Immunol* **5**, 1260-1265 (2004).
171. E. Vivier *et al.*, Innate or adaptive immunity? The example of natural killer cells. *Science* **331**, 44-49 (2011).

172. A. Muntasell *et al.*, NK Cell Infiltrates and HLA Class I Expression in Primary HER2. *Clin Cancer Res* **25**, 1535-1545 (2019).
173. J. Eckl *et al.*, Transcript signature predicts tissue NK cell content and defines renal cell carcinoma subgroups independent of TNM staging. *J Mol Med (Berl)* **90**, 55-66 (2012).
174. S. P. Schantz, N. G. Ordonez, Quantitation of natural killer cell function and risk of metastatic poorly differentiated head and neck cancer. *Nat Immun Cell Growth Regul* **10**, 278-288 (1991).
175. S. Nagaraj, D. I. Gabrilovich, Regulation of suppressive function of myeloid-derived suppressor cells by CD4+ T cells. *Semin Cancer Biol* **22**, 282-288 (2012).
176. V. Bronte *et al.*, Recommendations for myeloid-derived suppressor cell nomenclature and characterization standards. *Nat Commun* **7**, 12150 (2016).
177. F. Veglia, M. Perego, D. Gabrilovich, Myeloid-derived suppressor cells coming of age. *Nat Immunol* **19**, 108-119 (2018).
178. F. Veglia, E. Sanseviero, D. I. Gabrilovich, Myeloid-derived suppressor cells in the era of increasing myeloid cell diversity. *Nat Rev Immunol* **21**, 485-498 (2021).
179. Z. Wang *et al.*, A myeloid cell population induced by Freund adjuvant suppresses T-cell-mediated antitumor immunity. *J Immunother* **33**, 167-177 (2010).
180. J. Markowitz *et al.*, Nitric oxide mediated inhibition of antigen presentation from DCs to CD4. *Sci Rep* **7**, 15424 (2017).
181. S. Nagaraj *et al.*, Altered recognition of antigen is a mechanism of CD8+ T cell tolerance in cancer. *Nat Med* **13**, 828-835 (2007).
182. P. C. Rodríguez, A. C. Ochoa, Arginine regulation by myeloid derived suppressor cells and tolerance in cancer: mechanisms and therapeutic perspectives. *Immunol Rev* **222**, 180-191 (2008).
183. E. M. Hanson, V. K. Clements, P. Sinha, D. Ilkovitch, S. Ostrand-Rosenberg, Myeloid-derived suppressor cells down-regulate L-selectin expression on CD4+ and CD8+ T cells. *J Immunol* **183**, 937-944 (2009).
184. C. Lu, P. S. Redd, J. R. Lee, N. Savage, K. Liu, The expression profiles and regulation of PD-L1 in tumor-induced myeloid-derived suppressor cells. *Oncoimmunology* **5**, e1247135 (2016).
185. T. Iwata *et al.*, PD-L1(+)MDSCs are increased in HCC patients and induced by soluble factor in the tumor microenvironment. *Sci Rep* **6**, 39296 (2016).
186. Y. Pico de Coaña *et al.*, Ipilimumab treatment results in an early decrease in the frequency of circulating granulocytic myeloid-derived suppressor cells as well as their Arginase1 production. *Cancer Immunol Res* **1**, 158-162 (2013).
187. Y. Yang, C. Li, T. Liu, X. Dai, A. V. Bazhin, Myeloid-Derived Suppressor Cells in Tumors: From Mechanisms to Antigen Specificity and Microenvironmental Regulation. *Front Immunol* **11**, 1371 (2020).
188. F. Ghiringhelli *et al.*, Tumor cells convert immature myeloid dendritic cells into TGF-beta-secreting cells inducing CD4+CD25+ regulatory T cell proliferation. *J Exp Med* **202**, 919-929 (2005).
189. B. Huang *et al.*, Gr-1+CD115+ immature myeloid suppressor cells mediate the development of tumor-induced T regulatory cells and T-cell anergy in tumor-bearing host. *Cancer Res* **66**, 1123-1131 (2006).

190. P. Y. Pan *et al.*, Immune stimulatory receptor CD40 is required for T-cell suppression and T regulatory cell activation mediated by myeloid-derived suppressor cells in cancer. *Cancer Res* **70**, 99-108 (2010).
191. A. Stiff *et al.*, Nitric Oxide Production by Myeloid-Derived Suppressor Cells Plays a Role in Impairing Fc Receptor-Mediated Natural Killer Cell Function. *Clin Cancer Res* **24**, 1891-1904 (2018).
192. H. Li, Y. Han, Q. Guo, M. Zhang, X. Cao, Cancer-expanded myeloid-derived suppressor cells induce anergy of NK cells through membrane-bound TGF-beta 1. *J Immunol* **182**, 240-249 (2009).
193. E. Limagne *et al.*, Accumulation of MDSC and Th17 Cells in Patients with Metastatic Colorectal Cancer Predicts the Efficacy of a FOLFOX-Bevacizumab Drug Treatment Regimen. *Cancer Res* **76**, 5241-5252 (2016).
194. Y. Sato *et al.*, Characterization of the myeloid-derived suppressor cell subset regulated by NK cells in malignant lymphoma. *Oncoimmunology* **4**, e995541 (2015).
195. M. K. Brimnes *et al.*, Increased level of both CD4+FOXP3+ regulatory T cells and CD14+HLA-DR^{-}/low myeloid-derived suppressor cells and decreased level of dendritic cells in patients with multiple myeloma. *Scand J Immunol* **72**, 540-547 (2010).
196. P. Cheng *et al.*, Inhibition of dendritic cell differentiation and accumulation of myeloid-derived suppressor cells in cancer is regulated by S100A9 protein. *J Exp Med* **205**, 2235-2249 (2008).
197. J. Liu, X. Geng, J. Hou, G. Wu, New insights into M1/M2 macrophages: key modulators in cancer progression. *Cancer Cell Int* **21**, 389 (2021).
198. J. S. Byun, K. Gardner, Wounds that will not heal: pervasive cellular reprogramming in cancer. *Am J Pathol* **182**, 1055-1064 (2013).
199. M. Yin *et al.*, Tumor-associated macrophages drive spheroid formation during early transcoelomic metastasis of ovarian cancer. *J Clin Invest* **126**, 4157-4173 (2016).
200. M. Egawa *et al.*, Inflammatory monocytes recruited to allergic skin acquire an anti-inflammatory M2 phenotype via basophil-derived interleukin-4. *Immunity* **38**, 570-580 (2013).
201. L. A. Lievense *et al.*, Pleural Effusion of Patients with Malignant Mesothelioma Induces Macrophage-Mediated T Cell Suppression. *J Thorac Oncol* **11**, 1755-1764 (2016).
202. Y. Xu *et al.*, Immunosuppressive tumor-associated macrophages expressing interlukin-10 conferred poor prognosis and therapeutic vulnerability in patients with muscle-invasive bladder cancer. *J Immunother Cancer* **10**, (2022).
203. D. W. Beury *et al.*, Cross-talk among myeloid-derived suppressor cells, macrophages, and tumor cells impacts the inflammatory milieu of solid tumors. *J Leukoc Biol* **96**, 1109-1118 (2014).
204. K. Movahedi *et al.*, Different tumor microenvironments contain functionally distinct subsets of macrophages derived from Ly6C(high) monocytes. *Cancer Res* **70**, 5728-5739 (2010).
205. Y. Togashi, K. Shitara, H. Nishikawa, Regulatory T cells in cancer immunosuppression - implications for anticancer therapy. *Nat Rev Clin Oncol* **16**, 356-371 (2019).

206. G. Hu, Z. Liu, C. Zheng, S. G. Zheng, Antigen-non-specific regulation centered on CD25+Foxp3+ Treg cells. *Cell Mol Immunol* **7**, 414-418 (2010).
207. H. Nishikawa *et al.*, CD4+ CD25+ T cells responding to serologically defined autoantigens suppress antitumor immune responses. *Proc Natl Acad Sci U S A* **100**, 10902-10906 (2003).
208. K. Kurose *et al.*, Increase in activated Treg in TIL in lung cancer and in vitro depletion of Treg by ADCC using an antihuman CCR4 mAb (KM2760). *J Thorac Oncol* **10**, 74-83 (2015).
209. W. H. Fridman, F. Pagès, C. Sautès-Fridman, J. Galon, The immune contexture in human tumours: impact on clinical outcome. *Nat Rev Cancer* **12**, 298-306 (2012).
210. C. Li, P. Jiang, S. Wei, X. Xu, J. Wang, Regulatory T cells in tumor microenvironment: new mechanisms, potential therapeutic strategies and future prospects. *Mol Cancer* **19**, 116 (2020).
211. Y. Ohue, H. Nishikawa, Regulatory T (Treg) cells in cancer: Can Treg cells be a new therapeutic target? *Cancer Sci* **110**, 2080-2089 (2019).
212. T. Takahashi *et al.*, Immunologic self-tolerance maintained by CD25+CD4+ naturally anergic and suppressive T cells: induction of autoimmune disease by breaking their anergic/suppressive state. *Int Immunol* **10**, 1969-1980 (1998).
213. X. Cao *et al.*, Granzyme B and perforin are important for regulatory T cell-mediated suppression of tumor clearance. *Immunity* **27**, 635-646 (2007).
214. L. S. Walker, D. M. Sansom, The emerging role of CTLA4 as a cell-extrinsic regulator of T cell responses. *Nat Rev Immunol* **11**, 852-863 (2011).
215. O. S. Qureshi *et al.*, Trans-endocytosis of CD80 and CD86: a molecular basis for the cell-extrinsic function of CTLA-4. *Science* **332**, 600-603 (2011).
216. Y. Maeda *et al.*, Detection of self-reactive $CD8^+$ T cells with an anergic phenotype in healthy individuals. *Science* **346**, 1536-1540 (2014).
217. A. L. Mellor, D. H. Munn, IDO expression by dendritic cells: tolerance and tryptophan catabolism. *Nat Rev Immunol* **4**, 762-774 (2004).
218. K. E. de Visser, J. A. Joyce, The evolving tumor microenvironment: From cancer initiation to metastatic outgrowth. *Cancer Cell* **41**, 374-403 (2023).
219. Y. Jiang, Y. Li, B. Zhu, T-cell exhaustion in the tumor microenvironment. *Cell Death Dis* **6**, e1792 (2015).
220. C. Dobie, D. Skropeta, Insights into the role of sialylation in cancer progression and metastasis. *Br J Cancer* **124**, 76-90 (2021).
221. R. Beatson *et al.*, The mucin MUC1 modulates the tumor immunological microenvironment through engagement of the lectin Siglec-9. *Nat Immunol* **17**, 1273-1281 (2016).
222. J. E. Hudak, S. M. Canham, C. R. Bertozzi, Glycocalyx engineering reveals a Siglec-based mechanism for NK cell immunoevasion. *Nat Chem Biol* **10**, 69-75 (2014).
223. A. J. Petty *et al.*, Hedgehog signaling promotes tumor-associated macrophage polarization to suppress intratumoral CD8+ T cell recruitment. *J Clin Invest* **129**, 5151-5162 (2019).
224. M. C. Takenaka *et al.*, Control of tumor-associated macrophages and T cells in glioblastoma via AHR and CD39. *Nat Neurosci* **22**, 729-740 (2019).

225. Y. Zhu *et al.*, Disruption of tumour-associated macrophage trafficking by the osteopontin-induced colony-stimulating factor-1 signalling sensitises hepatocellular carcinoma to anti-PD-L1 blockade. *Gut* **68**, 1653-1666 (2019).
226. D. A. Thomas, J. Massagué, TGF-beta directly targets cytotoxic T cell functions during tumor evasion of immune surveillance. *Cancer Cell* **8**, 369-380 (2005).
227. R. Khazen *et al.*, Melanoma cell lysosome secretory burst neutralizes the CTL-mediated cytotoxicity at the lytic synapse. *Nat Commun* **7**, 10823 (2016).
228. S. Lucotti, C. M. Kenific, H. Zhang, D. Lyden, Extracellular vesicles and particles impact the systemic landscape of cancer. *EMBO J* **41**, e109288 (2022).
229. H. Peinado *et al.*, Melanoma exosomes educate bone marrow progenitor cells toward a pro-metastatic phenotype through MET. *Nat Med* **18**, 883-891 (2012).
230. N. M. Anderson, M. C. Simon, The tumor microenvironment. *Curr Biol* **30**, R921-R925 (2020).
231. R. L. Barrett, E. Puré, Cancer-associated fibroblasts and their influence on tumor immunity and immunotherapy. *Elife* **9**, (2020).
232. Y. Deng *et al.*, Hepatic carcinoma-associated fibroblasts enhance immune suppression by facilitating the generation of myeloid-derived suppressor cells. *Oncogene* **36**, 1090-1101 (2017).
233. J. T. Cheng *et al.*, Hepatic carcinoma-associated fibroblasts induce IDO-producing regulatory dendritic cells through IL-6-mediated STAT3 activation. *Oncogenesis* **5**, e198 (2016).
234. T. Kato *et al.*, Cancer-Associated Fibroblasts Affect Intratumoral CD8 + and FoxP3 + T Cells Via IL6 in the Tumor Microenvironment. *Clin Cancer Res* **24**, 4820-4833 (2018).
235. M. A. Lakins, E. Ghorani, H. Munir, C. P. Martins, J. D. Shields, Cancer-associated fibroblasts induce antigen-specific deletion of CD8. *Nat Commun* **9**, 948 (2018).
236. M. R. Nazareth *et al.*, Characterization of human lung tumor-associated fibroblasts and their ability to modulate the activation of tumor-associated T cells. *J Immunol* **178**, 5552-5562 (2007).
237. I. V. Pinchuk *et al.*, PD-1 ligand expression by human colonic myofibroblasts/fibroblasts regulates CD4+ T-cell activity. *Gastroenterology* **135**, 1228-1237, 1237.e1221-1222 (2008).
238. K. Ford *et al.*, NOX4 Inhibition Potentiates Immunotherapy by Overcoming Cancer-Associated Fibroblast-Mediated CD8 T-cell Exclusion from Tumors. *Cancer Res* **80**, 1846-1860 (2020).
239. S. S. Said, W. N. Ibrahim, Cancer Resistance to Immunotherapy: Comprehensive Insights with Future Perspectives. *Pharmaceutics* **15**, (2023).
240. P. A. Ott *et al.*, An immunogenic personal neoantigen vaccine for patients with melanoma. *Nature* **547**, 217-221 (2017).
241. Z. M. Herrera, T. C. Ramos, Pilot study of a novel combination of two therapeutic vaccines in advanced non-small-cell lung cancer patients. *Cancer Immunol Immunother* **63**, 737-747 (2014).
242. J. Raja, J. M. Ludwig, S. N. Gettinger, K. A. Schalper, H. S. Kim, Oncolytic virus immunotherapy: future prospects for oncology. *J Immunother Cancer* **6**, 140 (2018).

243. Y. Zhang, Z. Zhang, The history and advances in cancer immunotherapy: understanding the characteristics of tumor-infiltrating immune cells and their therapeutic implications. *Cell Mol Immunol* **17**, 807-821 (2020).
244. G. Wei *et al.*, Emerging immune checkpoints in the tumor microenvironment: Implications for cancer immunotherapy. *Cancer Lett* **511**, 68-76 (2021).
245. J. Larkin *et al.*, Combined Nivolumab and Ipilimumab or Monotherapy in Untreated Melanoma. *N Engl J Med* **373**, 23-34 (2015).
246. J. D. Twomey, B. Zhang, Cancer Immunotherapy Update: FDA-Approved Checkpoint Inhibitors and Companion Diagnostics. *AAPS J* **23**, 39 (2021).
247. T. N. Gide *et al.*, Distinct Immune Cell Populations Define Response to Anti-PD-1 Monotherapy and Anti-PD-1/Anti-CTLA-4 Combined Therapy. *Cancer Cell* **35**, 238-255.e236 (2019).
248. C. Robert *et al.*, Pembrolizumab versus ipilimumab in advanced melanoma (KEYNOTE-006): post-hoc 5-year results from an open-label, multicentre, randomised, controlled, phase 3 study. *Lancet Oncol* **20**, 1239-1251 (2019).
249. M. Łuksza *et al.*, A neoantigen fitness model predicts tumour response to checkpoint blockade immunotherapy. *Nature* **551**, 517-520 (2017).
250. T. J. de Vries *et al.*, Heterogeneous expression of immunotherapy candidate proteins gp100, MART-1, and tyrosinase in human melanoma cell lines and in human melanocytic lesions. *Cancer Res* **57**, 3223-3229 (1997).
251. J. D. Possick, Pulmonary Toxicities from Checkpoint Immunotherapy for Malignancy. *Clin Chest Med* **38**, 223-232 (2017).
252. C. H. Chang *et al.*, Metabolic Competition in the Tumor Microenvironment Is a Driver of Cancer Progression. *Cell* **162**, 1229-1241 (2015).
253. W. J. Murphy, D. L. Longo, The Surprisingly Positive Association Between Obesity and Cancer Immunotherapy Efficacy. *JAMA* **321**, 1247-1248 (2019).
254. J. M. Pitt *et al.*, Resistance Mechanisms to Immune-Checkpoint Blockade in Cancer: Tumor-Intrinsic and -Extrinsic Factors. *Immunity* **44**, 1255-1269 (2016).
255. C. Liu, M. Yang, D. Zhang, M. Chen, D. Zhu, Clinical cancer immunotherapy: Current progress and prospects. *Front Immunol* **13**, 961805 (2022).
256. S. A. Rosenberg *et al.*, Observations on the systemic administration of autologous lymphokine-activated killer cells and recombinant interleukin-2 to patients with metastatic cancer. *N Engl J Med* **313**, 1485-1492 (1985).
257. L. Zhao, Y. J. Cao, Engineered T Cell Therapy for Cancer in the Clinic. *Front Immunol* **10**, 2250 (2019).
258. M. V. Maus, C. H. June, Making Better Chimeric Antigen Receptors for Adoptive T-cell Therapy. *Clin Cancer Res* **22**, 1875-1884 (2016).
259. S. Vairy, J. L. Garcia, P. Teira, H. Bittencourt, CTL019 (tisagenlecleucel): CAR-T therapy for relapsed and refractory B-cell acute lymphoblastic leukemia. *Drug Des Devel Ther* **12**, 3885-3898 (2018).
260. Y. Ping, C. Liu, Y. Zhang, T-cell receptor-engineered T cells for cancer treatment: current status and future directions. *Protein Cell* **9**, 254-266 (2018).
261. F. Fang, W. Wang, M. Chen, Z. Tian, W. Xiao, Technical advances in NK cell-based cellular immunotherapy. *Cancer Biol Med* **16**, 647-654 (2019).
262. E. Liu *et al.*, Use of CAR-Transduced Natural Killer Cells in CD19-Positive Lymphoid Tumors. *N Engl J Med* **382**, 545-553 (2020).

263. S. R. Gill *et al.*, Metagenomic analysis of the human distal gut microbiome. *Science* **312**, 1355-1359 (2006).
264. R. Sender, S. Fuchs, R. Milo, Revised Estimates for the Number of Human and Bacteria Cells in the Body. *PLoS Biol.* **14**, e1002533 (2016).
265. S. Carding, K. Verbeke, D. T. Vipond, B. M. Corfe, L. J. Owen, Dysbiosis of the gut microbiota in disease. *Microb. Ecol. Health Dis.* **26**, 26191 (2015).
266. J. Durack, S. V. Lynch, The gut microbiome: Relationships with disease and opportunities for therapy. *J. Exp. Med.* **216**, 20-40 (2019).
267. M. Arumugam *et al.*, Enterotypes of the human gut microbiome. *Nature* **473**, 174-180 (2011).
268. E. Rinninella *et al.*, What is the Healthy Gut Microbiota Composition? A Changing Ecosystem across Age, Environment, Diet, and Diseases. *Microorganisms* **7**, 14 (2019).
269. H. J. Flint, K. P. Scott, P. Louis, S. H. Duncan, The role of the gut microbiota in nutrition and health. *Nature Reviews Gastroenterology & Hepatology* **9**, 577-589 (2012).
270. M. J. Butel, A. J. Waligora-Dupriet, S. Wydau-Dematteis, The developing gut microbiota and its consequences for health. *J Dev Orig Health Dis* **9**, 590-597 (2018).
271. S. Arboleya *et al.*, Establishment and development of intestinal microbiota in preterm neonates. *FEMS Microbiol. Ecol.* **79**, 763-772 (2012).
272. D. A. Sela, D. A. Mills, Nursing our microbiota: molecular linkages between bifidobacteria and milk oligosaccharides. *Trends Microbiol.* **18**, 298-307 (2010).
273. T. Jost, C. Lacroix, C. Braegger, C. Chassard, Impact of human milk bacteria and oligosaccharides on neonatal gut microbiota establishment and gut health. *Nutr. Rev.* **73**, 426-437 (2015).
274. C. Palmer, E. M. Bik, D. B. DiGiulio, D. A. Relman, P. O. Brown, Development of the human infant intestinal microbiota. *PLoS Biol.* **5**, e177 (2007).
275. M. Fallani *et al.*, Determinants of the human infant intestinal microbiota after the introduction of first complementary foods in infant samples from five European centres. *Microbiology* **157**, 1385-1392 (2011).
276. L. Zhuang *et al.*, Intestinal Microbiota in Early Life and Its Implications on Childhood Health. *Genomics Proteomics Bioinformatics* **17**, 13-25 (2019).
277. E. Rackaityte *et al.*, Viable bacterial colonization is highly limited in the human intestine in utero. *Nat Med* **26**, 599-607 (2020).
278. N. Li *et al.*, Memory CD4(+) T cells are generated in the human fetal intestine. *Nat Immunol* **20**, 301-312 (2019).
279. K. Aagaard *et al.*, The placenta harbors a unique microbiome. *Sci Transl Med* **6**, 237ra265 (2014).
280. M. C. Collado, S. Rautava, J. Aakko, E. Isolauri, S. Salminen, Human gut colonisation may be initiated in utero by distinct microbial communities in the placenta and amniotic fluid. *Sci Rep* **6**, 23129 (2016).
281. M. E. Perez-Muñoz, M. C. Arrieta, A. E. Ramer-Tait, J. Walter, A critical assessment of the "sterile womb" and "in utero colonization" hypotheses: implications for research on the pioneer infant microbiome. *Microbiome* **5**, 48 (2017).

282. J. S. Leiby *et al.*, Lack of detection of a human placenta microbiome in samples from preterm and term deliveries. *Microbiome* **6**, 196 (2018).
283. K. M. Kennedy *et al.*, Questioning the fetal microbiome illustrates pitfalls of low-biomass microbial studies. *Nature* **613**, 639-649 (2023).
284. Y. Shao *et al.*, Stunted microbiota and opportunistic pathogen colonization in caesarean-section birth. *Nature* **574**, 117-121 (2019).
285. M. A. Koch *et al.*, Maternal IgG and IgA Antibodies Dampen Mucosal T Helper Cell Responses in Early Life. *Cell* **165**, 827-841 (2016).
286. W. Zheng *et al.*, Microbiota-targeted maternal antibodies protect neonates from enteric infection. *Nature* **577**, 543-548 (2020).
287. T. Vatanen *et al.*, Genomic variation and strain-specific functional adaptation in the human gut microbiome during early life. *Nat Microbiol* **4**, 470-479 (2019).
288. R. Verma *et al.*, Cell surface polysaccharides of Bifidobacterium bifidum induce the generation of Foxp3+ regulatory T cells. *Sci Immunol* **3**, (2018).
289. B. M. Henrick *et al.*, Bifidobacteria-mediated immune system imprinting early in life. *Cell* **184**, 3884-3898.e3811 (2021).
290. J. H. Niess, G. Adler, Enteric flora expands gut lamina propria CX3CR1+ dendritic cells supporting inflammatory immune responses under normal and inflammatory conditions. *J Immunol* **184**, 2026-2037 (2010).
291. H. H. Smits *et al.*, Selective probiotic bacteria induce IL-10-producing regulatory T cells in vitro by modulating dendritic cell function through dendritic cell-specific intercellular adhesion molecule 3-grabbing nonintegrin. *J Allergy Clin Immunol* **115**, 1260-1267 (2005).
292. Y. Belkaid, T. W. Hand, Role of the microbiota in immunity and inflammation. *Cell* **157**, 121-141 (2014).
293. P. Calder, Feeding the immune system. *The Proceedings of the Nutrition Society* **72**, 1-11 (2013).
294. C. Jung, J. P. Hugot, F. Barreau, Peyer's Patches: The Immune Sensors of the Intestine. *Int J Inflam* **2010**, 823710 (2010).
295. C. Da Silva, C. Wagner, J. Bonnardel, J. P. Gorvel, H. Lelouard, The Peyer's Patch Mononuclear Phagocyte System at Steady State and during Infection. *Front Immunol* **8**, 1254 (2017).
296. A. Habtezion, L. P. Nguyen, H. Hadeiba, E. C. Butcher, Leukocyte Trafficking to the Small Intestine and Colon. *Gastroenterology* **150**, 340-354 (2016).
297. M. Buettner, U. Bode, Lymph node dissection--understanding the immunological function of lymph nodes. *Clin. Exp. Immunol.* **169**, 205-212 (2012).
298. C. Chassard, C. Lacroix, Carbohydrates and the human gut microbiota. *Current Opinion in Clinical Nutrition & Metabolic Care* **16**, 453-460 (2013).
299. A. Pingitore *et al.*, The diet-derived short chain fatty acid propionate improves beta-cell function in humans and stimulates insulin secretion from human islets in vitro. *Diabetes Obes Metab* **19**, 257-265 (2017).
300. L. Zhao *et al.*, Gut bacteria selectively promoted by dietary fibers alleviate type 2 diabetes. *Science* **359**, 1151-1156 (2018).
301. S. K. Jacobi, J. Odle, Nutritional factors influencing intestinal health of the neonate. *Adv Nutr* **3**, 687-696 (2012).

302. D. Rios-Covian *et al.*, Intestinal Short Chain Fatty Acids and their Link with Diet and Human Health. *Front Microbiol* **7**, 185 (2016).
303. P. Guilloteau *et al.*, From the gut to the peripheral tissues: the multiple effects of butyrate. *Nutr Res Rev* **23**, 366-384 (2010).
304. R. Lucas Lopez, M. J. Grande Burgos, A. Galvez, R. Perez Pulido, The human gastrointestinal tract and oral microbiota in inflammatory bowel disease: a state of the science review. *Apmis* **125**, 3-10 (2017).
305. C. Bourriaud *et al.*, Butyrate production from lactate by human colonic microflora. *Reprod. Nutr. Dev.* **42**, S55-S55 (2002).
306. S. Fukuda *et al.*, Bifidobacteria can protect from enteropathogenic infection through production of acetate. *Nature* **469**, 543-547 (2011).
307. R. Di Cagno *et al.*, Synthesis of gamma-aminobutyric acid (GABA) by Lactobacillus plantarum DSM19463: functional grape must beverage and dermatological applications. *Appl. Microbiol. Biotechnol.* **86**, 731-741 (2010).
308. F. Scaldaferri, M. Pizzoferrato, V. Gerardi, L. Lopetuso, A. Gasbarrini, The gut barrier: new acquisitions and therapeutic approaches. *J Clin Gastroenterol* **46 Suppl**, S12-17 (2012).
309. S. C. Bischoff *et al.*, Intestinal permeability--a new target for disease prevention and therapy. *BMC Gastroenterol* **14**, 189 (2014).
310. L. Wrzosek *et al.*, Bacteroides thetaiotaomicron and Faecalibacterium prausnitzii influence the production of mucus glycans and the development of goblet cells in the colonic epithelium of a gnotobiotic model rodent. *BMC Biol.* **11**, 61 (2013).
311. F. Yan *et al.*, A Lactobacillus rhamnosus GG-derived soluble protein, p40, stimulates ligand release from intestinal epithelial cells to transactivate epidermal growth factor receptor. *J. Biol. Chem.* **288**, 30742-30751 (2013).
312. E. Cario, G. Gerken, D. K. Podolsky, Toll-like receptor 2 controls mucosal inflammation by regulating epithelial barrier function. *Gastroenterology* **132**, 1359-1374 (2007).
313. N. H. Salzman, M. A. Underwood, C. L. Bevins, Paneth cells, defensins, and the commensal microbiota: a hypothesis on intimate interplay at the intestinal mucosa. *Semin. Immunol.* **19**, 70-83 (2007).
314. Y. Kumagai, S. Akira, Identification and functions of pattern-recognition receptors. *J Allergy Clin Immunol* **125**, 985-992 (2010).
315. R. Shin, M. Suzuki, Y. Morishita, Influence of intestinal anaerobes and organic acids on the growth of enterohaemorrhagic Escherichia coli O157:H7. *J. Med. Microbiol.* **51**, 201-206 (2002).
316. M. Bohnhoff, C. P. Miller, W. R. Martin, RESISTANCE OF THE MOUSE'S INTESTINAL TRACT TO EXPERIMENTAL SALMONELLA INFECTION. I. FACTORS WHICH INTERFERE WITH THE INITIATION OF INFECTION BY ORAL INOCULATION. *J. Exp. Med.* **120**, 805-816 (1964).
317. J. M. Pickard, M. Y. Zeng, R. Caruso, G. Núñez, Gut microbiota: Role in pathogen colonization, immune responses, and inflammatory disease. *Immunol. Rev.* **279**, 70-89 (2017).
318. H. Schaffler, A. Breitruck, Clostridium difficile - From Colonization to Infection. *Front Microbiol* **9**, 646 (2018).

319. T. Hrncir, Gut Microbiota Dysbiosis: Triggers, Consequences, Diagnostic and Therapeutic Options. *Microorganisms* **10**, (2022).
320. C. Manichanh, N. Borruel, F. Casellas, F. Guarner, The gut microbiota in IBD. *Nat Rev Gastroenterol Hepatol* **9**, 599-608 (2012).
321. D. Gevers *et al.*, The treatment-naive microbiome in new-onset Crohn's disease. *Cell Host Microbe* **15**, 382-392 (2014).
322. X. C. Morgan *et al.*, Dysfunction of the intestinal microbiome in inflammatory bowel disease and treatment. *Genome Biol* **13**, R79 (2012).
323. Z. K. Wang *et al.*, Intestinal microbiota pathogenesis and fecal microbiota transplantation for inflammatory bowel disease. *World J Gastroenterol* **20**, 14805-14820 (2014).
324. H. Sokol *et al.*, Faecalibacterium prausnitzii is an anti-inflammatory commensal bacterium identified by gut microbiota analysis of Crohn disease patients. *Proc Natl Acad Sci U S A* **105**, 16731-16736 (2008).
325. C. Tang *et al.*, Inhibition of Dectin-1 Signaling Ameliorates Colitis by Inducing Lactobacillus-Mediated Regulatory T Cell Expansion in the Intestine. *Cell Host Microbe* **18**, 183-197 (2015).
326. B. Kleessen, A. J. Kroesen, H. J. Buhr, M. Blaut, Mucosal and invading bacteria in patients with inflammatory bowel disease compared with controls. *Scand J Gastroenterol* **37**, 1034-1041 (2002).
327. I. Ahmed, B. C. Roy, S. A. Khan, S. Septer, S. Umar, Microbiome, Metabolome and Inflammatory Bowel Disease. *Microorganisms* **4**, (2016).
328. K. Hou *et al.*, Microbiota in health and diseases. *Signal Transduct Target Ther* **7**, 135 (2022).
329. O. Gaidai, Y. Cao, S. Loginov, Global Cardiovascular Diseases Death Rate Prediction. *Curr Probl Cardiol* **48**, 101622 (2023).
330. S. H. Zeisel, M. Warrier, Trimethylamine N-Oxide, the Microbiome, and Heart and Kidney Disease. *Annu Rev Nutr* **37**, 157-181 (2017).
331. C. Roncal *et al.*, Trimethylamine-N-Oxide (TMAO) Predicts Cardiovascular Mortality in Peripheral Artery Disease. *Sci Rep* **9**, 15580 (2019).
332. L. Liu, J. R. Huh, K. Shah, Microbiota and the gut-brain-axis: Implications for new therapeutic design in the CNS. *EBioMedicine* **77**, 103908 (2022).
333. H. Braak, R. A. de Vos, J. Bohl, K. Del Tredici, Gastric alpha-synuclein immunoreactive inclusions in Meissner's and Auerbach's plexuses in cases staged for Parkinson's disease-related brain pathology. *Neurosci Lett* **396**, 67-72 (2006).
334. M. G. Cersosimo, E. E. Benarroch, Pathological correlates of gastrointestinal dysfunction in Parkinson's disease. *Neurobiol Dis* **46**, 559-564 (2012).
335. F. Scheperjans *et al.*, Gut microbiota are related to Parkinson's disease and clinical phenotype. *Mov Disord* **30**, 350-358 (2015).
336. S. Eyvazi *et al.*, The oncogenic roles of bacterial infections in development of cancer. *Microb. Pathog.* **141**, 104019 (2020).
337. R. Tavares, S. K. Pathak, Helicobacter pylori Secreted Protein HP1286 Triggers Apoptosis in Macrophages via TNF-Independent and ERK MAPK-Dependent Pathways. *Front Cell Infect Microbiol* **7**, 58 (2017).
338. C. Y. Kao, B. S. Sheu, J. J. Wu, Helicobacter pylori infection: An overview of bacterial virulence factors and pathogenesis. *Biomed J* **39**, 14-23 (2016).

339. T. Scanu *et al.*, Salmonella Manipulation of Host Signaling Pathways Provokes Cellular Transformation Associated with Gallbladder Carcinoma. *Cell Host Microbe* **17**, 763-774 (2015).
340. A. D. Kostic *et al.*, Genomic analysis identifies association of Fusobacterium with colorectal carcinoma. *Genome Res.* **22**, 292-298 (2012).
341. A. I. Ojesina *et al.*, Landscape of genomic alterations in cervical carcinomas. *Nature* **506**, 371-375 (2014).
342. A. Marengo, C. Rosso, E. Bugianesi, Liver Cancer: Connections with Obesity, Fatty Liver, and Cirrhosis. *Annu. Rev. Med.* **67**, 103-117 (2016).
343. C. Ma *et al.*, Gut microbiome-mediated bile acid metabolism regulates liver cancer via NKT cells. *Science* **360**, (2018).
344. V. S. Akshintala, R. Talukdar, V. K. Singh, M. Goggins, The Gut Microbiome in Pancreatic Disease. *Clin Gastroenterol Hepatol* **17**, 290-295 (2019).
345. M. Vetizou *et al.*, Anticancer immunotherapy by CTLA-4 blockade relies on the gut microbiota. *Science* **350**, 1079-1084 (2015).
346. E. Vogtmann, J. J. Goedert, Epidemiologic studies of the human microbiome and cancer. *Br J Cancer* **114**, 237-242 (2016).
347. J. Li *et al.*, Individuality and ethnicity eclipse a short-term dietary intervention in shaping microbiomes and viromes. *PLoS Biol* **20**, e3001758 (2022).
348. E. Nova, S. Gómez-Martinez, R. González-Soltero, The Influence of Dietary Factors on the Gut Microbiota. *Microorganisms* **10**, (2022).
349. J. Ramirez *et al.*, Antibiotics as Major Disruptors of Gut Microbiota. *Front Cell Infect Microbiol* **10**, 572912 (2020).
350. C. K. Stein-Thoeringer *et al.*, A non-antibiotic-disrupted gut microbiome is associated with clinical responses to CD19-CAR-T cell cancer immunotherapy. *Nat Med* **29**, 906-916 (2023).
351. K. A. Lee *et al.*, Cross-cohort gut microbiome associations with immune checkpoint inhibitor response in advanced melanoma. *Nat Med* **28**, 535-544 (2022).
352. L. Derosa *et al.*, Intestinal Akkermansia muciniphila predicts clinical response to PD-1 blockade in patients with advanced non-small-cell lung cancer. *Nat Med* **28**, 315-324 (2022).
353. N. Iida *et al.*, Commensal bacteria control cancer response to therapy by modulating the tumor microenvironment. *Science* **342**, 967-970 (2013).
354. S. Viaud *et al.*, The intestinal microbiota modulates the anticancer immune effects of cyclophosphamide. *Science* **342**, 971-976 (2013).
355. A. M. McKee *et al.*, Antibiotic-induced disturbances of the gut microbiota result in accelerated breast tumor growth. *iScience* **24**, 103012 (2021).
356. C. Buchta Rosean *et al.*, Preexisting Commensal Dysbiosis Is a Host-Intrinsic Regulator of Tissue Inflammation and Tumor Cell Dissemination in Hormone Receptor-Positive Breast Cancer. *Cancer Res* **79**, 3662-3675 (2019).
357. T. Y. Feng *et al.*, Reciprocal Interactions Between the Gut Microbiome and Mammary Tissue Mast Cells Promote Metastatic Dissemination of HR+ Breast Tumors. *Cancer Immunol Res* **10**, 1309-1325 (2022).
358. J. D. Ransohoff *et al.*, Antimicrobial exposure is associated with decreased survival in triple-negative breast cancer. *Nat Commun* **14**, 2053 (2023).

359. S. Morrell *et al.*, Antibiotic exposure within six months before systemic therapy was associated with lower cancer survival. *J Clin Epidemiol* **147**, 122-131 (2022).
360. B. E. Wilson, B. Routy, A. Nagrial, V. T. Chin, The effect of antibiotics on clinical outcomes in immune-checkpoint blockade: a systematic review and meta-analysis of observational studies. *Cancer Immunol Immunother* **69**, 343-354 (2020).
361. L. Derosa *et al.*, Negative association of antibiotics on clinical activity of immune checkpoint inhibitors in patients with advanced renal cell and non-small-cell lung cancer. *Ann Oncol* **29**, 1437-1444 (2018).
362. A. Sivan *et al.*, Commensal Bifidobacterium promotes antitumor immunity and facilitates anti-PD-L1 efficacy. *Science* **350**, 1084-1089 (2015).
363. L. F. Mager *et al.*, Microbiome-derived inosine modulates response to checkpoint inhibitor immunotherapy. *Science* **369**, 1481-1489 (2020).
364. E. Ansaldo *et al.*, *Akkermansia muciniphila* induces intestinal adaptive immune responses during homeostasis. *Science* **364**, 1179-1184 (2019).
365. A. Montalban-Arques *et al.*, Commensal Clostridiales strains mediate effective anti-cancer immune response against solid tumors. *Cell Host Microbe* **29**, 1573-1588.e1577 (2021).
366. G. Gao *et al.*, Adjunctive probiotic lactobacillus rhamnosus probio-M9 administration enhances the effect of anti-PD-1 antitumor therapy via restoring antibiotic-disrupted gut microbiota. *Front Immunol* **12**, 772532 (2021).
367. T. Tanoue *et al.*, A defined commensal consortium elicits CD8 T cells and anti-cancer immunity. *Nature* **565**, 600-605 (2019).
368. N. Chaput *et al.*, Baseline gut microbiota predicts clinical response and colitis in metastatic melanoma patients treated with ipilimumab. *Ann Oncol* **28**, 1368-1379 (2017).
369. Y. Zheng *et al.*, Gut microbiome affects the response to anti-PD-1 immunotherapy in patients with hepatocellular carcinoma. *J Immunother Cancer* **7**, 193 (2019).
370. M. C. Andrews *et al.*, Gut microbiota signatures are associated with toxicity to combined CTLA-4 and PD-1 blockade. *Nat Med* **27**, 1432-1441 (2021).
371. R. C. Simpson *et al.*, Diet-driven microbial ecology underpins associations between cancer immunotherapy outcomes and the gut microbiome. *Nat Med* **28**, 2344-2352 (2022).
372. J. A. McCulloch *et al.*, Intestinal microbiota signatures of clinical response and immune-related adverse events in melanoma patients treated with anti-PD-1. *Nat Med* **28**, 545-556 (2022).
373. V. Gopalakrishnan *et al.*, Gut microbiome modulates response to anti-PD-1 immunotherapy in melanoma patients. *Science* **359**, 97-103 (2018).
374. B. Routy *et al.*, Gut microbiome influences efficacy of PD-1-based immunotherapy against epithelial tumors. *Science* **359**, 91-97 (2018).
375. E. N. Baruch *et al.*, Fecal microbiota transplant promotes response in immunotherapy-refractory melanoma patients. *Science* **371**, 602-609 (2021).
376. D. Davar *et al.*, Fecal microbiota transplant overcomes resistance to anti-PD-1 therapy in melanoma patients. *Science* **371**, 595-602 (2021).

377. N. Dizman *et al.*, Nivolumab plus ipilimumab with or without live bacterial supplementation in metastatic renal cell carcinoma: a randomized phase 1 trial. *Nat Med* **28**, 704-712 (2022).
378. G. Alessandri, D. van Sinderen, M. Ventura, The genus bifidobacterium: From genomics to functionality of an important component of the mammalian gut microbiota running title: Bifidobacterial adaptation to and interaction with the host. *Comput Struct Biotechnol J* **19**, 1472-1487 (2021).
379. A. O'Callaghan, D. van Sinderen, Bifidobacteria and Their Role as Members of the Human Gut Microbiota. *Front Microbiol* **7**, 925 (2016).
380. X. Xiong, S. L. Loo, L. Zhang, M. M. Tanaka, Modelling the effect of birth and feeding modes on the development of human gut microbiota. *Proc Biol Sci* **288**, 20201810 (2021).
381. C. Alcon-Giner *et al.*, Microbiota supplementation with *Bifidobacterium* and *Lactobacillus* modifies the preterm infant gut microbiota and metabolome: an observational study. *Cell Rep Med* **1**, 100077 (2020).
382. D. Dilli *et al.*, The propre-save study: effects of probiotics and prebiotics alone or combined on necrotizing enterocolitis in very low birth weight infants. *J Pediatr* **166**, 545-551.e541 (2015).
383. T. D. Braga, G. A. da Silva, P. I. de Lira, M. de Carvalho Lima, Efficacy of Bifidobacterium breve and Lactobacillus casei oral supplementation on necrotizing enterocolitis in very-low-birth-weight preterm infants: a double-blind, randomized, controlled trial. *Am J Clin Nutr* **93**, 81-86 (2011).
384. S. K. Patole *et al.*, Benefits of Bifidobacterium breve M-16V Supplementation in Preterm Neonates - A Retrospective Cohort Study. *PLoS One* **11**, e0150775 (2016).
385. W. H. Organization, *WHO recommendations for care of the preterm or low-birth-weight infant*. (2022).
386. Y. Yoon, G. Kim, B. N. Jeon, S. Fang, H. Park, Strain-Specific Enhances the Efficacy of Cancer Therapeutics in Tumor-Bearing Mice. *Cancers (Basel)* **13**, (2021).
387. S. H. Lee *et al.*, Bifidobacterium bifidum strains synergize with immune checkpoint inhibitors to reduce tumour burden in mice. *Nat Microbiol* **6**, 277-288 (2021).
388. V. Matson *et al.*, The commensal microbiome is associated with anti-PD-1 efficacy in metastatic melanoma patients. *Science* **359**, 104-108 (2018).
389. H. Zafar, M. H. Saier, Gut *Bacteroides* species in health and disease. *Gut Microbes* **13**, 1-20 (2021).
390. G. P. Rodriguez-Castaño *et al.*, Starch Utilization Promotes Quercetin Degradation and Butyrate Production by. *Front Microbiol* **10**, 1145 (2019).
391. W. Elhenawy, M. O. Debelyy, M. F. Feldman, Preferential packing of acidic glycosidases and proteases into Bacteroides outer membrane vesicles. *mBio* **5**, e00909-00914 (2014).
392. M. Chatzidaki-Livanis, M. J. Coyne, L. E. Comstock, An antimicrobial protein of the gut symbiont Bacteroides fragilis with a MACPF domain of host immune proteins. *Mol Microbiol* **94**, 1361-1374 (2014).

393. S. Fonseca *et al.*, Extracellular vesicles produced by the human gut commensal bacterium. *Front Microbiol* **13**, 1050271 (2022).
394. L. Durant *et al.*, Bacteroides thetaiotaomicron-derived outer membrane vesicles promote regulatory dendritic cell responses in health but not in inflammatory bowel disease. *Microbiome* **8**, 88 (2020).
395. E. J. Jones *et al.*, The Uptake, Trafficking, and Biodistribution of Bacteroides thetaiotaomicron Generated Outer Membrane Vesicles. *Front Microbiol* **11**, 57 (2020).
396. S. Wu *et al.*, A human colonic commensal promotes colon tumorigenesis via activation of T helper type 17 T cell responses. *Nat Med* **15**, 1016-1022 (2009).
397. M. Vétizou *et al.*, Anticancer immunotherapy by CTLA-4 blockade relies on the gut microbiota. *Science* **350**, 1079-1084 (2015).
398. Y. K. Lee *et al.*, The Protective Role of *Bacteroides fragilis* in a Murine Model of Colitis-Associated Colorectal Cancer. *mSphere* **3**, (2018).
399. J. Huang *et al.*, Metagenomic and metabolomic analyses reveal synergistic effects of fecal microbiota transplantation and anti-PD-1 therapy on treating colorectal cancer. *Front Immunol* **13**, 874922 (2022).
400. M. R. Rubinstein *et al.*, Fusobacterium nucleatum promotes colorectal carcinogenesis by modulating E-cadherin/β-catenin signaling via its FadA adhesin. *Cell Host Microbe* **14**, 195-206 (2013).
401. C. Xue *et al.*, Current understanding of the intratumoral microbiome in various tumors. *Cell Rep Med* **4**, 100884 (2023).
402. D. Nejman *et al.*, The human tumor microbiome is composed of tumor type-specific intracellular bacteria. *Science* **368**, 973-980 (2020).
403. G. D. Poore *et al.*, Microbiome analyses of blood and tissues suggest cancer diagnostic approach. *Nature* **579**, 567-574 (2020).
404. S. Parida *et al.*, A Procarcinogenic Colon Microbe Promotes Breast Tumorigenesis and Metastatic Progression and Concomitantly Activates Notch and β-Catenin Axes. *Cancer Discov* **11**, 1138-1157 (2021).
405. L. T. Geller *et al.*, Potential role of intratumor bacteria in mediating tumor resistance to the chemotherapeutic drug gemcitabine. *Science* **357**, 1156-1160 (2017).
406. S. Pushalkar *et al.*, The Pancreatic Cancer Microbiome Promotes Oncogenesis by Induction of Innate and Adaptive Immune Suppression. *Cancer Discov* **8**, 403-416 (2018).
407. L. Parhi *et al.*, Breast cancer colonization by Fusobacterium nucleatum accelerates tumor growth and metastatic progression. *Nat Commun* **11**, 3259 (2020).
408. A. Fu *et al.*, Tumor-resident intracellular microbiota promotes metastatic colonization in breast cancer. *Cell* **185**, 1356-1372.e1326 (2022).
409. Z. A. Rizvi *et al.*, High-salt diet mediates interplay between NK cells and gut microbiota to induce potent tumor immunity. *Sci Adv* **7**, eabg5016 (2021).
410. G. Zhu *et al.*, Intratumour microbiome associated with the infiltration of cytotoxic CD8+ T cells and patient survival in cutaneous melanoma. *Eur J Cancer* **151**, 25-34 (2021).
411. J. J. Tsay *et al.*, Airway Microbiota Is Associated with Upregulation of the PI3K Pathway in Lung Cancer. *Am J Respir Crit Care Med* **198**, 1188-1198 (2018).

412. D. Qu *et al.*, Intratumoral Microbiome of Human Primary Liver Cancer. *Hepatol Commun* **6**, 1741-1752 (2022).
413. M. J. Bender *et al.*, Dietary tryptophan metabolite released by intratumoral Lactobacillus reuteri facilitates immune checkpoint inhibitor treatment. *Cell* **186**, 1846-1862.e1826 (2023).
414. B. Aykut *et al.*, The fungal mycobiome promotes pancreatic oncogenesis via activation of MBL. *Nature* **574**, 264-267 (2019).
415. L. Narunsky-Haziza *et al.*, Pan-cancer analyses reveal cancer-type-specific fungal ecologies and bacteriome interactions. *Cell* **185**, 3789-3806.e3717 (2022).
416. F. Gao *et al.*, The effect of the intratumoral microbiome on tumor occurrence, progression, prognosis and treatment. *Front Immunol* **13**, 1051987 (2022).
417. F. P. Breitwieser, M. Pertea, A. V. Zimin, S. L. Salzberg, Human contamination in bacterial genomes has created thousands of spurious proteins. *Genome Res* **29**, 954-960 (2019).
418. M. Steinegger, S. L. Salzberg, Terminating contamination: large-scale search identifies more than 2,000,000 contaminated entries in GenBank. *Genome Biol* **21**, 115 (2020).
419. A. Gihawi, C. S. Cooper, D. S. Brewer, Caution regarding the specificities of pan-cancer microbial structure. *Microb Genom* **9**, (2023).
420. A. Gihawi *et al.*, Major data analysis errors invalidate cancer microbiome findings. *bioRxiv*, (2023).
421. F. C. C. d. M. Noel, T. S. Vincent, P. Manon van der, W. Jelle, N. Jacques, Absence of Lipopolysccharide (LPS) expression in Breast Cancer Cells. *bioRxiv*, 2023.2008.2028.555057 (2023).
422. H. C. Descamps, B. Herrmann, D. Wiredu, C. A. Thaiss, The path toward using microbial metabolites as therapies. *EBioMedicine* **44**, 747-754 (2019).
423. Q. Yang *et al.*, A Review of Gut Microbiota-Derived Metabolites in Tumor Progression and Cancer Therapy. *Adv Sci (Weinh)* **10**, e2207366 (2023).
424. A. Koh, F. De Vadder, P. Kovatcheva-Datchary, F. Bäckhed, From Dietary Fiber to Host Physiology: Short-Chain Fatty Acids as Key Bacterial Metabolites. *Cell* **165**, 1332-1345 (2016).
425. N. Singh *et al.*, Activation of Gpr109a, receptor for niacin and the commensal metabolite butyrate, suppresses colonic inflammation and carcinogenesis. *Immunity* **40**, 128-139 (2014).
426. S. Lavoie *et al.*, Expression of Free Fatty Acid Receptor 2 by Dendritic Cells Prevents Their Expression of Interleukin 27 and Is Required for Maintenance of Mucosal Barrier and Immune Response Against Colorectal Tumors in Mice. *Gastroenterology* **158**, 1359-1372.e1359 (2020).
427. J. Qiu *et al.*, Acetate Promotes T Cell Effector Function during Glucose Restriction. *Cell Rep* **27**, 2063-2074.e2065 (2019).
428. M. Luu *et al.*, Microbial short-chain fatty acids modulate CD8 + T cell responses and improve adoptive immunotherapy for cancer. *Nat Commun* **12**, 4077 (2021).
429. Q. Zhang *et al.*, Lactobacillus plantarum-derived indole-3-lactic acid ameliorates colorectal tumorigenesis via epigenetic regulation of CD8. *Cell Metab* **35**, 943-960.e949 (2023).

430. H. Wang *et al.*, The microbial metabolite trimethylamine N-oxide promotes antitumor immunity in triple-negative breast cancer. *Cell Metab* **34**, 581-594.e588 (2022).
431. K. Walczak, W. A. Turski, G. Rajtar, Kynurenic acid inhibits colon cancer proliferation in vitro: effects on signaling pathways. *Amino Acids* **46**, 2393-2401 (2014).
432. L. Vettore, R. L. Westbrook, D. A. Tennant, New aspects of amino acid metabolism in cancer. *Br J Cancer* **122**, 150-156 (2020).
433. J. J. Cho *et al.*, Manumycin A from a new Streptomyces strain induces endoplasmic reticulum stress-mediated cell death through specificity protein 1 signaling in human oral squamous cell carcinoma. *Int J Oncol* **47**, 1954-1962 (2015).
434. J. Angelin, M. Kavitha, Exopolysaccharides from probiotic bacteria and their health potential. *Int J Biol Macromol* **162**, 853-865 (2020).
435. M. M. P. Oerlemans, R. Akkerman, M. Ferrari, M. T. C. Walvoort, P. de Vos, Benefits of bacteria-derived exopolysaccharides on gastrointestinal microbiota, immunity and health. *Journal of Functional Foods* **76**, 104289 (2021).
436. C. Ferrario *et al.*, Modulation of the eps-ome transcription of bifidobacteria through simulation of human intestinal environment. *FEMS Microbiol Ecol* **92**, fiw056 (2016).
437. A. Fuso *et al.*, Feeding Lactic Acid Bacteria with Different Sugars: Effect on Exopolysaccharides (EPS) Production and Their Molecular Characteristics. *Foods* **12**, (2023).
438. M. Korakli, M. G. Gänzle, R. F. Vogel, Metabolism by bifidobacteria and lactic acid bacteria of polysaccharides from wheat and rye, and exopolysaccharides produced by Lactobacillus sanfranciscensis. *J Appl Microbiol* **92**, 958-965 (2002).
439. N. Salazar, M. Gueimonde, A. M. Hernández-Barranco, P. Ruas-Madiedo, C. G. de los Reyes-Gavilán, Exopolysaccharides produced by intestinal Bifidobacterium strains act as fermentable substrates for human intestinal bacteria. *Appl Environ Microbiol* **74**, 4737-4745 (2008).
440. P. Ruas-Madiedo *et al.*, Exopolysaccharides produced by Lactobacillus and Bifidobacterium strains abrogate in vitro the cytotoxic effect of bacterial toxins on eukaryotic cells. *J Appl Microbiol* **109**, 2079-2086 (2010).
441. J. B. Ewaschuk *et al.*, Secreted bioactive factors from Bifidobacterium infantis enhance epithelial cell barrier function. *Am J Physiol Gastrointest Liver Physiol* **295**, G1025-1034 (2008).
442. M. H. Lin *et al.*, A novel exopolysaccharide from the biofilm of Thermus aquaticus YT-1 induces the immune response through Toll-like receptor 2. *J Biol Chem* **286**, 17736-17745 (2011).
443. R. Graveline, M. Segura, D. Radzioch, M. Gottschalk, TLR2-dependent recognition of Streptococcus suis is modulated by the presence of capsular polysaccharide which modifies macrophage responsiveness. *Int Immunol* **19**, 375-389 (2007).
444. K. R. Hughes *et al.*, Bifidobacterium breve reduces apoptotic epithelial cell shedding in an exopolysaccharide and MyD88-dependent manner. *Open Biol* **7**, (2017).

445. Y. Murofushi *et al.*, The toll-like receptor family protein RP105/MD1 complex is involved in the immunoregulatory effect of exopolysaccharides from Lactobacillus plantarum N14. *Mol Immunol* **64**, 63-75 (2015).
446. S. E. Hardison, G. D. Brown, C-type lectin receptors orchestrate antifungal immunity. *Nat Immunol* **13**, 817-822 (2012).
447. M. Ujita *et al.*, Carbohydrate binding specificity of recombinant human macrophage beta-glucan receptor dectin-1. *Biosci Biotechnol Biochem* **73**, 237-240 (2009).
448. E. L. Adams *et al.*, Differential high-affinity interaction of dectin-1 with natural or synthetic glucans is dependent upon primary structure and is influenced by polymer chain length and side-chain branching. *J Pharmacol Exp Ther* **325**, 115-123 (2008).
449. E. P. McGreal *et al.*, The carbohydrate-recognition domain of Dectin-2 is a C-type lectin with specificity for high mannose. *Glycobiology* **16**, 422-430 (2006).
450. S. I. Gringhuis, J. den Dunnen, M. Litjens, M. van der Vlist, T. B. Geijtenbeek, Carbohydrate-specific signaling through the DC-SIGN signalosome tailors immunity to Mycobacterium tuberculosis, HIV-1 and Helicobacter pylori. *Nat Immunol* **10**, 1081-1088 (2009).
451. J. L. Round *et al.*, The Toll-like receptor 2 pathway establishes colonization by a commensal of the human microbiota. *Science* **332**, 974-977 (2011).
452. B. A. Cobb, Q. Wang, A. O. Tzianabos, D. L. Kasper, Polysaccharide processing and presentation by the MHCII pathway. *Cell* **117**, 677-687 (2004).
453. W. M. Kalka-Moll *et al.*, Zwitterionic polysaccharides stimulate T cells by MHC class II-dependent interactions. *J Immunol* **169**, 6149-6153 (2002).
454. C. Hidalgo-Cantabrana *et al.*, Exopolysaccharide-producing Bifidobacterium animalis subsp. lactis strains and their polymers elicit different responses on immune cells from blood and gut associated lymphoid tissue. *Anaerobe* **26**, 24-30 (2014).
455. S. Fanning *et al.*, Bifidobacterial surface-exopolysaccharide facilitates commensal-host interaction through immune modulation and pathogen protection. *Proc Natl Acad Sci U S A* **109**, 2108-2113 (2012).
456. A. Hickey *et al.*, Exopolysaccharide Blocks Dendritic Cell Maturation and Activation of CD4. *Front Microbiol* **12**, 653587 (2021).
457. R. Yu, F. Zuo, H. Ma, S. Chen, Exopolysaccharide-Producing Bifidobacterium adolescentis Strains with Similar Adhesion Property Induce Differential Regulation of Inflammatory Immune Response in Treg/Th17 Axis of DSS-Colitis Mice. *Nutrients* **11**, (2019).
458. S. Yan *et al.*, A ropy exopolysaccharide producing strain Bifidobacterium longum subsp. longum YS108R alleviates DSS-induced colitis by maintenance of the mucosal barrier and gut microbiota modulation. *Food Funct* **10**, 1595-1608 (2019).
459. E. Schiavi *et al.*, Exopolysaccharide from Bifidobacterium longum subsp. longum 35624™ modulates murine allergic airway responses. *Benef Microbes* **9**, 761-773 (2018).
460. M. Ayyash *et al.*, Characterization, bioactivities, and rheological properties of exopolysaccharide produced by novel probiotic Lactobacillus plantarum C70 isolated from camel milk. *Int J Biol Macromol* **144**, 938-946 (2020).

461. Y. Kim, S. Oh, H. S. Yun, S. H. Kim, Cell-bound exopolysaccharide from probiotic bacteria induces autophagic cell death of tumour cells. *Lett Appl Microbiol* **51**, 123-130 (2010).
462. M. Ayyash *et al.*, Physicochemical, bioactive and rheological properties of an exopolysaccharide produced by a probiotic Pediococcus pentosaceus M41. *Carbohydr Polym* **229**, 115462 (2020).
463. W. Vollmer, D. Blanot, M. A. de Pedro, Peptidoglycan structure and architecture. *FEMS Microbiol Rev* **32**, 149-167 (2008).
464. A. J. Wolf, D. M. Underhill, Peptidoglycan recognition by the innate immune system. *Nat Rev Immunol* **18**, 243-254 (2018).
465. R. Dziarski, D. Gupta, Mammalian PGRPs: novel antibacterial proteins. *Cell Microbiol* **8**, 1059-1069 (2006).
466. K. Sekine *et al.*, A new morphologically characterized cell wall preparation (whole peptidoglycan) from Bifidobacterium infantis with a higher efficacy on the regression of an established tumor in mice. *Cancer Res* **45**, 1300-1307 (1985).
467. J. Y. Kim, H. J. Woo, Y.-S. Kim, H. J. Lee, Screening for antiproliferative effects of cellular components from lactic acid bacteria against human cancer cell lines. *Biotechnology Letters* **24**, 1431-1436 (2002).
468. M. A. Müller-Anstett *et al.*, Staphylococcal peptidoglycan co-localizes with Nod2 and TLR2 and activates innate immune response via both receptors in primary murine keratinocytes. *PLoS One* **5**, e13153 (2010).
469. M. Pyclik, D. Srutkova, M. Schwarzer, S. Górska, Bifidobacteria cell wall-derived exo-polysaccharides, lipoteichoic acids, peptidoglycans, polar lipids and proteins - their chemical structure and biological attributes. *Int J Biol Macromol* **147**, 333-349 (2020).
470. H. Mizuno *et al.*, Lipoteichoic Acid Is Involved in the Ability of the Immunobiotic Strain. *Front Immunol* **11**, 571 (2020).
471. K. A. Kline, K. W. Dodson, M. G. Caparon, S. J. Hultgren, A tale of two pili: assembly and function of pili in bacteria. *Trends Microbiol* **18**, 224-232 (2010).
472. A. Basset *et al.*, Toll-like receptor (TLR) 2 mediates inflammatory responses to oligomerized RrgA pneumococcal pilus type 1 protein. *J Biol Chem* **288**, 2665-2675 (2013).
473. H. L. Tytgat *et al.*, Probiotic Gut Microbiota Isolate Interacts with Dendritic Cells via Glycosylated Heterotrimeric Pili. *PLoS One* **11**, e0151824 (2016).
474. F. Turroni *et al.*, Role of sortase-dependent pili of Bifidobacterium bifidum PRL2010 in modulating bacterium-host interactions. *Proc Natl Acad Sci U S A* **110**, 11151-11156 (2013).
475. M. Toyofuku, N. Nomura, L. Eberl, Types and origins of bacterial membrane vesicles. *Nat Rev Microbiol* **17**, 13-24 (2019).
476. A. Kulp, M. J. Kuehn, Biological functions and biogenesis of secreted bacterial outer membrane vesicles. *Annu. Rev. Microbiol.* **64**, 163-184 (2010).
477. C. Schwechheimer, M. J. Kuehn, Outer-membrane vesicles from Gram-negative bacteria: biogenesis and functions. *Nat. Rev. Microbiol.* **13**, 605-619 (2015).
478. S. Wang, J. Gao, Z. Wang, Outer membrane vesicles for vaccination and targeted drug delivery. *Wiley Interdiscip Rev Nanomed Nanobiotechnol* **11**, e1523 (2019).

479. E. D. Avila-Calderón *et al.*, Outer Membrane Vesicles of Gram-Negative Bacteria: An Outlook on Biogenesis. *Front Microbiol* **12**, 557902 (2021).
480. A. E. Sjöström, L. Sandblad, B. E. Uhlin, S. N. Wai, Membrane vesicle-mediated release of bacterial RNA. *Sci Rep* **5**, 15329 (2015).
481. Z. Li, A. J. Clarke, T. J. Beveridge, A major autolysin of Pseudomonas aeruginosa: subcellular distribution, potential role in cell growth and division and secretion in surface membrane vesicles. *J. Bacteriol.* **178**, 2479-2488 (1996).
482. A. Olofsson *et al.*, Biochemical and functional characterization of Helicobacter pylori vesicles. *Mol. Microbiol.* **77**, 1539-1555 (2010).
483. C. Schwechheimer, M. J. Kuehn, Synthetic effect between envelope stress and lack of outer membrane vesicle production in Escherichia coli. *J. Bacteriol.* **195**, 4161-4173 (2013).
484. O. Y. Kim *et al.*, Bacterial outer membrane vesicles suppress tumor by interferon-gamma-mediated antitumor response. *Nat Commun* **8**, 626 (2017).
485. M. Li *et al.*, Bacterial outer membrane vesicles as a platform for biomedical applications: An update. *J Control Release*, (2020).
486. M. M. Tomayko, C. P. Reynolds, Determination of subcutaneous tumor size in athymic (nude) mice. *Cancer Chemother Pharmacol* **24**, 148-154 (1989).
487. I. R. Serghiou *et al.*, An efficient method for high molecular weight bacterial DNA extraction suitable for shotgun metagenomics from skin swabs. *Microb Genom* **9**, (2023).
488. Y. Huang *et al.*, Genetically Engineered Bacterial Outer Membrane Vesicles with Expressed Nanoluciferase Reporter for i*n Vivo* Bioluminescence Kinetic Modeling through Noninvasive Imaging. *ACS Appl Bio Mater* **2**, 5608-5615 (2019).
489. K. Moor *et al.*, Peracetic Acid Treatment Generates Potent Inactivated Oral Vaccines from a Broad Range of Culturable Bacterial Species. *Front Immunol* **7**, 34 (2016).
490. P. Ruas-Madiedo, Detection, Isolation, and Purification of Bifidobacterial Exopolysaccharides. *Methods Mol Biol* **2278**, 101-115 (2021).
491. R. Stentz *et al.*, A bacterial homolog of a eukaryotic inositol phosphate signaling enzyme mediates cross-kingdom dialog in the mammalian gut. *Cell Rep* **6**, 646-656 (2014).
492. K. H. Kim, J. M. Sederstrom, Assaying Cell Cycle Status Using Flow Cytometry. *Curr Protoc Mol Biol* **111**, 28.26.21-28.26.11 (2015).
493. J. Chong, D. S. Wishart, J. Xia, Using MetaboAnalyst 4.0 for Comprehensive and Integrative Metabolomics Data Analysis. *Curr Protoc Bioinformatics* **68**, e86 (2019).
494. Z. Pang *et al.*, Using MetaboAnalyst 5.0 for LC-HRMS spectra processing, multi-omics integration and covariate adjustment of global metabolomics data. *Nat Protoc* **17**, 1735-1761 (2022).
495. N. F. Alikhan *et al.*, Dynamics of Salmonella enterica and antimicrobial resistance in the Brazilian poultry industry and global impacts on public health. *PLoS Genet* **18**, e1010174 (2022).
496. Y. Lu *et al.*, MicrobiomeAnalyst 2.0: comprehensive statistical, functional and integrative analysis of microbiome data. *Nucleic Acids Res* **51**, W310-W318 (2023).

497. M. A. E. Lawson *et al.*, Breast milk-derived human milk oligosaccharides promote Bifidobacterium interactions within a single ecosystem. *ISME J* **14**, 635-648 (2020).
498. S. Chen, Y. Zhou, Y. Chen, J. Gu, fastp: an ultra-fast all-in-one FASTQ preprocessor. *Bioinformatics* **34**, i884-i890 (2018).
499. R. R. Wick, L. M. Judd, C. L. Gorrie, K. E. Holt, Unicycler: Resolving bacterial genome assemblies from short and long sequencing reads. *PLoS Comput Biol* **13**, e1005595 (2017).
500. D. H. Parks, M. Imelfort, C. T. Skennerton, P. Hugenholtz, G. W. Tyson, CheckM: assessing the quality of microbial genomes recovered from isolates, single cells, and metagenomes. *Genome Res* **25**, 1043-1055 (2015).
501. T. Seemann, Prokka: rapid prokaryotic genome annotation. *Bioinformatics* **30**, 2068-2069 (2014).
502. C. Camacho *et al.*, BLAST+: architecture and applications. *BMC Bioinformatics* **10**, 421 (2009).
503. L. Wang *et al.*, Exopolysaccharide, Isolated From a Novel Strain Bifidobacterium breve lw01 Possess an Anticancer Effect on Head and Neck Cancer. *Front Microbiol* **10**, 1044 (2019).
504. C. L. M. Gilchrist, Y. H. Chooi, clinker & clustermap.js: automatic generation of gene cluster comparison figures. *Bioinformatics* **37**, 2473-2475 (2021).
505. J. Junick, M. Blaut, Quantification of human fecal bifidobacterium species by use of quantitative real-time PCR analysis targeting the groEL gene. *Appl Environ Microbiol* **78**, 2613-2622 (2012).
506. M. J. Peña, S. T. Tuomivaara, B. R. Urbanowicz, M. A. O'Neill, W. S. York, Methods for structural characterization of the products of cellulose- and xyloglucan-hydrolyzing enzymes. *Methods Enzymol* **510**, 121-139 (2012).
507. K. R. Anumula, P. B. Taylor, A comprehensive procedure for preparation of partially methylated alditol acetates from glycoprotein carbohydrates. *Anal Biochem* **203**, 101-108 (1992).
508. S. Nechuta *et al.*, A pooled analysis of post-diagnosis lifestyle factors in association with late estrogen-receptor-positive breast cancer prognosis. *Int J Cancer* **138**, 2088-2097 (2016).
509. M. Ewertz *et al.*, Effect of obesity on prognosis after early-stage breast cancer. *J Clin Oncol* **29**, 25-31 (2011).
510. N. M. Y. Teng, C. A. Price, A. M. McKee, L. J. Hall, S. D. Robinson, Exploring the impact of gut microbiota and diet on breast cancer risk and progression. *Int J Cancer* **149**, 494-504 (2021).
511. G. D. Sepich-Poore *et al.*, The microbiome and human cancer. *Science* **371**, (2021).
512. L. Zitvogel *et al.*, Cancer and the gut microbiota: an unexpected link. *Sci Transl Med* **7**, 271ps271 (2015).
513. J. L. Wang *et al.*, Infection, antibiotic therapy and risk of colorectal cancer: a nationwide nested case-control study in patients with Type 2 diabetes mellitus. *Int J Cancer* **135**, 956-967 (2014).
514. M. Uribe-Herranz *et al.*, Gut microbiota modulate dendritic cell antigen presentation and radiotherapy-induced antitumor immune response. *J Clin Invest* **130**, 466-479 (2020).

515. G. Longhi, D. van Sinderen, M. Ventura, F. Turroni, Microbiota and Cancer: The Emerging Beneficial Role of Bifidobacteria in Cancer Immunotherapy. *Front Microbiol* **11**, 575072 (2020).
516. M. J. Allegrezza *et al.*, Trametinib Drives T-cell-Dependent Control of KRAS-Mutated Tumors by Inhibiting Pathological Myelopoiesis. *Cancer Res* **76**, 6253-6265 (2016).
517. A. I. Riggio, K. E. Varley, A. L. Welm, The lingering mysteries of metastatic recurrence in breast cancer. *Br J Cancer* **124**, 13-26 (2021).
518. A. G. Waks, E. P. Winer, Breast Cancer Treatment: A Review. *JAMA* **321**, 288-300 (2019).
519. P. C. Hagen, J. W. Skelley, Efficacy of Bifidobacterium Species in Prevention of Necrotizing Enterocolitis in Very-Low Birth Weight Infants. A Systematic Review. *J Pediatr Pharmacol Ther* **24**, 10-15 (2019).
520. M. O'Reilly, G. Mellotte, B. Ryan, A. O'Connor, Gastrointestinal side effects of cancer treatments. *Ther Adv Chronic Dis* **11**, 2040622320970354 (2020).
521. M. Camilleri, Leaky gut: mechanisms, measurement and clinical implications in humans. *Gut* **68**, 1516-1526 (2019).
522. S. Guo *et al.*, Secretions of Bifidobacterium infantis and Lactobacillus acidophilus Protect Intestinal Epithelial Barrier Function. *J Pediatr Gastroenterol Nutr* **64**, 404-412 (2017).
523. R. Al-Sadi *et al.*, Enhances the Intestinal Epithelial Tight Junction Barrier and Protects against Intestinal Inflammation by Targeting the Toll-like Receptor-2 Pathway in an NF-κB-Independent Manner. *Int J Mol Sci* **22**, (2021).
524. J. Cortes *et al.*, Pembrolizumab plus Chemotherapy in Advanced Triple-Negative Breast Cancer. *N Engl J Med* **387**, 217-226 (2022).
525. M. F. Fernandez *et al.*, Breast Cancer and Its Relationship with the Microbiota. *Int J Environ Res Public Health* **15**, (2018).
526. Y. Shi *et al.*, Intratumoral accumulation of gut microbiota facilitates CD47-based immunotherapy via STING signaling. *J Exp Med* **217**, (2020).
527. S. Pal *et al.*, The microbiome restrains melanoma bone growth by promoting intestinal NK and Th1 cell homing to bone. *J Clin Invest* **132**, (2022).
528. H. Raskov, A. Orhan, J. P. Christensen, I. Gögenur, Cytotoxic CD8. *Br J Cancer* **124**, 359-367 (2021).
529. H. Hosseini *et al.*, Early dissemination seeds metastasis in breast cancer. *Nature* **540**, 552-558 (2016).
530. A. D. Waldman, J. M. Fritz, M. J. Lenardo, A guide to cancer immunotherapy: from T cell basic science to clinical practice. *Nat Rev Immunol* **20**, 651-668 (2020).
531. A. Reuben *et al.*, TCR Repertoire Intratumor Heterogeneity in Localized Lung Adenocarcinomas: An Association with Predicted Neoantigen Heterogeneity and Postsurgical Recurrence. *Cancer Discov* **7**, 1088-1097 (2017).
532. B. T. Fife, J. A. Bluestone, Control of peripheral T-cell tolerance and autoimmunity via the CTLA-4 and PD-1 pathways. *Immunol Rev* **224**, 166-182 (2008).
533. O. Michielin, M. B. Atkins, H. B. Koon, R. Dummer, P. A. Ascierto, Evolving impact of long-term survival results on metastatic melanoma treatment. *J Immunother Cancer* **8**, (2020).

534. T. A. Olsen *et al.*, Racial Differences in Clinical Outcomes for Metastatic Renal Cell Carcinoma Patients Treated With Immune-Checkpoint Blockade. *Front Oncol* **11**, 701345 (2021).
535. M. J. Grant, R. S. Herbst, S. B. Goldberg, Selecting the optimal immunotherapy regimen in driver-negative metastatic NSCLC. *Nat Rev Clin Oncol* **18**, 625-644 (2021).
536. L. Ruiz, S. Delgado, P. Ruas-Madiedo, B. Sánchez, A. Margolles, Bifidobacteria and Their Molecular Communication with the Immune System. *Front Microbiol* **8**, 2345 (2017).
537. C. Milani *et al.*, The First Microbial Colonizers of the Human Gut: Composition, Activities, and Health Implications of the Infant Gut Microbiota. *Microbiol Mol Biol Rev* **81**, (2017).
538. C. Robertson *et al.*, Incidence of necrotising enterocolitis before and after introducing routine prophylactic. *Arch Dis Child Fetal Neonatal Ed* **105**, 380-386 (2020).
539. P. Golstein, G. M. Griffiths, An early history of T cell-mediated cytotoxicity. *Nat Rev Immunol* **18**, 527-535 (2018).
540. N. Zhang, M. J. Bevan, CD8(+) T cells: foot soldiers of the immune system. *Immunity* **35**, 161-168 (2011).
541. P. Ramesh, R. Shivde, D. Jaishankar, D. Saleiro, I. C. Le Poole, A Palette of Cytokines to Measure Anti-Tumor Efficacy of T Cell-Based Therapeutics. *Cancers (Basel)* **13**, (2021).
542. K. Hallermalm *et al.*, Tumor necrosis factor-alpha induces coordinated changes in major histocompatibility class I presentation pathway, resulting in increased stability of class I complexes at the cell surface. *Blood* **98**, 1108-1115 (2001).
543. A. V. Collins *et al.*, The interaction properties of costimulatory molecules revisited. *Immunity* **17**, 201-210 (2002).
544. R. A. Colvin, G. S. Campanella, J. Sun, A. D. Luster, Intracellular domains of CXCR3 that mediate CXCL9, CXCL10, and CXCL11 function. *J Biol Chem* **279**, 30219-30227 (2004).
545. C. I. Liakou *et al.*, CTLA-4 blockade increases IFNgamma-producing CD4+ICOShi cells to shift the ratio of effector to regulatory T cells in cancer patients. *Proc Natl Acad Sci U S A* **105**, 14987-14992 (2008).
546. D. Ng Tang *et al.*, Increased frequency of ICOS+ CD4 T cells as a pharmacodynamic biomarker for anti-CTLA-4 therapy. *Cancer Immunol Res* **1**, 229-234 (2013).
547. V. Chew, H. C. Toh, J. P. Abastado, Immune microenvironment in tumor progression: characteristics and challenges for therapy. *J Oncol* **2012**, 608406 (2012).
548. H. C. DeGrendele, M. Kosfiszer, P. Estess, M. H. Siegelman, CD44 activation and associated primary adhesion is inducible via T cell receptor stimulation. *J Immunol* **159**, 2549-2553 (1997).
549. T. L. Murphy, K. M. Murphy, Dendritic cells in cancer immunology. *Cell Mol Immunol* **19**, 3-13 (2022).
550. G. Alessandri, M. C. Ossiprandi, J. MacSharry, D. van Sinderen, M. Ventura, Bifidobacterial Dialogue With Its Human Host and Consequent Modulation of the Immune System. *Front Immunol* **10**, 2348 (2019).

551. J. L. Galeano Niño *et al.*, Effect of the intratumoral microbiota on spatial and cellular heterogeneity in cancer. *Nature* **611**, 810-817 (2022).
552. E. Abdolalipour *et al.*, Evaluation of the antitumor immune responses of probiotic Bifidobacterium bifidum in human papillomavirus-induced tumor model. *Microb Pathog* **145**, 104207 (2020).
553. A. M. Morton *et al.*, Endoscopic photoconversion reveals unexpectedly broad leukocyte trafficking to and from the gut. *Proc Natl Acad Sci U S A* **111**, 6696-6701 (2014).
554. G. Berg *et al.*, Microbiome definition re-visited: old concepts and new challenges. *Microbiome* **8**, 103 (2020).
555. M. R. Fernandes, P. Aggarwal, R. G. F. Costa, A. M. Cole, G. Trinchieri, Targeting the gut microbiota for cancer therapy. *Nat Rev Cancer* **22**, 703-722 (2022).
556. A. J. Gonzales-Luna, T. J. Carlson, K. W. Garey, Emerging Options for the Prevention and Management of Clostridioides difficile Infection. *Drugs* **83**, 105-116 (2023).
557. S. G. Kalathil, Y. Thanavala, Importance of myeloid derived suppressor cells in cancer from a biomarker perspective. *Cell Immunol* **361**, 104280 (2021).
558. A. E. Stenzel, S. I. Abrams, K. B. Moysich, A Call for Epidemiological Research on Myeloid-Derived Suppressor Cells in Ovarian Cancer: A Review of the Existing Immunological Evidence and Suggestions for Moving Forward. *Front Immunol* **10**, 1608 (2019).
559. A. M. van der Leun, D. S. Thommen, T. N. Schumacher, CD8. *Nat Rev Cancer* **20**, 218-232 (2020).
560. K. J. Hiam-Galvez, B. M. Allen, M. H. Spitzer, Systemic immunity in cancer. *Nat Rev Cancer* **21**, 345-359 (2021).
561. F. Sallusto, D. Lenig, R. Förster, M. Lipp, A. Lanzavecchia, Two subsets of memory T lymphocytes with distinct homing potentials and effector functions. *Nature* **401**, 708-712 (1999).
562. Q. Liu, Z. Sun, L. Chen, Memory T cells: strategies for optimizing tumor immunotherapy. *Protein Cell* **11**, 549-564 (2020).
563. A. Kallies, D. Zehn, D. T. Utzschneider, Precursor exhausted T cells: key to successful immunotherapy? *Nat Rev Immunol* **20**, 128-136 (2020).
564. F. Petitprez, M. Meylan, A. de Reyniès, C. Sautès-Fridman, W. H. Fridman, The Tumor Microenvironment in the Response to Immune Checkpoint Blockade Therapies. *Front Immunol* **11**, 784 (2020).
565. S. J. Gaudino, P. Kumar, Cross-Talk Between Antigen Presenting Cells and T Cells Impacts Intestinal Homeostasis, Bacterial Infections, and Tumorigenesis. *Front Immunol* **10**, 360 (2019).
566. Y. Chen *et al.*, Tumor-associated macrophages: an accomplice in solid tumor progression. *J Biomed Sci* **26**, 78 (2019).
567. J. Gao, Y. Liang, L. Wang, Shaping Polarization Of Tumor-Associated Macrophages In Cancer Immunotherapy. *Front Immunol* **13**, 888713 (2022).
568. M. Nouri-Shirazi *et al.*, Dendritic cells capture killed tumor cells and present their antigens to elicit tumor-specific immune responses. *J Immunol* **165**, 3797-3803 (2000).

569. J. You, H. Dong, E. R. Mann, S. C. Knight, P. Yaqoob, Probiotic modulation of dendritic cell function is influenced by ageing. *Immunobiology* **219**, 138-148 (2014).
570. A. L. Hart *et al.*, Modulation of human dendritic cell phenotype and function by probiotic bacteria. *Gut* **53**, 1602-1609 (2004).
571. Q. Li *et al.*, Oral administration of. *Oncoimmunology* **10**, 1868122 (2021).
572. A. Rivière, M. Selak, D. Lantin, F. Leroy, L. De Vuyst, Bifidobacteria and Butyrate-Producing Colon Bacteria: Importance and Strategies for Their Stimulation in the Human Gut. *Front Microbiol* **7**, 979 (2016).
573. S. J. Yoon *et al.*, -derived short-chain fatty acids and indole compounds attenuate nonalcoholic fatty liver disease by modulating gut-liver axis. *Front Microbiol* **14**, 1129904 (2023).
574. S. Deleu, K. Machiels, J. Raes, K. Verbeke, S. Vermeire, Short chain fatty acids and its producing organisms: An overlooked therapy for IBD? *EBioMedicine* **66**, 103293 (2021).
575. B. Chrisman *et al.*, The human "contaminome": bacterial, viral, and computational contamination in whole genome sequences from 1000 families. *Sci Rep* **12**, 9863 (2022).
576. C. D. Johnston, S. Bullman, The tumour-associated microbiome. *Nat Rev Gastroenterol Hepatol* **19**, 347-348 (2022).
577. E. Riquelme *et al.*, Tumor Microbiome Diversity and Composition Influence Pancreatic Cancer Outcomes. *Cell* **178**, 795-806.e712 (2019).
578. C. M. Dejea *et al.*, Patients with familial adenomatous polyposis harbor colonic biofilms containing tumorigenic bacteria. *Science* **359**, 592-597 (2018).
579. A. Kozajda, K. Jeżak, A. Kapsa, Airborne Staphylococcus aureus in different environments-a review. *Environ Sci Pollut Res Int* **26**, 34741-34753 (2019).
580. M. Battaglia, L. A. Garrett-Sinha, Staphylococcus xylosus and Staphylococcus aureus as commensals and pathogens on murine skin. *Lab Anim Res* **39**, 18 (2023).
581. P. Wilmes *et al.*, The gut microbiome molecular complex in human health and disease. *Cell Host Microbe* **30**, 1201-1206 (2022).
582. N. Hasan, H. Yang, Factors affecting the composition of the gut microbiota, and its modulation. *PeerJ* **7**, e7502 (2019).
583. P. Zhang, Influence of Foods and Nutrition on the Gut Microbiome and Implications for Intestinal Health. *Int J Mol Sci* **23**, (2022).
584. J. Schmid, V. Sieber, B. Rehm, Bacterial exopolysaccharides: biosynthesis pathways and engineering strategies. *Front Microbiol* **6**, 496 (2015).
585. R. Touré, E. Kheadr, C. Lacroix, O. Moroni, I. Fliss, Production of antibacterial substances by bifidobacterial isolates from infant stool active against Listeria monocytogenes. *J Appl Microbiol* **95**, 1058-1069 (2003).
586. N. Darvishi, N. A. Fard, M. Sadrnia, Genomic and proteomic comparisons of bacteriocins in probiotic species. *Biotechnol Rep (Amst)* **31**, e00654 (2021).
587. F. A. Martinez, E. M. Balciunas, A. Converti, P. D. Cotter, R. P. de Souza Oliveira, Bacteriocin production by Bifidobacterium spp. A review. *Biotechnol Adv* **31**, 482-488 (2013).
588. J. Tan *et al.*, Evaluation of an Antibiotic Cocktail for Fecal Microbiota Transplantation in Mouse. *Front Nutr* **9**, 918098 (2022).

589. M. Tsikala-Vafea, N. Belani, K. Vieira, H. Khan, D. Farmakiotis, Use of antibiotics is associated with worse clinical outcomes in patients with cancer treated with immune checkpoint inhibitors: A systematic review and meta-analysis. *Int J Infect Dis* **106**, 142-154 (2021).
590. J. Laiño, J. Villena, P. Kanmani, H. Kitazawa, Immunoregulatory Effects Triggered by Lactic Acid Bacteria Exopolysaccharides: New Insights into Molecular Interactions with Host Cells. *Microorganisms* **4**, (2016).
591. S. E. Jones, M. L. Paynich, D. B. Kearns, K. L. Knight, Protection from intestinal inflammation by bacterial exopolysaccharides. *J Immunol* **192**, 4813-4820 (2014).
592. I. Speciale *et al.*, Bifidobacterium bifidum presents on the cell surface a complex mixture of glucans and galactans with different immunological properties. *Carbohydr Polym* **218**, 269-278 (2019).
593. M. Luu, A. Visekruna, Microbial metabolites: novel therapeutic tools for boosting cancer therapies. *Trends Cell Biol* **31**, 873-875 (2021).
594. M. G. Chevrette *et al.*, Microbiome composition modulates secondary metabolism in a multispecies bacterial community. *Proc Natl Acad Sci U S A* **119**, e2212930119 (2022).
595. N. Castro-Bravo, J. M. Wells, A. Margolles, P. Ruas-Madiedo, Interactions of Surface Exopolysaccharides From *Bifidobacterium* and *Lactobacillus* Within the Intestinal Environment. *Front Microbiol* **9**, 2426 (2018).
596. S. K. Mazmanian, C. H. Liu, A. O. Tzianabos, D. L. Kasper, An immunomodulatory molecule of symbiotic bacteria directs maturation of the host immune system. *Cell* **122**, 107-118 (2005).
597. R. Inturri *et al.*, Chemical and biological properties of the novel exopolysaccharide produced by a probiotic strain of Bifidobacterium longum. *Carbohydr Polym* **174**, 1172-1180 (2017).
598. C. Sabater *et al.*, Exopolysaccharide Producing *Bifidobacterium animalis* subsp. *lactis* Strains Modify the Intestinal Microbiota and the Plasmatic Cytokine Levels of BALB/c Mice According to the Type of Polymer Synthesized. *Front Microbiol* **11**, 601233 (2020).
599. M. J. Kang *et al.*, Structural analysis and prebiotic activity of exopolysaccharide produced by probiotic strain. *Food Sci Biotechnol* **32**, 517-529 (2023).
600. A. Wallimann *et al.*, An Exopolysaccharide Produced by Bifidobacterium longum 35624® Inhibits Osteoclast Formation via a TLR2-Dependent Mechanism. *Calcif Tissue Int* **108**, 654-666 (2021).
601. S. Lebeer, J. Vanderleyden, S. C. De Keersmaecker, Host interactions of probiotic bacterial surface molecules: comparison with commensals and pathogens. *Nat Rev Microbiol* **8**, 171-184 (2010).
602. S. Goyal, J. C. Castrillón-Betancur, E. Klaile, H. Slevogt, The Interaction of Human Pathogenic Fungi With C-Type Lectin Receptors. *Front Immunol* **9**, 1261 (2018).
603. J. Tang, G. Lin, W. Y. Langdon, L. Tao, J. Zhang, Regulation of C-Type Lectin Receptor-Mediated Antifungal Immunity. *Front Immunol* **9**, 123 (2018).
604. S. Cohen-Kedar *et al.*, Human intestinal epithelial cells respond to β-glucans via Dectin-1 and Syk. *Eur J Immunol* **44**, 3729-3740 (2014).

605. H. Feinberg *et al.*, Mechanism of pathogen recognition by human dectin-2. *J Biol Chem* **292**, 13402-13414 (2017).
606. W. B. Coley, The treatment of malignant tumors by repeated inoculations of erysipelas. With a report of ten original cases. 1893. *Clin Orthop Relat Res*, 3-11 (1893).
607. J. Bickels, Y. Kollender, O. Merinsky, I. Meller, Coley's toxin: historical perspective. *Isr Med Assoc J* **4**, 471-472 (2002).
608. E. F. McCarthy, The toxins of William B. Coley and the treatment of bone and soft-tissue sarcomas. *Iowa Orthop J* **26**, 154-158 (2006).
609. D. Dutta, S. H. Lim, Bidirectional interaction between intestinal microbiome and cancer: opportunities for therapeutic interventions. *Biomark Res* **8**, 31 (2020).
610. F. Badie *et al.*, Use of *Salmonella* Bacteria in Cancer Therapy: Direct, Drug Delivery and Combination Approaches. *Front Oncol* **11**, 624759 (2021).
611. S. Patyar *et al.*, Bacteria in cancer therapy: a novel experimental strategy. *J Biomed Sci* **17**, 21 (2010).
612. M. Luo *et al.*, Bacteria-mediated cancer therapy: A versatile bio-sapper with translational potential. *Front Oncol* **12**, 980111 (2022).
613. Y. Chen *et al.*, Genetically engineered oncolytic bacteria as drug delivery systems for targeted cancer theranostics. *Acta Biomater* **124**, 72-87 (2021).
614. L. P. Jahromi, G. Fuhrmann, Bacterial extracellular vesicles: Understanding biology promotes applications as nanopharmaceuticals. *Adv Drug Deliv Rev* **173**, 125-140 (2021).
615. A. L. Carvalho *et al.*, Bioengineering commensal bacteria-derived outer membrane vesicles for delivery of biologics to the gastrointestinal and respiratory tract. *J Extracell Vesicles* **8**, 1632100 (2019).
616. A. L. Carvalho *et al.*, Use of bioengineered human commensal gut bacteria-derived microvesicles for mucosal plague vaccine delivery and immunization. *Clin Exp Immunol* **196**, 287-304 (2019).
617. K. L. Maughan, M. A. Lutterbie, P. S. Ham, Treatment of breast cancer. *Am Fam Physician* **81**, 1339-1346 (2010).
618. S. Al-Nasiry, N. Geusens, M. Hanssens, C. Luyten, R. Pijnenborg, The use of Alamar Blue assay for quantitative analysis of viability, migration and invasion of choriocarcinoma cells. *Hum Reprod* **22**, 1304-1309 (2007).
619. A. A. Ahmed, M. Abedalthagafi, Cancer diagnostics: The journey from histomorphology to molecular profiling. *Oncotarget* **7**, 58696-58708 (2016).
620. G. J. Yuen, E. Demissie, S. Pillai, B lymphocytes and cancer: a love-hate relationship. *Trends Cancer* **2**, 747-757 (2016).
621. P. Berraondo *et al.*, Cytokines in clinical cancer immunotherapy. *Br J Cancer* **120**, 6-15 (2019).
622. C. Rébé, F. Ghiringhelli, Interleukin-1β and Cancer. *Cancers (Basel)* **12**, (2020).
623. P. S. Steeg, Tumor metastasis: mechanistic insights and clinical challenges. *Nat Med* **12**, 895-904 (2006).
624. D. Jorgovanovic, M. Song, L. Wang, Y. Zhang, Roles of IFN-γ in tumor progression and regression: a review. *Biomark Res* **8**, 49 (2020).
625. N. Wang *et al.*, CXCL1 derived from tumor-associated macrophages promotes breast cancer metastasis via activating NF-κB/SOX4 signaling. *Cell Death Dis* **9**, 880 (2018).

626. H. Dillekås, M. S. Rogers, O. Straume, Are 90% of deaths from cancer caused by metastases? *Cancer Med* **8**, 5574-5576 (2019).
627. D. N. Huggins *et al.*, Characterizing Macrophage Diversity in Metastasis-Bearing Lungs Reveals a Lipid-Associated Macrophage Subset. *Cancer Res* **81**, 5284-5295 (2021).
628. S. S. Alhudaithi *et al.*, Local Targeting of Lung-Tumor-Associated Macrophages with Pulmonary Delivery of a CSF-1R Inhibitor for the Treatment of Breast Cancer Lung Metastases. *Mol Pharm* **17**, 4691-4703 (2020).
629. T. Kitamura *et al.*, Monocytes Differentiate to Immune Suppressive Precursors of Metastasis-Associated Macrophages in Mouse Models of Metastatic Breast Cancer. *Front Immunol* **8**, 2004 (2017).
630. D. Y. Oh *et al.*, Toward a better understanding of T cells in cancer. *Cancer Cell* **39**, 1549-1552 (2021).
631. M. Hassanein, J. A. Anderson, Refusal of animal-derived medical products in a paediatric setting: Ethical issues. *Paediatr Child Health* **26**, 99-102 (2021).
632. S. P. Sattar, M. Shakeel Ahmed, F. Majeed, F. Petty, Inert medication ingredients causing nonadherence due to religious beliefs. *Ann Pharmacother* **38**, 621-624 (2004).
633. R. Stentz *et al.*, The Proteome of Extracellular Vesicles Produced by the Human Gut Bacteria Bacteroides thetaiotaomicron. *Appl Environ Microbiol* **88**, e0053322 (2022).
634. O. Y. Kim *et al.*, Bacterial outer membrane vesicles suppress tumor by interferon-γ-mediated antitumor response. *Nat Commun* **8**, 626 (2017).
635. L. Ai *et al.*, Prognostic role of myeloid-derived suppressor cells in cancers: a systematic review and meta-analysis. *BMC Cancer* **18**, 1220 (2018).
636. V. Gujrati *et al.*, Bioengineered bacterial outer membrane vesicles as cell-specific drug-delivery vehicles for cancer therapy. *ACS Nano* **8**, 1525-1537 (2014).
637. C. G. England, E. B. Ehlerding, W. Cai, NanoLuc: A Small Luciferase Is Brightening Up the Field of Bioluminescence. *Bioconjug Chem* **27**, 1175-1187 (2016).
638. D. Li, L. Zhu, Y. Wang, X. Zhou, Y. Li, Bacterial outer membrane vesicles in cancer: Biogenesis, pathogenesis, and clinical application. *Biomed Pharmacother* **165**, 115120 (2023).
639. B. Hoesel, J. A. Schmid, The complexity of NF-κB signaling in inflammation and cancer. *Mol Cancer* **12**, 86 (2013).
640. M. Karin, Nuclear factor-kappaB in cancer development and progression. *Nature* **441**, 431-436 (2006).
641. C. J. Kearney *et al.*, Tumor immune evasion arises through loss of TNF sensitivity. *Sci Immunol* **3**, (2018).
642. A. Montfort *et al.*, The TNF Paradox in Cancer Progression and Immunotherapy. *Front Immunol* **10**, 1818 (2019).
643. M. Oft, IL-10: master switch from tumor-promoting inflammation to antitumor immunity. *Cancer Immunol Res* **2**, 194-199 (2014).
644. D. Zheng, T. Liwinski, E. Elinav, Interaction between microbiota and immunity in health and disease. *Cell Res* **30**, 492-506 (2020).

645. J. F. Toso *et al.*, Phase I study of the intravenous administration of attenuated Salmonella typhimurium to patients with metastatic melanoma. *J Clin Oncol* **20**, 142-152 (2002).
646. C. P. Day, G. Merlino, T. Van Dyke, Preclinical mouse cancer models: a maze of opportunities and challenges. *Cell* **163**, 39-53 (2015).
647. C. M. Mastroianni *et al.*, Preferences of patients with advanced colorectal cancer for treatment with oral or intravenous chemotherapy. *Patient* **1**, 181-187 (2008).
648. Y. Shiravand *et al.*, Immune Checkpoint Inhibitors in Cancer Therapy. *Curr Oncol* **29**, 3044-3060 (2022).
649. Q. Chen *et al.*, Bioengineering Bacterial Vesicle-Coated Polymeric Nanomedicine for Enhanced Cancer Immunotherapy and Metastasis Prevention. *Nano Lett* **20**, 11-21 (2020).
650. Y. Li *et al.*, Bacterial Outer Membrane Vesicles Presenting Programmed Death 1 for Improved Cancer Immunotherapy. *ACS Nano* **14**, 16698-16711 (2020).
651. T. R. Marzoog *et al.*, Bacterial extracellular vesicles induced oxidative stress and mitophagy through mTOR pathways in colon cancer cells, HT-29: Implications for bioactivity. *Biochim Biophys Acta Mol Cell Res* **1870**, 119486 (2023).
652. Y. Jiang *et al.*, Bifidobacterium-derived membrane vesicles inhibit triple-negative breast cancer growth by inducing tumor cell apoptosis. *Mol Biol Rep* **50**, 7547-7556 (2023).
653. E. F. Giunta *et al.*, Baseline IFN-γ and IL-10 expression in PBMCs could predict response to PD-1 checkpoint inhibitors in advanced melanoma patients. *Sci Rep* **10**, 17626 (2020).
654. K. S. Saini, C. Twelves, Determining lines of therapy in patients with solid cancers: a proposed new systematic and comprehensive framework. *Br J Cancer* **125**, 155-163 (2021).
655. S. C. Wei, C. R. Duffy, J. P. Allison, Fundamental Mechanisms of Immune Checkpoint Blockade Therapy. *Cancer Discov* **8**, 1069-1086 (2018).
656. Y. Yao *et al.*, The Role of Microbiota in Infant Health: From Early Life to Adulthood. *Front Immunol* **12**, 708472 (2021).
657. W. Y. Cheng, C. Y. Wu, J. Yu, The role of gut microbiota in cancer treatment: friend or foe? *Gut* **69**, 1867-1876 (2020).
658. M. Ratner, Seres's pioneering microbiome drug fails mid-stage trial. *Nat Biotechnol* **34**, 1004-1005 (2016).
659. V. B. Young, Unexpected Results From a Phase 2 Trial of a Microbiome Therapeutic for Clostridioides difficile Infection: Lessons for the Future. *Clin Infect Dis* **72**, 2141-2143 (2021).
660. L. C. Beck *et al.*, Strain-specific impacts of probiotics are a significant driver of gut microbiome development in very preterm infants. *Nat Microbiol* **7**, 1525-1535 (2022).
661. Q. Li *et al.*, Oral administration of *Bifidobacterium breve* promotes antitumor efficacy via dendritic cells-derived interleukin 12. *Oncoimmunology* **10**, 1868122 (2021).
662. R. Hansen *et al.*, A Double-Blind, Placebo-Controlled Trial to Assess Safety and Tolerability of (Thetanix) Bacteroides thetaiotaomicron in Adolescent Crohn's Disease. *Clin Transl Gastroenterol* **12**, e00287 (2020).

663. V. Kästele *et al.*, Intestinal-derived ILCs migrating in lymph increase IFNγ production in response to Salmonella Typhimurium infection. *Mucosal Immunol* **14**, 717-727 (2021).
664. E. C. Mackley *et al.*, CCR7-dependent trafficking of RORγ^{+} ILCs creates a unique microenvironment within mucosal draining lymph nodes. *Nat Commun* **6**, 5862 (2015).
665. S. A. Houston *et al.*, The lymph nodes draining the small intestine and colon are anatomically separate and immunologically distinct. *Mucosal Immunol* **9**, 468-478 (2016).
666. M. Tomura *et al.*, Monitoring cellular movement in vivo with photoconvertible fluorescence protein "Kaede" transgenic mice. *Proc Natl Acad Sci U S A* **105**, 10871-10876 (2008).
667. M. E. Mnich, R. van Dalen, N. M. van Sorge, C-Type Lectin Receptors in Host Defense Against Bacterial Pathogens. *Front Cell Infect Microbiol* **10**, 309 (2020).
668. J. D. Martínez *et al.*, Unraveling Sugar Binding Modes to DC-SIGN by Employing Fluorinated Carbohydrates. *Molecules* **24**, (2019).
669. S. J. van Vliet, L. C. Paessens, V. C. Broks-van den Berg, T. B. Geijtenbeek, Y. van Kooyk, The C-type lectin macrophage galactose-type lectin impedes migration of immature APCs. *J Immunol* **181**, 3148-3155 (2008).